SUMMARY

DEBRIS MOTION AND INJURY RELATIONSHIPS
IN ALL HAZARD ENVIRONMENTS

Final Report

by

A. Longinow
A. Wiedermann
S. Citko
N. Iwankiw

for

July 1976

DCPA Review Notice

SUMMARY REPORT

Study Objective

The main objective of this study was to verify and develop casualty (injury and fatality) relationships for people located in conventional buildings when subjected to man-made and natural disaster environments. The emphasis is on the direct effects as produced by megaton-range nuclear weapons. Limited consideration is given to an examination of debris effects produced by a tornado.

Casualty Assessment

Recognizing the importance of being able to predict the long term survivability of people in population centers subjected to a nuclear weapon attack, an effort was devoted to a review and selection of casualty criteria applicable to the evaluation of casualties in a nuclear weapon environment. This was a day effort in this study. It was useful in validating casualty functions developed in previous studies and in providing a basis for categorizing impact casualties in several categories with respect to type and level of injury. To this end, currently available literature in this field from a number of different sources including drop tests, sled tests, vibration tests, animal tests, accident data and analytic simulation studies were reviewed with the object of verifying and selecting impact casualty criteria that are applicable for evaluation of casualties in a nuclear weapon blase environment. Impact criteria previously produced by White and his coworkers (Ref. 1) were reviewed and verified in the context of other currently available data. These criteria were subsequently extended for use with appropirate simulation models.

To provide for a clearer distinction between injuries to different parts of the body produced by impact, an additional simulation model was developed. This is a two dimensional

A conventional tornado wind environment, together with a simple aerodynamic drag model is used to establish debris trajectories and corresponding hazards for one severe tornado wind field.

Conclusions and recommendations resulting from this effort are presented in Chapter 6 in the context of the overall civil defense problem. Results of this study provide the civil defense planner with a set of countermeasures that can be used in allocating certain categories of existing shelter space in accordance to its effectiveness in saving lives.

REPORT DOCUMENTATION PAGE		READ INSTRUCTIONS BEFORE COMPLETING FORM
1. REPORT NUMBER	2. GOVT ACCESSION NO.	3. RECIPIENT'S CATALOG NUMBER
4. TITLE (and Subtitle) DEBRIS MOTION AND INJURY RELATIONSHIPS IN ALL HAZARD ENVIRONMENTS		5. TYPE OF REPORT & PERIOD COVERED Final Report 6/74 - 6/75
		6. PERFORMING ORG. REPORT NUMBER J6334
7. AUTHOR(s) A. Longinow, A. Wiedermann, S. Citko, N. Iwankiw		8. CONTRACT OR GRANT NUMBER(s) DCPA01-74-C-0251
9. PERFORMING ORGANIZATION NAME AND ADDRESS IIT Research Institute 10 West 35th Street Chicago, Illinois 60616		10. PROGRAM ELEMENT, PROJECT, TASK AREA & WORK UNIT NUMBERS Work Unit 1614E
11. CONTROLLING OFFICE NAME AND ADDRESS Defense Civil Preparedness Agency Washington, D.C. 20301		12. REPORT DATE July 1976
		13. NUMBER OF PAGES 236
14. MONITORING AGENCY NAME & ADDRESS(if different from Controlling Office)		15. SECURITY CLASS. (of this report) Unclassified
		15a. DECLASSIFICATION/DOWNGRADING SCHEDULE

16. DISTRIBUTION STATEMENT (of this Report)

Approved for public release; distribution unlimited

17. DISTRIBUTION STATEMENT (of the abstract entered in Block 20, if different from Report)

18. SUPPLEMENTARY NOTES

19. KEY WORDS (Continue on reverse side if necessary and identify by block number)

Civil Defense, Nuclear Weapons, Tornado, Wind, Personnel Shelter, Blast Effects, Casualties, Survivors, Damage, Impact

20. ABSTRACT (Continue on reverse side if necessary and identify by block number)

This report contains the results of a study concerned with producing casualty (injury and fatality) relationships for people located in conventional buildings when subjected to man-made and natural disaster hazard environments. Emphasis is on the direct effects produced by nuclear weapons. Limited consideration is given to debris effects produced by a tornado.

DD FORM 1473 1 JAN 73   EDITION OF 1 NOV 65 IS OBSOLETE

20.

The key portion of this effort was concerned with selecting impact casualty criteria and developing a simulation model for people subjected to blast winds and debris. Portions of available literature dealing with impact casualties are reviewed and discussed. Impact casualty criteria applicable for evaluating casualties in a nuclear weapon blast environment are selected. A two-dimensional, articulated man simulation model developed herein is described.

People survivability estimates for people located in conventional basements of multisotry buildings subjected to blast effects of megaton range nuclear weapons are presented. Results are presented for full basements with one-way and two-way (flat plate, flat slab) reinforced concrete overhead floor systems and large V/A (basement volume to entranceway area) ratios, i.e., large basements with proportionally small entranceways in which blast penetration is not a significant hazard. A separate task is devoted to basements having small V/A ratios. The transient air velocity field which may exist in such basements is modeled. This model is used in conjunction with a simple drag-type transport model to examine the impact hazard to personnel

A limited effort is devoted to evaluating debris hazards posed by a tornado. A conventional tornado wind environment together with a simple aerodynamic model is used to establish hazards posed by debris for one severe tornado wind field.

DEBRIS MOTION AND INJURY RELATIONSHIPS
IN ALL HAZARD ENVIRONMENTS

DCPA Contract DCPA01-74-C-0251
DCPA Work Unit 1614E

Final Report
by

A. Longinow
A. Wiedermann
S. Citko
N. Iwankiw

for

Defense Civil Preparedness Agency
Washington, D.C.   20301

July 1976

Approved for public release;
distribution unlimited.

DCPA Review Notice

FORWARD

This is the final report on IITRI Project J6334, entitled "Debris Motion and Injury Relationships in all Hazard Environments." It was performed for the Defense Civil Preparedness Agency under Contract No. DCPA01-74-C-0251, Work Unit 1614E. The study was initiated on April 15, 1974 and was completed November 15, 1975.

The study was performed in the Structural Analysis Section, Engineering Mechanics Division of IIT Research Institute. The following IITRI personnel contributed to this effort: A. Longinow, A. Wiedermann, S. Citko and N. Iwankiw. The study was monitored by Mr. D. A. Bettge of DCPA. The many useful suggestions provided by Mr. Bettge in the course of this project are gratefully acknowledged.

<div style="text-align:right">

Respectfully Submitted,
IIT RESEARCH INSTITUTE
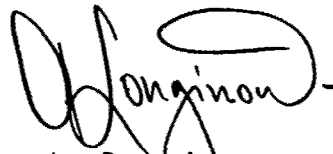
A. Longinow
Project Engineer

</div>

APPROVED:

K. E. McKee
Director of Research
Engineering Mechanics Division

ABSTRACT

This report contains the results of a study concerned with producing casualty (injury and fatality) relationships for people located in conventional buildings when subjected to man-made and natural disaster hazard environments. Emphasis is on the direct effects produced by nuclear weapons. Limited consideration is given to debris effects produced by a tornado.

The key portion of this effort was concerned with selecting impact casualty criteria and developing a simulation model for people subjected to blast winds and debris. Portions of available literature dealing with impact casualties are reviewed and discussed. Impact casualty criteria applicable for evaluating casualties in a nuclear weapon blast environment are selected. A two-dimensional, articulated man simulation model developed herein is described.

People survivability estimates for people located in conventional basements of multistory buildings subjected to blast effects of megaton range nuclear weapons are presented. Results for full basements with one-way and two-way (flat plate, flat slab) reinforced concrete overhead floor systems and large V/A (basement volume to entranceway area) ratios, i.e., large basements with proportionally small entranceways in which blast penetration is not a significant hazard. A separate task is devoted to basements having small V/A ratios. The transient air velocity field which may exist in such basements is modeled. This model is used in conjunction with a simple drag-type transport model to examine the impact hazard to personnel.

A limited effort is devoted to evaluating debris hazards posed by a tornado. A conventional tornado wind environment together with a simple aerodynamic model is used to establish hazards posed by debris for one severe tornado wind field.

CONTENTS

CONTENTS (Concl)

ILLUSTRATIONS

ILLUSTRATIONS (Contd)

ILLUSTRATIONS (Concl)

LIST OF TABLES

CHAPTER 1

INTRODUCTION

The primary objective of the effort described herein was to produce casualty (injury and fatality) relationships for people located in conventional buildings when subjected to hazards produced by man-made and natural disaster environments. Although the emphasis is on the direct effects produced by megaton-range nuclear weapons, some consideration is given to debris effects produced by a tornado.

Recognizing the importance of being able to predict long term survivability of people in population centers subjected to a nuclear weapon attack, a task was devoted to selecting casualty criteria and developing a more complete people response simulation model. This was a key effort in this study. Currently available literature in this field from a number of different sources including drop tests, sled tests, vibration tests, animal tests, accident data and analytic simulation studies were reviewed with the object of selecting impact casualty (injury and fatality) criteria that are adaptable to the evaluation of impact casualties in a nuclear weapon environment. Impact criteria previously produced by White and his coworkers (Ref. 11) were reviewed in the context of other available data and were selected for use with the "rigid block" simulation model.

To provide for a clearer distinction between injuries to different parts of the body produced by impact, an additional simulation model was developed. This is a two-dimensional, seven segment model (see Figure 10) simulating an individual. It is capable of approximating forces experienced by an individual during impact with a hard surface and when being translated by the blast winds. The level of casualty experienced can be estimated by relating the strain energy produced at impact to casualty criteria which were developed (Table 7, Ref. 32) from available data based on the strain energy approach. Although crude,

1

this method is believed to be an improvement over the previous method using the rigid block simulation model. Review of casualty data and description of simulation models is contained in Chapter 2.

To provide for a better understanding as to protection afforded by conventional basements against the effects of blast produced by megaton-range nuclear weapons, a sample of basements was analyzed in this study.

Chapter 3 contains people survivability results for basements of multistory buildings with overhead slab at grade and such that the V/A (basement volume to entranceway area) ratio is large, i.e., large basements with proportionally small entranceways. In such basements the primary casualty mechanism is debris produced by the collapse of the overhead slab (floor) system. Two types of overhead floor systems were considered, i.e., one-way slabs (simply-supported and two-span continuous) and square two-way slabs without beams or girders, i.e., flat plates and flat slabs. This sample of floor systems includes representative ranges of the usual design parameters, i.e., span, concrete strength, steel strength and design live load.

Chapter 4 considers the blast wind hazard in basement areas when the overhead slab does not fail. The transient air velocity field which may exist in a conventional basement when exposed to the air blast effects of a nominal megaton-range nuclear weapon in its Mach region has been modeled. This simulation model was used in conjunction with a simple drag type transport model to examine the translational and impact behavior of personnel located in various positions throughout the basement area. This effort has indicated that a significant hazard exists and has indentified some of the mechanisms and parameters that influence the hazard level.

A limited effort (see Chapter 5) was devoted to the evaluation of the debris hazard produced by tornado exposure. An approach is formulated and is based, in part, upon a blend of deterministic calculations and probabilistic estimates. A conventional tornado

2

wind environment, together with a simple aerodynamic drag model is used to establish debris trajectories and corresponding hazards for one severe tornado wind field.

Conclusions and recommendations resulting from this effort are presented in Chapter 6 in the context of the overall civil defense problem. Results of this study provide the civil defender with a set of countermeasures that can be used in allocating certain categories of existing shelter space in accordance to its effectiveness in saving lives.

CHAPTER 2

ASSESSMENT OF CASUALTIES IN A DIRECT EFFECTS ENVIRONMENT

2.1 CATEGORIZATION OF THE EFFECTS OF BLAST

Biological effects of blast have been arbitrarily divided
into several categories, i.e., primary, secondary and tertiary
effects (Refs. 14, 22). Body damage produced by the primary
effects is that associated with variations in environmental pres-
sure. Injuries involve the air-containing organs, e.g., the
sinuses, ears, lungs and gastrointestinal tract. Secondary
effects include those injuries resulting from the impact of pene-
trating and nonpenetrating missiles energized by ground shock,
overpressures and dynamic pressures. A wide variety of injuries
is seen ranging from slight lacerations to penetrating and per-
forating lesions due to flying debris, including glass fragments
and other frangible materials. This also includes crushing (im-
pact) injuries produced by the collapse of inhabited structures.
Tertiary effects include injuries that occur as a consequence
of actual displacement of an individual by winds that accompany
the propagation of the blast wave. Injuries may be first pro-
duced during the accelerative phase of movement because of dif-
ferential velocities imparted to various portions of the body.
However, for the overpressure range of interest (1 psi to 15 psi)
major trauma will be more prevalent and severe during decelera-
tion, particularly as a result of impact with hard surfaces.
Injuries in this category are expected to bear a resemblance to
those observed with victims of falls, automobile accident and aero-
plane crashes; e.g. abrasions, lacerations, contusions, fractures,
and rupture of, and damage to, the internal organs, including the
heart, lungs, liver, spleen, brain, and spinal chord (Ref. 22).

2.2 CASUALTY MECHANISMS

For people in the upper stories of buildings subjected to
the direct effects of nuclear weapons, casualties (injuries and
fatalities) are expected to be produced by thermal radiation,
prompt nuclear radiation, dynamic pressure and debris.

2.2.1 Thermal Radiation

Burn casualties will result when window coverings (blinds, shades, etc.) are not provided or are inadequate and when people are in direct line of sight with the blast source.

2.2.2 Prompt Nuclear Radiation

Radiation casualties will be produced when the mass thickness between the people and the source is not adequate.

2.2.3 Dynamic Pressure

High velocity winds associated with the passage of the blast wave will cause people to lose balance, be rotated and translated, and impact with floors, walls, furniture, etc. When translation is terminated within the building, impact with the ground plane (grassy lawn, garden earth, concrete, asphalt, etc.) will occur or people will be blown out of buildings from various stories.

2.3.4 Debris

In addition to setting people in motion, dynamic pressures will cause loose or previously attached objects to be set in motion. Building components such as window frames and glass, mounted equipment furnishings, walls and partitions separated by the blast loading become moving, potentially lethal debris under the action of blast winds. These can interact with people located in their paths producing impact casualties.

People located in partial basements with windows (see Figure 1(a)) face a similar set of casualty mechanisms as do people in the upper stories. In full basements, i.e., those without windows and with overhead slab at grade (see Figure 1(b)) impact is expected to be the primary casualty mechanism and is brought into play by the breakup and collapse of the overhead floor system.

6
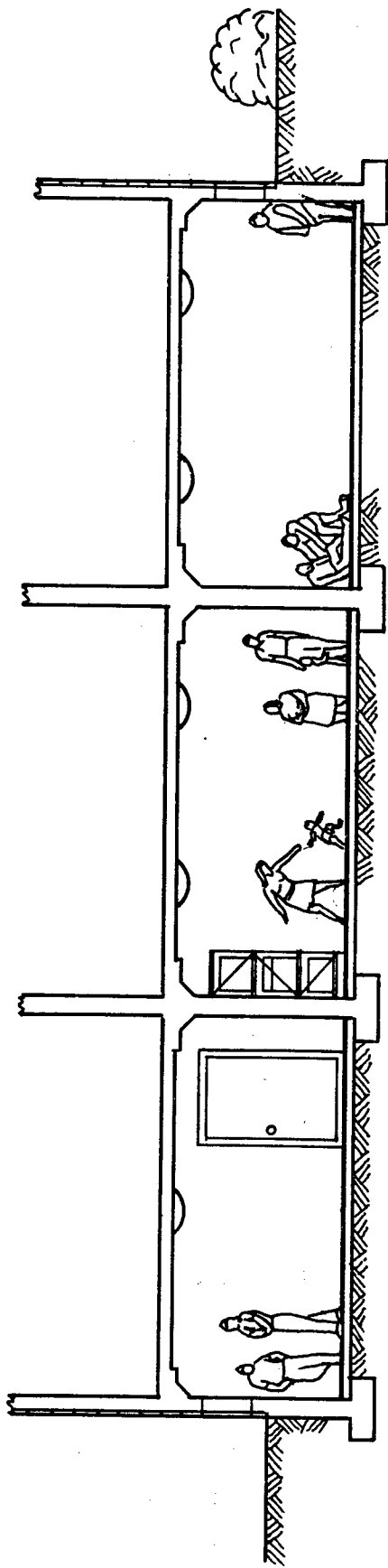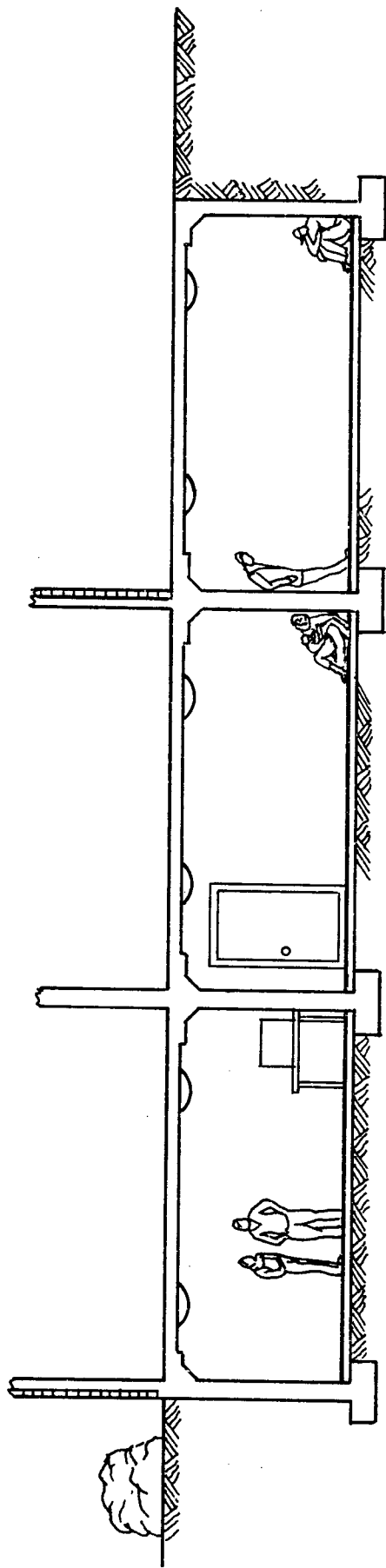
a) Partial Basement

b) Full Basement

Figure 1 Examples of Partial and Full Basements

7

People are thus subject to impact as a result of being set in motion by the blast winds, by airborne, sliding or falling debris or some combination of these casualty mechanisms.

Impact, blast or penetrating, is a significant casualty mechanism for people in the upper stories and in basements. In those instances where thermal and prompt nuclear radiation may be considered as insignificant (which represents a large number of practical cases), impact is then the only casualty mechanism.

Criteria which are specifically oriented for assessing casualties in buildings subjected to the direct effects of nuclear weapons are limited. Impact criteria (Ref. 14) used in previous studies (Refs. 15, 16, 17) were derived by the use of a great deal of bioengineering judgement on numerous related experiences such as accidental free-falls, scaled animal data, war related bomb data, military aircraft pilot ejection studies, etc.

A literature review was conducted in the course of this study with the aim of possibly enlarging the capability of current casualty criteria so as to allow prediction of injuries and fatalities for a broader class of casualties and with a higher level of confidence than was possible previously. The emphasis of this review was on casualties produced by impact. Results are discussed in the following paragraphs. This is followed by a summary of tentative casualty criteria applicable to a blast environment together with a description of several simulation models used to predict impact casualty mechanisms as a function of weapon yield, range, building characteristics, location and initial position of people.

2.3 IMPACT

Impacts involving the human body are among the most common phenomena of life. There are few violent, natural or man-made disasters in which impact is not a significant casualty mechanism. Impact is the primary casualty producer in vehicular collisions and is therefore of interest in this field with respect to regional and whole body tolerances as a function of body orientation and type of restraint device. For very similar

8

reasons, impact is also of interest in aviation medical research. A large quantity of currently available literature on impact injury tolerance originated in the interest of vehicular and aeroplane safety.

Impact is characterized by forces of very rapid onset, short duration and high magnitude. Such forces are produced by abrupt acceleration, deceleration or sudden contact, e.g., a person in the free-field striking the ground or an object. In the case of sudden contact, impact can be penetrating or nonpenetrating.

Sustained acceleration studies on humans are (and have been) performed using instruments such as the centrifuge. A large quantity of this work deals with accelerations in the range from 1 to 15 g and higher, and with durations ranging upward from somewhere in the vicinity of 5 sec. This does not fall in the category of impact. Impact involves time intervals which may be stated approximately as ranging from 1 sec. downward, often measurable in terms of one-hundredth or one-thousandth of a second.

An examination of the effects produced by acceleration in these two general areas reveals that one of the distinctions between them is that in the former (i.e., long-term sustained acceleration), fluid shifts within the body dominate. In other words, the time period is sufficiently great such that the normal distribution of blood among the various vessels and organs of the body is affected. Also, the hydraulic pressure in the vessels in particular areas may be elevated to the point where hemorrhage or loss of blood into the tissues occurs. Often the heart is unable to cope with pressures so generated and consequently there may be collapse of veins and even actual emptying of the heart.

In the case of impact, on the other hand, the duration of the force on the body is too brief to bring these hydraulic effects into play and therefore other effects dominate.

Impact forces are dissipated by the deformation (and/or rupture) of body tissues, external environment (restraint system, striking surface, etc.) and displacement of body organs. Impacts of low order produce effects generally limited to discomfort; these may be more painful but they are less threatening to life. When the effects are more severe, actual damage to body structure and interference with function may occur. Damage may range from that which is slight and repairable, to complete disintegration.

Human tolerance to impact can be defined as the level of some predetermined parameter at which a physical reaction end point is produced in the individual(s) subjected to the impact. The predetermined parameter can be: pressure, deformation, velocity, acceleration, etc. The physical reaction end point can be: painful reaction, limit of voluntary tolerance, injury threshold, LD_{50} value, limit of survival, etc.

Our current state of knowledge concerning human impact tolerances is very incomplete. While most human volunteer studies have been conducted on young, healthy male subjects under rigidly controlled conditions with careful medical monitoring, they have been voluntarily terminated at levels below that of irreversible injury. No experimental impact data are available for females, children, or other segments of the population.

The influence of age is suggested by the data collected by Stech and Payne (Ref. 20) who present an extrapolation of available data to find that the vertebral end plate breaking strength reduces to zero at approximately 119 years of age. This extrapolation is based on limited cadaver data and may be crude, however it does emphasize the significance of age on the level of injury and time to recovery for identical conditions of impact.

To assess the ability of the human body to withstand impact and, subsequently, to establish levels of estimated injury probability, it is necessary to obtain and analyze data on actual exposures to impact. In general, there are two sources of data, i.e., controlled experiments using volunteer subjects and

accidental (involuntary) exposures. It is obviously undesirable to injure subjects in test situations. Thus the data resulting from tests tend to consist of subjective responses or reports of no injury. Accident data, on the other hand, very often include injury levels ranging from mild to lethal; however the circumstances surrounding the exposure are generally ill-defined.

Tests have been conducted at various laboratories using live human subjects, human cadavers and live animals. Most of the work that is currently reported is directed at reducing highway casualties. Snyder (Ref. 8) reviews some 446 technical papers on this subject and provides a very comprehensive state-of-the-art review of "Human Impact Tolerance" up to approximately August 1970. Snyder concludes that current knowledge on human tolerance to impact must still be considered very general and fragmentary. "Some ballpark human tolerance limits have been established which a healthy young male cannot exceed without the probability of injury or fatal trauma" (Ref. 8). The following paragraphs of this narrative discuss some of these tolerance limits and results which are considered to be pertinent in assigning injury criteria to impacts produced in a blast environment.

2.4 SOME RELATED IMPACT EXPERIENCE

Figure 2 is a compilation of human impact experience obtained from several sources such as DeHaven (Ref. 18), Snyder (Ref. 19) and others. This chart (Ref. 23) was constructed assuming uniform acceleration or deceleration in accordance with the equation:

$$a = \frac{v^2}{2h} \tag{1}$$

where

a - acceleration (deceleration)

v - initial or final velocity (v is used as the ordinate in Figure 2)

h - acceleration or deceleration distance (h is used as the abscissa in Figure 2)
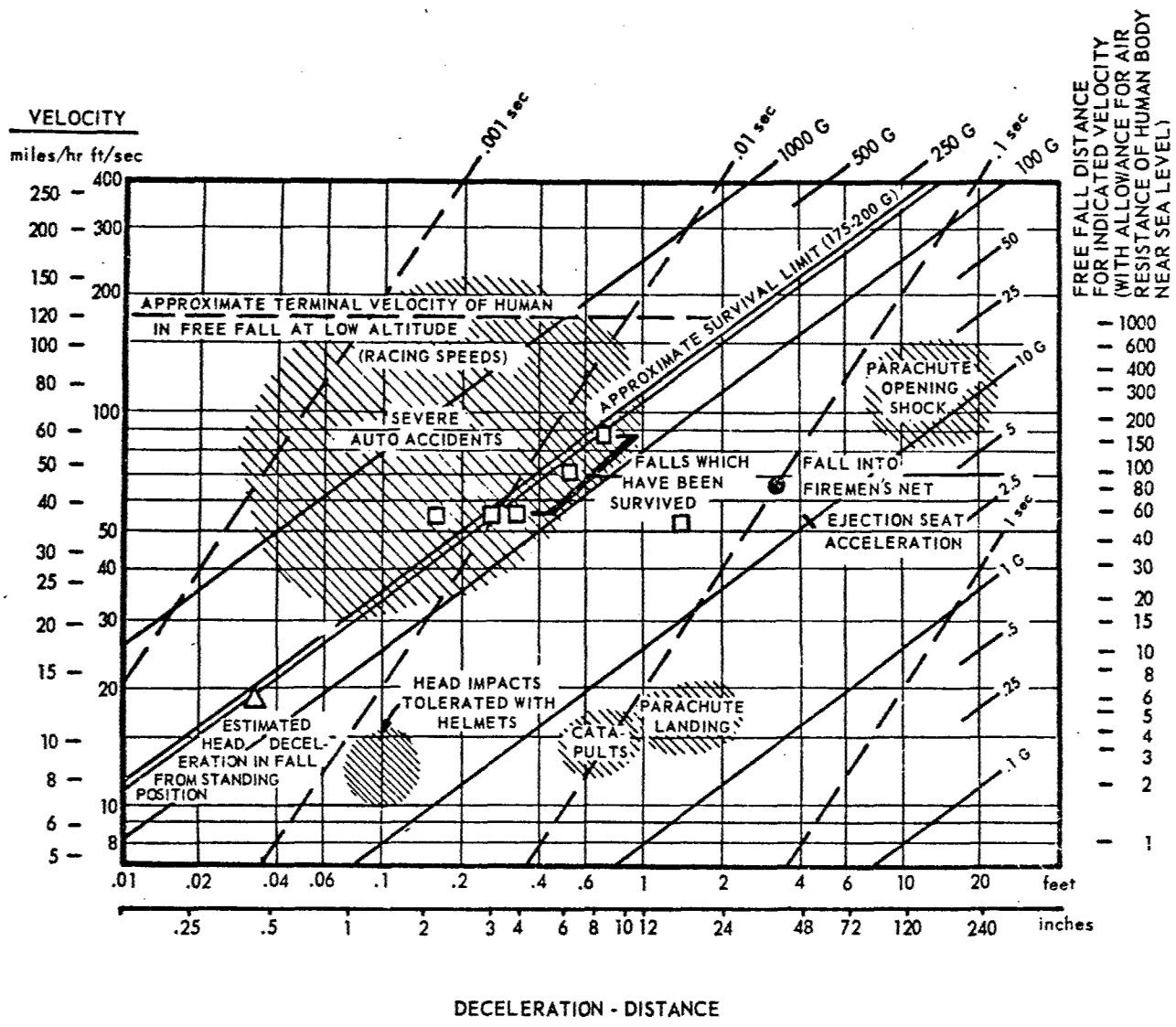
Figure 2   Velocity-Distance-Time-Acceleration Chart

The chart was constructed using logarithmic scales and the acceleration is found on the angularly-oriented solid line coordinate sytem in G units. The time involved in a given case of uniform acceleration may be determined from the angularly oriented dashed-line coordinate system.

Data points with hollow squares are for free falls of 50-150 ft with survival. The triangle represents an estimate of deceleration of a human head experienced in a fall from a standing position with the head hitting a hard surface. There are a number of other cases of more and less extreme impacts with survival for free falls from 5 to 275 ft (Ref. 19), however the deceleration distance is not always available. Based largely on the survived fall data shown, a tentative survival limit, indicated by the double diagonal line (175-200 G) was established. Parameter values corresponding to this line should be used with caution, since in addition to the four parameters (v,s,g,t) which collectively define impact in Figure 2, a number of associated biophysical parameters influence the corresponding impact casualty and degree of survival.

2.5 HEAD IMPACT

Injury to the head is the most frequent and severe result of impact. Head injuries were found to occur in about 80 percent of the automotive accidents and are considered to be the prime cause of fatalities. The distribution of accident injuries in motor vehicle occupants with respect to various parts of the body in the mid-60's was approximately as follows (Ref. 1):

        Head   -   80 percent
        Legs   -   42 percent
        Arms   -   35 percent
        Chest   -   25 percent
        Spine   ⎫
        Abdomen   ⎬   20 percent
        Pelvis   ⎭

The sum of these percentages is greater than 100 percent because

in any one accident one frequently finds injuries to multiple portions of the body. The head is also involved in 50 percent of persons injured in motorcycle accidents (Ref. 2) and in about 70 percent of persons injured in accidental falls in the home (Ref. 3). It is expected that head injuries produced by impact would constitute a significant fraction of all impact injuries that would be produced in a blast environment.

The tolerance level of the living, human brain to impact appears to be unknown at this time. Concussion, which is considered as the minimal pathophysiologic disturbance of the brain resulting from impact, is often used as the end point in studies of brain injury. Concussion is defined (Ref. 4) as a condition of lowered functional activity, without visible structural change, produced in an organ by a shock (as by a fall or blow). Such lowered functional activity in the head can be unconsciousness which often occurs immediately after an impact. Concussion is a form of brain injury, frequently reversible but potentially fatal, and associated (in the human) with amnesia. Its mechanism does not appear to be known at this time.

According to most published information, the primary injury to be avoided is not so much structural damage to the skull but rather injury to the brain. Head impact can produce injury to the brain before its intensity is sufficiently great to cause skull fracture.

Gurdjian and his coworkers in studies of impact energy required to fracture the human skull (Refs. 5, 6, 7) have shown that while about 25 in.-lb of energy were required to fracture dry skulls, significantly more energy was required to fracture an intact head. The additional energy was absorbed by the scalp (hair and head contents) when the intact head was tested. Energy levels required to cause fracture in intact heads ranged from 400 to 1,000 in.-lb with an average at about 600 in.-lb. In performing these experimental studies, the skulls (or intact heads) were allowed to drop onto a steel plate and the impact energy was measured as the weight of the dropping mass times the drop height.

Although some differences were found in energy required to produce fracture due to blows in different locations, the tests were not extensive enough to determine that these differences were significant. Gurdjian (Ref. 6) indicates that greater variations were found in energy requirements to produce fracture with a blow in any single location of different skulls than were found from one position to another on the same skull. According to Snyder (Ref. 8), "Force (fracture) tolerance at the side of the skull appears to be about one-half that found for the frontal region."

A tolerance curve for frontal (forehead) impact of the human head on a hard surface is shown in Figure 3 (Ref. 8) It was developed at Wayne State University based on cadaver skull fracture and the observed onset of concussion in animals. Ordinate is the "effective" acceleration (deceleration) level and the abscissa indicates the duration of the corresponding pulse. This curve is purported to delineate the tolerance to impact-induced acceleration before the occurrence of moderate concussion in man. Values lying above the curve are regarded as dangerous to life, values below are considered tolerable.

The usefulness of the WSU (Wayne State University) curve is limited since is is based primarily on frontal head impact to a hard (unyielding) surface. It throws little light on head impact tolerances when other types of surfaces and other impact locations on the head are considered.

The curve shown in Figure 3 was plotted using the following values from Ref. 8 which are based on the Wayne curve and have been proposed as tolerable.

180 G for 2 ms	85 G for 7 ms
132 G for 3 ms	80 G for 8 ms
110 G for 4 ms	74 G for 10 ms
100 G for 5 ms	57 G for 20 ms
90 G for 6 ms	
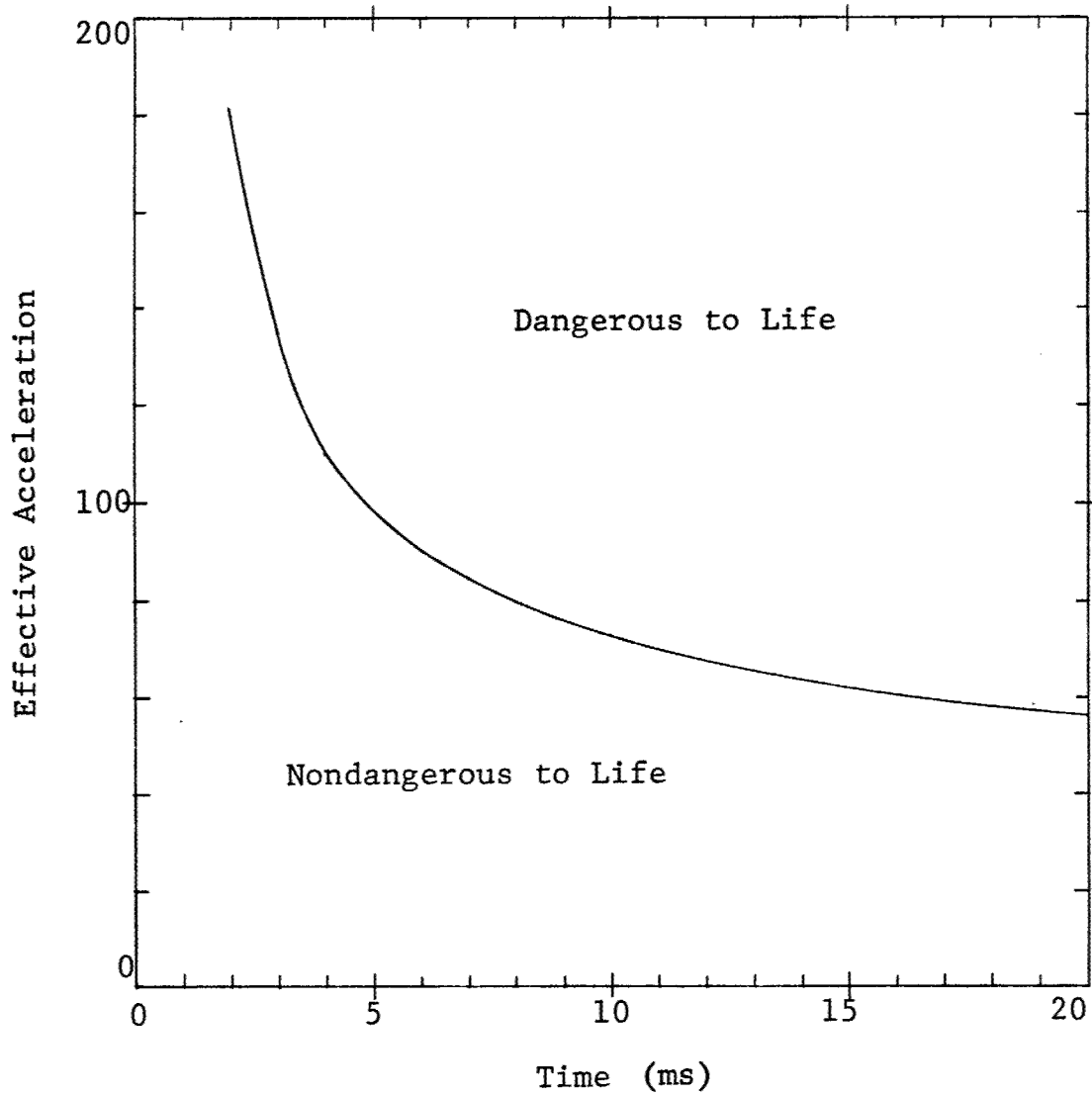
Figure 3   Wayne State University Cerebral Concussion Tolerance Curve

A brief discussion of the applicability of the WSU curve with respect to long duration impacts is given in Ref. 9.

A useful mathematical model for indicating the possibility of incipient head injury is described by Gadd (Ref. 10). This is called the severity index (I) and is defined as follows:

$$I = \int a^n \, dt \qquad (2)$$

where:

a = acceleration, force, or pressure of the response function producing threshold of injury of a given degree

n = weighting factor greater than 1

t = time in seconds

Integration of this function in accordance with Equation (2) yields a number (index) which is applicable to a particular level of injury and whose numerical value varies depending upon whether it is developed in terms of acceleration, force, deformation, or some other indication of loading intensity.

The weighting factor may be thought of as recognizing that the lower portions of the pulse contribute very little to the injury, but that the more intensive portions contribute to a disproportionately great degree.

To use Equation (2) to estimate the level of injury of a given type, two judgements must be made from available bio-mechanics data as follows:

1. The appropriate weighting exponent must be selected. For internal injury to the head from frontal blows an exponent of 2.5 has been used (Ref. 10). This is based on the slope of the Wayne animal impact data representing dangerous concussion.

2. The maximum value (left-hand side) of Equation (2) which can be sustained without danger to life must also be selected if absolute rather than relative estimates are to be made. A numerical value of

1000 for the <u>threshold of serious internal head injury in frontal impact</u> is suggested in Ref. 10. For this value of I, the function "a" (acceleration, deceleration) should be in g-units.

The severity index function is obviously not applicable beyond a certain pulse duration. Although not specifically stated, Ref. 10 seems to indicate that 50 ms is a reasonable upper limit for impact durations.

The severity index criterion appears to be preferable to indexes such as the WSU curve because inherent in its formulation is the premise that injury is a function of loading intensity, pulse shape and duration.

In order to assess impact injuries that would be produced in a blast environment, White and his coworkers (Ref. 11) have examined available head impact data in the light of a blast environment produced by the detonation of a nuclear weapon and have produced the following, tentative criteria.

Table 1

TENTATIVE CRITERIA FOR TERTIARY BLAST EFFECTS
INVOLVING IMPACT

(After White et al, Ref. 11)

Condition, Critical Organ or Event	Related Impact Velocity fps
Skull Fracture	
Mostly "Safe"	10
Threshold	13
50 Percent	18
Near 100 Percent	23

White states (Ref. 11) that these criteria are given as a guide for assessing the various levels of decelerative injury involving

the human head in a blast environment. Since it is difficult to
know with any degree of certainty which portion of the head will
be subject to impacts in such an environment, the criteria are
given in terms of impact velocity rather than acceleration-time
data. Reference 11 does not discuss or speculate on the prob-
able levels of injury associated with these impact velocities.
Criteria given in Table 1 are based on a review of all avail-
able data though primarily on Refs. 12 and 13. In a later
publication (Ref. 14) by White and his coworkers these criteria
were reviewed. However, no new information was found in the
literature to warrant any changes. Review of related data as
part of the present study has uncovered no new data or criteria
to warrant any changes either.

These criteria (Table 1) were adapted in this (and pre-
vious studies (Refs. 15, 16, 17) for assessing the surviv-
ability of people in conventional buildings subjected to blast
environments produced by nuclear weapons. The interpretation
placed on these criteria, and the manner in which they are used
in performing such assessments is discussed in a subsequent sec-
tion of this chapter.

2.6 FREE-FALLS AND WHOLE BODY IMPACT

Reported free-falls in the United States occur at a rate
approaching 50 per day due to accident, suicide or homicide
(Ref. 8) and thus present an unusual opportunity to study the
effects of impact on humans at levels far above those possible
in the laboratory.

The first attempts to study free-fall cases in a scientific
manner is generally attributed to DeHaven (Ref. 18). In 1942
he reported on eight free-falls which included both accidents
and suicide attempts. DeHaven defines a free-fall as being a
fall which is free of any obstructions other than that encountered
at its termination.

Of the eight cases analyzed by DeHaven, seven were such that the height of fall was known exactly. These seven involved both men and women whose ages ranged from 21 to 42. There were no fatalities and whatever injuries were incurred were all followed by full recovery.

Two of the cases (1 and 5) were falls to soil. One fell 55 ft (v_i* = 54 fps) landing on the left side and back with no apparent injuries. The other fell 93 ft (v_i = 73 fps) landing in a nearly supine position on the right side and back.

Two of the cases (6 and 7) were falls onto automobiles, where the force of the body demolished the car structure (roof, hood, fenders) without excessive injuries to the body. One fell 108 ft (v_i = 79 fps) from a 10th story window and landed on the hood and fenders of an automobile, face down. "This man sustained a depressed frontal fracture of the skull, but the immediate cause of this injury was not determined. He had bounced from the car to the pavement. Head injuries observed in like accidents have occurred as a result of bouncing from a decelerative structure to a hard surface." (Ref. 18). This person survived the fall and achieved full recovery. In the second case, a man jumped from the roof of a 14 story building, falling 146 ft (v_i = 86 fps) onto the top and rear of the deck of a coupe and landing in a supine position. The man experienced numerous fractures and suffered moderate shock but was conscious. He survived the fall and achieved full recovery.

In case 3, a wooden fence was demolished by some anterior portion of the chest or abdomen, with trivial injury. The height of fall was 72 ft. In case 2, the force of the fall demolished roof planking and broke three 6-in. by 2-in. beams, with only one skeletal fracture and little other injury. The height of fall was 66 ft. In case 4, a 1.5-in. by 1.5-in. structural T was deflected 13 in. by the anterior portion of the chest. Injuries were minor and recovery uneventful. The height of fall was 74 ft. Cases studied by DeHaven are briefly summarized in Table 2. He

---

*v_i = Impact velocity corrected for air resistance

Table 2

SUMMARY OF FREE-FALL DATA (Ref. 18)

Case	Sex M or F	Age	Height ft-in.	Weight lb	Height of Fall ft	Impact Velocity fps	Deceleration Distance In.	Average Gravity Increase G	Landing Surface of Object	Landing Position	Incurred Injuries
1	F	42	5-2	125	55	54	4	140	Well packed soil	Left side and back	No evidence of injuries
2	F	27	5-3	120	66	60	*	*	Wooden roof	Head first with progressive contact of shoulders and back	Lacerations, abrasions, fracture of sixth cervical vertebra
3	F	36	5-4	115	72	65	*	*	Wood and wire fence	Jack-knifed over the fence face down	No evidence of injuries
4	F	30	5-6	122	74	66	Variable	Not estimated	Iron bar, metal screens, a skylight of wired glass and a metal lath ceiling	Prone, face downward	Contusions, lacerations, rib fractures
5	F	21	5-7	115	93	73	∿6	∿166	Freshly turned soil	Nearly supine, on the right side and back	Fractured rib and wrist
6	M	42	*	*	108	79	6 to 12	100 to 200	Hood and fenders of a car	Face downward	Depressed frontal skull fracture
7	M	27	5-7	140	146	86	∿5	Not estimated	Roof and rear of a car	Semisupine	Numerous fractures and some internal injuries

* Unknown

21

concludes that "the human body can tolerate and expend a force of two hundred times the force of gravity for brief intervals during which the force acts in transverse relation to the long axis of the body" (Ref. 18).

DeHavens' data are included herein as an illustration that the human body can be quite resistant to substantial falls depending on the particular circumstances of impact, i.e., type of impacting surface and area of body impacted. The particular sample of data presented is not statistically valid since DeHaven used only data points in which the individuals survived the free-fall incident, which constitutes a biased sample.

Since the publication of these data (Ref. 18), numerous other studies of accidental free-falls on children and adults, suicides, high divers, skiers etc. have occurred and are reported in the literature (Refs. 19, 20, 21).

With the objective of formulating criteria for assessing impact injuries (other than to the head alone) in a blast environment, White and his coworkers (Ref. 22) performed a series of drop tests on mice, rats, guinea pigs and rabbits. Impact velocity associated with 50 percent mortality (LD_{50}) was calculated for each. These results were subsequently scaled in terms of mean body weight to determine the corresponding impact velocity for man (70 kg animal). Using such experimental results coupled by a review of related information (such as free-fall data discussed previously) in the light of a blast environment, the tentative criteria shown in Table 3 were produced.

These data were subsequently revised. Reference 14 states that, "following the emergence of the large- and small-animal differences in tolerance to blast overpressure, it was obvious that the earlier estimate of the 50 percent lethal velocity for whole-body impact derived from rodent data (Ref. 22) would need updating." Results of this updating are shown in Table 3 in the column labeled revised data. The revised data are based, at least in part, on information reported by Lewis (Ref. 21).

22

Table 3

TENTATIVE CRITERIA FOR INDIRECT (TERTIARY) BLAST EFFECTS
INVOLVING IMPACT

(After White el at, Refs. 11, 14)

Condition, Critical Organ or Event	Related Impact Velocity fps	
Survivability with Total Body Impact	Previous Data (Ref. 11)	Revised Data (Ref. 14)
Mostly Safe	10	10
Lethality Threshold	20	21
Lethality 50 Percent	26	54
Lethality Near 100 Percent	30	138

In Ref. 20, Stech and Payne describe the analysis of moun-
taineering free-fall data from the accident reports of the
American Alpine Club. The method used in analyzing these data
was to assign an injury severity rating to each reported acci-
dent, using the available information in the accident report and
rating the severity with the scale developed by Aviation Crash
Injury Research at Cornell Aeronautical Laboratories. The mid-
point of the injury severity scale was taken as the point repre-
senting 50 percent probability of major injury. Using this
value, an estimated value of 53 fps (impact velocity) was
found for the 50 percent probability of major injury for impact
in the transverse direction, i.e., prone or supine. It is inter-
esting to compare this value with the 54 fps total body impact
velocity for the 50 percent probability of lethality obtained by
White et al (see Table 3) using a different set of free-fall
data and a different data analysis procedure. Obviously, 50
percent probability of major injury is not necessarily equivalent
to 50 percent probability of lethality.

The revised impact criteria shown in Table 3 were adapted
in this (and previous) studies (Refs. 15, 16, 17) for assessing
the survivability of people in conventional buildings subjected
to blast environments produced by nuclear weapons. The inter-
pretation placed on these criteria, and the manner in which they

are used in performing such assessments are discussed in a subsequent section of this chapter.

2.7 INJURY SCALES

The most widely known and used injury scales in this country are those which were produced in connection with automobile accident investigations. An injury scale (Refs. 24, 25) is an essential analytic tool for the comparison of injury and injury severity. Five separate criteria scales are used for scaling injuries that commonly occur in automobile accidents. These are the following:

1. Energy Dissipation Scale (ED). This scale is used to rank injuries by the amount of energy dissipated in producing the injury. Although some undisputed bench marks of injury-related energy dissipation are available in the literature, most of the rankings included in this scale are based on the consensus of clinical judgements of the members of the subcommittee responsible for its development.

2. Threat to Life Scale (TL). The purpose of this scale is to identify those injuries which result in loss of life. The rankings in this scale are based entirely on clinical judgements and reflect current treatment ability of medical facilities.

3. Permanent Impairment Scale (PI). This is an identification scale to determine and rank injuries which result in permanent impairment or disability. The scaling is based on the average permanent disability produced by a given diagnosis. Although variation in any one case is considerable, such averages have been used for many years by insurance companies.

4. Treatment Period Scale (TP). The treatment period used in establishing the rankings of this scale represents the time during which the injured is unable to work. This scale together with the PI

scale can be used to approximate the economic
effects of the incurred injury.

5. Incidence Scale (IN). This scale is used to esti-
   mate the incidence of given diagnosis (injury).
   Estimates included are based on personal experience
   of individuals who developed the scale plus statis-
   tics of automobile accident injuries.

The AIS (Abbreviated Injury Scale, Refs. 24 and 25) has
fairly wide applicability and is a compromise between the ED
and TL scales briefly described. In this scale each diagnosis
is ranked using a 1-9 gradation as follows:

Injury Category	AIS Rating
No Injury or Minor Injury	1
Moderate	2
Severe (Non-Life-Threatening)	3
Severe (Life-Threatening, Survival Probable)	4
Critical (Survival Uncertain)	5
Fatal	6,7,8,9

There are five injury categories and the units 6 to 9 are neces-
sary to reflect various degrees of fatalness. A 6 denotes that
a patient received an injury which is usually fatal, but is an
isolated injury. A higher ranking number is assigned when a
patient receives multiple fatal injuries. A higher ranking num-
ber also denotes extremely severe single injuries such as a
crushed chest. The AIS scale includes a list of probable inju-
ries that could be associated with each of the five injury cate-
gories. This scale has the potential of being used in conjunc-
tion with a set of impact velocities (such as Figure 2) so as
to describe probable impact injuries in a blast environment.

2.8 TENTATIVE CRITERIA FOR THE EVALUATION OF IMPACT
    CASUALTIES IN A BLAST ENVIRONMENT

Based on the review of currently available information of
impact effects on people, the impact criteria put together by

25

White and his coworkers (Ref. 14) still provide the most concise and convenient set of casualty assessment data for a blast environment. Presently they do not appear to have been superceded. These criteria, which were previously discussed in Sections 2.5 and 2.6 of this chapter, related impact velocity to a probability of skull fracture in the case of head impact and to the probability of lethality in the case of total body impact. They are summarized in Table 4. Table 5 lists the type of injuries that are expected to be associated with blast translation (decelerative tumbling) and in the present case refers to whole body impact. Corresponding tentative criteria for debris impact are given in Table 6.

For purposes of assessing casualties in a blast environment produced by nuclear weapons, the head and whole body impact criteria given in Table 4 are interpreted and extended as indicated in Figures 4 and 5 for head and whole body impact respectively.

Referring to Figure 4, it will be noted that, in accord with the data given in Table 4, no measurable injuries are expected at impact velocities (to any portion of the head) less than 10 fps. In the range from 10 to 13 fps the probability of (recoverable) injury increases linearly such that in the vicinity of 13 fps it is essentially 100 percent. The associated probability of fatality is essentially zero. At higher impact velocities the probability of injury (excluding fatality) decreases with increasing probability of fatality. Thus at a head impact velocity of 18 fps a person has the same chance of recoverable injury as of fatality. Similarly, for total body impact up to approximately 20 fps, all injuries are assumed to be reversible, and therefore no probability of fatality is associated with total body impact velocities less than 20 fps. For total body impact in excess of 20 fps, fatalities are assumed to occur. Probability of fatality increases with impact velocity while the probability of reversible injury decreases. Thus at lower velocities (say in the neighborhood of 20 fps) the probability of injury is high and the probability of fatality low.

Table 4

TENTATIVE CRITERIA FOR INDIRECT BLAST EFFECTS
INVOLVING IMPACT (Ref. 14)

Condition, Critical Organ or Event	Related Impact Velocity fps
Skull Fracture	
Mostly "Safe"	10
Threshold	13
50 Percent	18
Near 100 Percent	23
Total Body Impact	
Mostly "Safe"	10
Lethality Threshold	21
Lethality 50 Percent	54
Lethality Near 100 Percent	138

Table 5

BASIC PATHOLOGICAL LESIONS ASSOCIATED
WITH INDIRECT BLAST TRANSLATIONAL INJURY
(Whole Body Impact)

1. Fracture of body structures of the calvaria, face and vertebral column with associated concussion or paralysis.

2. Fractures of long bones of the extremities -- simple or compound.

3. Rib fracture with all associated complications.

4. Rupture of internal organs with associated bleeding, development of infection or respiratory insufficiency.

5. Large area soft tissue injury with associated crush syndrome.

Table 6

TENTATIVE CRITERIA FOR INDIRECT BLAST EFFECTS INVOLVING SECONDARY MISSILES (Ref. 14)

Kind of Missile	Critical Organ or Event	Related Impact Velocity fps
Nonpenetrating 10-lb object	Cerebral Concussion	
	● Mostly "Safe"	10
	● Threshold	15
	Skull Fracture	
	● Mostly "Safe"	10
	● Threshold	15
	● Near 100 Percent	23
Penetrating 10-gm glass fragments	Skin Laceration	
	● Threshold	50
	Serious Wounds	
	● Threshold	100
	● 50 Percent	180
	● Near 100 Percent	300
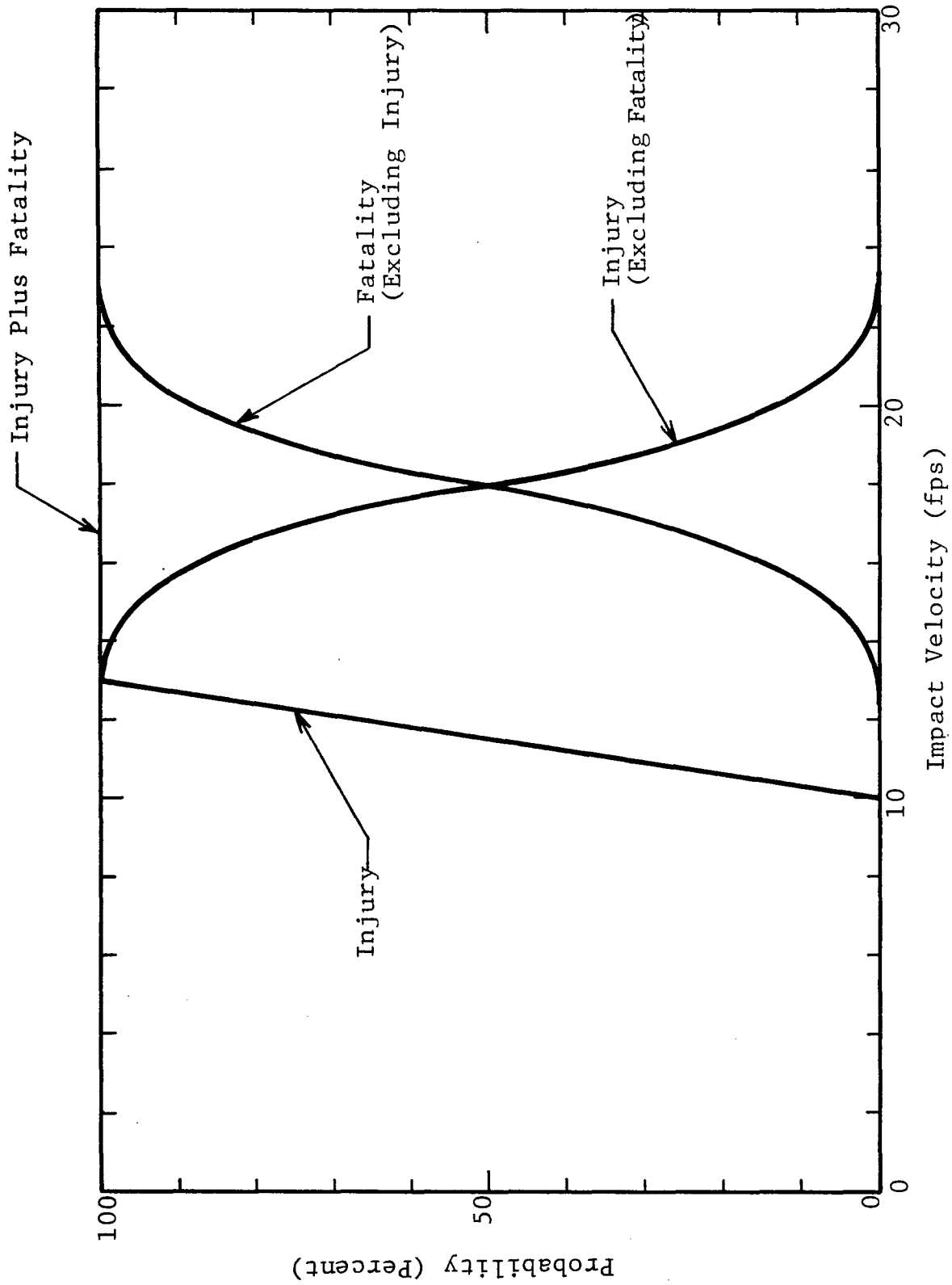
Figure 4   Variation of Probability of Injury and/or Fatality
with Head Impact Velocity
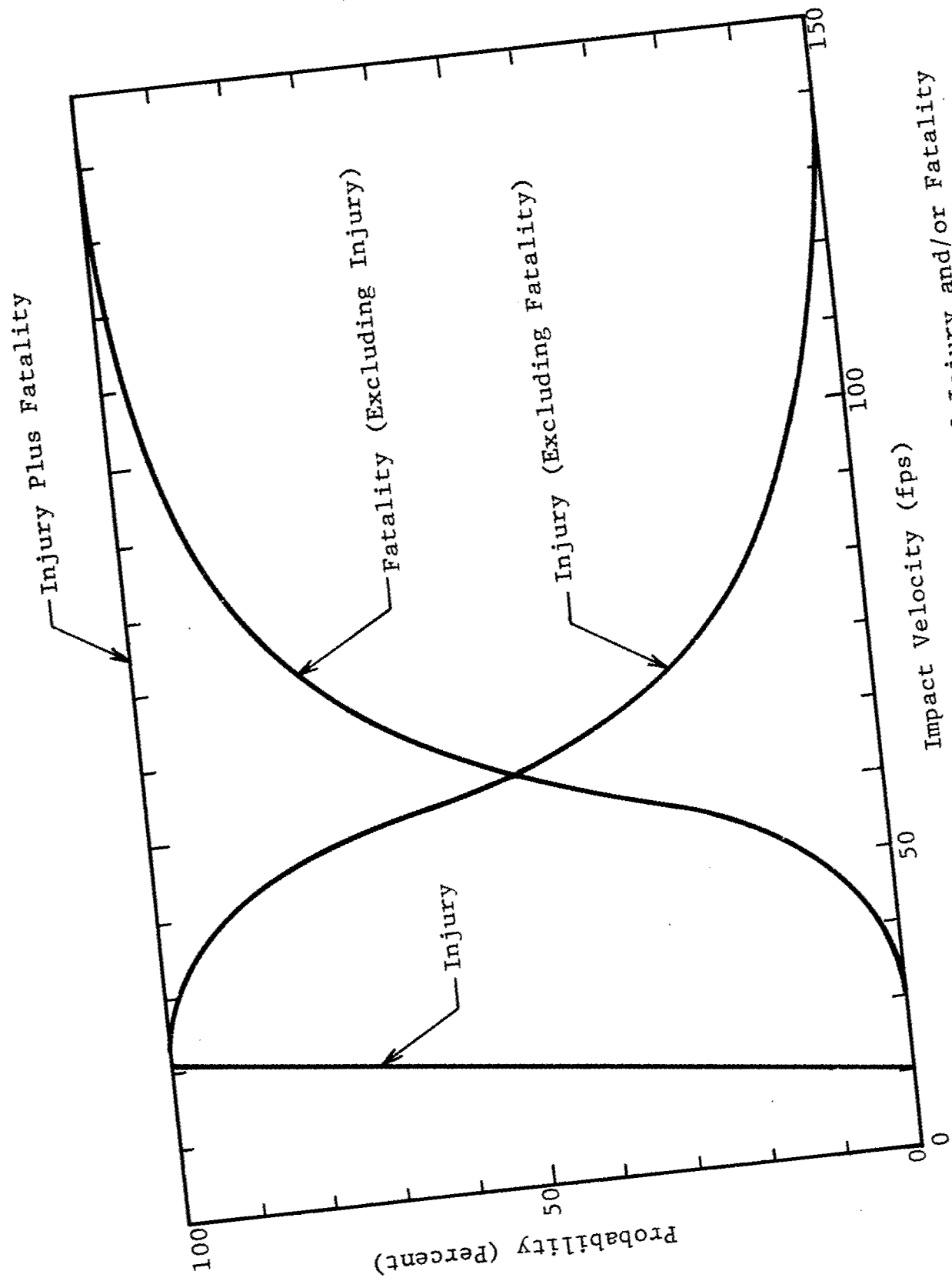
Figure 5   Variation of Probability of Injury and/or Fatality
with Whole Body Impact Velocity

At the high end, 138 fps, the probability of a reversible injury is essentially zero and therefore the probability of fatality essentially certain. Similar reasoning is applied to debris data (Table 5) though corresponding curves are not included in this report.

In the light of the complexities that are potentially present in a nuclear weapon blast environment (such as a variety of different impact surfaces, multiple impacts for any one person due to decelerative tumbling by the long duration blast loading, a variety of different debris sizes coupled with a probable lack of immediate medical attention), the interpretation given to White's data is considered as reasonable with the current state of-the-art.

Simulation models used for predicting impacts and corresponding impact intensitites in a blast environment are briefly described in the following sections.

2.9 GROSS RESPONSE SIMULATION MODEL

A rectangular block free to translate and rotate in two dimensions is used to simulate the gross response of a person subjected to dynamic pressure produced by the detonation of a nuclear weapon. The basic geometry is as indicated in Figure 6(a). The simulated person is defined by four corner points where points 1 and 2 define the feet and points 3 and 4 the head. The dashed line is used to identify the front and the back of the individual in the plotted output. Thus with points 2 and 3 identifying the front, Figure 6(a), represents a standing individual facing to the right.

Under the action of dynamic pressure a person would be subjected to diffraction, drag, lift and contact forces. Contact forces come into play when impact with the floor, wall or the ground plane occurs. Diffraction loading occurs when the shock front interacts with the individual and lasts approximately for the time required for the wave to clear around him. This loading
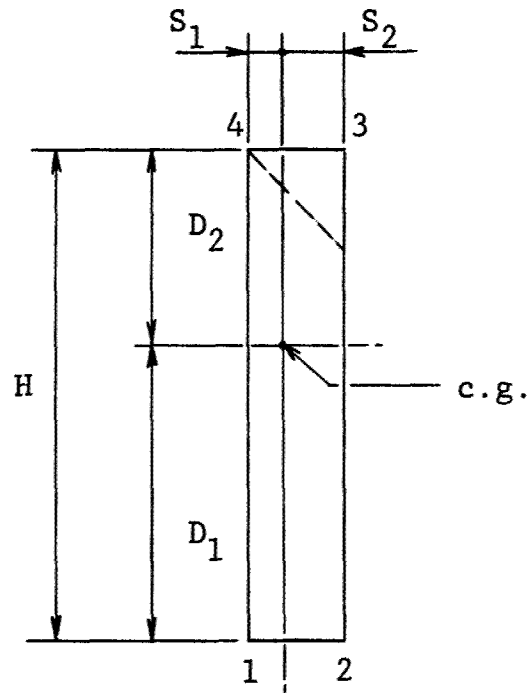
a) Geometry
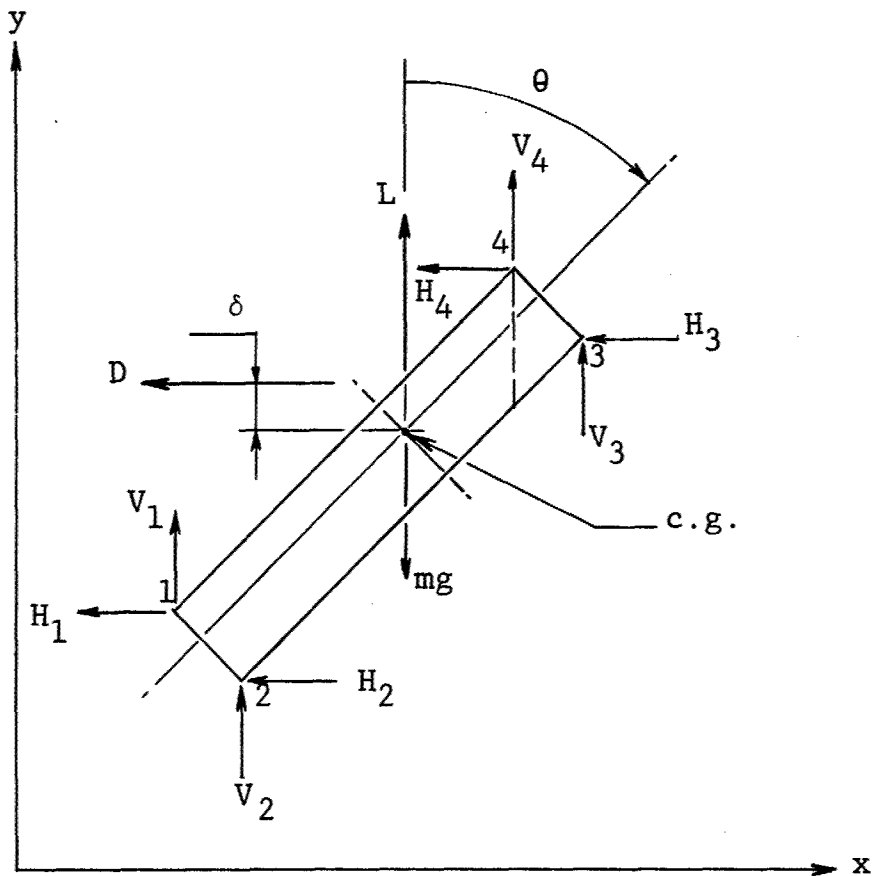
b) Lift, Drag and Contact Forces

Figure 6   Gross Response Simulation Model
(Tumbling Man)

is considered in this simulation model and is treated in a manner similar to that suggested in Ref. 26.

Drag (D) and lift (L) forces are assumed to act on the individual as indicated in Figure 6(b). These forces are defined as follows.

$$D = q(t) \, A_d(\theta) \tag{3}$$

$$L = q(t) \, A_\ell(\theta) \tag{4}$$

Where $q(t)$ is the dynamic pressure of the flow and A_d, A_ℓ are the position dependent drag and lift areas respectively. The particular dynamic pressure time history used in any one case is the free field dynamic pressure modified by dominant local conditions such as building geometry, aperture (window and door) size and location, and room geometry.

The human body is similar in aerodynamic shape to a cylinder with a height-to-width ratio between 4 and 7 (Ref. 27). Since people vary significantly in size and proportions, the selection of a reference area is difficult. Hoerner (Ref. 27) presents the drag of an average man* in the form of a drag area D/q. Drag area values were obtained from wind tunnel tests at wind speeds between 100 and 200 fps. These values are as follows:

A_{dmax} = Maximum drag area = 9 sq ft   (Standing, facing in the direction of wind)

A_{dmin} = Minimum drag area = 1.2 sq ft (Prone, facing up, parallel to the direction of wind)

$A_{\ell max}$ = Maximum lift area = L/q

≈ 2.5 sq ft

The lift area, $A_{\ell max}$, is based on aerodynamic tests of ski-jumpers. This value is for the typical "flying" position, with the body leaning forward against and into the air (Ref. 27).

---

*Weight = 165 lb,   H = 5.9 ft, V = 2.6 ft^3, S = 20 ft^2

The drag and lift area values given are used as end points in computing the drag and lift forces acting on an individual caught up in a dynamic pressure stream. Intermediate values are obtained using the following relationships (Ref. 28).

$$A_d = A_{dmin} + (A_{dmax} - A_{dmin}) \sin^2(\theta - \pi/2) \qquad (5)$$

$$A_\ell = A_{\ell max} \sin(2\theta - \pi) \qquad (6)$$

The variations of drag and lift areas are shown in Figure 7. Thus when $\theta = 0$, $A_d = A_{dmax} = 9$ sq ft and $A_\ell = 0$, and when $\theta = \pi/2$, $A_d = A_{dmin} = 1.2$ sq ft and $A_\ell = 0$.

Rotation is produced because the drag force is assumed to act through the center of pressure, i.e., the center of projected area (see Figure 6(b)) and thus has an eccentricity relative to the center of gravity. This eccentricity (δ) is

$$\delta = (H/2 - D_1)\cos\theta + 1/2(S_1 - S_2)\sin\theta$$

The lift force is assumed to act through the center of gravity (c.g.) and therefore has no associated eccentricity.

The final set of forces which may act on the individual are contact forces due to impact with a horizontal or vertical sur-face. Contact forces are assumed to occur at corner points only and are determined as indicated in Figure 8 and by the use of the following relationships.

The following forces apply (where the subscript i refers to the specific corner point in contact: $i = 1,2,3$ or 4):

For contact with a horizontal surface (floor, ground):

$$V_i = -K_\ell \, y_i \qquad y_i < 0 \quad \text{and} \quad \dot{y}_i < 0$$

$$= -K_u \, y_i \qquad y_i < 0 \qquad \dot{y}_i \geq 0$$

$$= 0 \qquad y_i > 0$$

$$H_i = \mu V_i \ (|\dot{x}_i|/\dot{x}_i)$$

34
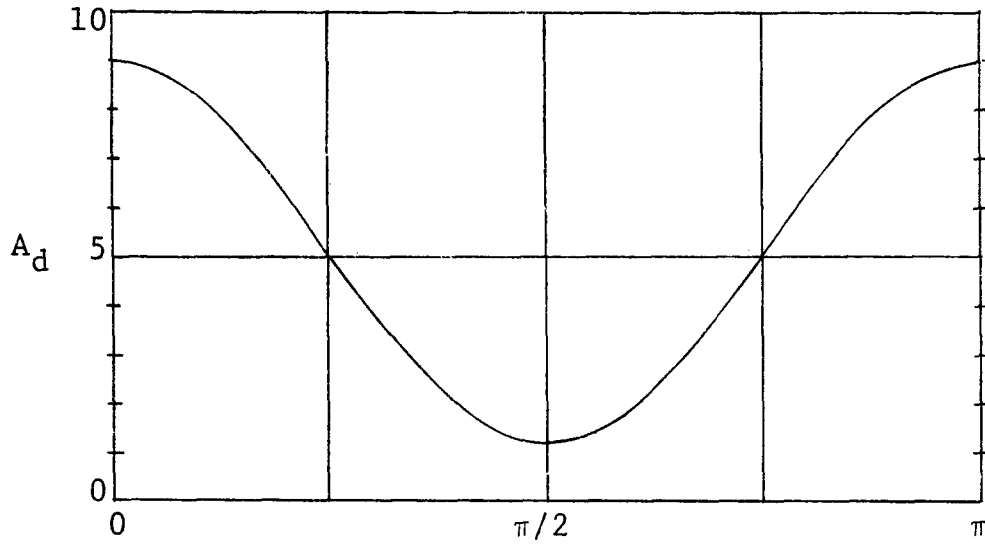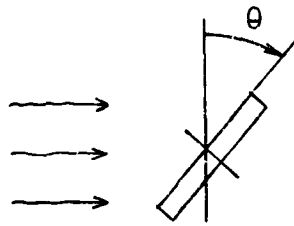
a) Variation of Drag Area (A_d) with θ
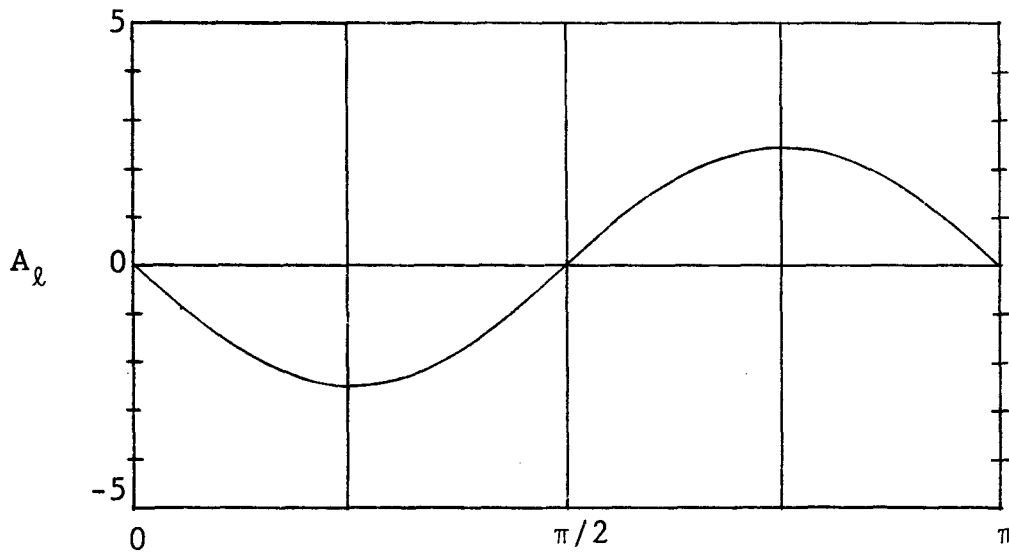
b) Variation of Lift Area (A_ℓ) with θ

Figure 7   Variation of Drag and Lift Areas
with Orientation
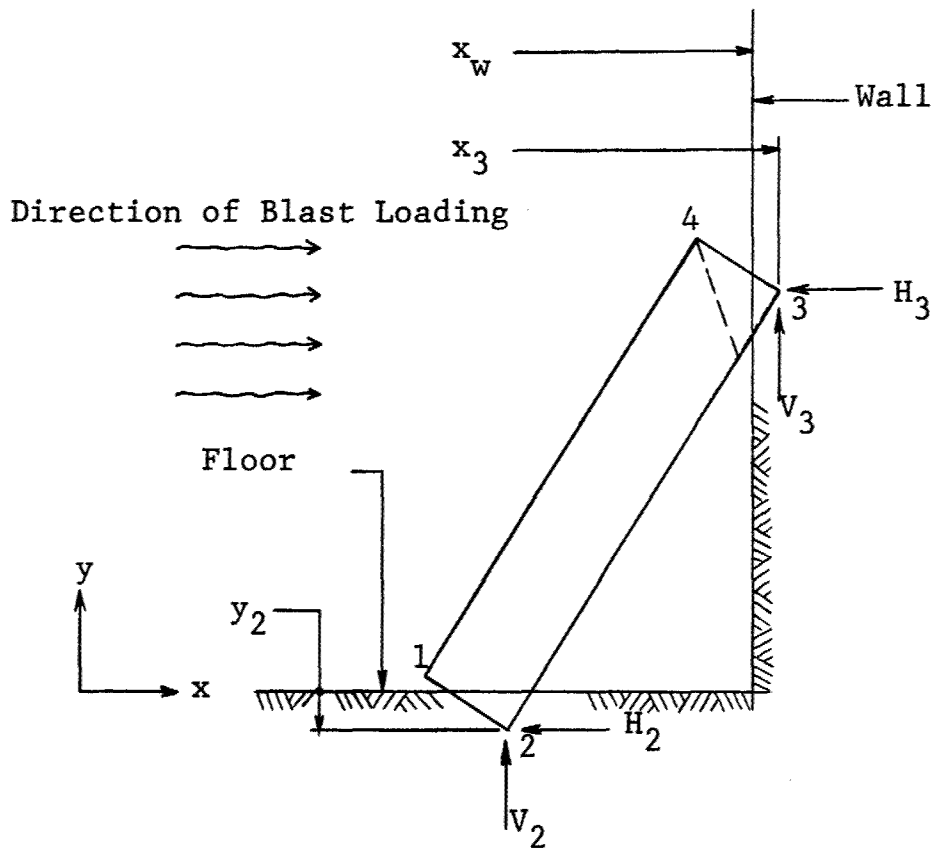
a) Example of Contact Force Designation
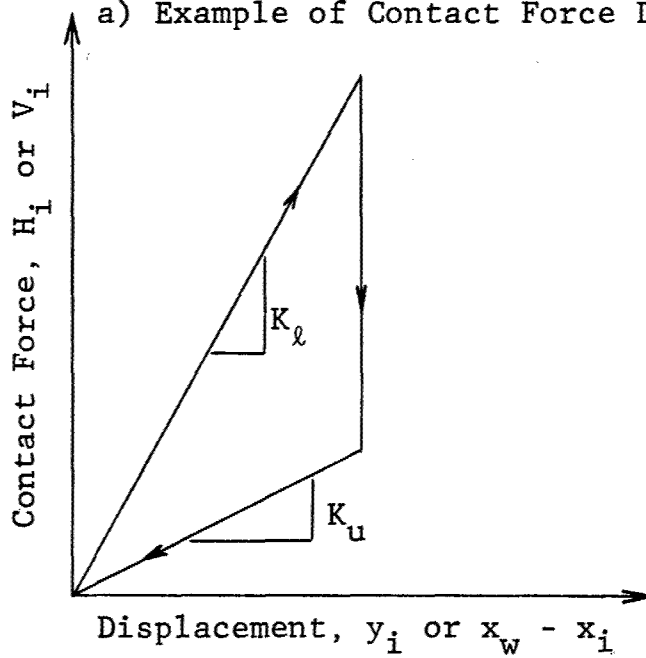
b) Contact Force Magnitude

Figure 8   Definition of Contact Forces Produced by Impact

For contact with a vertical surface (wall):

$$H_i = K_\ell(x_i - x_w) \qquad x_i > x_w \quad \text{and} \quad \dot{x}_i > 0$$

$$ = K_u(x_i - x_w) \qquad x_i > x_w \quad \text{and} \quad \dot{x}_i \leq 0$$

$$ = 0 \qquad\qquad\qquad x_i < x_w$$

$$V_i = \mu H_i(|\dot{y}_i|/\dot{y}_i)$$

where

x_w - coordinate of the wall

K_ℓ - spring constant for loading

K_u - spring constant for unloading

μ - coefficient of friction

see Figures 8(a)
and 8(b)

The reason for using the two different spring constants (see Figure 8(b)) is to provide an approximate means for dissipating energy during impact.

With the forces and geometry having been defined, the governing equations for computing the trajectory of an individual caught up in a dynamic pressure stream (Figure 6(b)) are given as follows:

$$M\ddot{x} + D + H_1 + H_2 + H_3 + H_4 = 0$$

$$M\ddot{y} - L - V_1 - V_2 - V_3 - V_4 = 0$$

$$I\ddot{\theta} + D\delta - H_1(D_1\cos\theta - S_1\sin\theta) - H_2(D_1\cos\theta + S_2\sin\theta)$$

$$+ H_3(D_2\cos\theta - S_2\sin\theta) + H_4(D_2\cos\theta - S_1\sin\theta)$$

$$- V_1(D_1\sin\theta + S_1\cos\theta) - V_2(D_1\sin\theta - S_2\cos\theta)$$

$$+ V_3(D_2\sin\theta + S_2\cos\theta) + V_4(D_2\sin\theta - S_1\cos\theta) = 0 \quad (7)$$

These, and the previous equations given form the basis of the "Gross Response Simulation Model." This computer program accepts data on room geometry (length and height), story height,

story length and location and position (standing, prone) of the occupant being analyzed. For a given blast loading, which is applied as described previously, the routine computes the trajectory of the occupant keeping track of his impact velocities with horizontal and/or vertical surfaces. These velocities are then compared with casualty criteria so as to estimate the extent of casualty experienced.

Some results obtained by the use of this simulation model are shown in Figure 9(a), (b), (c) and (d). In each case, an individual located essentially in the open (as far as shielding is concerned) is subjected to the diffraction loading and the dynamic pressure which is essentially that of the free-field. Weapon blast environments are for a 1 MT weapon and are referenced to the free-field overpressure.

In Figure 9(a) and (b) an individual is located on the second story of an "open"* building and 10 ft from the edge. The blast wave originates to the left of the individual. At the range of 2 psi (Figure 9(a)) he is moved, loses balance but does not fall off the building. At the range of 4 psi he is blown off the building and impacts the ground plane without tumbling. A similar problem is considered in Figure 9(c) and (d) except that we are here dealing with a simulated individual on the ground floor of the same building. At the range of 4 psi his response for the first 0.6 sec is identical to that of Figure 9(b), after which he is moved approximately an additional 10 ft before impacting with the ground. Figure 9(d) is the same problem at the 16 psi range. In this more intense blast environment the individual is lofted and translated, impacting a wall 60 ft from his initial position.

The following "average man" data were used in simulating the individual described.

---

*weak walled, framed building

38
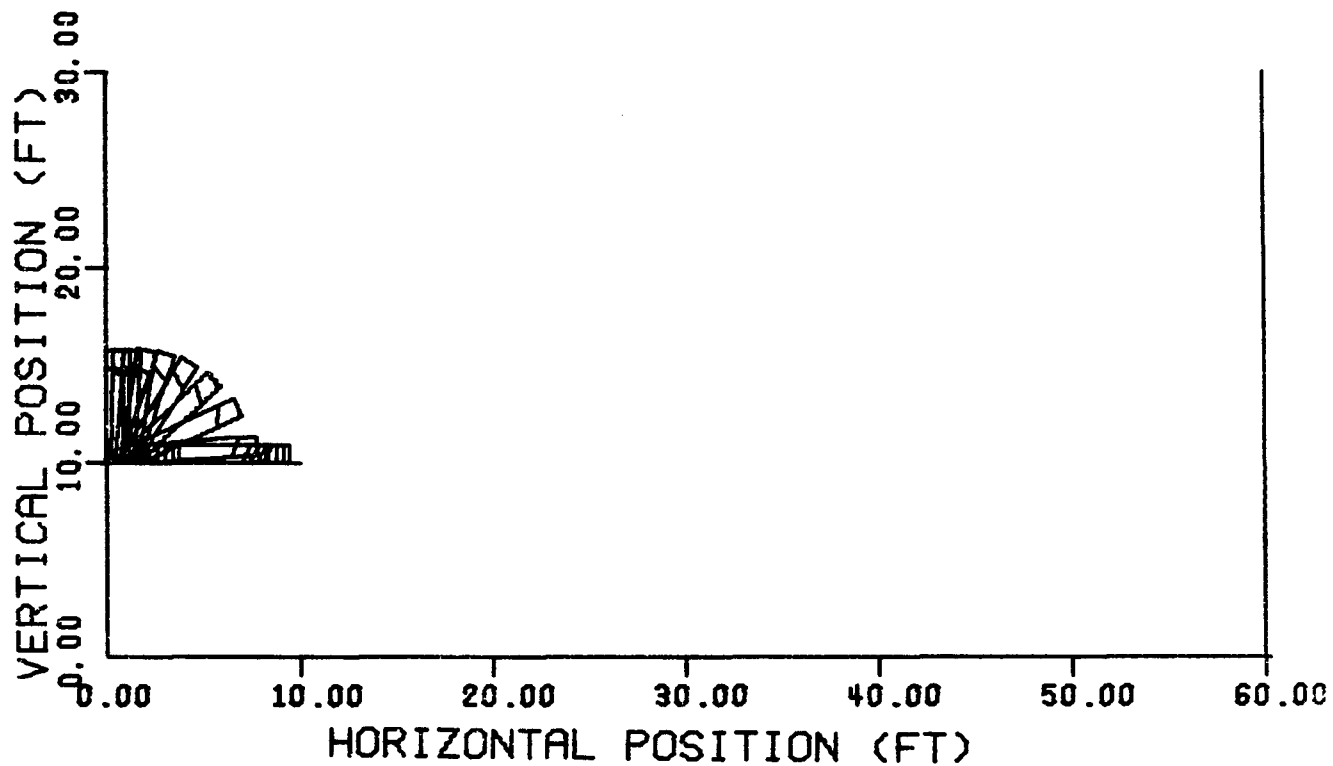
a) Free-Field Overpressure, 2 psi
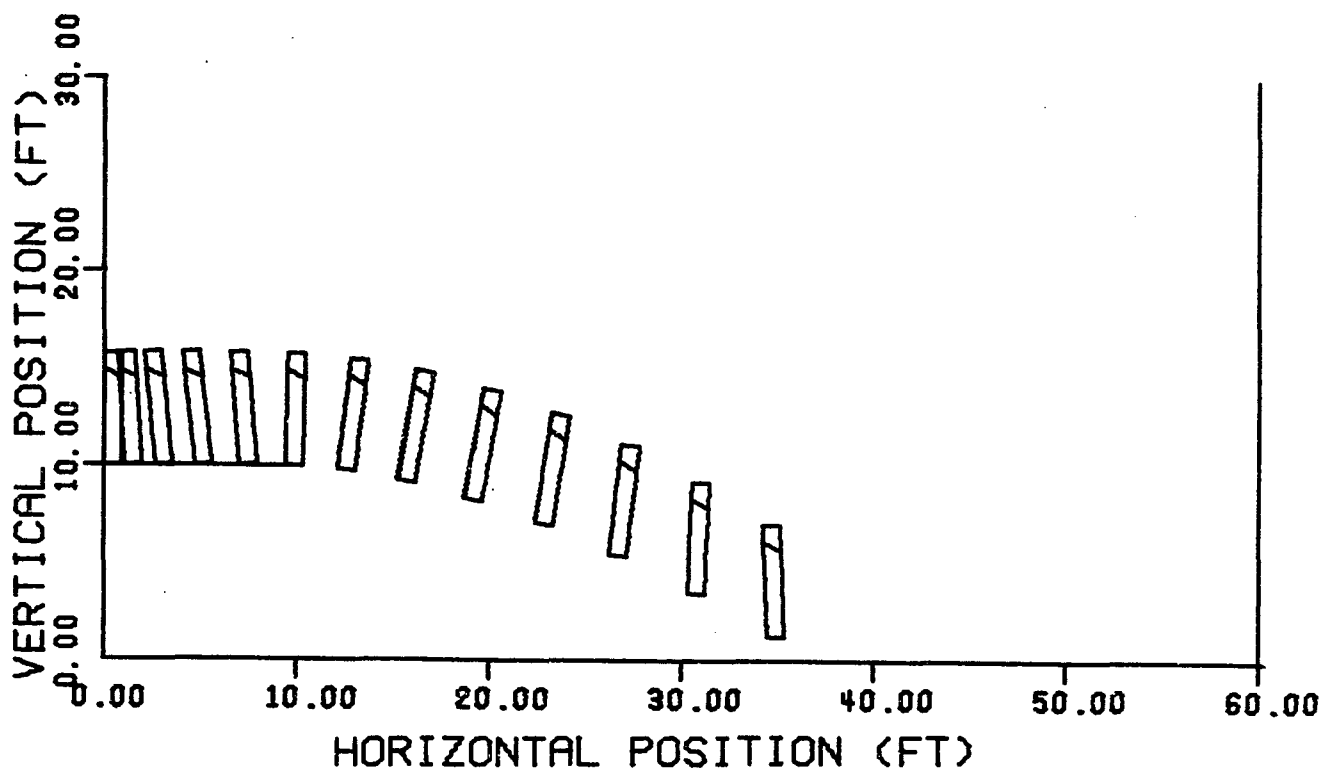
b) Free-Field Overpressure, 4 psi

Figure 9   Blast Trajectory of Simulated Man

39
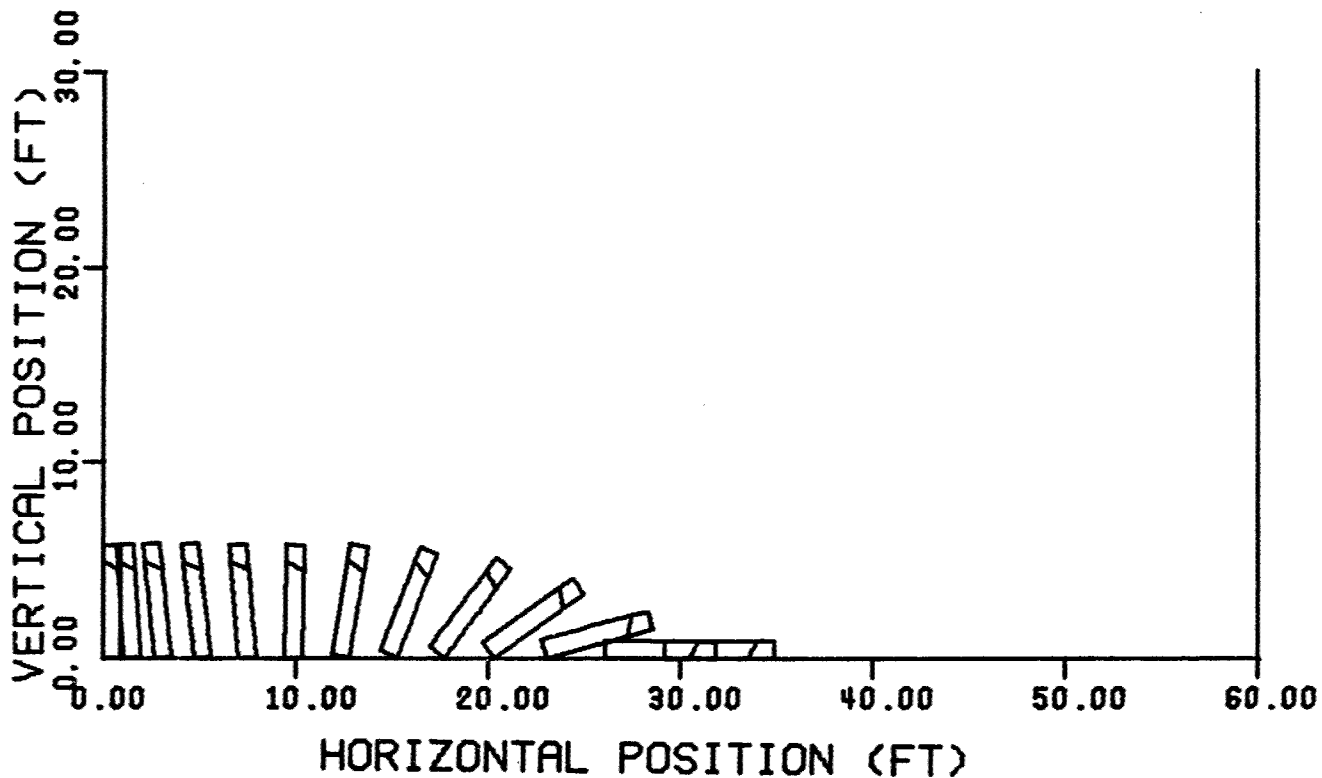
c) Free-Field Overpressure, 4 psi
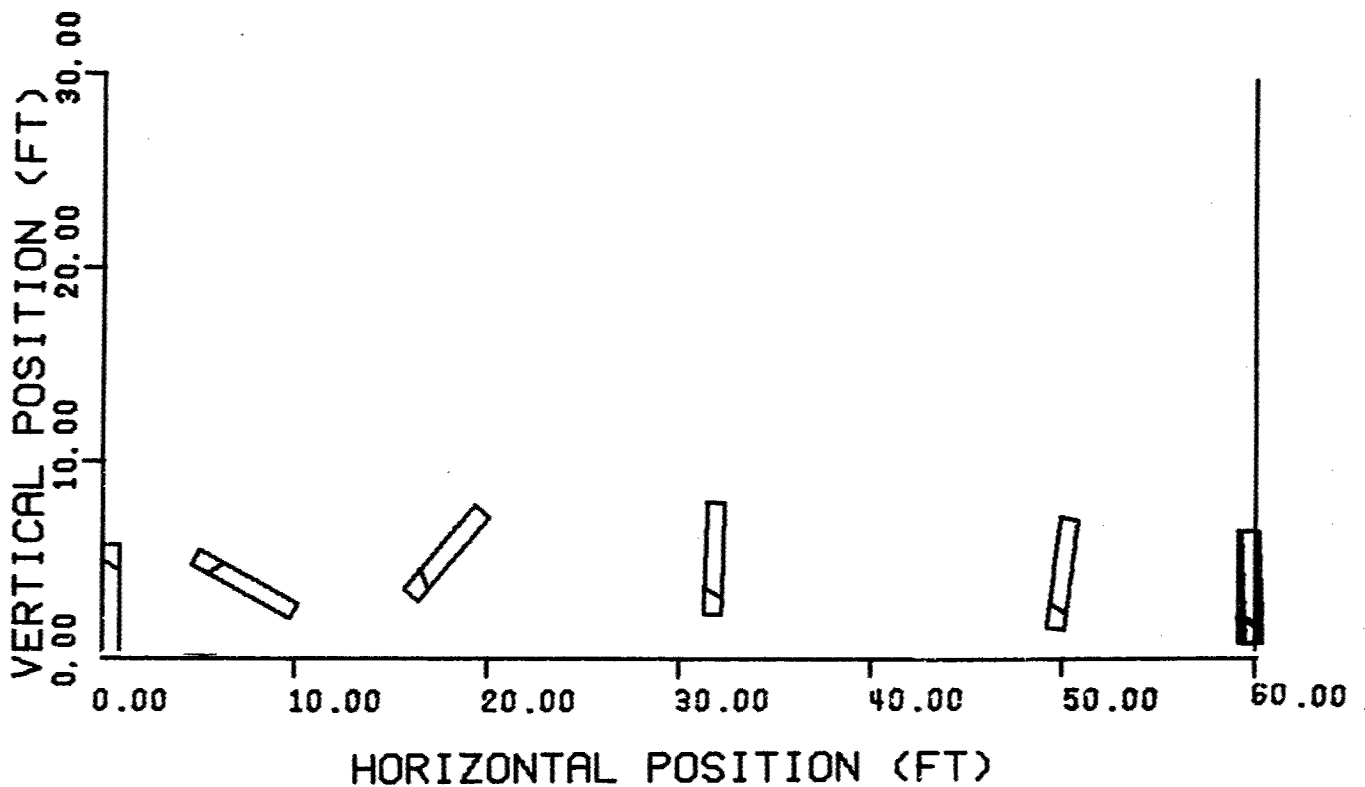
d) Free-Field Overpressure, 16 psi

Figure 9 Blast Trajectory of Simulated Man (Concl)

Weight   165   lb   ⎫
Height, H   5.77   ft   ⎪
Height to c.g., D_1 3.20   ft   ⎬ (see Figure 6)
            S_1 0.29   ft   ⎪
            S_2 0.625 ft   ⎭

Width (out of plane)   1.56   ft
Moment of inertia   8.58   (lb-sec^2-ft)

$K_\ell = 1.65 \times 10^5$ lb/ft ⎫ loading and unloading
$K_u = 1.65 \times 10^3$ lb/ft   ⎬ spring constants (see Figure 8(b)
                                 ⎭

μ = coefficient of friction = 0.25

2.10 ARTICULATED MAN SIMULATION MODEL

The articulated model was developed as a tool for evaluating
the effects of impact in a blast environment on a somewhat more
detailed level than is possible with the single, rigid block
model described previously. In this simulation, the individual
is modeled by means of seven elliptical cylinders interconnected
with six flexible joints as shown in Figure 10. Since only planar
motions are allowed, this results in 21 degrees of freedom. The
simulated man can contact three surfaces described by coordinates
X1,Y1,X2,Y2 in the fixed global coordinate system. Local coor-
dinate systems X(I), Y(I) are fixed along the principal axes of
each elliptical element. The two horizontal contact surfaces
represent the building floor and the ground surface. The vertical
surface represents a wall which has not yielded at the time contact
is made.

Forces acting on any element of the simulated man include
gravity, joint, contact, aerodynamic and pressure forces. The
gravity force is merely the weight of the element directed in
the global negative Y direction. Each element has springs resist-
ing motion in the local X(I) and Y(I) directions as well as tor-
sional springs resisting rotation at each joint associated with
the element. The total stiffness at a joint consists of a com-
bination of the stiffnesses associated with the two elements
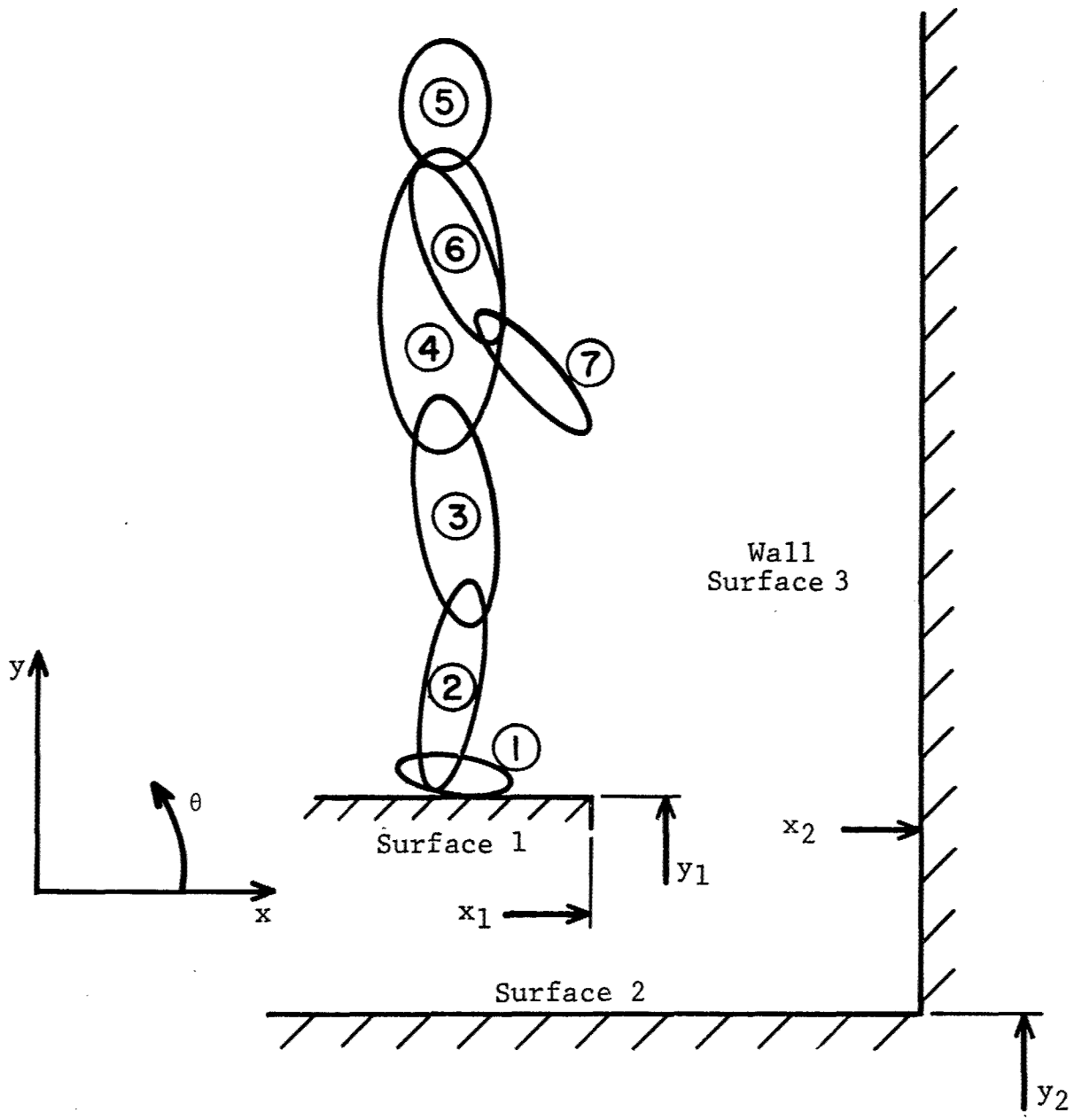
Figure 10   Articulated Man   Simulation Model

joined. Force-deflection characteristics of the springs are general piecewise linear functions.

Normal and frictional contact forces acting between an element and three possible contact surfaces are modeled as piecewise linear functions of the contact interference volume. They are assumed to act through the centroid of this volume. The contact interference volume is defined as the volume of an element that would extend beyond a contact surface if there were no deformation. Different functions are used for deformation and restoration.

Initial velocities can be applied to all or several components of the model. Aerodynamic forces are determined for each element using the following relationships:

$$D = q(t) A_d (\theta)$$

$$L = q(t) A_\ell (\theta)$$

(8)

where D is the drag force, L the lift force, q(t) is the dynamic pressure, and A_d, A_ℓ are the effective drag and lift areas respectively. These relationships are the same as those used with the single rigid block model except that A_d and A_ℓ are drag and lift areas of elliptic cylinders. The variation of A_d and A_ℓ with orientation is described using Equations (5) and (6), where θ is the angle from the direction of the relative blast wave velocity to the minor diameter of the particular elliptic element.

Physical data describing the size, weight and joint positions of the elliptical elements were obtained from Refs. 29, 30 and 31. These data correspond closely with the 50th percentile American male. Surface contact force and joint torsional spring data are approximately the same as those used in Ref. 31. Since a "hard-stop" was used at the ends of the range of normal motions of the joints in this reference, these torsional spring data were altered to approximate the large increase in the stiffness at these positions. Deflections in this range would ordinarily indicate injury, probably fatal in the case of the neck joints.

43

Figure 11 illustrates a typical result using this model. In this example, a standing individual at a large window (not shown), with his back to the direction of blast is subjected to overpressure at the range of 10 psi. A partial trajectory is given at increments of 0.1 sec. This figure also shows a piece of debris (modeled as an elliptical cylinder) which becomes separated from the upper portion of the front wall. This model considers the interaction of a single debris piece with the simulated man.

2.11 Summary, Conclusions and Recommendations

This chapter contains a review of the current state-of-the-art of impact injury assessment as this relates to people subjected to a blast environment produced by the detonation of nuclear weapons. Based on this review, casualty criteria previously compiled by White and his coworkers (Ref. 14) were verified and selected. These criteria were then extended (interpreted) as shown in Figures 4 and 5 for predicting the probability of injury and fatality for head and whole body impact.

Simulation models used for impact intensity prediction are also described. This includes the "rigid block" and the "articulated man" models. The rigid block model is a revised version of that previously reported in Ref. 16. The articulated man model was developed and verified mostly in the course of the effort reported herein.

Impact casualty criteria selected are fairly adequate for a gross, relative evaluation of casualties using the "rigid block" model since in using this model it is difficult to isolate and identify local impacts to the thorax, abdomen, upper and lower legs, upper and lower arms, neck etc. For a finer and a more realistic gradation of injuries a different simulation model and an additional set of casualty ranking criteria are required. The articulated man simulation model may be used for this purpose. Impacts to the various parts of the body may be evaluated using the "strain energy density" method considered by Krouskop and his

44
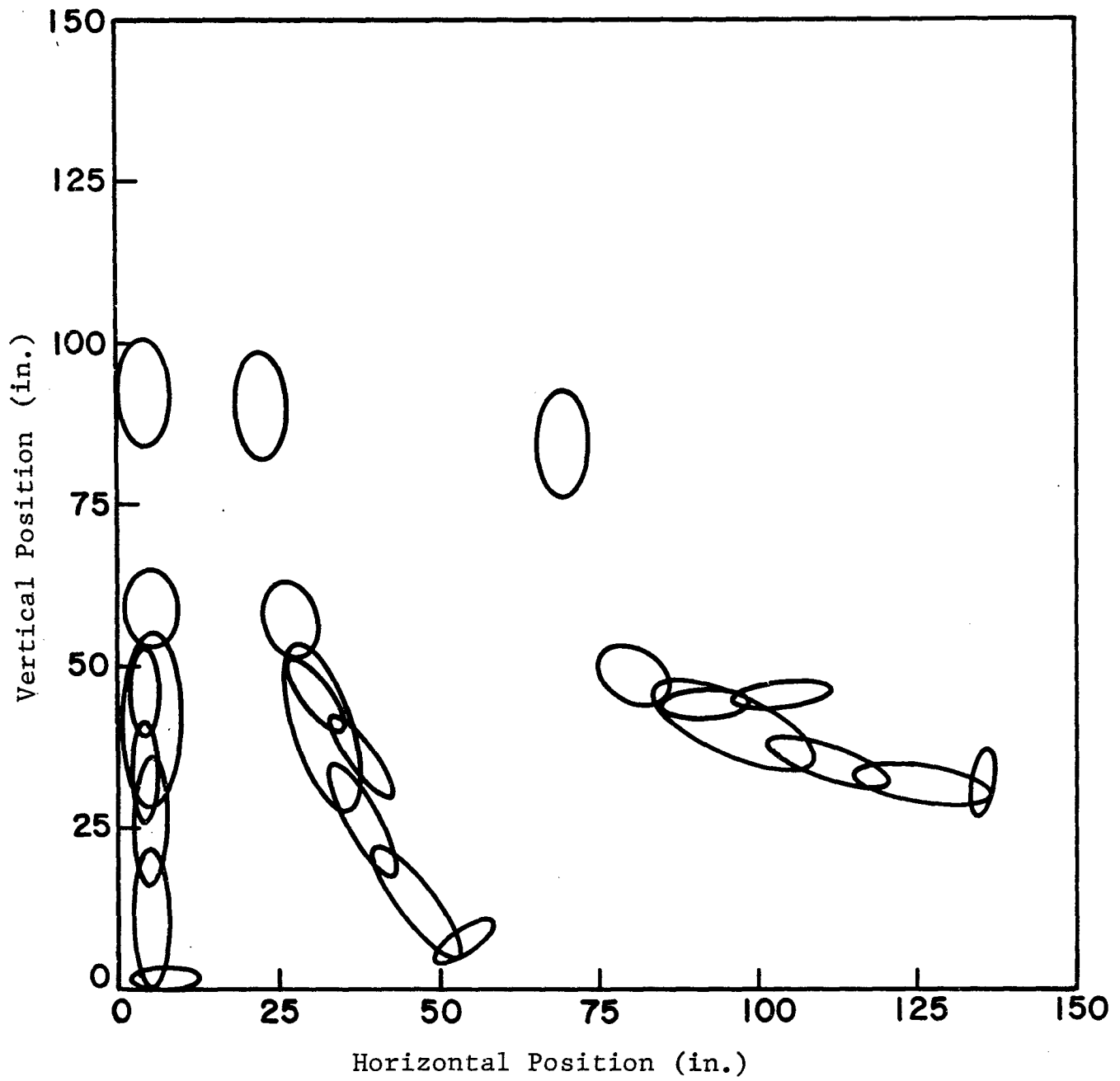
Figure 11 Blast Trajectory of Simulated Man

coworkers in Ref. 32. This method may be described as follows.

1. Determine accelerations, forces and stresses experienced by the various body segments (see Figures 10 and 11) and joints of the simulated person during motion and impact.

   The articulated man simulation model keeps track of the time-dependent joint forces and body segment accelerations as the man tumbles and articulates when driven by the blast winds. Contact forces produced at impact are also time-dependent and are computed using the "contact interference volume" approach. The influence of the impact force on the response of other body segments is also determined.

2. Calculate the strain energy in each body segment based on the information determined in the previous step.

   For a single member (such as the arm for example) subjected to a concentric axial impact load in the elastic range this is computed using the following equation - (Energy Density = $ED = \sigma^2/2E$), where σ is the stress and E the effective modulus of elasticity of tissue material.

3. Compare the ED values with casualty criteria to determine the level of casualty.

   Table 7 (Ref. 32) is a set of injury threshold indices for various parts of the body expressed in terms of energy density. They were apparently determined based on a review of recorded experiences and experiments such as were reviewed and discussed in this chapter. Trauma corresponding to the six categories of injury level are identified in Table 2.8. This table is based on the abbreviated injury scale discussed previously in section 2.7, Krouskop suggests that the highest injury level that occurs in a particular body area is assigned to the entire body area.

   The specific method (and data, Table 7) used by Krouskop is very crude and needs a great deal of work. However aside from Ref. 32, this is the first attempt to quantify injury categories comprising an injury scale (Table 8). It provides a start on the basis of which casualty evaluation criteria relative to a nuclear weapon environment can be built. We recommend that a reasonable version of this method be developed and used for civil defense purposes.

Table 7

INJURY THRESHOLD INDEX

Injury Level	Head	Thorax	Abdomen	Upper Arm	Lower Arm	Upper Leg	Lower Leg
No Injury	< 60	< 60	< 60	< 60	< 60	< 60	< 60
Minor (1)	> 60	> 60	> 60	> 60	> 60	> 60	> 60
Moderate (2)	>150	>200	>150	>150	>150	>150	>150
Severe (3)	>280	>350		>215	>215	>215	>215
Serious (4)	>400	>775		>725	>725	>725	>725
Critical (5)	>650	>1100		>1200	>1200	>1200	>1200
Fatal (6)	>800	>1700	>1150				

All values are reported in $\dfrac{in.-lbs}{in.^3}$

47

Table 8

TYPICAL INJURIES THAT CONSTITUTE THE INJURY LEVELS
DEFINED IN THE INJURY INDEX

Injury Index	Head	Thorax	Abdomen
1-Minor	Headache, Dizziness, Whiplash Complaint, Eye Abrasions, Fracture of Teeth	Muscle Ache, Bruises, Stiffness	Muscle Ache, Bruises
2-Moderate	Brief Unsonsciousness, Undisplaced Fractures of Head and Face, Severe Whiplash Complaint, Disfiguring Lacerations	Simple Fracture, Major Contusions	Major Contusions
3-Severe	Displaced Fractures, Extended Unconsciousness, Spinal Fracture, Loss of Eye	Multiple Fractures, Rupture of Diaphragm, Lung Contusion	Contusion of Organs, Bladder Rupture, Vertical Spinal Fracture
4-Serious	Unconscious over 15 min. with Abnormal Neurological Signs, Compound Skull Fracture	Open Chest Wounds	Internal Lacerations, Spinal Fracture with Paraplegia
5-Critical	Cerebral Injury with Unconsciousness over 24 hr., Cervical Spine Injury with Quadriplegia	Chest Injuries with Respiratory Embarrassment, Aortic Lacerations, Myocardial Rupture with Circulatory Embarassment	Rupture of Internal Organs
6-Fatal	Fatal Lesions	Fatal Lesions	Fatal Lesions

Table 8 (Concl)

Injury Index	Upper Arm	Lower Arm	Upper Leg	Lower Leg
0—No Injury	None	None	None	None
1—Minor	Muscle Ache, Sore Joints	Muscle Ache, Sore Joints, Broken Fingers	Muscle Ache, Sore Joints	Muscle Arch, Sore Joints, Broken Toes
2—Moderate	Major Sprain, Undisplaced Fractures	Major Sprain, Undisplaced Fractures, Compound Fractures of Fingers	Major Sprain, Undisplaced Fractures	Major Sprain, Undisplaced Fractures, Compound Fracture of Toes
3—Severe	Displaced or Open Simple Fractures, Dislocation of Major Joints	Displaced or Open Simple Fractures, Dislocation of Major Joints, Amputation of Fingers	Displaced or Open Simple Fractures, Dislocation of Major Joints	Displaced of Open Simple Fractures, Dislocation of Major Joints, Amputation of Toes
4—Serious	Multiple Fractures	Multiple Fractures	Multiple Fractures	Multiple Fractures
5—Critical	Amputation		Amputation	
6—Fatal				

CHAPTER 3

PEOPLE SURVIVABILITY IN CONVENTIONAL BASEMENTS

3.1 <u>INTRODUCTION</u>

This chapter contains the results of analyses that were per-
formed to gain a better understanding as to the levels of protec-
tion afforded by conventional basements against the effects of
blast produced by the detonation of megaton-range nuclear weapons.
Protection referred to depends on a number of parameters which
include:

1. <u>Type of overhead floor system</u> - this involves the
   design live load, span lengths, end conditions,
   material strengths and workmanship.

2. <u>Degree of basement exposure</u> - this can range from a
   subbasement with few protected apertures to a par-
   tial basement with one or several exposed basement
   walls and many large apertures.

3. <u>Design criteria and age of structure</u> - this refers
   to the specific design code provisions as to type of
   concrete, steel, the placement of reinforcement, de-
   tails, and the degree of deterioration at the footings
   and elsewhere experienced since construction.

In this chapter we consider basements of multistory buildings
with overhead floor systems at grade. The V/A (basement <u>v</u>olume
to entranceway <u>a</u>rea) ratio is large. These are large basements
with proportionally small entranceway areas. This precludes the
production of significant casualties by blast winds entering base-
ment areas through failed or open entranceways. The influence of
blast winds on survivability of people in basements is discussed
in Chapter 4. On this basis, the primary casualty mechanism con-
sidered is impact which is produced by spalled chunks of concrete
from the overhead slab and the collapse of the slab itself.

51

Two types of overhead floor systems were considered, i.e., one-way slabs (simply-supported and two-span continuous) and two-way slabs without beams,i.e.,flat plates and flat slabs. They were designed using current engineering practice and design criteria as stipulated in ACI 318-63 (Ref. 38). The following parameters were varied over what are considered as representative ranges, i.e.,design live load (50 to 250 psf), span length (12 to 28 ft), concrete strength (3 ksi and 4 ksi), steel strength (40 ksi and 60 ksi). This set of designs is considered as representative of the current inventory of existing basements.

The designed floor systems were subsequently analyzed to determine people survivability. Both injuries and fatalities were considered. Results obtained are presented in the form of percent survivors (injured and uninjured) as a function of free-field overpressure at the site for several body positions and distributions of people.

These results are useful in isolating the importance of various design parameters, body positions and distributions of people on survivability in a blast environment. They provide the basis for the ranking of basement shelters in fair detail when field data are known. When detailed field data are not available, these results may be used for assigning lower and upper bound survivability values to individual basements based on the knowledge of the overhead floor system. These results provide information on the capabilities of these categories of shelters relative to other potential candidates.

3.2 ONE-WAY SLAB DESIGN AND ANALYSIS RESULTS

3.2.1 Design

One-way reinforced concrete slabs considered here include two basic types, i.e., simple span simply supported and two-span continuous over a central support. The basic basement geometry associated with these slabs is illustrated in Figure 12. Design parameters considered were varied over the ranges as indicated on page 54.
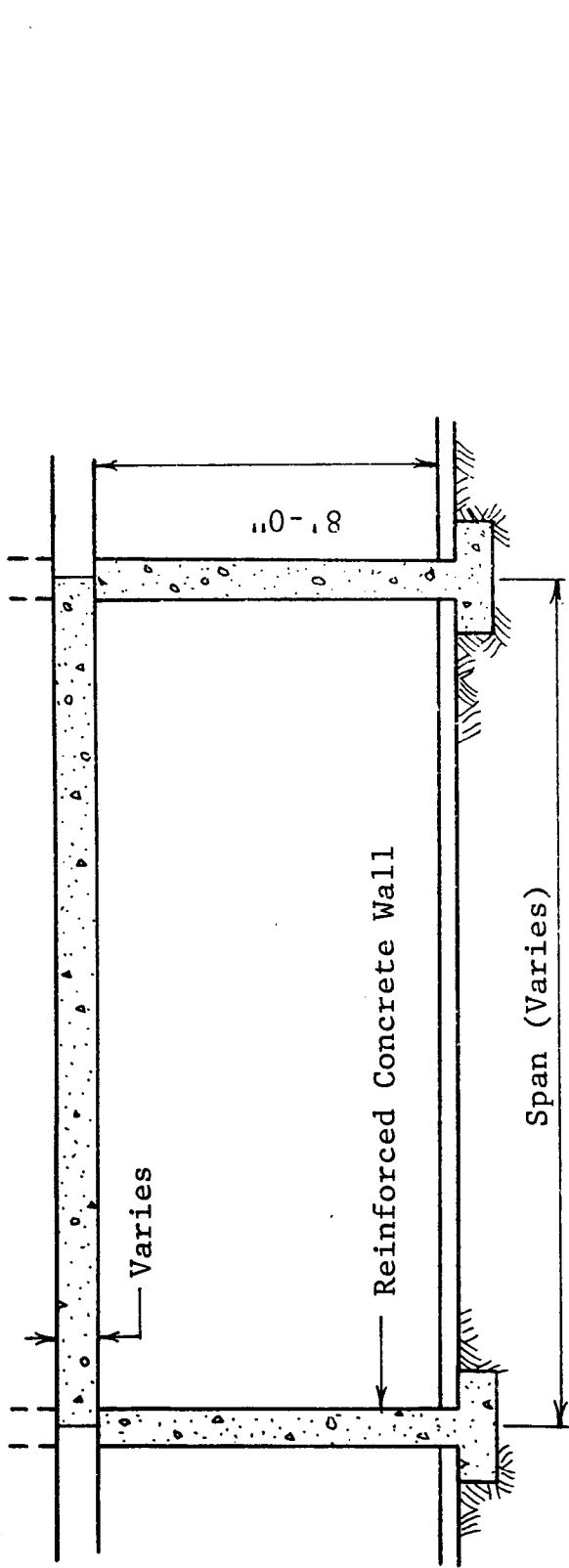
a) Simply Supported, One-Way Slabs
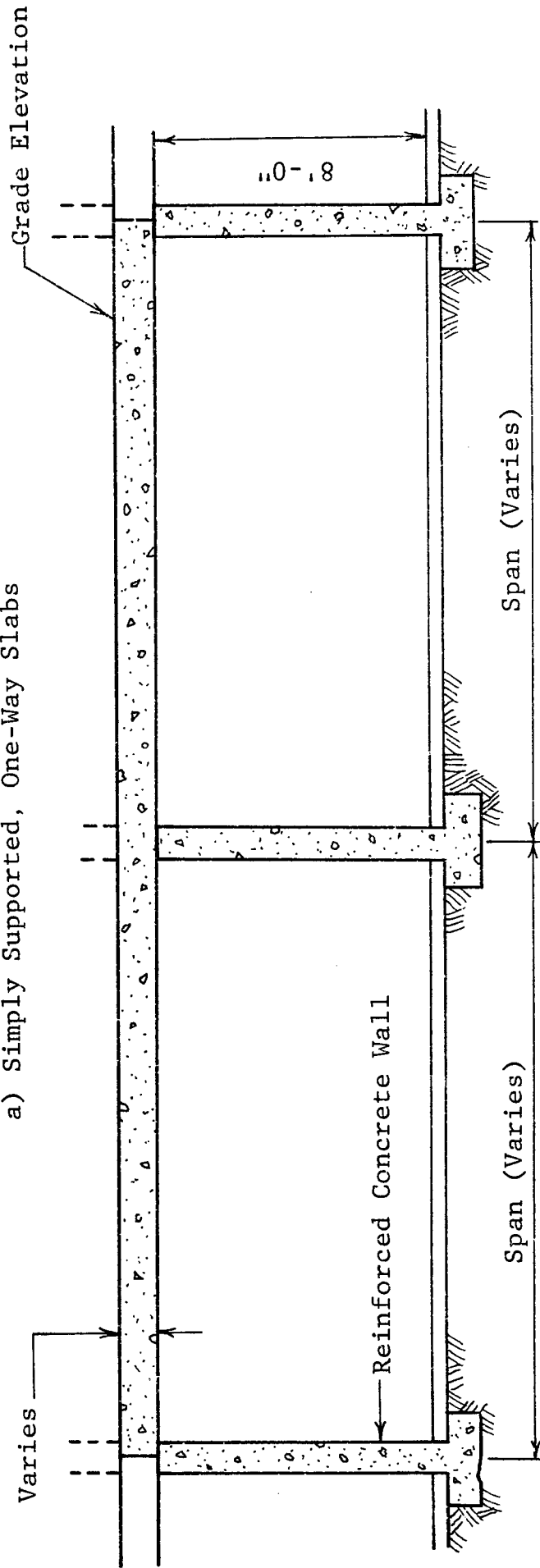
b) Two-Span Continuous, One-Way Slabs

Figure 12   Basic Basement Geometry for One-Way Slabs

53

Span length (simply supported)   - 12 ft, 16 ft, 20 ft

         (two-span continuous) - 16 ft, 20 ft, 24 ft, 28 ft

Design live load   - 50 psf, 80 psf, 125 psf, 250 psf

f'_c (ultimate compressive strength of concrete)   - 3 ksi, 4 ksi

f_y (yield strength of reinforcing steel)   - 40 ksi, 60 ksi

As indicated in Figure 12, a clear ceiling height of 8 ft was kept constant.

Slabs were designed using a procedure which utilizes the "Ultimate Strength Design" approach and satisfies the requirements of both the ACI 318-63 and ACI 318-71 "Building Code Requirements for Reinforced Concrete." To facilitate the design of these slabs, the procedure was programmed for electronic computation. For the purpose of illustrating the general procedure used in designing one-way slabs the design program for one-way simply-supported slabs is included in this section. This consists of a general flowchart (Figure 13), a program listing and a list of program variables (Table 9). The flowchart was simplified for illustration purposes and therefore does not include all of the logic indicated in the program listing.

3.2.2 Analysis

Slabs described in the previous section were analyzed with the object of identifying reasonable collapse mechanisms and determing corresponding collapse overpressures when subjected to the blast effects of a single, megaton-range nuclear weapon in its Mach region.

Collapse mechanisms were identified based on yield-line theory (Ref. 33), available experimental data (Refs. 34, 35, 36) 37) and engineering judgement. Based on this, it was assumed that the only reasonably admissable collapse mechanisms to consider are those shown in Figure 14.

54
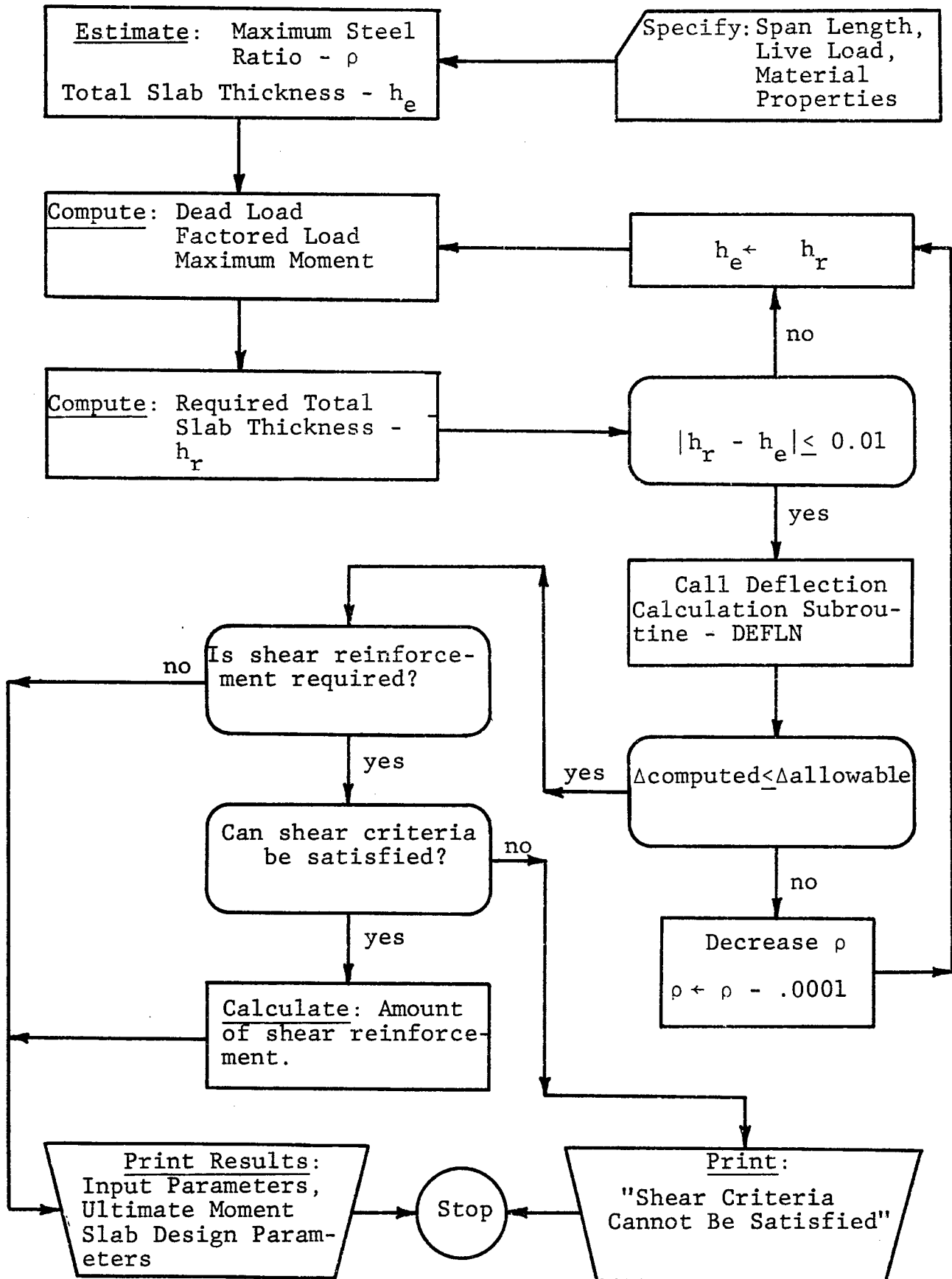
Figure 13   Flowchart for One-Way Slab Design Procedure

55

LISTING OF DESIGN PROGRAM FOR ONE-WAY
SIMPLY-SUPPORTED CONCRETE SLABS

```
C    THIS PROGRAM DESIGNS ONE-WAY SIMPLY-SUPPORTED REINFORCED
C      CONCRETE SLABS USING ACI 318-71 AND ALSO SATISFIES ACI 318-63.
C      DYNAMIC BLAST FAILURE OVERPRESSURES ARE ALSO CALCULATED.
C
       DIMENSION XLIVE(10)
       XLIVE(1)=50.0
       XLIVE(2)=80.0
       XLIVE(3)=125.0
       XLIVE(4)=250.0
C*****READ STEEL STRENGTH
     2 READ(5,1) FY
     1 FORMAT(F10.0)
C*****SET CONCRETE STRENGTH
       DO 100 KK=3000,4000,1000
       FC=KK
C*****PRINT  HEADING AND VALUES
       WRITE(6,3) FC,FY
     3 FORMAT('1********************************',/,' CONCRETE COMPRESSIVE
      *STRENGTH =',F10.3,' PSI',/,' STEEL YIELD STRENGTH =',9X,F10.3,
      +' PSI',///)
C*****MODULUS OF ELASTICITY
       ES=29000000.
       EC=150.**1.5*33.*FC**.5
       N=ES/EC
       XN=N
C*****CRACKING STRENGTH
       FR=7.5*FC**.5
C*****CONCRETE SHEAR STRENGTH
       VC=2.*FC**.5
C*****SIZE OF STRESS BLOCK
       B1=.85
       IF(FC.GT.4000.) B1=.85-.05/1000.*(FC-4000.)
C*****RHO BALANCED
       ROB=(.85*B1*FC/FY)*(87000./(87000.+FY))
C*****INCREMENT LIVE LOAD
       DO 101 LL=1,4
       WL=XLIVE(LL)
C*****WRITE HEADINGS
       WRITE(6,70) WL
    70 FORMAT(//,' LIVE LOAD =',F10.3,' PSF',//)
       WRITE(6,99)
    99 FORMAT (                          ' SPAN      MU(FT*LB)      D(IN)       H(
      *IN)',7X,  'AS(IN*IN/FT)',26X,'IE(IN**4)',6X,'P1(PSI)',8X,'P2(PSI)'
      *,///)
C*****INCREMENT SPAN LENGTH
       DO 15 L=12,20,2
       XL=L
    60 J=0
```

```
C*****ESTIMATE DEAD LOAD, REDUCE LIVE LOAD IF CRITERIA MET AND CALCULATE
C      FACTORED LOADS.
       RO=.75*ROB
       OW=RO*FY/FC
       H=XL*12./20.
       AREA=XL*XL
       WL1=WL
     7 WD=H*150./12.
       IF(AREA.LT.150.0.OR.WL1.GT.100.0) GO TO 501
       R=AREA*.0008
       WL=(1-R)*WL1
       RMAX1=.23*(1+WD/WL1)
       IF(R.LT.RMAX1.AND.R.LT.0.60) GO TO 501
       IF(RMAX1-.60) 502,502,503
   502 WL=(1-RMAX1)*WL1
       GO TO 501
   503 WL=.40*WL1
   501 CONTINUE
       WU=1.4*WD+1.7*WL
C*****CALCULATE MAX MOMENT AND DEPTH REQUIRED
       XMU=WU*XL*XL/8.
    54 D=SQRT(XMU/(.9*FC*OW*(1.-.59*OW)))
       XH=D+1.
C*****CHECK IF CALCULATED DEPTH AND ESTIMATED DEPTH ARE CLOSE ENOUGH.
C      IF THEY ARE, GO CHECK DEFLECTION.  IF THEY ARE NOT, GO AND
C      ITERATE AGAIN WITH THE CALCULATED VALUE AS THE ESTIMATE OF DEPTH.
       IF(ABS(XH-H)-.01) 8,8,9
     9 H=XH
       GO TO 7
C*****CHECK DEFLECTION CRITERIA.  IF NOT MET REDUCE RHO TO INCREASE DEPTH
C      AND THEN GO TO BEGINNING OF DESIGN PROCESS.
     8 AS=RO*12.*D
       CALL DEFLN(EC,FR,XN,XL,WD,WL,XH,D,AS,J)
       IF(J-1) 11,13,13
    11 RO =RO-.0001
       OW=RO*FY/FC
       H=XH
       GO TO 7
    13 AMIN=.0018*12.*XH
C*****CHECK MINIMUM STEEL AREA
       IF(AS.LT.AMIN) AS=AMIN
C*****EFFECTIVE MOMENT OF INERTIA
    12 XIE=.5*12.*D**3*(5.5*AS/(12.*D)+.083)
C*****CALL DYNAM TO CALCULATE DYNAMIC FAILURE OVERPRESSURES
       CALL DYNAM(XMU,XL,WD,XIE,EC,AS,D,FC,S1,S2,S3,P1,P2)
C*****WRITE SOME OF RESULTS
       WRITE(6,81)  XL,XMU,D,XH,AS,XIE,P1,P2
    81 FORMAT(1X,F4.1,F13.1,3X,F6.2,F10.2,F15.3,25X,F12.1,6X,F10.4,5X,
      *F10.4)
```

```
C*****CALCULATE MAX SHEAR STRESS, CALCULATE AMOUNT OF SHEAR REINFORCEMENT
C     REQUIRED AND ALSO CHECK IF SHEAR CRITERIA CAN BE SATISFIED.
      VU=WU*XL/2.-WU*D/12.
      SVU=VU/(.85*12.*D)
      SD=SVU-VC
      IF(SD) 20,20,21
   20 S=0.
      GO TO 30
   21 IF(SD-4.*FC**.5) 4,4,5
    4 S=.5*D
      GO TO 30
    5 IF(SD-8.*FC**.5) 40,40,50
   40 S=.25*D
      GO TO 30
C*****PRINT 'SHEAR CRITERIA CAN NOT BE SATISFIED'
   50 WRITE(6,51)
   51 FORMAT(55X,'SHEAR DESIGN CRITERIA NOT SATISFIED')
      GO TO 16
   30 AV=SD*12.*S/FY
C*****PRINT SHEAR AREA
      WRITE(6,25) AV
   25 FORMAT(55X,'AV=',F8.3,' IN*IN/FT')
C*****PRINT SLAB DISTANCES WHEN IT IS IN ITS FAILED POSITION
   16 WRITE(6,17) S1,S2,S3
   17 FORMAT( 90X,'S1 =',F5.2,3X,'S2 =',F5.2,3X,'S3 =',F5.2)
   15 CONTINUE
  101 CONTINUE
  100 CONTINUE
      GO TO 2
      END
```

```
      SUBROUTINE DEFLN(EC,FR,XN,XL,WD,WL,XH,D,AS,J)
C*****SUBROUTINE DEFLN CHECKS SLAB DEFLECTIONS AGAINST ALLOWABLE
C     DEFLECTIONS USING CODE REQUIREMENTS.  J=1 MEANS CRITERIA SATISFIED.
      XIG=XH**3
      C=XN*AS/12.*(SQRT(1.+2.*12.*D/(XN*AS))-1.)
      XIC=(12.*C**3)/3.+XN*AS*(D-C)**2
      XML=WL*XL*XL*12./8.
      XMAD=WD*XL*XL*12./8.
      XMADL=XMAD+.5*XML
      XMA=XMAD+XML
      XMCR=FR*XIG*2./XH
      XID=((XMCR/XMAD)**3)*XIG+(1.-(XMCR/XMAD)**3)*XIC
      XIDL=((XMCR/XMADL)**3)*XIG+(1.-(XMCR/XMADL)**3)*XIC
      XI=((XMCR/XMA)**3)*XIG+(1.-(XMCR/XMA)**3)*XIC
      IF(XMCR/XMAD.GT.1.) XID=XIG
      IF(XMCR/XMADL.GT.1.)XIDL=XIG
      IF(XMCR/XMA.GT.1.) XI=XIG
      DE=5.*(XL*12.)**2/(48.*EC)
      DL=DE*XML/XI
      DD=DE*XMAD/XID
      DLS=DE*.5*XML/XIDL
      DEF=DL+2.*DD+1.4*DLS
      IF(DL.LT.XL*12./360..AND.DEF.LT.XL*12./480.) J=1
      RETURN
      END
```

```
      SUBROUTINE DYNAN(XMU,XL,WD,XIE,EC,AS,D,FC,S1,S2,S3,P1,P2)
C*****SUBROUTINE DYNAM CALCULATES SLAB DYNAMIC FAILURE OVERPRESSURES AND
C     PERTINENT DIMENSIONS OF THE SLAB IN ITS FAILED POSITION.
      XK1=384.*EC*XIE/(5.*(XL*12.)**3)
      DMU=1.25/.9*XMU
      RY1=8.*DMU/XL
      RL1=RY1-WD*XL
      YE1=RY1/(XK1*12.)
      RU=AS/(12.*D)
      U1=.1/RU
      IF(U1.GT.30.) U1=30.
      YF1=U1*YE1
      FAC=1.-1./(2.*U1)
      P1=RL1*FAC/XL
      RY2=2.*RY1
      RL2=RY2-WD*XL/2.
      P2=RL2*FAC/(XL/2.)
      ALPHA=ACOS(8./XL)
      BETA=ATAN(YF1/(XL/2.))
      THETA=ALPHA-BETA
      SH=SQRT(YF1**2+(XL/2.)**2)
      S2=SH*SIN(THETA)
      S1=SH*COS(2.*BETA)
      PHI=3.1416/2.-ALPHA-BETA
      S3=S2-(SH-SH*COS(PHI))
      V1=.39*RL1+.11*P1*XL+WD*XL/2.
      V2=.39*RL2+.11*P2*XL/2.+WD*XL/4.
      DVC=2.*(1.25*FC)**.5
      DVU=12.*D*DVC
      IF(V1.GT.DVU) P1=0.
      IF(V2.GT.DVU) P2=0.
      P1=P1/144.
      P2=P2/144.
      RETURN
      END
```

60

Table 9

PROGRAM VARIABLES

FC	$= f'_c$	Concrete compressive strength, psi
FY	$= f_y$	Yield strength of reinforcing steel, psi
ES	$= E_s$	Modulus of elasticity for reinforcing steel, psi
EC	$= E_c$	Modulus of elasticity for concrete, psi
	E_c	$= w^{1.5} (33) \sqrt{f'_c}$ (ACI 318-71; 8.3.1)
	w	= Weight of concrete, lb/cu ft
N	$= n$	$= $ Modular ratio $= E_s/E_c$
FR	$= f_r$	= Modulus of rupture of concrete $= 7.5 \sqrt{f'_c}$, psi
VC	$= v_c$	= Nominal permissable shear stress carried by concrete, psi (ACI 318-71; 11.4)
ROB	$= \rho_b$	= Reinforcement ratio producing balanced condition (ACI 318-71; 10.3.3)
XL	$= \ell$	= Slab span length, ft
WL	$= W_\ell$	= Design live load, psf
RO	$= \rho$	= Ratio of tension reinforcement $= As/bd$
	b	= unit width of slab, in.
	d	= effective depth of slab, in.
XH	$= h$	= total depth of beam or slab section (h = d + 1), in.
WD	$= W_d$	= Design dead load, psf
WV	$= V$	= Factored design load = 1.4D + 1.7L, psf
	D	= Dead load, psf
XLIVE(I)	$= L$	= Live load, psf
XMV	$= M_v$	= Factored design load bending moment, ft-lb

Table 9 (Contd)

H	= h	=	Minimum allowable total depth of slab, in. (ACI 318-71; Table 9.5(a))
D	= d	=	Effective depth of slab, in.
AS	= A_s	=	Area of tension reinforcement, sq in.
AMIN	= $A_{s(min)}$	=	Minimum area of tension reinforcement
		=	0.0018bh (ACI 318-71; 7.13)
VU	= V_v	=	Total applied design shear force at section, lb
SVU	= u_v	=	Nominal total design shear stress, psi (ACI 318-71; 11.2.1)
S	= s	=	Shear reinforcement spacing in a direction parallel to the longitudinal reinforcement, in. (ACI 318-71; 11.1.4b)
AV	= A_v	=	Area of shear reinforcement, sq in.
XIG	= I_g	=	Gross moment of inertia of concrete section neglecting reinforcement, in.^{4}
C	= kd	=	Depth of uncracked section, in.
XIC	= I_{cr}	=	Moment of inertia of cracked, transformed section, in.^{4}
XMAD	= M_{ad}	=	Maximum dead load moment, in.-lb
XMADL	= M_{adl}	=	Maximum dead load plus 50% live load moment, in-lb
XML	= M_{al}	=	Maximum live load moment, in.-lb
XMRC	= M_{cr}	=	Cracking moment, in.-lb (ACI 318-71; 9.5.2.2)
XID	= I_{ed}	=	Effective moment of inertia for dead load deflection calculation, in.^{4}
XIDL	= $I_{ed\ell/2}$	=	Effective moment of inertia for immediate 50% live load deflection calculation, in.^{4}
XI	= $I_{ed\ell}$	=	Effective moment of inertia for immediate total live load deflection calculation, in.^{4}

Table 9 (Concl)

DL	$= \Delta_L$	= Immediate live load deflection, in.
DD	$= \Delta_D$	= Immediate dead load deflection, in.
DLS	$= \Delta_{LS}$	= Immediate 50% live load deflection, in.
DEF	$= \Delta_{LT}$	= Long term deflection $= \Delta_L + 2\Delta_D + 1.4\Delta_{LS}$
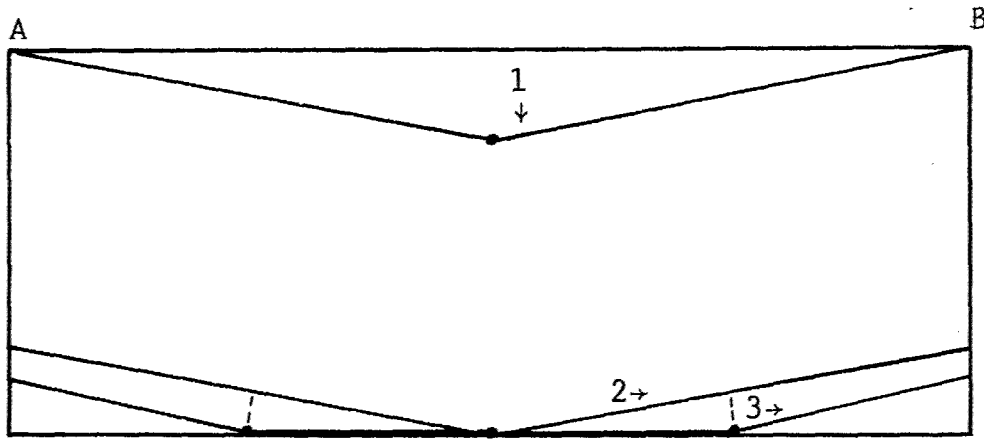
a) Symmetric Collapse Mode for Simply-Supported Slab
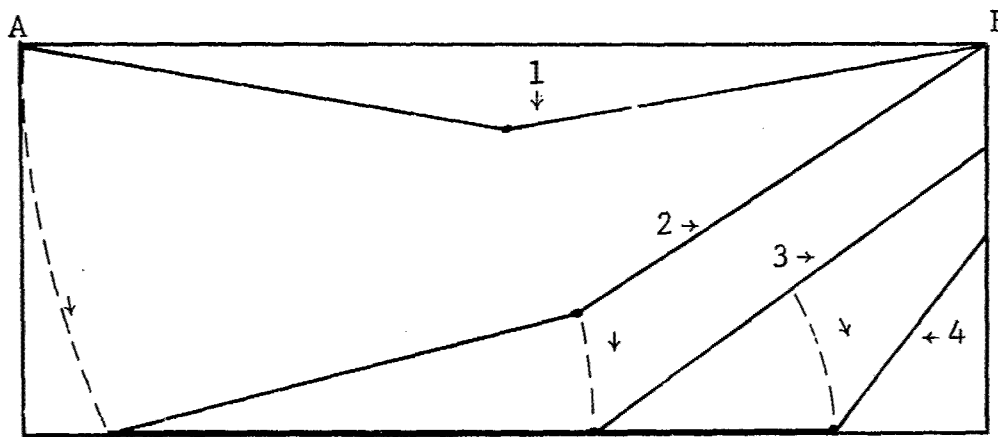
b) Unsymmetric Collapse Mode for Simply-Supported Slab
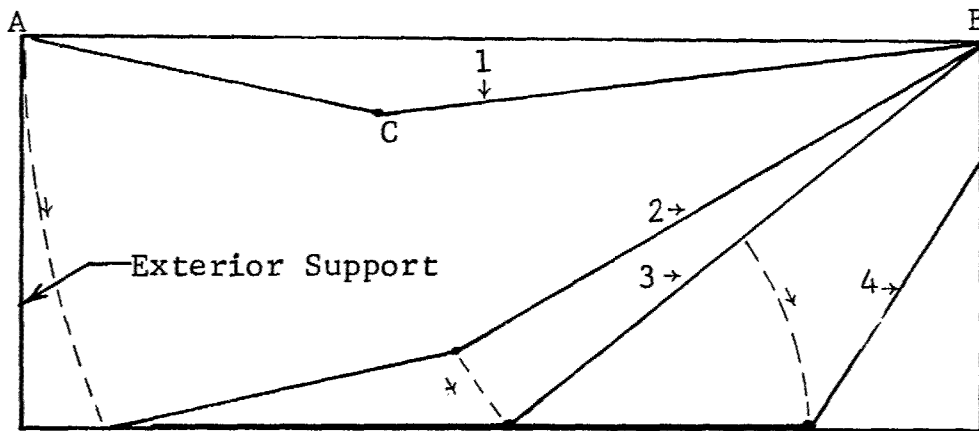
c) Collapse Mode for Two-Span Continuous Slab

Figure 14   Assumed Collapse Modes for One-Way Slabs

Experience and theory indicate that a uniform, simply-supported one-way slab subjected to a uniformly applied dynamic load of sufficiently high magnitude will develop a plastic hinge at midspan (the point of maximum moment). This produces an unstable condition resulting in collapse. A symmetric collapse mode is expected under symmetric and uniform conditions. However, since conditions are not expected to be ideally uniform in every case an unsymmetric mode is also considered. It is included as a reasonable alternate to account for the possibly significant movement of individual supports (basement walls) during the blast loading process and other variations producing unsymmetric response.

Since the likelihood of these collapse modes is not known, it is reasonable to assume that each of the three is equally likely. Assumptions described have some experimental basis. For example, in Ref. 35 approximately one-half of the symmetrically designed supported and loaded slabs experienced unsymmetric collapse.

After the slab has experienced its yield moment at overpressure Pl or higher (see position 1 in Figure 14 (a) and (b)), the subsequent symmetric and unsymmetric assumed modes of collapse are described as follows.

The symmetric collapse (Figure 14(a)) is followed by a stable postfailure position 2. At sufficiently high overpressures (P2 or higher) this is followed by failure and collapse of the half-spans resulting in postfailure position 3.

The unsymmetric collapse (Figure 14(b)) is assumed to include three events.

  a. Rotation of span about support point A or B resulting in unstable position 2.

  b. Further rotation and sliding resulting in stable position 3.

  c. Failure and collapse of half-span due to overpressure P2 or higher, resulting in postfailure position 4.

65

Only one collapse mode is assumed for the two-span continuous slab and is illustrated in Figure 14(c). After the slab has experienced overpressures of P1 or higher, it becomes a mechanism, i.e., plastic hinges have been formed at points C and B and the slab collapses. It is assumed to pull off support A, rotate about support B into unstable position 2 and further into stable position 3. If exposed to overpressures of P2 or higher, the propped part of the slab is assumed to form a plastic hinge at midspan, break loose at support B and then rotate and slide into postfailure position 4.

The structural analysis of the slabs was performed using blast-load design-analysis procedures of the type described in Chapters 7 and 8 of Ref. 38.

To facilitate the analysis, a small computer program was prepared which, in addition to computing the P1 and P2 values, also determined floor areas affected by the collapse of slabs based on assumptions described previously in this section.

Results are given in Table A.1, which is included in the Appendix. This includes all pertinent design parameters and peak overpressures (P1, P2) of long duration required to produce failure.

3.3 TWO-WAY SLAB DESIGN AND ANALYSIS RESULTS

3.3.1 Design

Typical square, interior panels (see Figure 15) were designed in accordance with ACI 318-63 (Ref. 39). The designs meet the requirements of Chapter 21, "Flat Slabs with Square or Rectangular Panels" and either Chapters 10 to 12 of Part IV-A, "Structural Analysis and Proportioning of Members - Working Stress Design," or Chapters 15 to 17 of Part IV-B, "Structural Analysis and Proportioning of Members - Ultimate Strength Design."

The design criteria were based on minimum volume of concrete through the use of minimum slab thickness and minimum column dimensions. These criteria were assumed to yield a reasonable-cost structure if not the least-cost structure, which would be dependent on actual construction costs at the time of construction.

66

L

L

Column Capital

Drop Panel

(a) Flat-Slab Floor

L

t

CAP

D

t_d

L

L

t
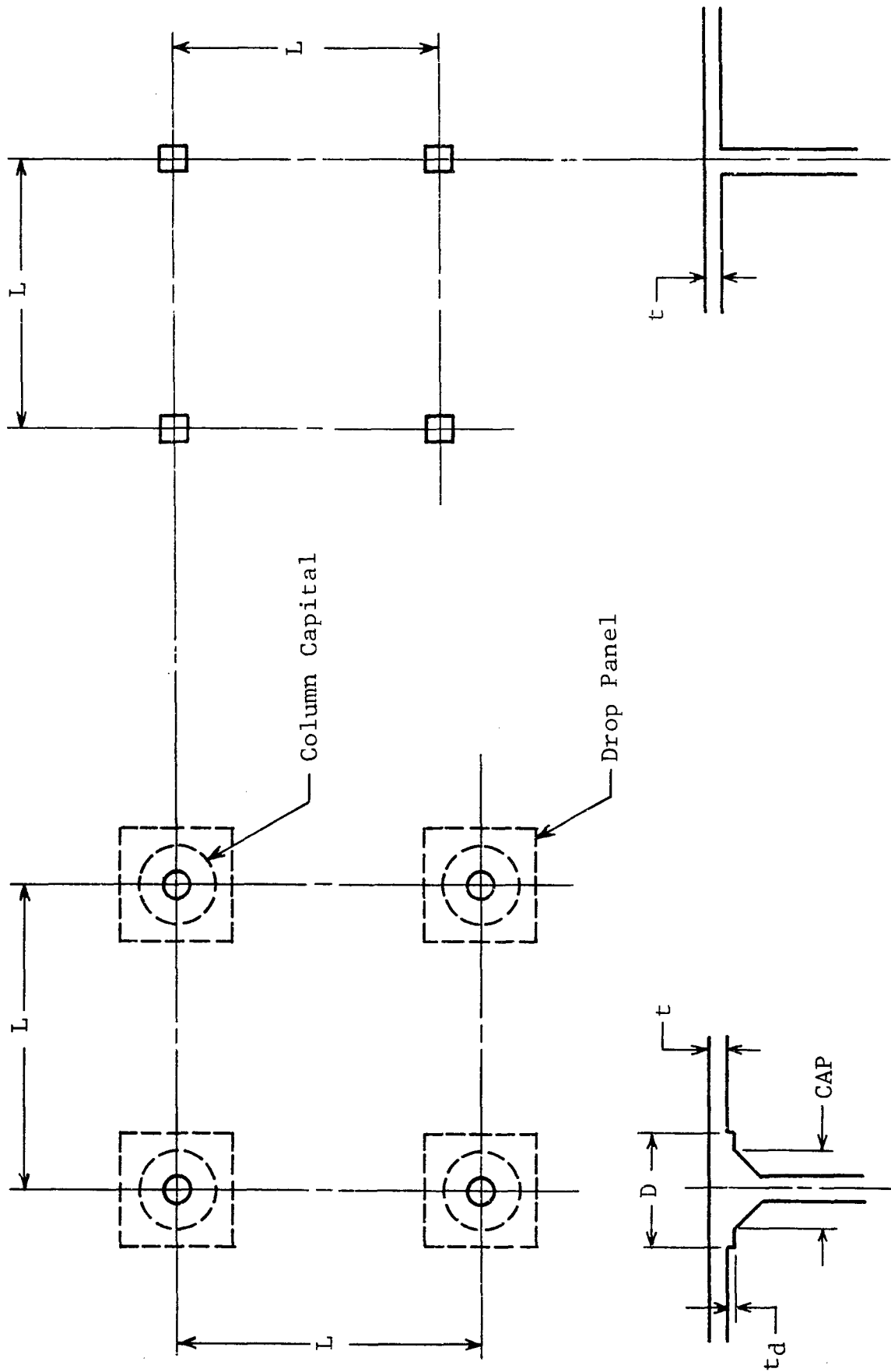
(b) Flat-Plate Floor

Figure 15   Flat-Slab, Flat-Plate Construction and Nomenclature

3.3.1.1 Design Parameters

Various combinations of the span length of the flat slab panel (center to center of supports), L, and uniformly distributed, nominal live load, W, were considered for flat slabs (plates) without drop panels, for flat slabs with drop panels, and for flat slabs with drop panels and column capitals. All combinations of L = 16, 20, 24, and 28 ft and W = 50, 80, 125, and 250 psf were considered for one or more types of flat slab. A matrix of design parameters used is given in Table 10. Story height, H, was assumed to be 12 ft.

The design load acting on the slab was assumed to be the nominal live load reduced in accordance with American Standard Building Code Requirements for Minimum Design Loads, A58.1-1955 (Ref. 40) for live loads less than 100 psf and surface area greater than 150 sq ft (Section 3.5.2), and the dead load consisting of the slab weight based on a unit weight of 150 pcf and an additional dead load of 10 psf. This combination of service loads was used in the working stress designs, and a combination of factored live and dead loads was used for the ultimate strength design.

Representative material strengths were considered. Compressive strengths of concrete, f'_c, were either 3,000 or 4,000 psi. Yield strengths of the steel reinforcement were either 40,000 or 60,000 psi.

Representative sizes of reinforcing bars and drop panel dimensions were obtained from the CRSI DESIGN HANDBOOK (Refs. 41, 42), Chapter 8 of the "Working Stress Design Manual," and Chapter 12 of the "Ultimate Strength Design Manual." These values were used since many structural engineers utilize the CRSI handbook for initial design configuration.

3.3.1.2 Design Process - Working Stress Design

Each design required several iterations to obtain the final design dimensions and slab weight that satisfied the ACI 318-63 requirements. The empirical method of Section 2104 of ACI 318-63 was used to obtain design moments rather than an elastic analysis.

68

Table 10

MATRIX OF TWO-WAY SLAB DESIGN PARAMETERS

Span / Live Load	16 ft	20 ft	24 ft	28 ft
50 psf	FP WSD	FP WSD	FP WSD	CAPS USD
80 psf	FS WSD	FS WSD	FS WSD	CAPS USD
125 psf	FS WSD	FS WSD	FS WSD	--
125 psf	FS USD	FS USD	FS USD	--
125 psf	CAPS USD	CAPS USD	CAPS USD	CAPS USD
250 psf	CAPS USD	CAPS USD	CAPS USD	CAPS USD

Notation: FP   - Flat plate
           FS   - Flat slab with drop panel and no capital
           CAPS - Flat slab with drop panel and capital
           WSD - Working stress design
           USD - Ultimate strength design

The slab thickness, t, at the center of the slab for slabs without drop panels must be at least 1/36, but not less than 5 in. nor

$$0.028L \left(1 - \frac{2c}{3L}\right) \sqrt{\frac{w'}{f_c'/2000}} + 1\ 1/2 \qquad (9)$$

where

    c = effective support size (column capital diameter
        or column dimension for no capital)

and

    w'= the uniformly distributed unit dead and live
        loads (Section 2104 (d) Slab Thickness).

For slabs with drop panels whose length is at least one-third the span length and whose projection below the slab is at least one-fourth the slab thickness, the slab thickness must be at least L/40 but not less than 4 in. nor

$$0.024L \left(1 - \frac{2c}{3L}\right) \sqrt{\frac{w'}{f_c'\ 2000}} + 1. \qquad (10)$$

The minimun column dimension shall not be less than 10 in. and must also provide a moment of inertia, I_c, of the gross concrete section not less than 1000 in.^{4} or less than

$$I_c = \frac{t^3 H}{0.5 + \frac{W_D}{W_L}} \qquad (11)$$

where W_D and W_L are the total dead and live loads on the panel respectively (Section 2104(b) Columns). Moment redistribution for smaller columns has not been considered.

    The first design step was to determine minimum slab thickness, minimum effective support size, and drop panel dimensions, when required, to satisfy the above requirements and to calculate the corresponding slab weight.

The <u>second design step</u> was to check the shearing stress on the section located a distance $d/2$ out from the periphery of the column, where d is the effective depth, the distance from the extreme compression fiber to the centroid of tension steel, in accordance with Section 1207 - Shear Stress in Slabs and Footings. If the nominal shear stress exceeds $2\sqrt{f'_c}$, the thickness at the critical section and/or the effective support size, c, must be increased until the nominal shear stress is below the allowable stress.

The <u>third design step</u> was to determine the numerical sum of the positive and negative bending moments in one direction of the panel, M_O. From Section 2104(f) - Bending Moment Coefficient

$$M_O = 0.09WLF(1 - \frac{2c}{3L})^2 \qquad (12)$$

where

W = total dead and live load on the panel

and

$$F = 1.15 - \frac{c}{L}, \text{ but not less than } 1.0. \qquad (13)$$

The <u>fourth design step</u> was to distribute the sum of the bending moments, M_O, among the critical positive and negative sections of the column and middle strips based on the percentages of Table 2104(f) for interior panels.

The <u>fifth design step</u> was to determine the effective depth, d, at each critical section and to calculate the required area of tension steel, A_t, to meet the requirements of Chapter 11 - Flexural Computations - Working Stress Design.

Minimum reinforcement cover of 3/4 in. was assumed for each design. Drop panel weight was included to determine an average uniformly distributed slab weight.

3.3.1.3 Design Process - Ultimate Strength Design

The working stress design process was modified for the ultimate strength design to meet the special ACI 318-63 requirements for ultimate strength design of flat slabs (Section 2101(e) Ultimate Strength Design).

The minimum slab thickness was a function of steel yield strength as shown in Table 2101(e) - Minimum Slab Thickness. The numerical sum of the positive and negative bending moments, M_o, was increased to

$$M_o = 0.10WLF(1 - \frac{2c}{3L})^2,\tag{14}$$

where

W is the factored load.

The <u>first design step</u> for ultimate strength design was to determine the minimum dimensions as in the working stress design. The increasing slab thickness with increased yield stress requirement of Table 2101(e) was incorporated into this step.

The <u>second design step</u> was to check the ultimate shear stress on the same critical section in accordance with Section 1707 - Shear Stress in Slabs and Footings.

The <u>third design step</u> was to determine

$$M_o = 0.10WLF(1 - \frac{2c}{3L})^2,\tag{15}$$

and the <u>fourth design step</u> was to again redistribute the bending moment, M_o, in accordance with Table 2104(f).

The <u>fifth design step</u> was to determine the effective depth at each critical section and to calculate the area of tension steel, A_s, required to meet provisions of Chapter 16 - Flexural Computations - Ultimate Strength Design.

3.3.2 Analysis

Two-way slabs described in the previous section were analyzed with the object of determining collapse overpressures when subjected to the blast effects of a single, megaton-range nuclear weapon in its Mach region.

Theory and experimental data indicate that two-way slabs of the type considered in this study will fail either in flexure (with yield lines forming along the lines of maximum moment) or in shear due to punching at the columns (Ref. 43). Flexural failure is the likely failure mechanism for flat slabs with column capitals while shear failure is the likely failure mechanism for flat plates.

Overpressures producing flexural or shear failure were determined using procedures of the type described in Chapters 7 and 8 of Ref. 38 or Chapter 7 of Ref. 44. Failure criteria used herein are described in the following paragraphs.

For the purpose of determining the number of survivors, two levels of slab failure are considered, i.e., incipient collapse and ultimate collapse. Loads producing incipient failure (collapse) are defined herein as the minimum values of flexural or shear resistance of the slab. Assumed failure mechanisms are shown in Figures 16 and 17. For incipient collapse, flexural failure is assumed to be controlled by a limiting ductility ratio characterized by the following deflection (see pp 7-8, Ref. 38):

$$y_f = \frac{0.10}{p} y_{el} \leq 30 \; y_{el} \tag{16}$$

Here, p is the reinforcement ratio at the center of the middle strip and y_{el} is the limiting elastic deflection. Shear failure is assumed to occur if the maximum calculated unit shear is larger than the ultimate (v_u) as specified in Chapter 17, Section 1707 of the ACI Building Code (Ref. 39). In computing v_u, the ultimate compressive strength of concrete is increased by 25 percent (Chapter 6, Ref. 39) to approximately account for the strain rate under dynamic loading.

73

Flexural failure as defined implies significant cracking and deformation of the concrete. However, in the majority of cases the slab is expected to remain suspended from its original supports. Shear failure used herein is based on a criterion which considers the strength of concrete but not steel. When failing in shear the slab is expected to undergo significant cracking, but is also expected to remain suspended in the majority of cases. Blast overpressure levels corresponding to incipient collapse identify a limiting condition on massive structural failure, and therefore a limiting condition on people survivability against the effects of building debris. For overpressures up to the one producing incipient collapse, the majority of shelter occupants are expected to be survivors relative to this casualty mechanism.

Blast overpressures producing ultimate collapse are used to determine the lower bound on survivability, i.e., blast overpressures at which no survivors are expected. Criteria used in estimating this condition are discussed next.

Assumed ultimate collapse mechanisms for flat slab-flat plate systems are illustrated in Figures 16 and 17 for initial flexural and shear failure respectively. In the case of initial flexural failure, the cone formed around each column (See Figure 16) increases due to excessive cracking and spalling of concrete. Only the bent bars are assumed to support the cracked slab, and collapse occurs when their ultimate tensile strength is reached. A similar collapse mechanism is assumed for the slab, which initially fails in shear (See Figure 17). The ultimate tensile strength of bent reinforcement was increased 25 percent to account for the strain rate and decreased 10 percent to account for the probable loss of strength due to the initial yielding.

Results are given in Table A.3 which is included in the Appendix. This includes all design and analysis data for each two-way slab considered in this effort.

74
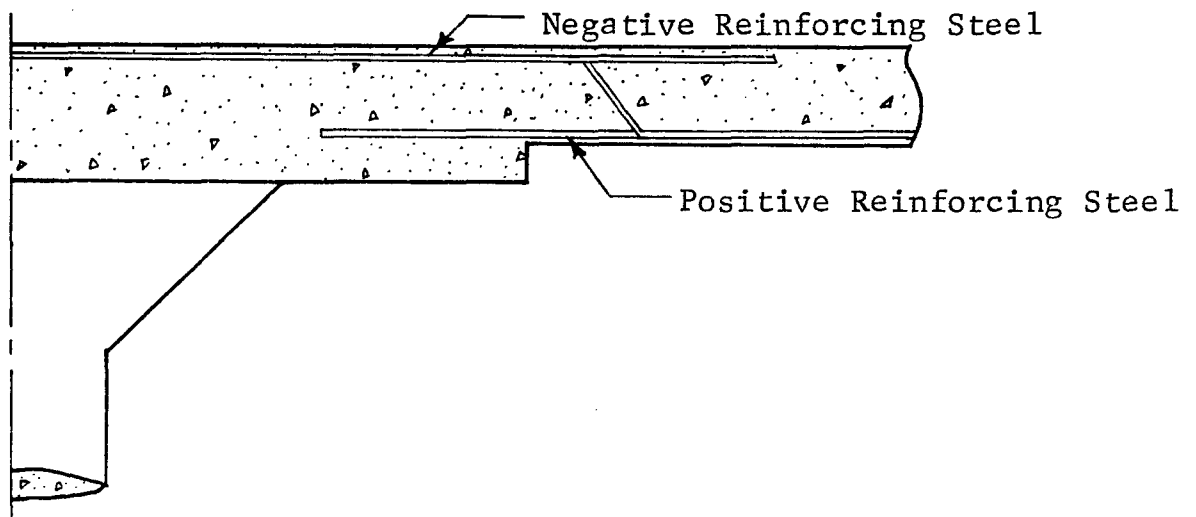
a) Initial Slab Configuration
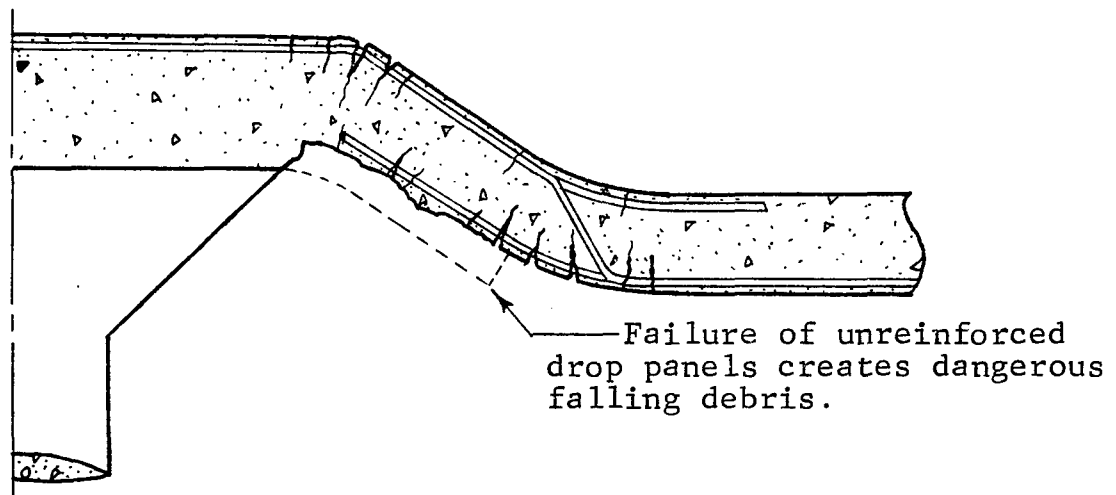
b) Flexural Failure of Concrete
   at Incipient Collapse
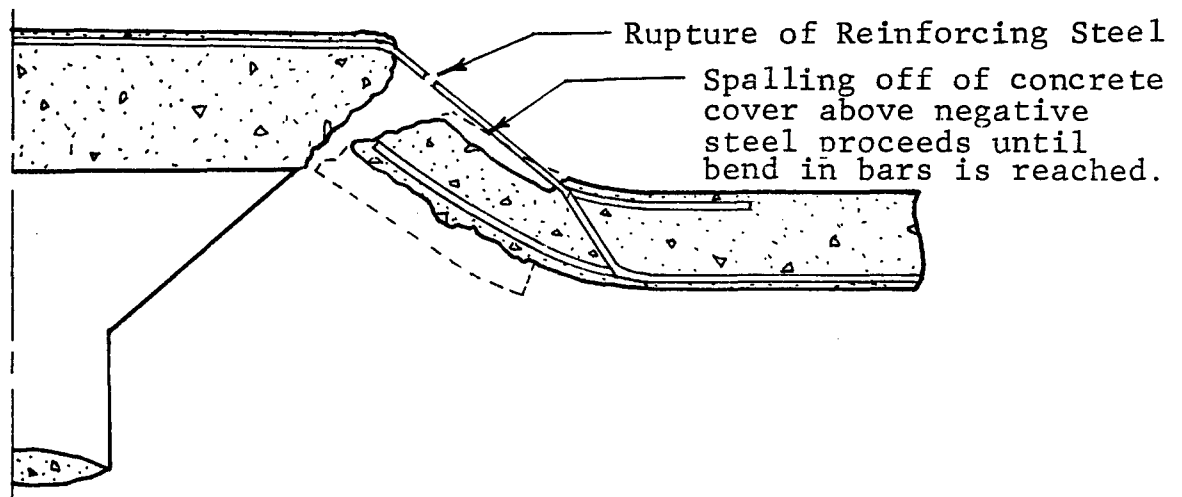
c) Rupture of Reinforcing Steel Leading to
   Ultimate Collapse of the Slab

Figure 16   Flexural Failure Mechanism
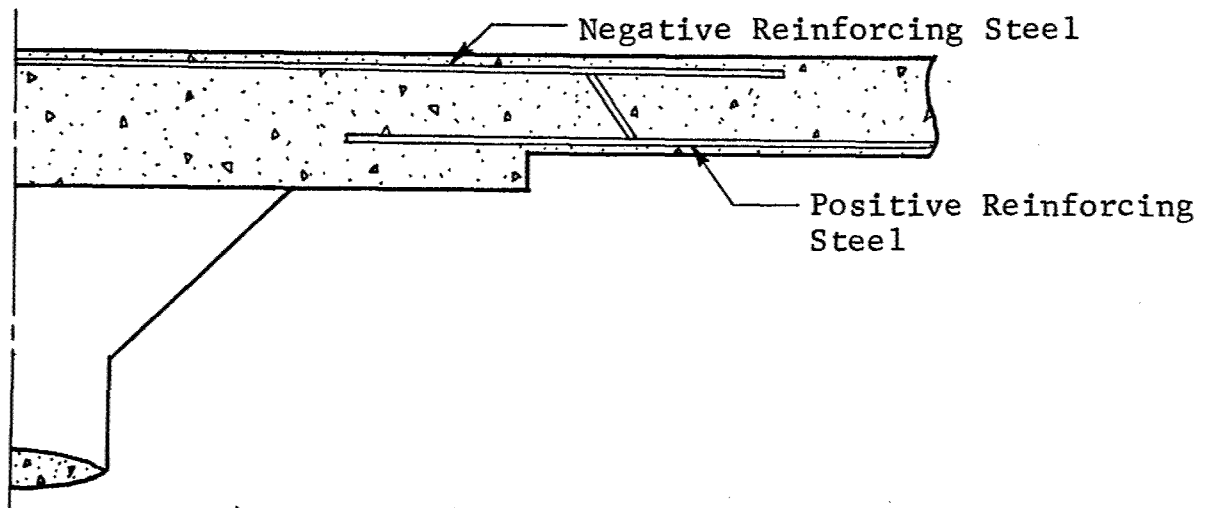
a) Initial Slab Configuration
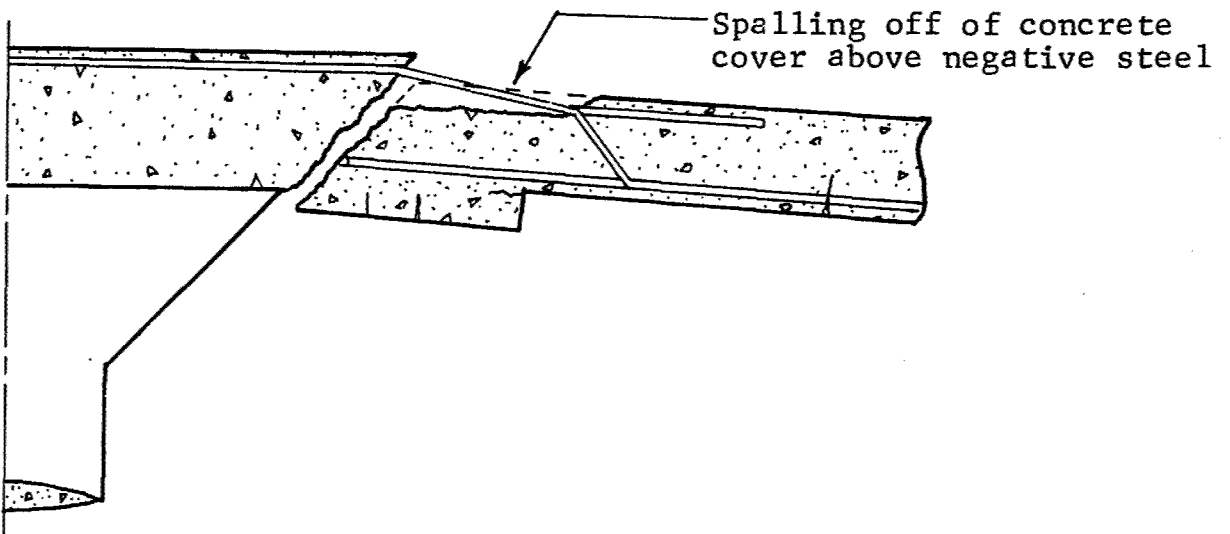
b) Shear Failure of Concrete at Incipient Collapse
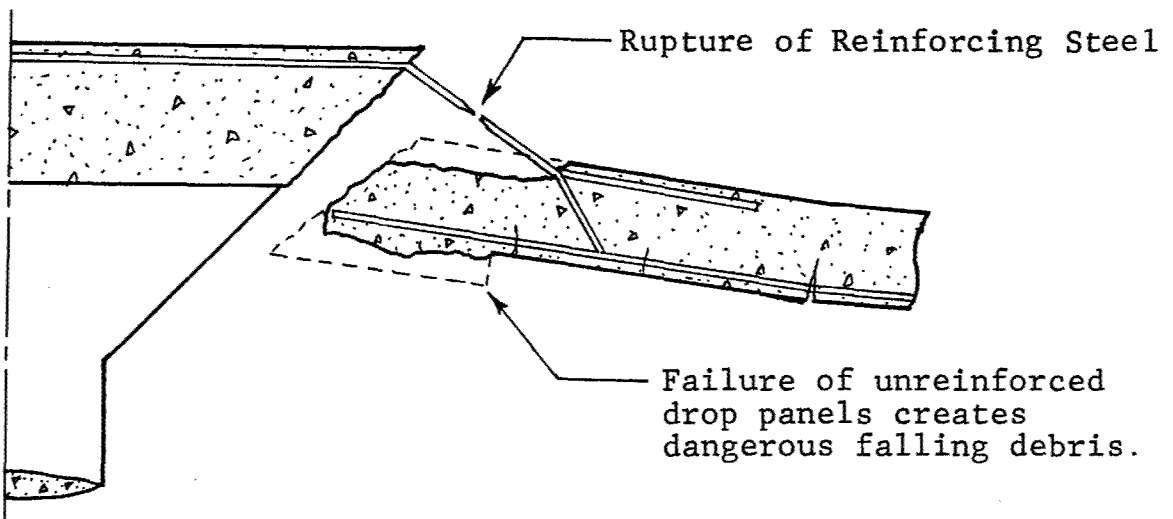
c) Rupture of Reinforcing Steel Leading to
   Ultimate Collapse of the Slab

Figure 17   Shear Failure Mechanism

3.4 INJURY AND FATALITY ESTIMATES (ONE-WAY SLABS)

3.4.1 Body Positions and Distribution of People

Five basic body positions and distributions were assumed as shown in Figure 18. They are: (1) standing, (2) sitting, (3) prone and perpendicular to the wall with head toward the wall, (4) prone and perpendicular to the wall with head away from the wall, and (5) prone and parallel to the wall.

These body positions were selected to gauge the relative effectiveness of one over the other assuming that such positions are strictly adhered to by shelter occupants. In cases where specific body positions are not strictly adhered to, random distributions of shelter occupants will exist. To consider such situations, two additional distributions of people were selected and are illustrated in Figure 19. In both cases people are assumed to be prone; (a) is the assumed random distribution along peripheral walls, and (b) is the assumed random distribution over the entire floor area. In summary, seven body positions and distributions of people were considered for basements having one-way reinforced concrete overhead floor systems. These are tabulated as follows (see Figure 18 and 19).

1. Standing along support walls

2. Sitting along support walls

3. Prone, perpendicular to the support wall with head away from the wall

4. Prone, perpendicular to the support wall with head toward the wall

5. Prone, parallel to the support walls

6. Random distribution of prone people along support walls only

7. Random distribution of prone people over the entire floor area
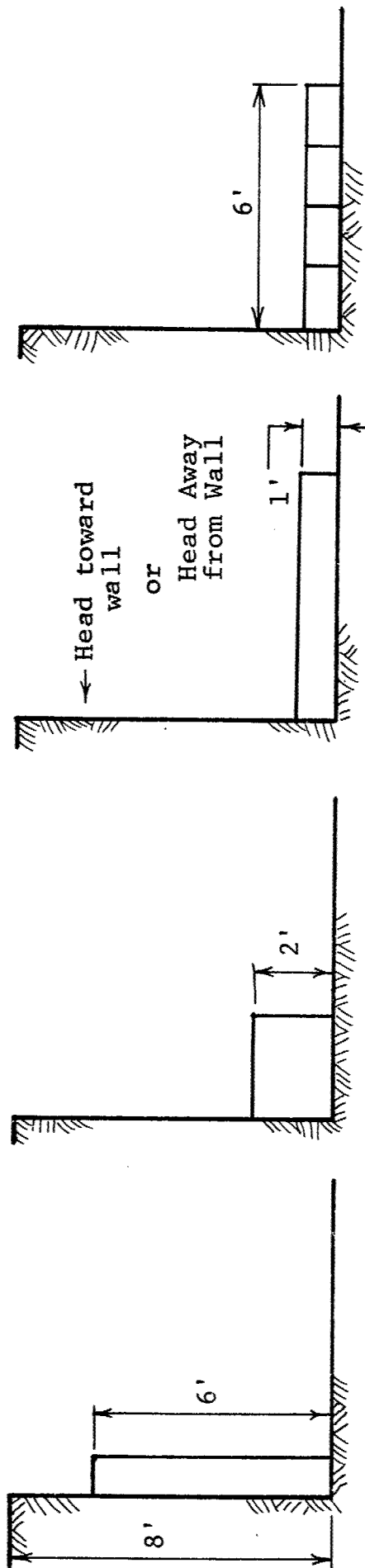
a) Elevation View

b) Plan View

Head toward wall

or

Head Away from Wall

6'

1'

2'

6'

8'

Prone, Parallel to Support Wall

Prone, Perpendicular to Support Wall

Sitting

Standing

6'

6'

2.5'

1'
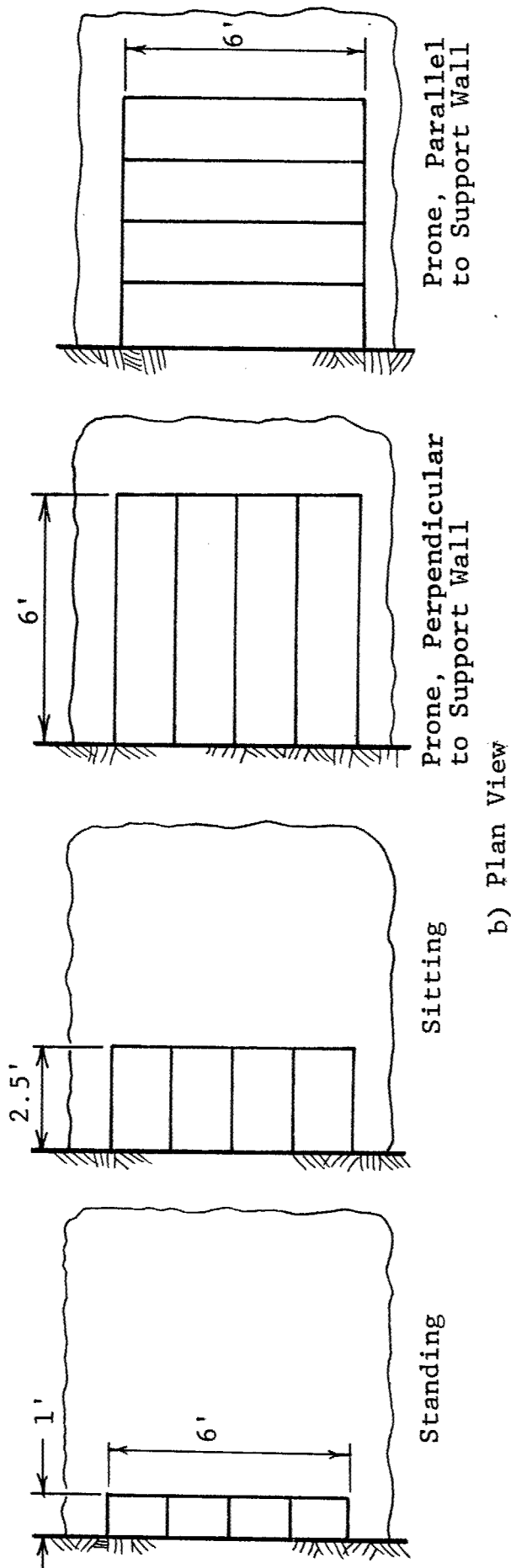
Figure 18   Body Positions for Personnel in Basements

X marks
location
of head
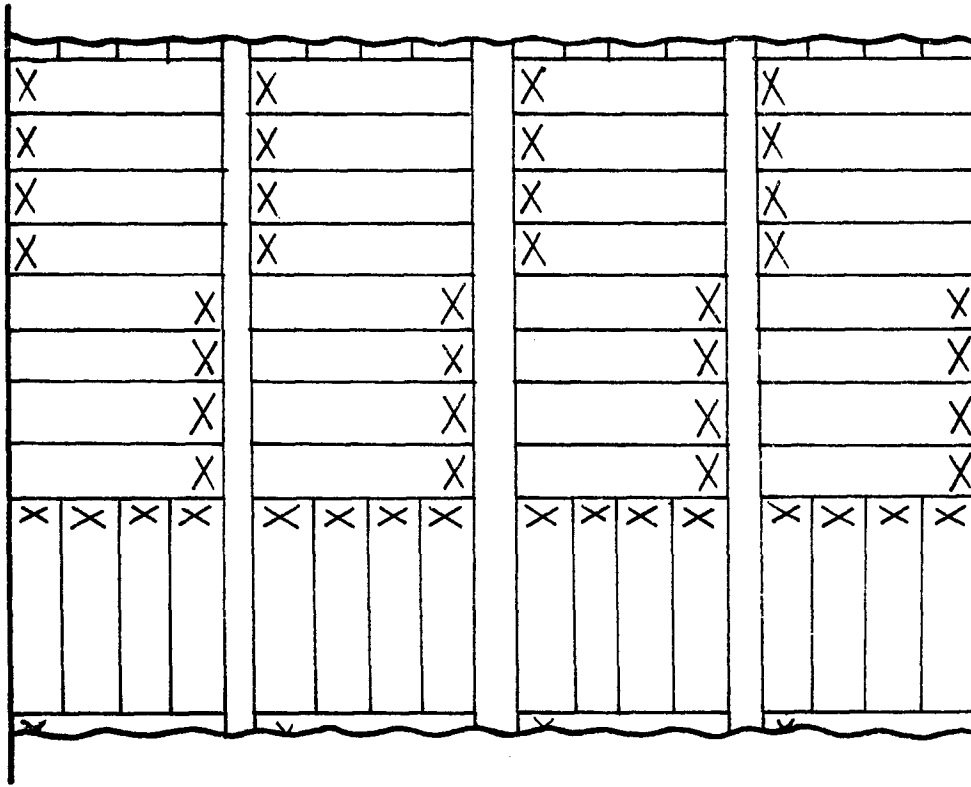
b) Uniformly Distributed
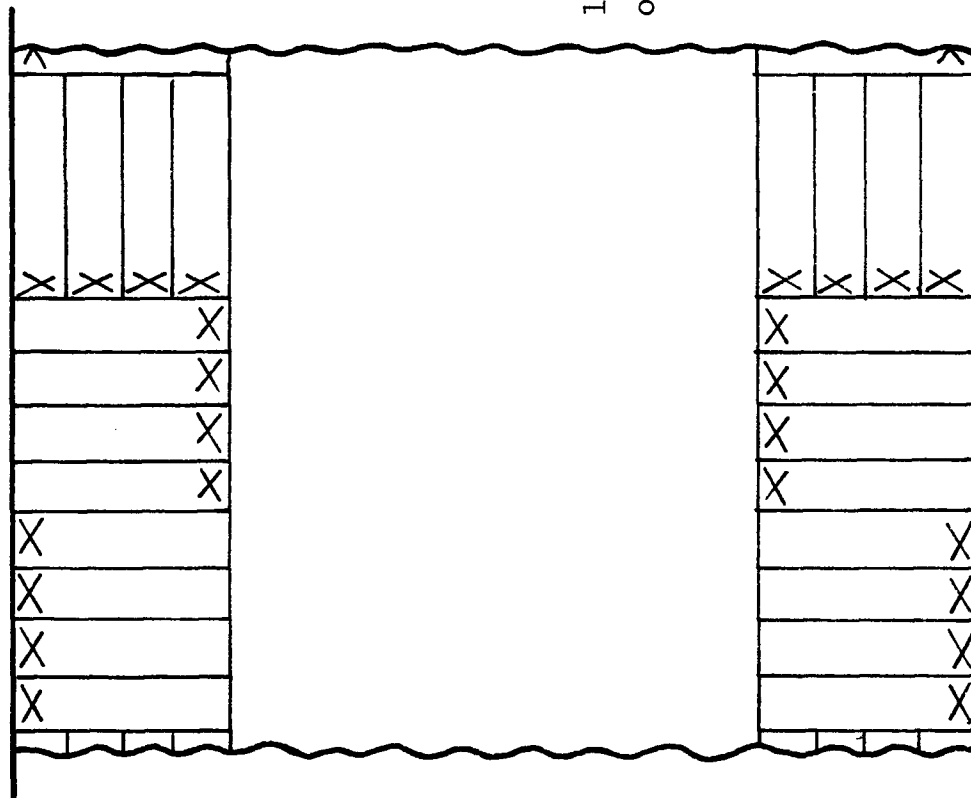
a) Along Support Wall

Figure 19   Assumed Random Distributions of Personnel

79

3.4.2 Estimation of Injury and Fatality

The primary casualty mechanism considered is debris from the breakup of the overhead basement slab. The process used in estimating debris casualties is one in which basement areas occupied by people (in the various positions)(Figures 18 and 19) are superimposed on basement areas affected by the collapsed slabs (Figure 14). The interaction of collapse modes with body positions provides a rough (though realistic) estimate of corresponding casualties. Impacts to the head or the thorax were assumed to produce fatality. Impact to or pinning of the legs was assumed to produce injury or fatality depending on the particular area or length affected. Small amounts of debris breaking from the slab during yielding were considered and were assumed to produce injuries.

The possibility of injured people being rescued in the post-attack period was not considered in making the final estimates. Injury and fatality estimates as produced herein are therefore a function of slab parameters and body positions of people occupying the shelter area.

Based on these assumptions, representative results for the random distribution of prone people over the entire floor area are given in Figure 20 and Figure 21. Figure 20(a) refers to a basement with a 12-ft simply supported one-way slab. For overpressures lower than P1 no casualties are expected. At overpressures higher than P1 but less than P2, total survivors are estimated at 13 percent of which 4 percent are injured. At overpressures of P2 or higher, total survivors are estimated at 8 percent of which 3 percent are injured.

Figure 20 also includes the upper and lower bounds on P1 and P2. Intermediate values are found in Table A.1 of the Appendix. Methods for predicting P1 and P2 overpressures are discussed in Section 3.3.2.

People survivability estimates for basements with one-way, two-span continuous slabs are given in Figure 21.

Note: These estimates are for random, uniform distribution of prone personnel over entire floor area

Percent Total Survivors

Percent Injured Survivors

	Lower Bound	Upper Bound
P1	1.15	4.63
P2	5.73	20.49

	Lower Bound	Upper Bound
P1	1.01	4.88
P2	5.57	22.24
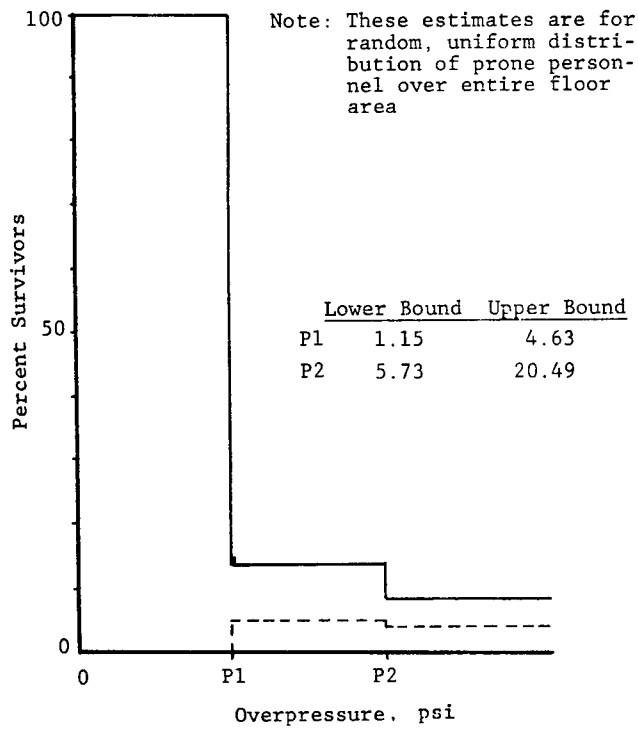
a) Slab Span, 12 ft

b) Slab Span, 16 ft

	Lower Bound	Upper Bound
P1	0.89	5.13
P2	5.54	24.05
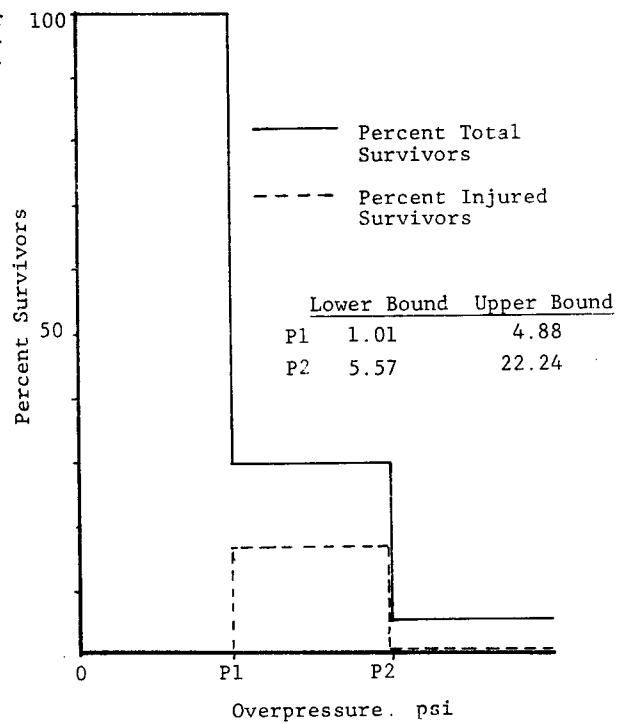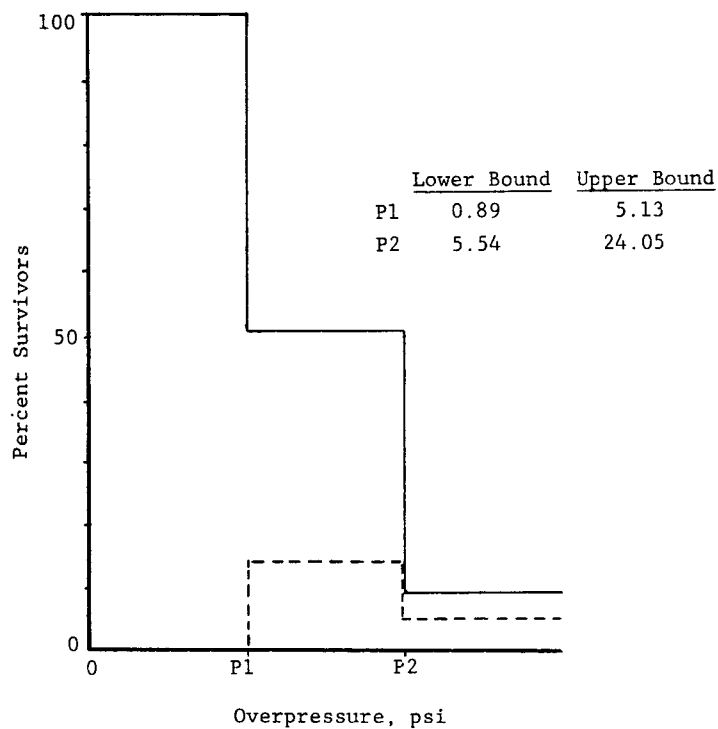
c) Slab Span, 20 ft

Figure 20 People Survivability Estimates for Basement Shelters With One-Way Simply-Supported Slabs

81
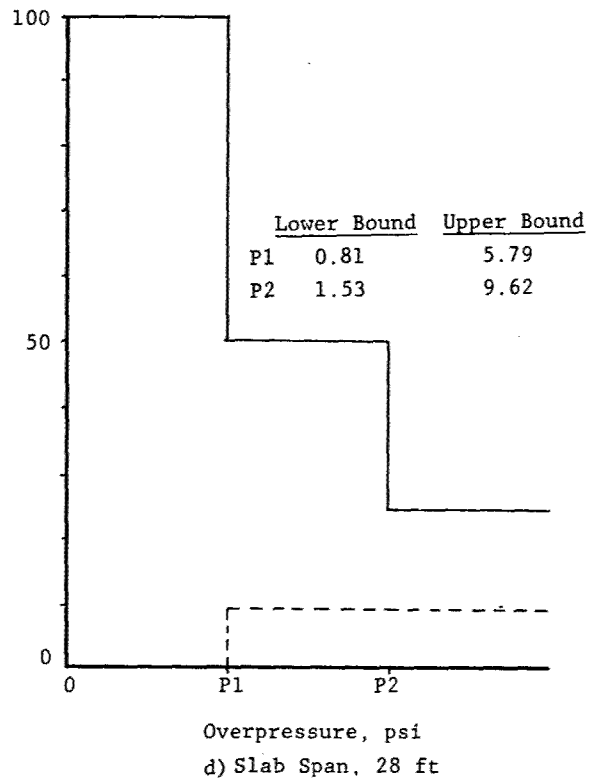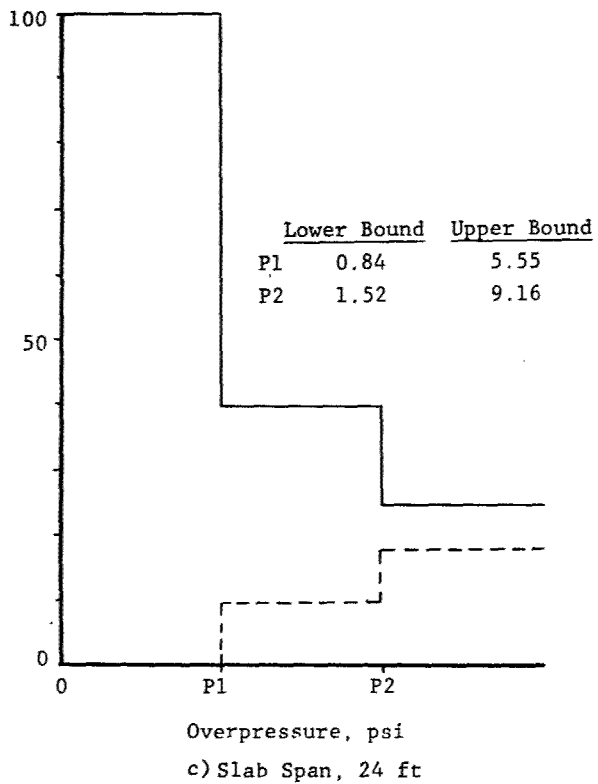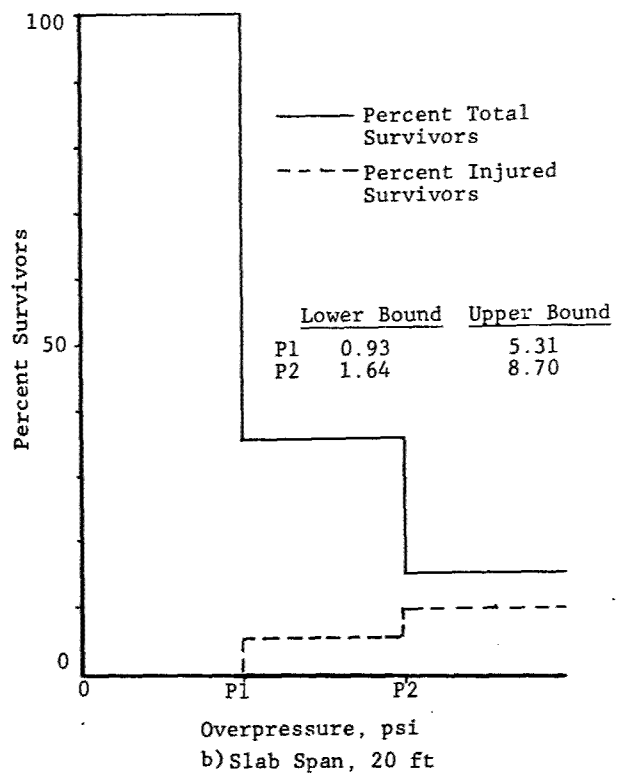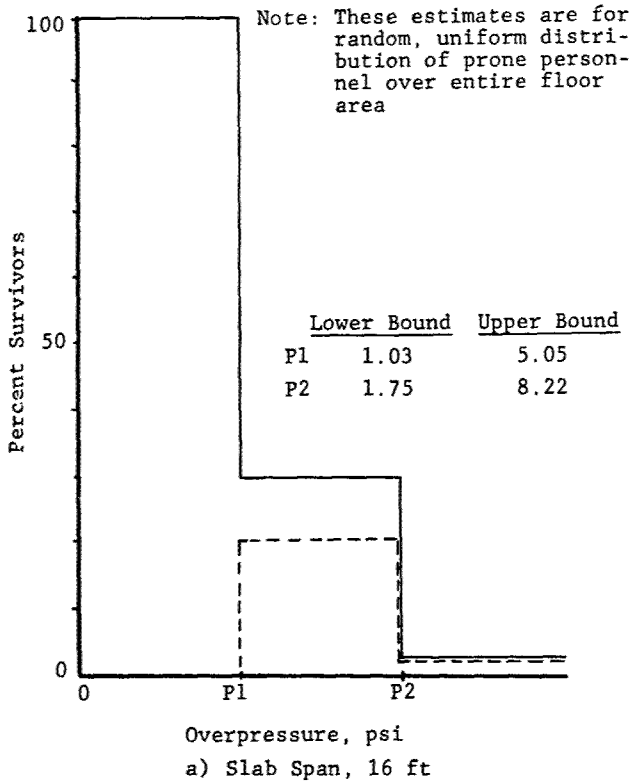
Figure 21   People Survivability Estimates for Basement Shelters
With Two-Span Continuous Overhead Slabs

82

Upper and lower bounds on people survivability for basements with one-way simply-supported slabs are given in Figure 22. These results are for the random distribution of prone personnel over the entire floor area. These bounds were obtained by varying all design parameters over their respective ranges. Design parameters and their corresponding ranges are discussed in Section 3.3.1.

Upper and lower bounds on people survivability for basements with one-way, two-span continuous slabs are given in Figure 23.

The effectiveness of the seven body positions and distributions on survivability is compared in Figure 24 and Figure 25. Results in Figure 25 are for basements with one-way simply supported slabs, those in Figure 25 are for basements with one-way two-span continuous slabs. These results are ranked in Table 11. As would be expected, body positions which are the closest to the wall and the floor offer the best protection. This includes the sitting and the prone, parallel to the wall positions. Standing along the support walls is the worst position in both cases. Differences between the remaining positions and distributions are not very significant.

3.5 INJURY AND FATALITY ESTIMATES (TWO-WAY SLABS)

The level of uncertainty associated with failure overpressures for two-way slabs is greater than for one-way slabs. Two-way slabs are more redundant. The response of redundant structures is generally more difficult to predict than that of simple structures especially in the postyield range. Also, there exists less experimental data on the response of two-way slabs than on one-way slabs.

Due to this uncertainty, an analysis to determine the relative effectiveness of the seven body positions and distributions (see Section 3.4.1) was not performed. A single body position, i.e., random distribution of prone people over the entire floor area was used in estimating casualties.
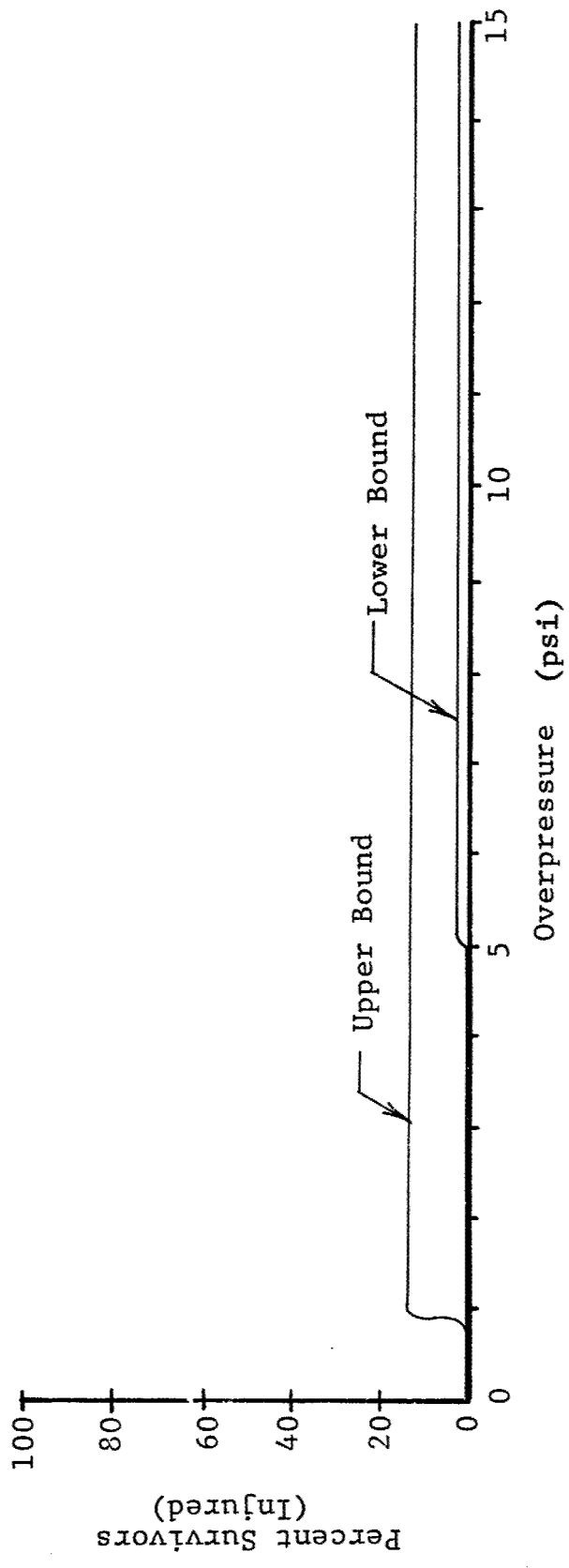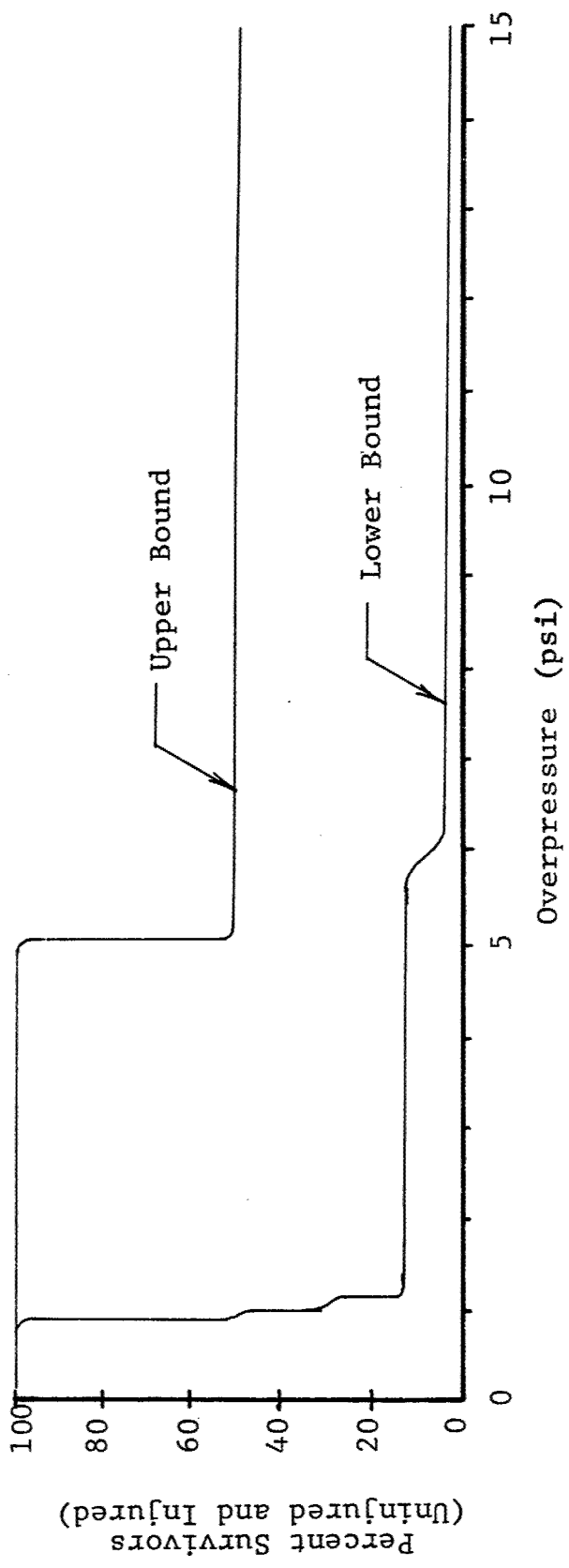
Figure 22   Upper and Lower Bound on Survivability and Injury for Simply-Supported Overhead Slabs
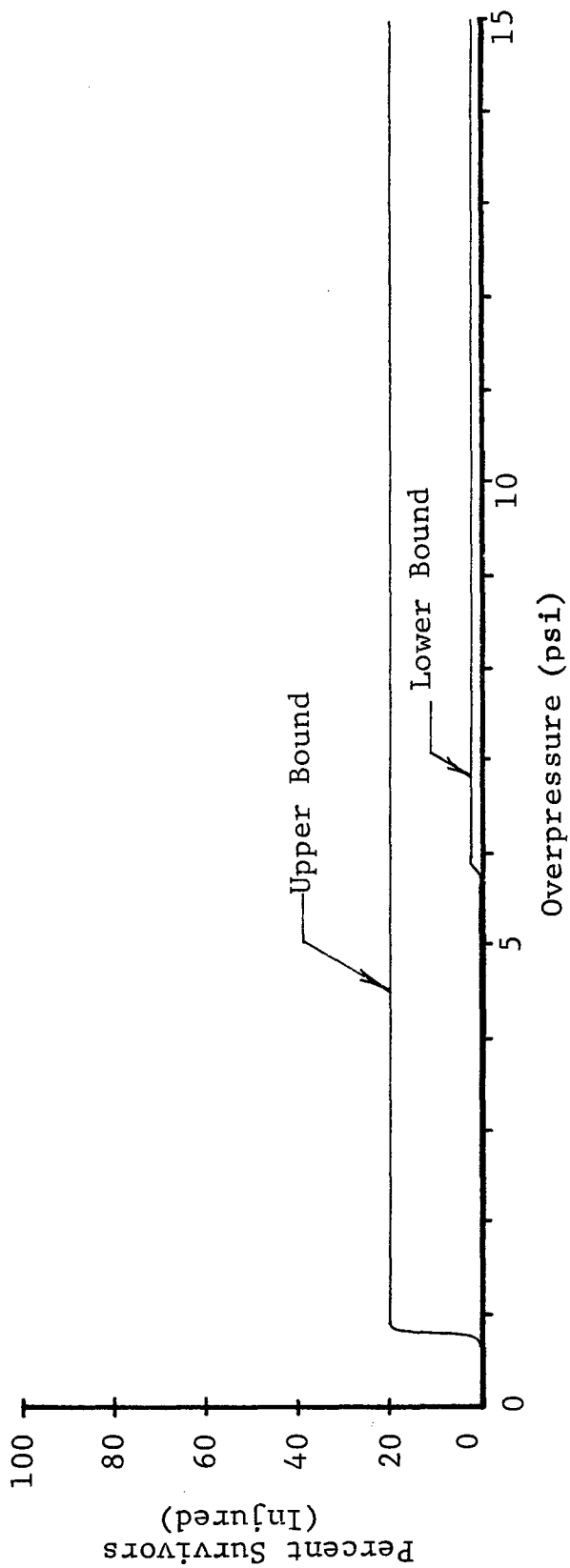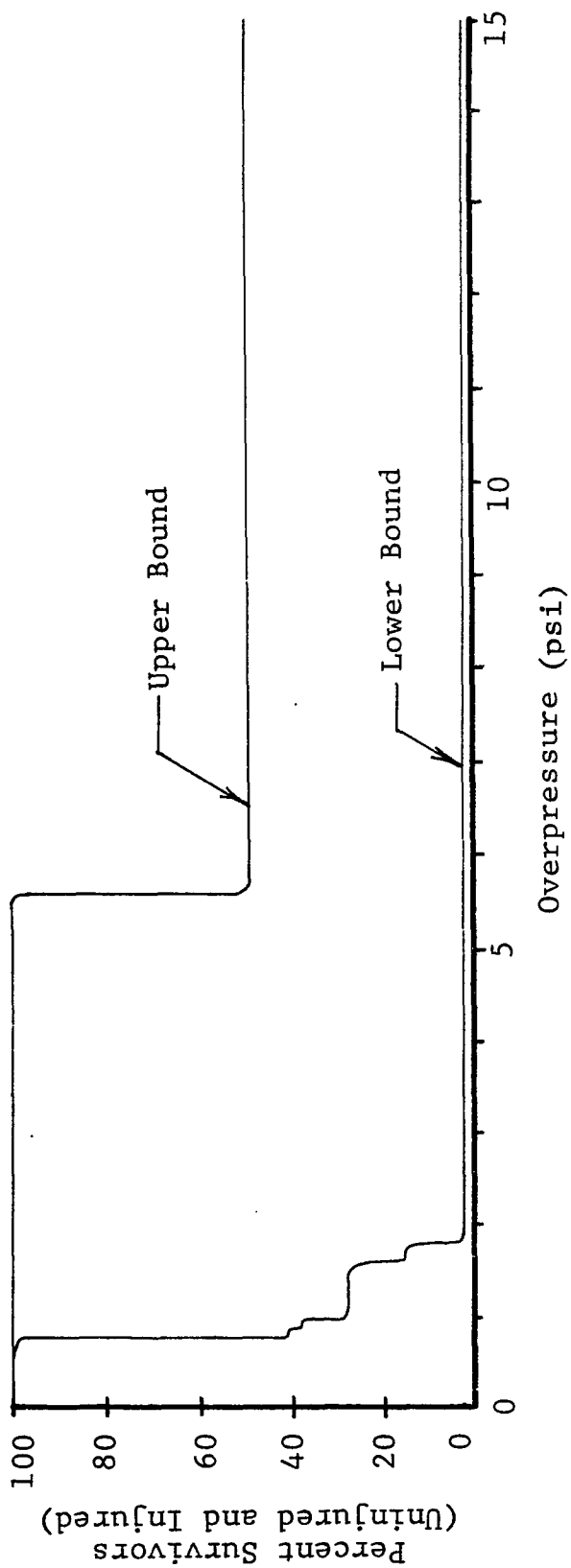
Figure 23   Upper and Lower Bounds on Survivability for Two-Span Continuous Overhead Slabs

85

Note: These results are for basements with one-way, simply supported slabs.

Standing along support walls

Sitting along support walls

Prone, perpendicular to the support walls (Head toward wall)

Prone, perpendicular to the support walls (Head away from the wall)

Prone, parallel to the support walls

Random distribution of prone people along support walls only

Random distribution of prone people over entire floor area

	Lower Bound	Upper Bound
P1	0.89	5.13
P2	5.54	24.05
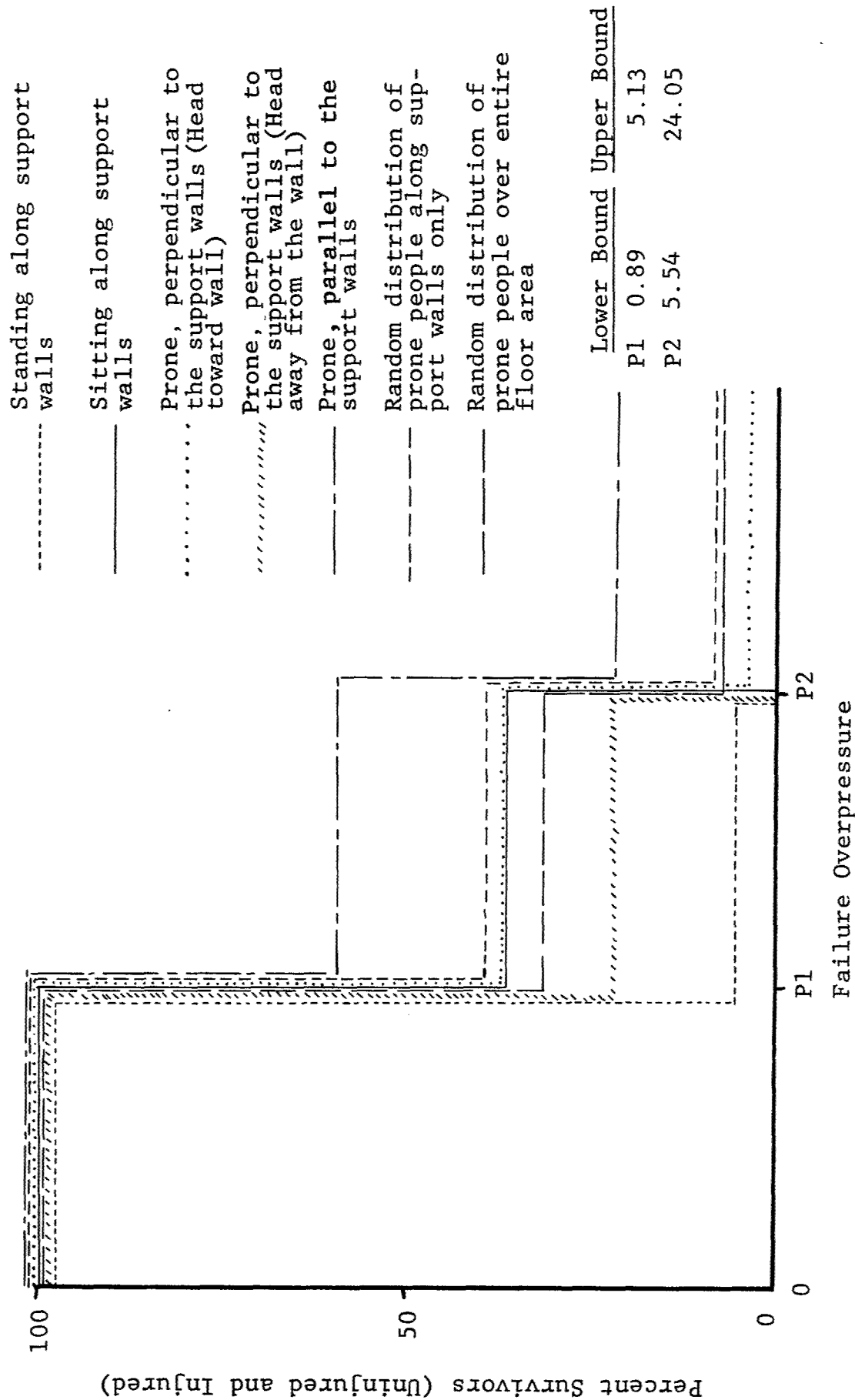
Figure 24   Effect of Body Position and Distribution on Survivability

Percent Survivors (Uninjured and Injured)

Failure Overpressure

Note: These results are for basements with one-way, two-span continuous slabs

		Lower Bound	Upper Bound
P1		0.81	5.05
P2		1.52	9.62

------- Standing along support walls

————— Sitting along support walls

· · · · · Prone, perpendicular to the support walls (Head toward wall)

//////// Prone, perpendicular to the support walls (Head away from wall)

————— Prone parallel to the support walls

— — — Random distribution of prone people along support walls only

—·—·— Random distribution of prone people over entire floor area

Percent Survivors (Uninjured and Injured)

Failure Overpressure

Figure 25 Effect of Body Position and Distribution on Survivability

87

Table 11

RANKING* OF BODY POSITIONS AND PEOPLE DISTRIBUTIONS

Basements with One-Way, Two-Span Continuous Overhead Slabs	Basements with One-Way, Simply-Supported Overhead Slabs
1. Sitting along support walls	1. Prone, parallel to the support walls
2. Prone, parallel to the support walls	2. Random distribution of prone people along support walls only
3. Prone, perpendicular to the support wall with head toward the wall	3. Sitting along support walls, or Random distribution of prone people over the entire floor area, or Prone, perpendicular to the support wall with head toward the wall
4. Random distribution of prone people along support walls only	4. Prone, perpendicular to the support wall with head away from the wall
5. Random distribution of prone people over entire floor area	5. Standing along support walls
6. Prone, perpendicular to the support wall with head away from the wall	
7. Standing along support walls	

*The ranking (1 best - 7 worst) is based on results given in Figures 24 and 25.

The analysis (see Section 3.3) dealing with the response of two-way slabs to blast loading was concerned with two levels of slab failure, i.e., incipient collapse and ultimate collapse. It is assumed that prior to incipient collapse there are essentially no fatalities and after ultimate collapse there are essentially no survivors. For lack of better criteria a linear relationship is used between these two points. Figure 26 illustrates these relationships. In this figure PI refers to incipient failure while PU refers to ultimate collapse. All personnel are survivors before and at PI, no survivors are expected at and after PU.

Injuries were assumed to start at 0.75 PI, increasing linearly to 25 percent of PI for slabs without drop panels and to 50 percent of PI for slabs with drop panels. Injuries prior to incipient collapse of the slab are assumed to be produced by chunks of concrete breaking loose from the slab and impacting people below. Injury assumptions used herein were made after examining test results such as are given in Refs. 34, 35, 36, 37, 43 and 45. Particular attention is called to Figure 4.23 of Ref. 24 which provides some indication on the quantity of loose debris covering the floor area. Also, refer to Figures 4.11, 4.12 and 4.13 of Ref. 45 which show the separation and collapse of drop panels and thus the creation of a hazardous (casualty-producing) condition before the ultimate collapse of the slab. Since drop panels are generally unreinforced, they are expected to fail and drop off as indicated in this test. This information was used as the basis for establishing the 50 percent injury level and the corresponding variation of injuries indicated in Figure 26(b).

For overpressure levels less than PI, injuries are assumed to be produced by falling chunks of concrete separated from the slab during its deformation. No fatalities are expected prior to PI. For overpressure levels greater than PI, both injuries and fatalities are expected to occur in approximately the proportions indicated in Figure 26. In this case, casualties are assumed to be produced by the collapse of the overhead slab and the trapping of injured survivors by large portions of the failed slab.
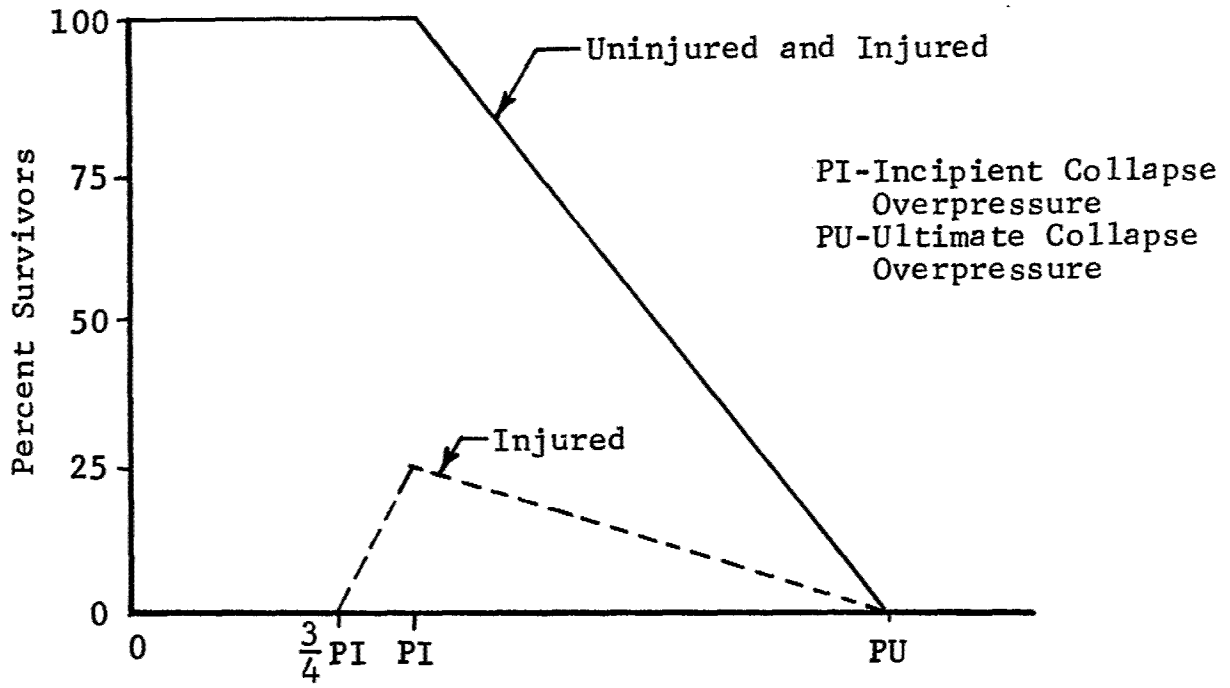
a) Flat Plate Overhead Floor System
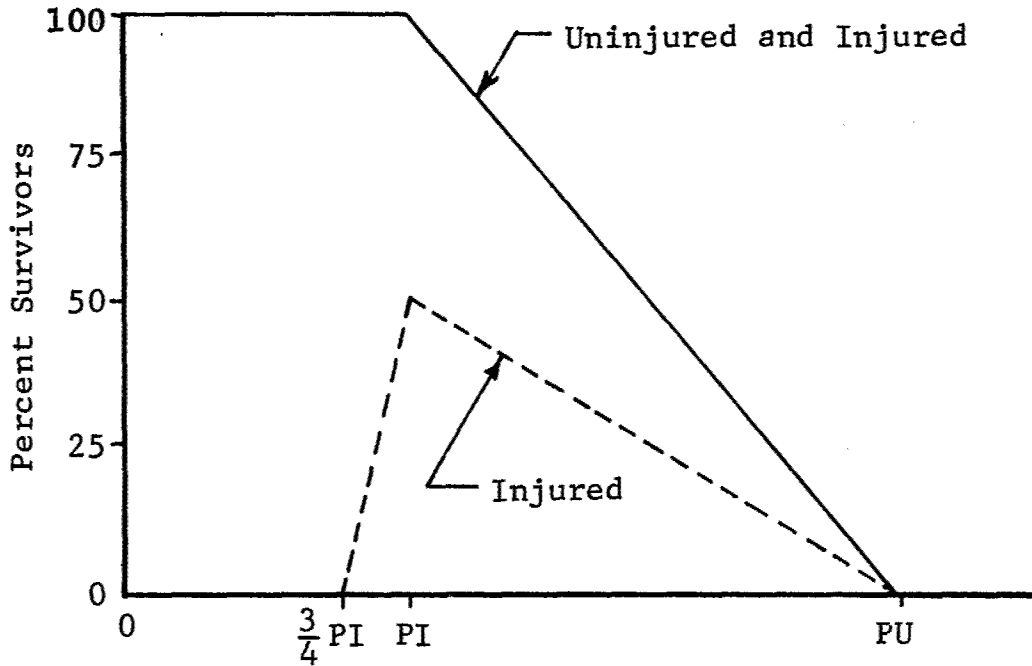
b) Flat Slab (With Drop Panel or
   With Drop Panel and Capital)
   Overhead Floor System

Figure 26   Estimate of Survivability and Injury
            for Two-Way Slabs

90

Results are summarized in Figure 26. Figure 26(a) is for people in basements with overhead systems consisting of flat plates and flat slabs without drop panels while Figure 26(b) is for flat slabs with drop panels.

Upper and lower bounds on PI and PU are given in Table 12 Intermediate values within these bounds are given in Table A.1 of the Appendix.

Using the results given in Table A.3 of the Appendix, lower and upper bound curves for total survivors and injured survivors were constructed and are presented in Figure 27. These results are divided in three categories, i.e., flat plates, flat slabs with drop panels and flat slabs with drop panels and column capitals.

It is interesting to note that the lower bound for the flat plate (Figure 27(a)) is higher than for the other two categories. This is principally due to the fact that this floor system does not have drop panels. Drop panels are generally unreinforced. They fail easily and are capable of producing significant casualties. Although this floor system has this advantage at low overpressures, its bounds are very narrow (see Figure 27(a),(b)). The other two categories of slabs offer protection over a distinctly wider range of overpressures.

3.6 SUMMARY, CONCLUSIONS AND RECOMMENDATIONS

To gain a better understanding as to the levels of protection afforded by existing conventional basements against the effects of blast, a series of survivability analyses for people located in several different basement types were performed.

Overhead floor systems considered included one-way slabs (simply supported and two-span continuous) and square two-way slabs (flat plate, flat slab with drop panels, flat slab with drop panels and column capitals). Slab design parameters constitute a representative (real world) range of spans, design live loads and material properties. The hazard load environment represents the blast effects of a single, megaton-range nuclear weapon. Structural analyses of slab response were based on current

91

Table 12

BOUNDS ON PI* AND PU*

PI		PU		Structural Member
Lower Bound	Upper Bound	Lower Bound	Upper Bound	
0.57	0.81	1.80	2.40	FP**
0.70	2.74	1.10	4.20	FS**
0.56	3.38	0.60	13.50	CAPS**

```
 * PI - Incipient Collapse Overpressure
   PU - Ultimate Collapse Overpressure

** FP - Flat plate
   FS - Flat slab with drop panel and no capital
 CAPS - Flat slab with drop panel and capital
```
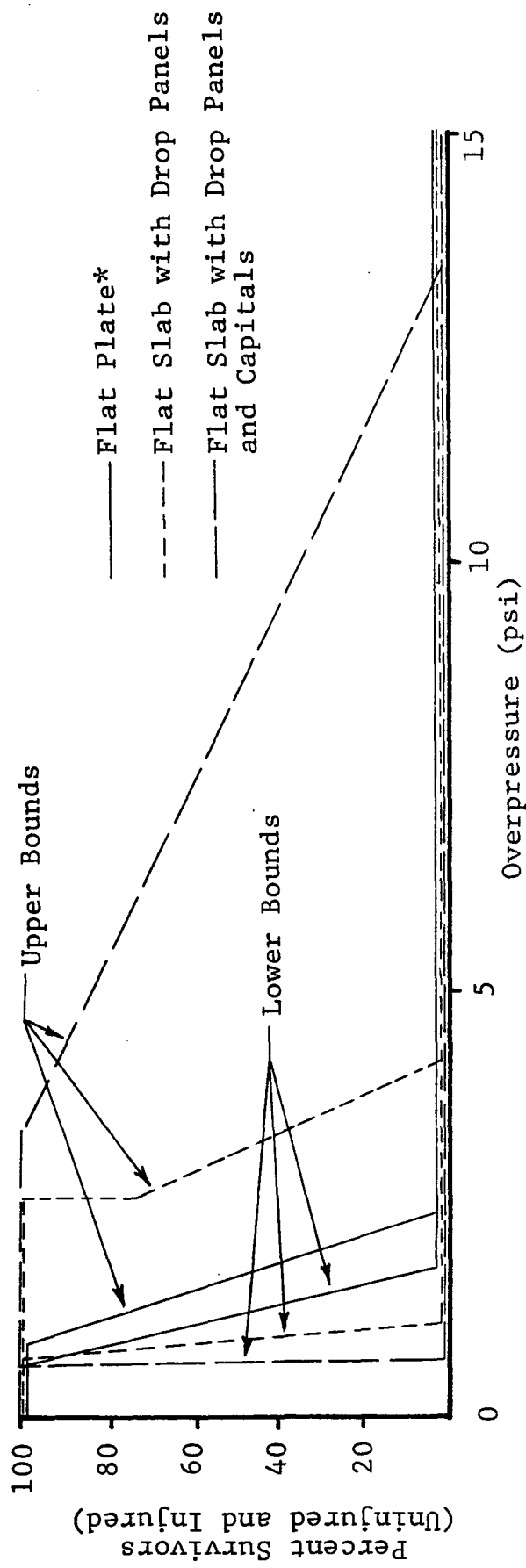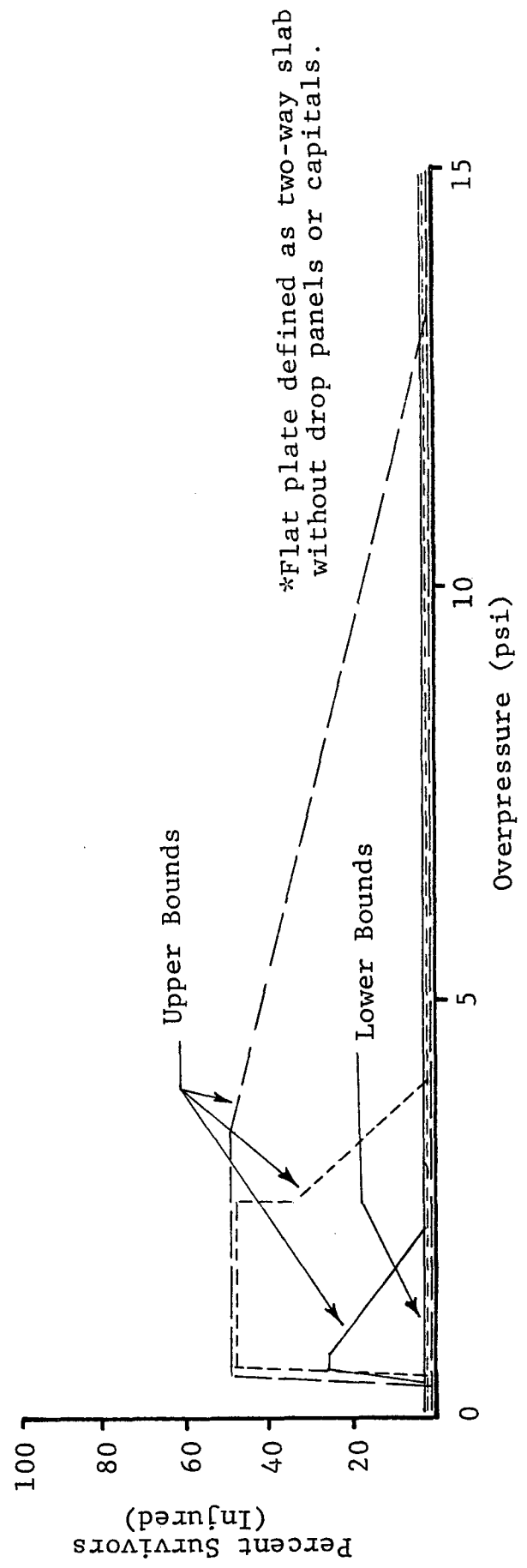
Figure 27 Upper and Lower Bound Estimates of Survivability and Injury for Two-Way Slabs

93

state-of-the-art techniques backed by series of experimental results, most of which were generated by WES at the request of DCPA. People survivability analyses were performed using the results of the structural analysis. Casualty mechanisms considered were impact and the trapping of people as the result of failure and collapse of the overhead slab. Casualty levels were identified by relating failed states of the slabs to areas where people would be located and their particular body positions at the time of slab failure. Slab collapse mechanisms and corresponding overpressure levels were identified with the aid of structural analyses.

Casualties that can be produced by blast winds entering basement areas through doors and windows were not considered in arriving at percent survivors. Thus, these results apply to small and moderate size basements with strong doors and no windows, or to large basements with proportionally small entrance areas. The influence of blast winds on people in basement areas is discussed in the following chapter. Based on results obtained, the following conclusions are made.

1. For one-way overhead floor systems, the most advantageous body positions are those which occupy the least space and are closest to the floor. This includes sitting along peripheral (support) walls and lying along and parallel to peripheral walls.

2. Predicted failure overpressures (P1 and P2) for one-way slabs, and incipient failure, (PI), and ultimate collapse, (PU), overpressures for two-way slabs correlate most directly with design live load.

3. Upper and lower bound estimates of total survivors and injured survivors were obtained for each slab type as a function of free-field overpressure incident on the slab. On the whole, basements with one-way slabs appear to provide better protection than two-way slabs. It would seem that the reverse would be true due to the redundancy of a two-way floor system; however, it must

be remembered that the redundancy of a typical two-way slab system isn't used for extra protection, but rather for a more economical design.

4. It was determined that greater protection for personnel in basements with one-way overhead slabs is afforded along the supporting walls (see conclusion 1). It is therefore recommended that any supplies, equipments and passageways be located in central areas with personnel along peripheral walls.

5. For two-way slabs it is recommended that one of two methods of placing reinforcement in the column strip be practiced so as to provide extra blast resistance. These methods are:(1) part of the reinforcement should consist of bent bars.(2) if only straight bars are used, then a portion of the positive reinforcement should be carried into the supports and be anchored so as to develop its yield at the perimeter of the capital or of the column if no capital is used. These methods would help to prevent the sudden collapse of slabs by causing them to be suspended by the reinforcement after flexural or shear failure has occurred. In other words, the aim is to insure that membrane action occurs and is sufficient to preclude sudden collapse.

6. It is recommended that reinforcement be provided in drop panels so as to preclude spalling and separation.

7. It is recommended that additional slab types prevalent in the total inventory of existing buildings be analyzed in the manner considered in this study. This would provide a better understanding of protection that is afforded by all basements of conventional buildings.

Slab systems that should be considered in future efforts should include the following:

● Two-way reinforced concrete slabs on steel beams

● Two-way reinforced concrete slabs on reinforced concrete beams

- Two-way steel decks on steel beams

- Two-way waffle slabs

- Reinforced concrete joist floor systems.

CHAPTER 4

FLOW INDUCED TRANSLATIONAL EFFECTS IN BASEMENT SHELTERS

4.1 BACKGROUND

This chapter presents the results of an initial effort to establish the probability of survival for personnel within conventional basement type shelters when subjected to blast wind induced translating effects generated by an atmospheric burst of a nominal, megaton-range nuclear weapon in its Mach region.

The detonation of a large nuclear weapon within the atmosphere generates a rather-well defined blast wave system which propagates outward from the burst point. This blast wave system will interact with the ground plane and its perturbations (hills, structures, etc.) altering the local blast environment to some extent. This blast environment is characterized by the presence of a shock discontinuity across which the air pressure increases. The pressure level then decreases, decaying down below the atmospheric level (entering the so-called negative phase) and then increases again, yet more slowly, until the ambient pressure level is reached. The air motion also undergoes a similar oscillatory (outward-inward) pattern. Structure geometries and orientations, shielding effects, and shelter entrance locations and configurations will further distort the fine details of the local blast environment. Ultimately the blast wave energy will propagate within an open shelter and induce a variety of rather intense flow regimes within the shelter. Personnel and objects located within these shelters will respond to the environment, in part, by being transported in some fashion (tumbled, slid, etc.) until the adverse environment is relieved or an impact with a wall or other ojbect occurs. The nature and intensity of an impact, if one occurs, will be dependent upon the many variables defining the explosion, the shelter, the object, and the location of the object and other objects with the shelter. The survivability of personnel to such impacts will be a function of the nature and intensity of the impact or perhaps impacts and

the complicated interactions of other adverse physiological effects such as blast overpressure exposure.

The current study is based upon the conditions of a surface burst of a 1 MT nuclear weapon with the shelter located in the Mach region. This restriction is not a limiting one as other weapon yields and burst conditions can be readily treated. However as an initial effort to establish the survivability levels of personnel in shelters due to impact conditions some restrictions and simplifications are required. The survivability question is a complex one and if an adequate prediction is to be made, then a comprehensive effort coupled with some attempt (perhaps experimental observations) to verify the more important aspects of this complex problem will have to be made. The basic elements of the problem can be categorized by the following steps or criteria:

a. Injury and fatality criteria
b. Impact and bounce conditions
c. Complete description of the transient air velocity field within the shelter
d. Development or adaptation of adequate translational models
e. Adequate selection of pertinent shelter parameter values.

In many instances these steps can be undertaken at several levels of sophistication and precision. Initially simple models and/or criteria can be used or established to obtain a rough estimate of the survivability levels for typical conditions of interest and to identify the critical aspects of the overall problem. Such a procedure is used in this effort.

The transient velocity field which will exist within the shelter will depend upon the geometry of the shelter and the size and location of the inlet opening or openings. Furthermore, the mass flow rate of air into and out of the interior shelter region or cavity will be a significant factor. The latter effect is a function of the volume-to-area (V/A) ratio of the shelter, where the pertinent area is the total inlet area. This effect will also be dependent upon the free-air blast environment.

Any attempt to define the transient velocity field within a
shelter will have to be limited to relatively simple configurations
such as rectangular rooms. Since the openings or inlets will fre-
quently occupy nearly the entire vertical height of the room and
since the plan (horizontal) dimensions of a room are generally much
larger than the vertical height, the flow within the shelter will
take place primarily in the horizontal plane. Thus a two-dimen-
sional flow model should be adequate to define the blast induced
velocity field and the basement shelter can then be characterized
simply by its width, W, and its length, H. The inlet area can be
connected to an equivalent inlet width, B, by dividing the inlet
area by the room height. At the present time the location of the
inlet has been restricted to the central location on one wall.
This wall is called the front wall. The identification of the
back and side walls follows naturally. Such a symmetric geometry
leads to the inclusion of the case where the axis of symmetry
(across which no flow of air occurs) can be treated as a wall.
The width of this reduced room and of the inlet correspond to the
related half-widths of the full room, and the inlet will now be
located at one extreme end of the front wall. Many rooms which
differ somewhat from these two geometric cases can be converted
to these geometries by neglecting some small geometric perturba-
tions and by utilizing average or effective values for some of
the shelter parameters. It should also be noted that the basic
geometry (a rectangular room with one centrally located inlet on
the front wall) can be combined with identical modules to yield
more complex configurations which contain multiple but similar
openings. Figure 28 illustrates a variety of room configurations
which can be treated. The use of the basic geometry and its var-
iant forms will provide a range of configurations which correspond
to most shelter geometries of interest.

A number of shelter sizes have been tentatively selected for
this study. Three large shelters were selected from Ref. 46
and two small basement shelters treated in another part of this
report were included to cover a rather wide range of probable sizes.

99

W

Axis of Symmetry

a) Basic Geometry

H

Front Wall

B

Inlet

W

Wall

H

Inlet

B

b) Reduced Geometry

Inlet

B

W

H

Axis of Symmetry

B

Inlet

c) Typical Expanded Configuration
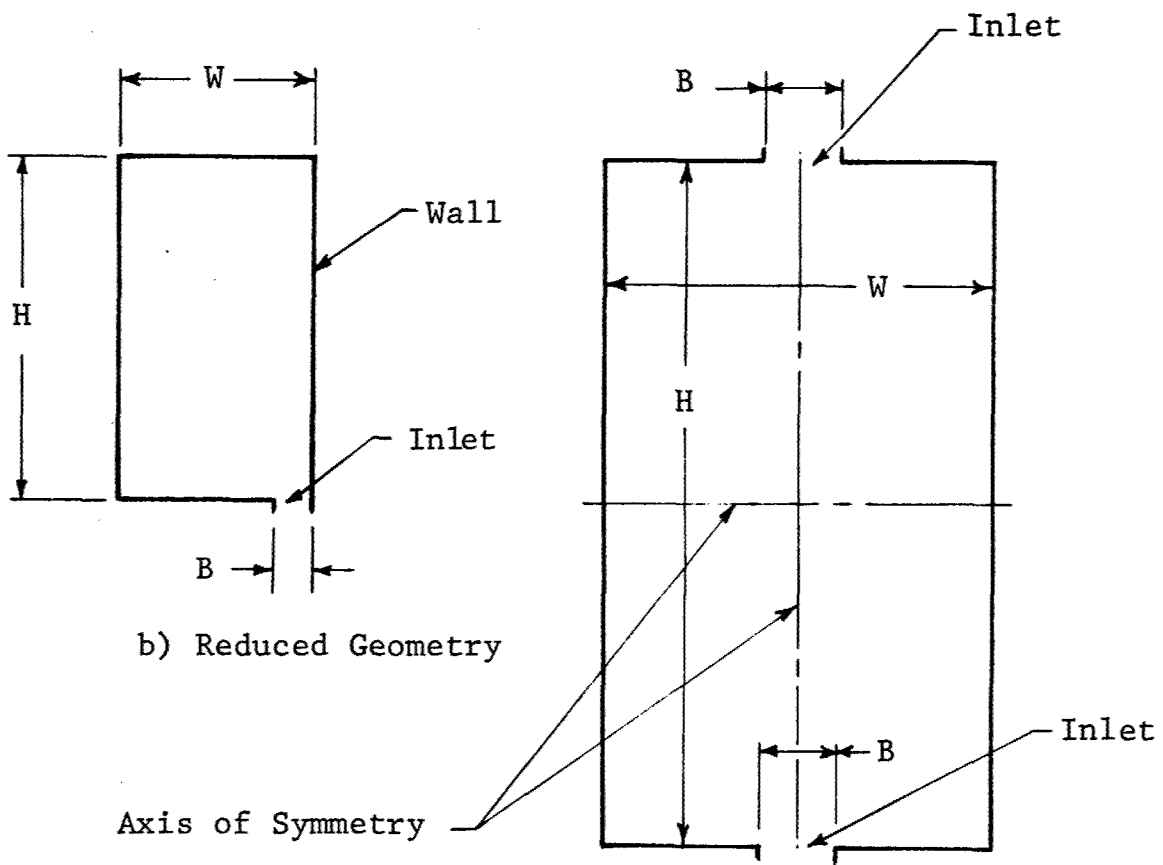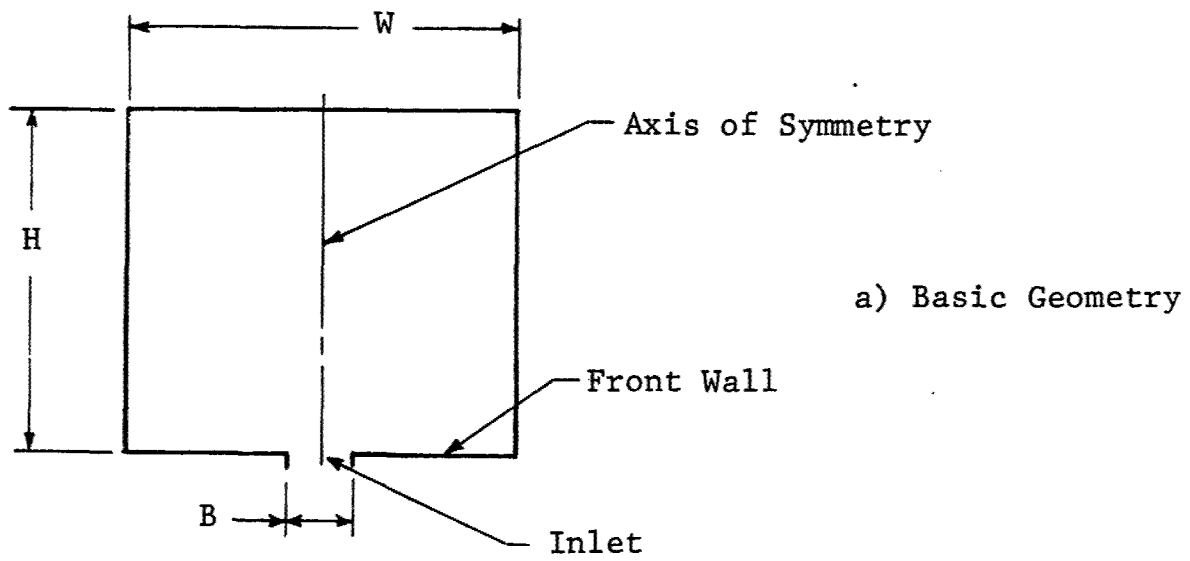
Figure 28   Room Configurations

100

Dimensions and parameter values for this range of shelter sizes are presented in Table 13. In most cases several inlet area values were selected, however it should be noted that multiple inlets will generally exist for the larger shelters. The number of inlets and/or their locations are not specifically defined at this stage. Furthermore, the fact that the rooms selected are square is of no particular significance. Other aspect ratios can be included at a future time. The sizes of the inlet areas were generally selected to obtain a desired volume-to-area ratio. This parameter will generally be larger for the larger shelter sizes.

Since the overall mass flow rate aspect of this problem is only dependent on one shelter variable (the volume-to-area ratio, V/A) auxiliary calculations were made for a range of this variable (from 200 to 4000 ft) and for a nominal range of peak free-field overpressure levels. Recall that the weapon size and burst condition have already been fixed. The overpressure values treated specifically include 2,6,10 and 15 psi. The cavity filling computer code of Ref. 47 was used for these calculations after some minor modifications needed to obtain the desired details were made. The inlet flow velocity histories corresponding to an overpressure of 10 psi are presented in Figure 29 At somewhat high overpressures the flow is initially choked and remains so for a short period of time. In those instances the inlet velocity remains constant for an appropriate period of time at a value of approximately 1100 fps. In this study standard ambient conditions for both pressure and temperature were used. This approximation is adequate since these variables are not very influential over their conventional ranges. The inlet flow velocity histories shown in Figure 42 are similar to those of the other overpressure levels with the exception that the initial value is lower for lower overpressure levels. The mass flow rate reaches a value of zero when the cavity (shelter) overpressure reaches its maximum value. The interior pressure increases from the time of shock arrival in a manner which can be roughly described as linear in form. The interior pressure then decays like the outside free-field overpressure decays, at essentailly the same value.

Table 13

SELECTED BASEMENT SHELTERS

Case No.	Volume, V (ft³)	Dimensions (ft x ft x ft)	Inlet Area, A (ft²)	V/A Ratio (ft)
A	4.0×10^5	200 x 200 x 10	400	1000
B1	10^5	100 x 100 x 10	25	4000
B2	10^5	100 x 100 x 10	100	1000
C1	3.6×10^4	60 x 60 x 10	10	3600
C2	3.6×10^4	60 x 60 x 10	50	720
D1	2048	16 x 16 x 8	2.05	1000
D2	2048	16 x 16 x 8	4.10	500
E1	6270	28 x 28 x 8	6.27	1000
E2	6270	28 x 28 x 8	12.54	500
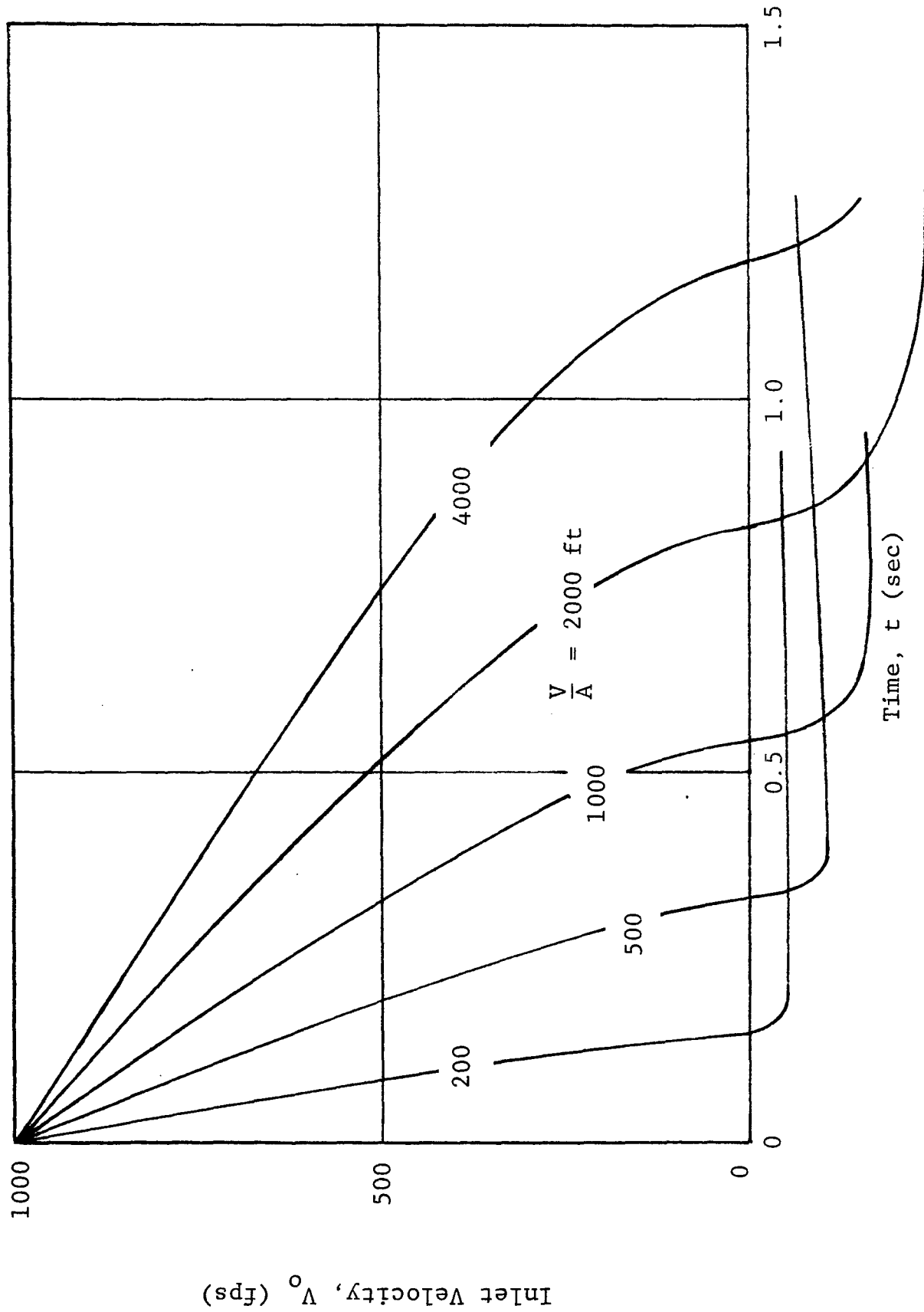
Figure 29   Inlet Flow Velocity Histories - p_i = 10 psi

103

This pressure decay period corresponds to the outflow (negative inlet velocity) interval shown in Figure 29. It lasts until the end of the positive phase duration of the overpressure which for the overpressure levels indicated is in the range of 2 to 3 sec. The peak magnitude of the inlet flow velocity is smaller during the outflow period than it is during the inflow period. During the negative phase of the overpressure the air within the shelter will continue to flow out of the region, however, at a substantially reduced rate. It would appear that, as a first order approximation, the inlet flow velocity can be set equal to zero during this late time period and thus enable the analyst to terminate the inlet flow in some reasonable manner. These cavity filling calculations have provided for a reasonable estimate of the inlet flow velocity histories for the range of overpressure of general interest. They also provide additional flow details. The air density within the cavity will vary somewhat as the cavity pressure varies, but over a narrower percentage range. Therefore for the current study a constant value is used. The standard ambient density is used in subsequent transport calculations although a value modified slightly to account for the overpressure level could also be applied. The cavity filling calculations also provide the maximum or peak pressure which exists within the shelter. This information for the range of shelter parameters of interest is shown in Figure 30. This figure illustrates the variation of peak average pressure within the shelter as a function of external free-field overpressure and the volume-to-inlet area ratio. These pressure levels are too low to produce noticeable casualties by themselves alone. Assuming "fast rising" pressure, the LD_{50} (50 percent probability of mortality value for man) is 61.5 psi (see p 28, Ref. 14).

The major task of this initial effort dealt with generating an adequate description of the transient velocity field within the basement shelter and then imposing this environment on objects within. Subsequently the resulting translation effects were observed. This has been done using a simple drag type translational model.
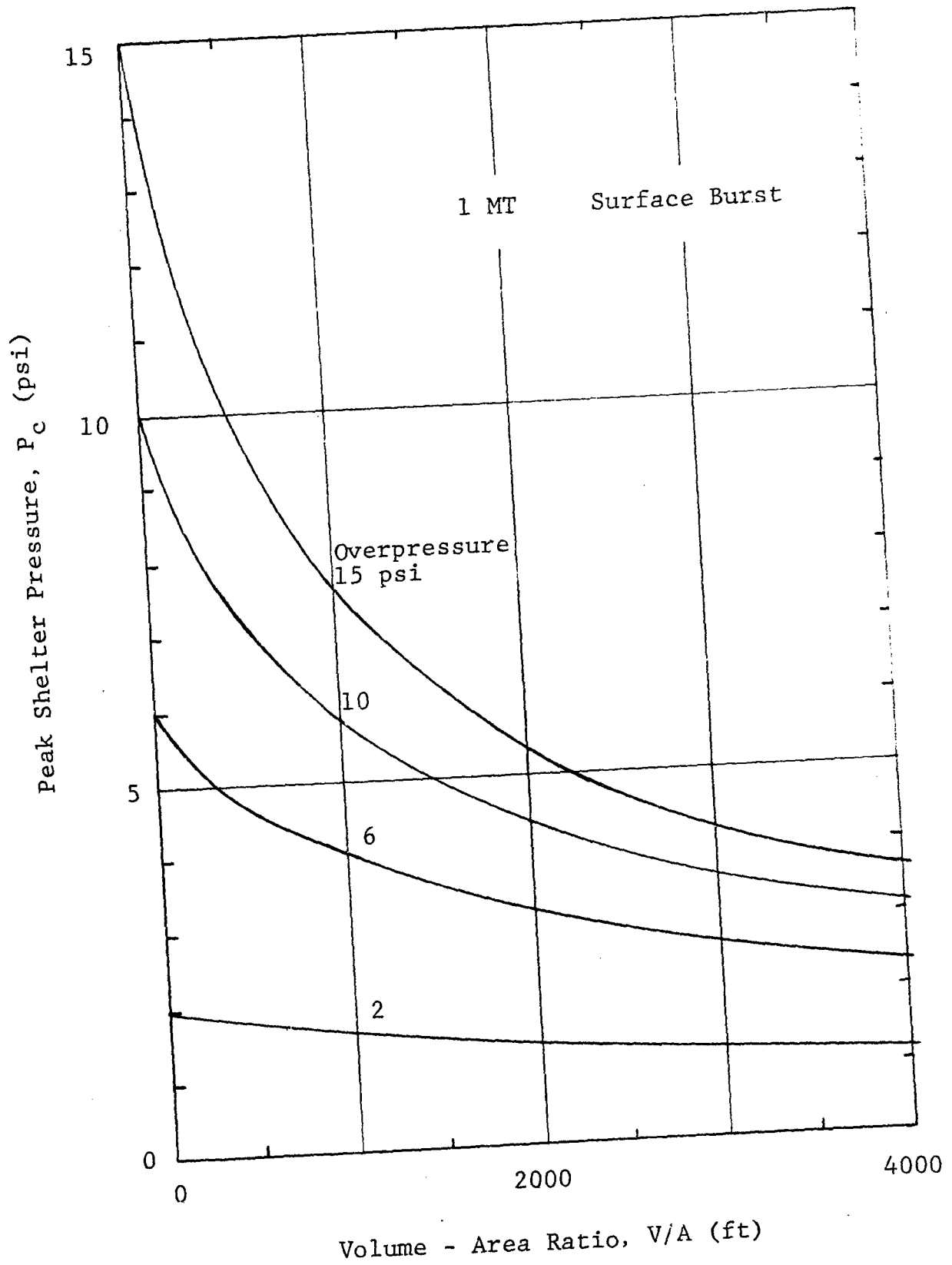
Figure 30   Peak Pressure Environment in Shelter

The calculations were carried out until an impact occurred at one of the room boundaries. Only the initial impact was considered. The conversion of this observed impact condition into a statement of survivability or injury level, although not explicitly made in this report, must involve some appropriate impact criteria. The criteria presented in Figures 4 and 5 should be adequate for initial estimates of survivability. It is apparent that multiple impact conditions may be common in the shelter environment, hence the rebound or "bounce" aspect of the problem must be introduced in some manner. At the present time a simple approach has been formulated, but not applied since the transport calculations were stopped after the first impact occurred. The approach which was formulated was that of using an analytical expression, specifically an exponential decay form, to reduce the normal component of the rebound velocity when normalized by the noraml component of the impact velocity. The exponential factor involves the normal component of the impact velocity and an appropriate critical velocity. A value of 50 fps was selected initially for this critical velocity. In this manner the rebound velocity is treated as a function of the impact velocity. The final selection of the analytical form and the value of the critical velocity should be based upon a separate impact analysis which can examine the influence of the effective spring constants and hysteresis characteristics of the impact materials (soft tissue, etc.) of interest to this study.

The use of a simple drag model to define the transport aspect of the problem also represents an initial step in this study. Such a transport model neglects the effects of gravity and the corresponding tumbling and sliding effects. It defines the motion of the object of the horizontal plane and should be applicable for the early phases of the motion of people initially in the standing position. Such a model can be easily expanded for some conditions or, supplanted by the use of a tumbling man model, such as that developed by IITRI (Ref. 16). Such refined transport models can be combined with the transient velocity field description to improve the accuracy of future transport and injury prediction.

106

4.2 TRANSIENT VELOCITY FIELDS IN BASEMENT SHELTERS

An adequate description of the transient air velocity varia-
tions throughout the shelter for the parameters of interest repre-
sents the driving force for the transport of objects within the
shelter, and as such, is a critical step in attaining the overall
objective of this part of the program. A previous discussion in
this chapter has indicated that a two-dimensional flow model
bounded by a horizontal rectangular region would be adequate for
this effort. Other more complex flow models may ultimately be
examined; however, the two-dimensional model should be an adequate
first step.

There are several approaches which could be followed to ob-
tain the needed flow details. One method would be to use an ap-
propriate gas dynamic or hydro code capability to numerically in-
tegrate the governing flow equations in a forward time stepping
manner and thus carry the solution to some late time point in the
flow process. A number of such solutions have been obtained for
basement type shelter geometries (see Refs. 48, 49) for over-
pressure levels of general interest. Such solutions are relative-
ly expensive to obtain. The flow solution could be obtained si-
multaneously with the solution of a transport problem (for one or
more objects) and then redone for other transport conditions. Or,
a given solution could be stored on tape and used repeatedly for
a wide variety of transport problems. The storage requirements
for a single velocity field solution (one shelter geometry at one
overpressure level) would be rather large since such solutions
frequently involve about 1000 node points (the spatial coordinates)
and perhaps well over 1000 time steps. This many time steps would
be needed to carry the solution out far enough in time. Undoubt-
edly, some economies could be generated by curve fitting over
coarser intervals in either space or time (or both). However, at
least two parameter values would have to be stored at each stor-
age unit. It appears at this time that for the many overpressure
levels of interest and the wide variety of shelter sizes and geom-
etries which may be examined, the above described approaches

are not economically feasible. The use of such an approach may
be appropriate as an accuracy check or at least as a consistency
check on other methods. The accuracy of these numerical solutions
is, of course, limited; however, these types of solutions should
be quite adequate for the goal of survivability prediction.

Experimental methods have been used in the past to obtain
solutions of such complex transient multidimensional gas dynamic
flows. The scaled shock tube type experiments were generally
limited to obtaining information relating to pressure variations.
Very little success was achieved in observing flow velocities of
air particles. Nonetheless such experiments did provide an insight
into a number of complex phenomena, such as shock diffraction ef-
fects and vortex growth and transport.

The approach which was selected for obtaining a description
of the transient air velocity troughout a shelter is that of syn-
thesizing the velocity field analytically by using a number of
functional terms to define the magnitude of the velocity vector
components. The bases for this development are all the known ap-
plicable solutions such as the numerical solutions given in
Refs. 48 and 49. The adequacy and accuracy of such an approach
has not yet been demonstrated; however, the initial results are
promising. Accuracy is being sacrificed to some degree but this
approach does permit many flow solutions to be generated at a very
low cost. The following paragraphs describe the development of
the synthetic process and indicate the current state of develop-
ment of the velocity field approximation.

Velocity diagrams for three time values (measured by Cycle
number which is a time indicator used in Ref. 48) are presented
in Figures 31 - 33. These details were taken from Ref. 48
and correspond to a square shelter with a 25 percent opening in
the center of the front wall. The solution was obtained for a
specific shock tube condition on a small-scale model; the peak
overpressure was approximately 5 psi. The effective duration
is such that this solution is applicable to the general range of
parameter values of interest to the current problem. These three

108

Back Wall
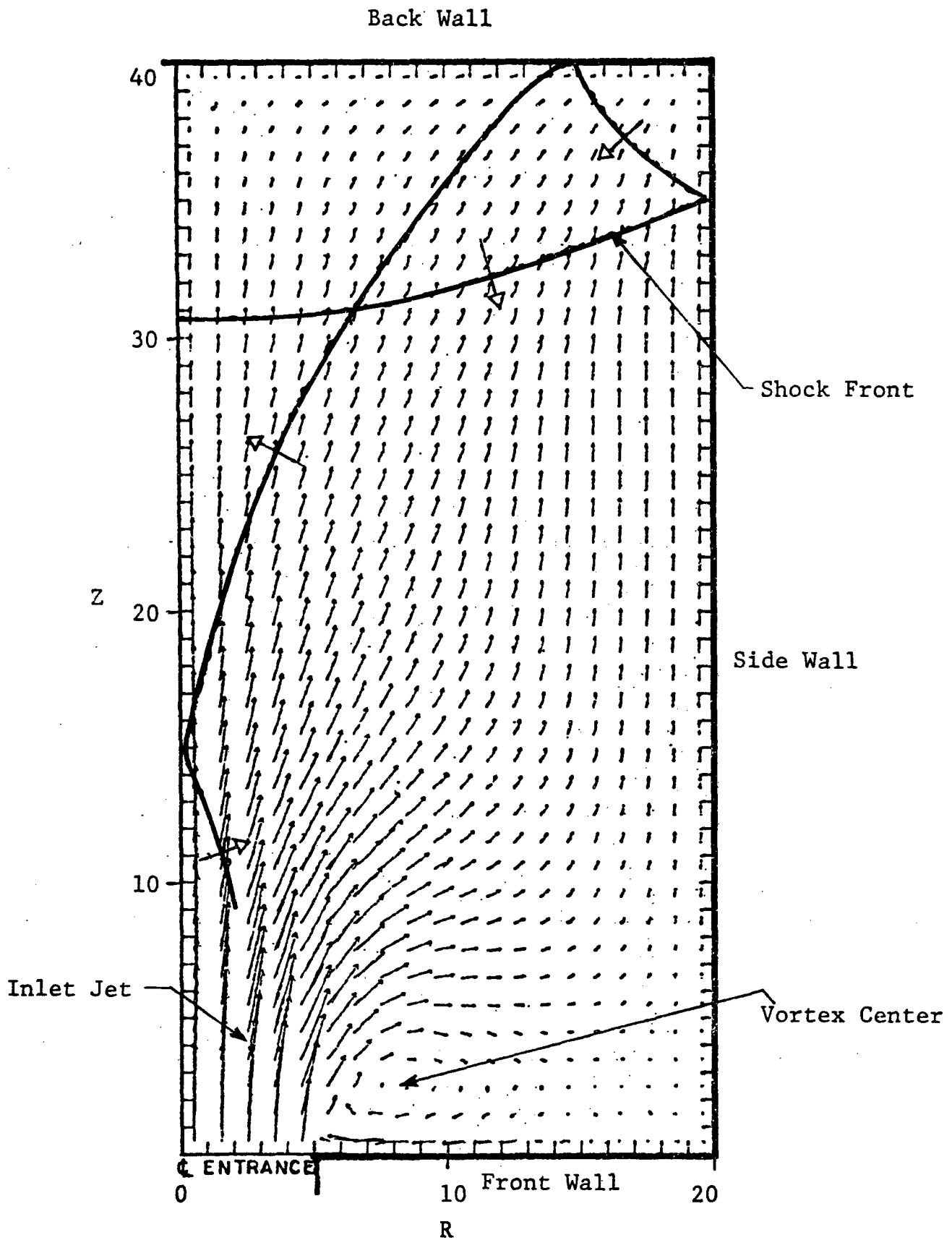
Figure 31 Velocity Diagram - Cycle 150

Back Wall
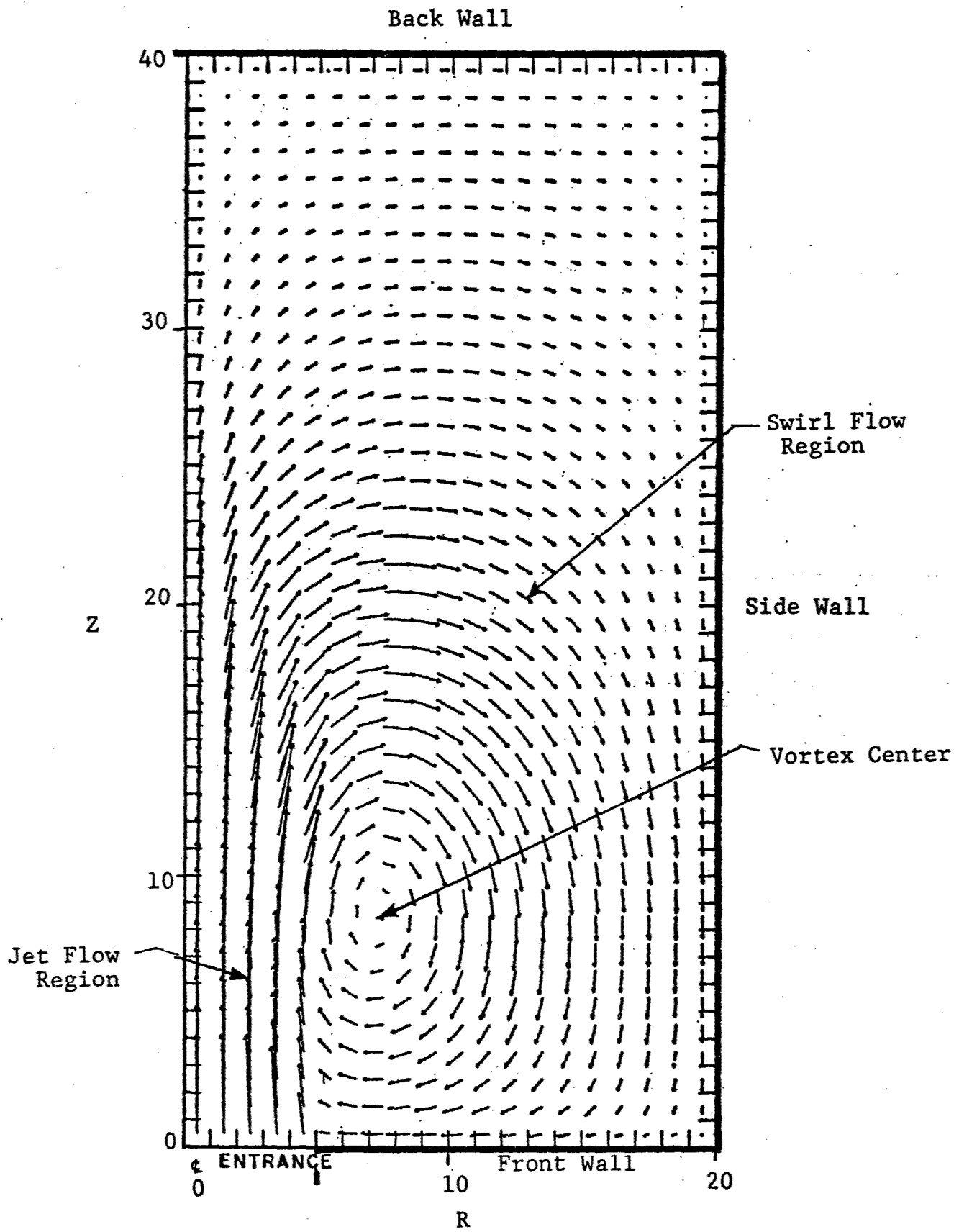
Figure 32 Velocity Diagram - Cycle 275

110
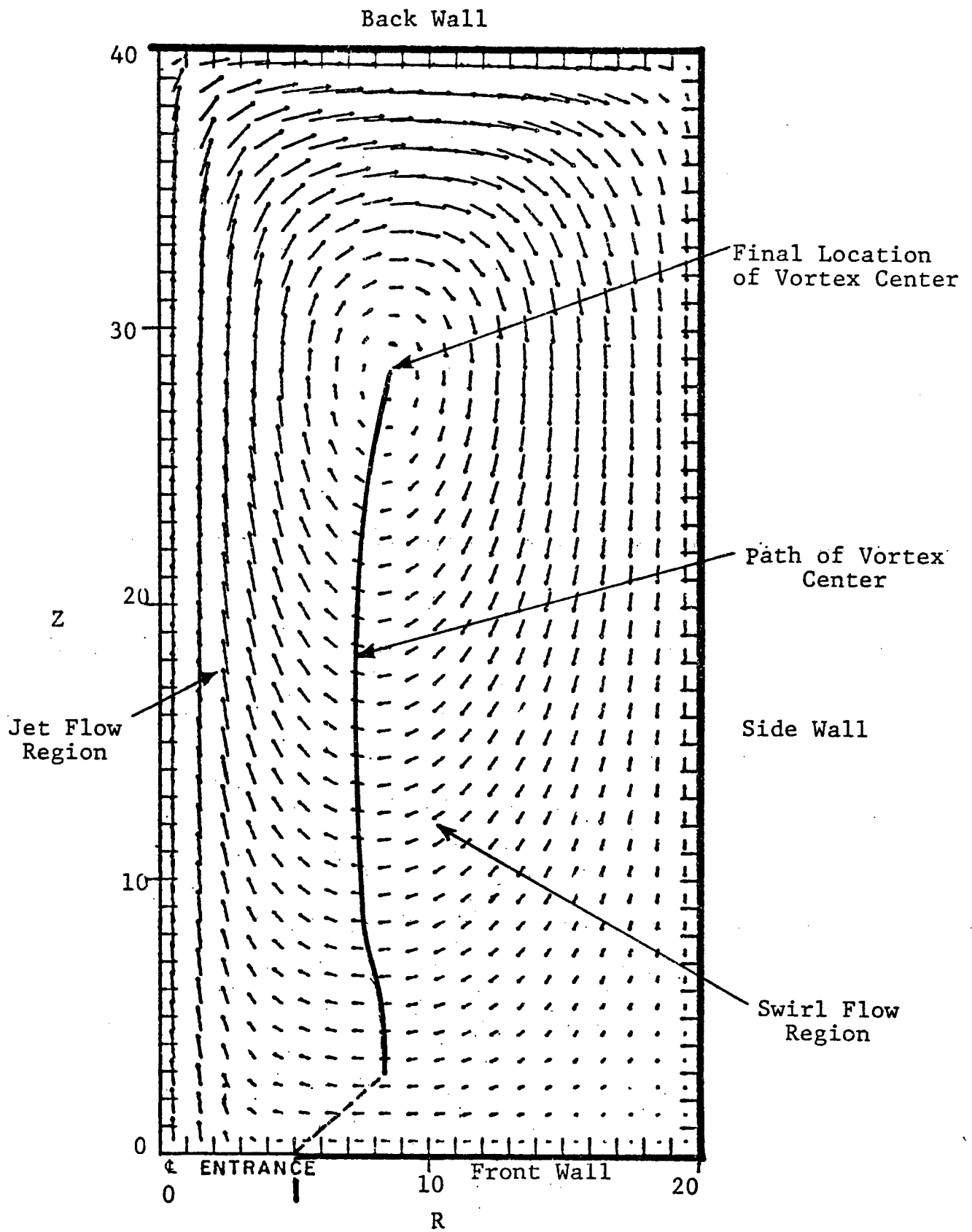
Figure 33 Velocity Diagram - Cycle 750

diagrams are presented to demonstrate the general nature of the flow regimes which will exist within the shelter.

A shock wave will propagate through the inlet, diffract around the geometric features and then propagate out into the shelter interior. In this manner the first motions of the air within the cavity are induced. The details of this initial flow will be influenced, in part, by exterior perturbations and distortions of the local exterior blast environment and by the geometric details of the entranceway. For purposes of the current program these fine, perhaps randomly occurring, details are of secondary importance and can be eliminated by considering a simplified model or configuration. Thus, the initial process can be idealized by a cylindrical disturbance source emanating from the inlet position ($R=0$, $Z=0$ in Figure 31). The strength of these pressure waves will be relatively weak such that their propagation speed can be characterized adequately by a constant wave speed, c, say the ambient speed of sound of air (1130 fps). These waves will interact with the solid boundaries or walls of the room, by reflecting and propagating back into the interior regions of the shelter. In Figure 31 the disturbance (shock front) has reflected from the back wall and is moving back toward the entrance. The disturbance has also reflected from the side wall and, in fact, has already reached the axis of symmetry at some positions in the shelter. The result of these reflections is to turn the blast induced flow such that the normal components of the velocity at the walls are zero. At this time an inlet jet is forming in addition to a swirl flow near the edge of the inlet. The swirl flow field is due to the formation of a vortex whose center is identified in this figure. The pressure disturbances will reverberate between the various solid boundaries of the room and decay in strength. These disturbances will also interact with the rather strong vortex flow. Shock tube experiments have shown that such an interaction generally results in the destruction (by dispersion) of the shock front and for this reason the more transient wave aspects of the flow disappears. Thus a description of the velocity field must contain a contribution which is referred to herein as the

112

"nonsteady" phase. This contribution exists from the time of shock arrival (a convenient zero time reference point) until a time of approximately 2H/c which corresponds to the double transit time of the disturbance within the room. This contribution must account for the air motion induced by the expansion of the pressure wave into the shelter interior and the modifying contribution made by the wall reflections.

Figure 32 illustrates the nature of the flow after the initial phase has ended. The flow is changing more slowly. The inlet jet is completely formed and extends further into the room. It has already adjusted to the finite length of the region available to it. The swirl flow region has grown in size and now occupies the entire shelter area. The center of the vortex is moving slowly toward the rear of the shelter. Thus two significant flow features are present at this time interval; a stabilized inlet jet flow and a moving swirl flow region. These naturally form two additional velocity contributing terms in the velocity field model.

Figure 33 illustrates the velocity field at a later time. The velocity of the air at the inlet region has decayed substantially. The movement of the vortex center has stopped due to its interaction with the back boundary; thus, the swirl flow has stabilized in position and is decaying in intensity. The path of the vortex center is shown in Figure 33 and indicates its rather well defined movement. Similar vector diagrams have been examined from other related numerical solutions and the above described general features are common to each solution. Unfortunately these available numerical solutions were not extended sufficiently in time to define the outflow aspects of the velocity field. It is clear that the jet flow is replaced by some type of sink flow (the sink being located at the inlet of the shelter) and that the intensity of the flows is greatly diminished. The swirl flow may persist for some short time after the outflow begins but no data are currently available to establish this aspect of the flow. If it does exist its intensity will probably be small.

The current velocity field model which was used in this study consists of four component parts defining: (1) the nonsteady blast diffraction effects, (2) the inlet jet flow, (3) the swirl flow, and (4) the outflow flow contributions. These parts have been written in a computer subroutine form for use in subsequent transport calculations. The following paragraphs present the most significant aspects of these component parts and are followed by a discussion of the method used to combine the parts. Due to the symmetry of the basic geometry the velocity field need only be defined for the reduced geometric case. Each submodel defines the velocity field components U and V at a given time, t and position (x,y). The velocity components U and V correspond respectively to an orthogonal x and y coordinate system whose origin is at the center of the inlet on the front wall. The positive x-direction is into the room toward the back wall of the shelter, thus $0 \leq x \leq H$. The positive y-direction is from the center of the inlet toward the side wall, thus $0 \leq y \leq W$.

The nonsteady flow submodel is applicable during the time interval $0 \leq t \leq 2H/c$ during which the inlet velocity, V_o, is varying slowly with time (see Figure 29). An examination of the available numerical solutions during this early time period indicated that the velocity distribution behind the initially expanding disturbance (i.e., no wall reflections) is primarily radial in direction and increases in intensity from an essentially zero value at the shock front to the inlet value at the origin. The wave shape is relatively constant, and nearly linear, hence a self-similar solution in the variable (R/R_s) can be formulated, where R is the radial distance of the position (x,y) from the origin and R_s is the range of the disturbance. This range is simply the product of the wave speed and the elapsed time $(R_s = ct)$ recalling that the flow starts when t=0. The development procedure was iterative in nature, being modified as the various submodels were combined and adjusted to obtain a reasonably good comparison over the full field of interest and for the various times at which velocity vector data was available. As a result the self-similar solution for the velocity

114

magnitude, V_n took on the form

$$V_n = V_2(1 - \frac{R}{R_s})e^{-\frac{R}{R_s}} \cos(0.8\alpha), \qquad 0 \leq R \leq R_s \qquad (17)$$

where V_2 is the contribution of the inlet velocity V_o allocated to the nonsteady flow contribution and α is the position angle measured from the x-axis. The wall reflections are flow adjustments dictated by the physical requirement that the normal component of the velocity at the wall vanish. This requirement could be met easily by using a method of images. Thus the velocity at a given point could be made up of many vector contributions. Eight sources were selected, two in the x-direction and four in the y-direction. Only two were needed in the x-direction since the applicability of the nonsteady model was prelimited by $t \leq 2H/c$. Four image positions in the y direction will allow for four reverberations in this direction and thus be applicable to narrow shelters where $ZW \leq H$. Narrower shelter geometries can be treated by increasing the number of source points. It should be noted that for each of the sources used, the velocity contribution vanishes whenever the apparent range (distance from the source) is greater than the disturbance range.

The current jet flow submodel was patterned after the jet model described in Ref. 47. The latter model corresponded to a free standing jet and is applicable for shelters which are very large compared to the inlet width, B, of the jet. These types of jets can be very long, in fact at a distance of 100B the flow velocity is still approximately 10 percent of the inlet value. Since the shelter sizes and configurations of interest of the order of say 10B, the back and perhaps the side walls will influence the jet flow field. The analytic form used in Ref. 47 was simplified slightly with respect to the velocity distribution at any distance x from the inlet. The primary influence of the back wall is to decelerate the jet flow such that the velocity vanishes at the back wall. The current version of the jet submodel merely applies a factor $(1-x/H)$ to the free jet solution to satisfy this requirement; the free jet conditions being defined by an inlet magnitude

V_1 which represents that portion of the inlet velocity, V_o, that is allocated to the jet flow contribution. The free jet is narrow enough such that side wall interactions will not occur for the shelter aspect ratios (W/H) being considered. An earlier version of the jet submodel was based upon an image procedure to satisfy the zero velocity requirement at both the back and front wall. This model required some 20 to 40 images (i.e., velocity contribution) plus a final correction procedure to obtain flow details similar to those obtained by the current simple version.

The development of the swirl flow submodel represents the most difficult flow regime to model because of its rather long-lasting moving nature and because it covers the entire shelter area. The current version may require some additional modification, although their effects may be small. The motion of the vortex center is rather well defined. After a short induction period it moves at a relatively constant speed, until it approaches its final position of approximately 0.7H. The path occurs at a near constant value of y of approximately 1.8B for wide rooms. An adjustment was introduced for narrower rooms such that when W approaches B (an unrealistic width) the value of y was equal to B. The speed at which the vortex center moves is approximately 200 to 250 fps for the various solutions and times examined; a value of 225 fps was selected for the current model. It should be noted that this narrow range of vortex center speed is consistent with vortex motion observations made many years ago while studying shock diffraction effects on objects in shock tube experiments (i.e., approximately 20 percent of the shock velocity). The direction of flow (i.e., the streamlines) in the swirl flow region is roughly elliptical around the center of the vortex and the flow extends rather deeply into the corners. This feature was approximated by selecting a fourth order relationship between the variables Δx and Δy which define the position relative to the vortex center. In this manner the flow direction, that is the ratio of the velocity components, was defined for every point within the limiting streamline. The velocity was assumed to vanish outside of the limiting streamline; that is, at the corner regions. The

116

magnitude of the velocity also depends upon the absolute distance of the position (x,y) from the center of the vortex. The magnitude of the velocity is essentially zero at the vortex center and then increases in a roughly linear fashion until it reaches its maximum magnitude at a distance approximately equal to B. For larger distances the velocity decreases at nearly constant circulation conditions. Finally some minor adjustments were incorporated into the magnitude calculation to reflect the fact that the intensity of the swirl flow increased with vortex center displacement.

The outflow submodel is relatively simple in concept and does not include any swirl flow features. Basically during the outflow phase a sink type of flow should exist. The strength of the sink is given by the value of the inlet velocity. The flow will be primarily radial in direction and the magnitude will decrease with increasing distance from the sink. The magnitude of the velocity should be essentially zero at the walls of the shelter. Two factors were used to reduce the magnitude of the velocity. First a simple finite sink type relationship was used. Specifically this took the form

$$\left(\frac{1}{1 + \frac{D}{2B}} \right) \tag{18}$$

where D is the distance from the origin. Secondly a factor to account for the finite size of the room was introduced. This factor took the form

$$\left(1 - \frac{D}{D_m}\right) \tag{19}$$

where D_m was the maximum room dimension along the ray passing through the point of interest. In this manner the zero velocity condition at the walls was achieved.

In describing some of the above velocity submodels, reference was made to a contribution of the inlet velocity which was allocated

to the particular flow regime. The intensity of the flow and its variation with time have been keyed to the intensity of the inlet flow. The inlet flow for a given condition was determined from cavity filling calculations. Whenever more than one flow regime coexists and contributes to the inlet flow magnitude the component parts (such as V_1 and V_2 for the jet flow and nonsteady flow contributions) must make up the whole (i.e., equal to V_o). During the nonsteady flow period $0 \leq t \leq 2H/c$ when the jet flow is in a growth phase, the driving velocity for the nonsteady flow was expressed by the following relationship,

$$V_2 = V_o (1 - \frac{tc}{2H})^2 \tag{20}$$

The swirl flow growth was also related to the intensity of the inlet flow; however, since this flow does not directly involve the mass flow at the inlet, its relationship is not necessarily influenced by other flow regimes. The driving velocity, V_3, was defined by the relationships

$$\left.\begin{aligned} V_3 &= V_o \frac{tc}{4H}, & 0 \leq t \leq 4H/c \\ V_3 &= V_o, & 4H/c \leq t \end{aligned}\right\} \tag{21}$$

During the outflow period all of the inlet flow velocity is allocated to the outflow submodel since it is the only flow regime which is assumed to exist at that time. Finally, after the positive phase duration of the overpressure has elapsed, the inlet flow is very small and has been assumed to vanish. In this time interval it has been assumed that a quiescent flow state exists within the shelter and thus the velocity is assumed to vanish everywhere.

The above relationships as well as some of the details of the submodels have been developed and further modified to achieve as accurate a comparison with the existing velocity information as possible. Although this development is not necessarily complete,

118

it appears that an acceptable level of accuracy has been achieved. It is difficult to make any blanket statements regarding accuracy; however, the reader is entitled to an impression in this area. For this reason the following estimate of the accuracy is presented. For the vast majority of the flow region, especially where the magnitude of the velocity is the largest, the magnitude of the velocity is accurate to approximately ± 25 percent and its direction is accurate to approximately ± 20 degrees. Uncertainties of these magnitudes will probably exist whenever the conversion of any real life shelter and the related weapon effects details are idealized to arrive at a specific prediction of the flow environment.

4.3 TRANSLATION ENVIRONMENTS IN SHELTERS

The translational effects of objects or people located within the subject shelters has been partially evaluated by using a simple drag type of translational model and neglecting the effects of gravity, rotation and ground interactions. Other, more complex transport models can be applied with relative ease. A computer code was written for this drag type model which called upon the previously discussed air velocity description subroutines to define the aerodynamic condition at the current location of the object. The inlet flow velocity histories (see Figure 29) were curve fitted and a number of parameters were established with which to define this flow as a function of both overpressure and shelter volume-to-area ratio. The current version of the transport code is applicable to the basic and reduced shelter geometries identified in Figure 28. In each of these cases the solid walls must be identified in order that an impact condition can be identified. The air velocity model does not discriminate between a solid wall and an axis of symmetry, since in both cases the normal component of the velocity at these boundaries is equal to zero. It is expected that the current code will be modified to treat a variety of expanded shelter configurations which are characterized by multiple inlets. The current code does consider rebound and multiple impact conditions; however, this feature has not been used as yet to evaluate impact conditions within the shelter.

A series of transport impact calculations were made for shelter cases C,D and E (see Table 13). The drag characteristics of the object were similar for those used in Ref. 16 for the case of a standing man. The results are presented in Figures 37 through 40 and are expressed in terms of trajectories and the magnitude of the normal component of the impact velocity for the first impact. The latter value is indicated for a number of initial positions of the object within the shelter and several contours of constant impact intensity are shown. These correspond generally to the 10,25,50 and 100 fps values and represent nominal bounds for injury and fatality conditions for both head impact and total body impact conditions. The angle of incidence at the time of impact is evident from the trajectory results. Other details, such as time of impact and velocity history are available but are not presented with these initial results.

Figure 34 presents the results for shelter Case E2 when it is exposed to a 6 psi overpressure blast environment. The maximum overpressure which exists in the shelter in this instance is approximately 4.7 psi (see Figure 30). The most severe impact condition occurs, as expected, at those initial object positions just inside the inlet. These objects move straight back and impact the rear wall. It should be noted that although the impact velocities for objects located along the axis of symmetry near the back wall may be acceptably low; these objects may be subject to object-to-object impacts from objects closer to the inlet and thus generate an unacceptable impact condition. These calculations show that somewhat less intense impacts occur for another region which is located near the rear of the shelter and at the edge of the jet. Similar results for this shelter case are shown in Figure 35 and 36 respectively for the 10 and 15 psi overpressure exposure situation. The peak overpressure within the shelter for the latter case is approximately 10 psi. The intensity of the impact velocity has increased appreciably and the size of the critical area has grown. Figure 37 presents some additional trajectory details for the latter condition and identifies the boundary walls at which objects initially located in certain parts of the shelter

120

V/A = 500 ft   10 < V_i < 25 fps

0.6

4.0   0.2

11.7

1.0   0.7

←Jet Boundary

7.3

34.6   0.6   0.1

a) Trajectories   b) Impact Velocities, V_i (fps)
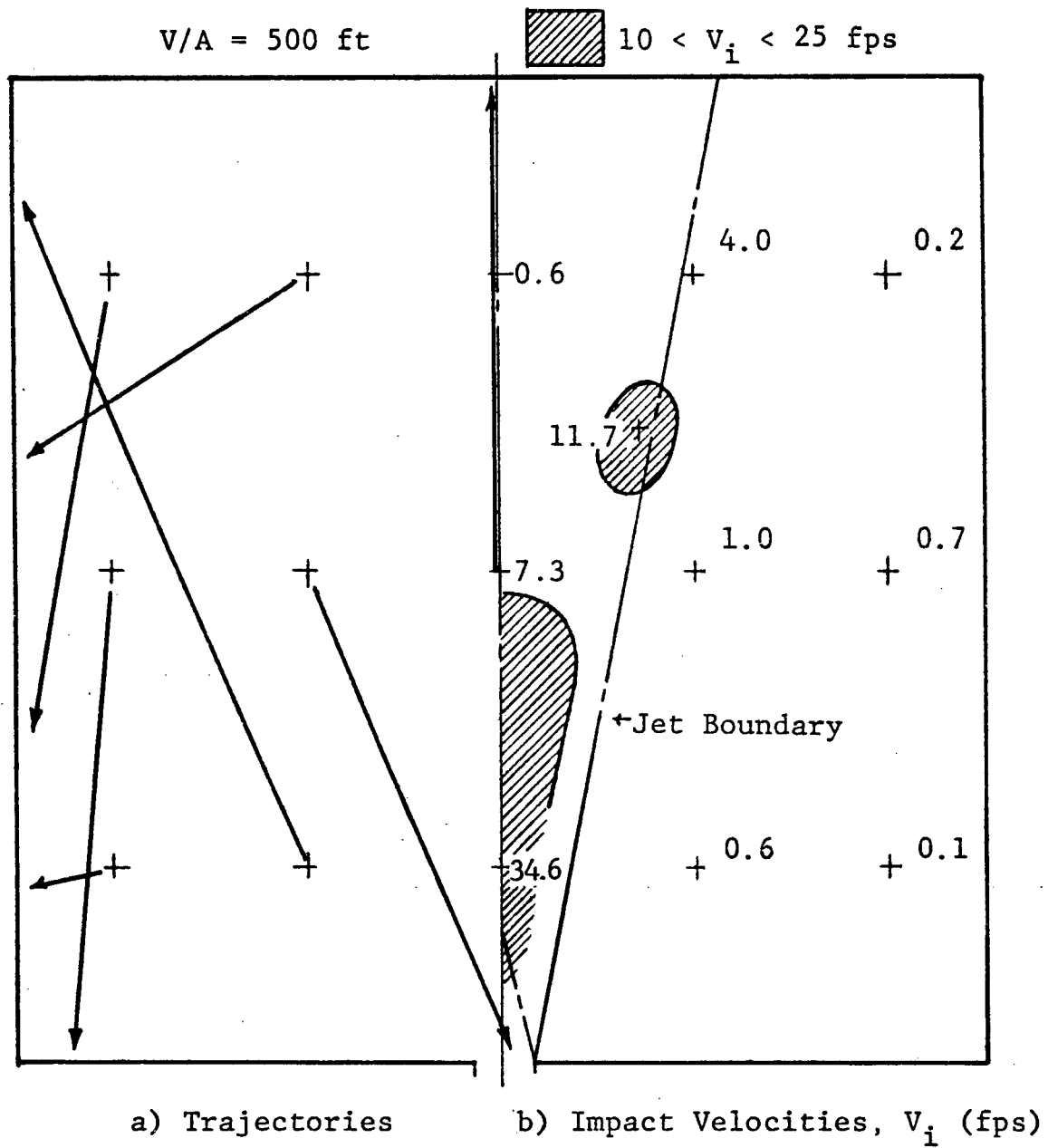
Figure 34   Transport Environment - Case E2 - 6 psi

121

V/A = 500 ft

10 < V_i < 25 fps

25 < V_i

a) Trajectories

b) Impact Velocities, V_i (fps)
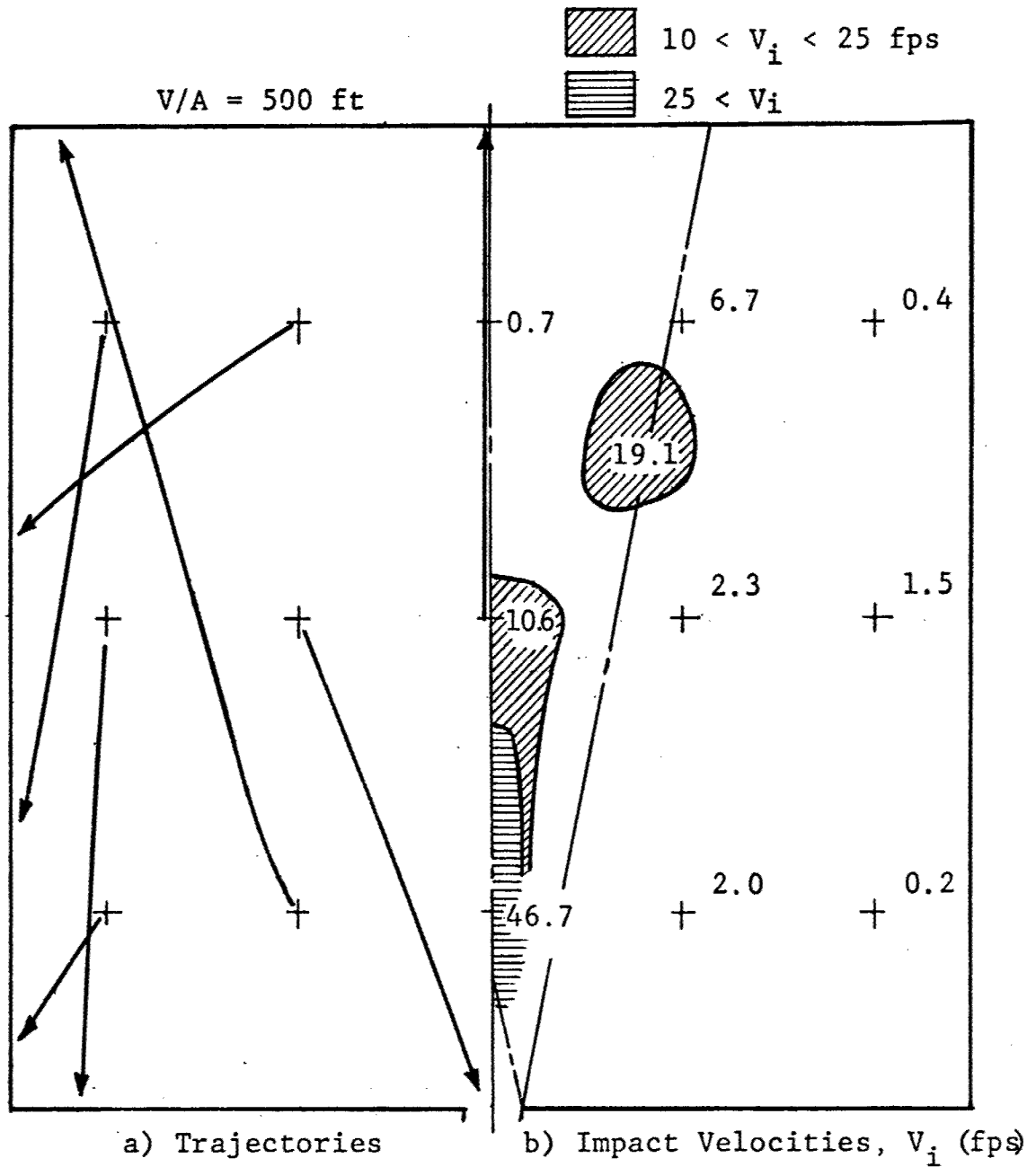
Figure 35   Transport Environment - Case E2 - 10 psi

122

V/A = 500 ft

$10 < V_i < 25$ fps

$25 < V_i$

a) Trajectories

b) Impact Velocities, V_i (fps)
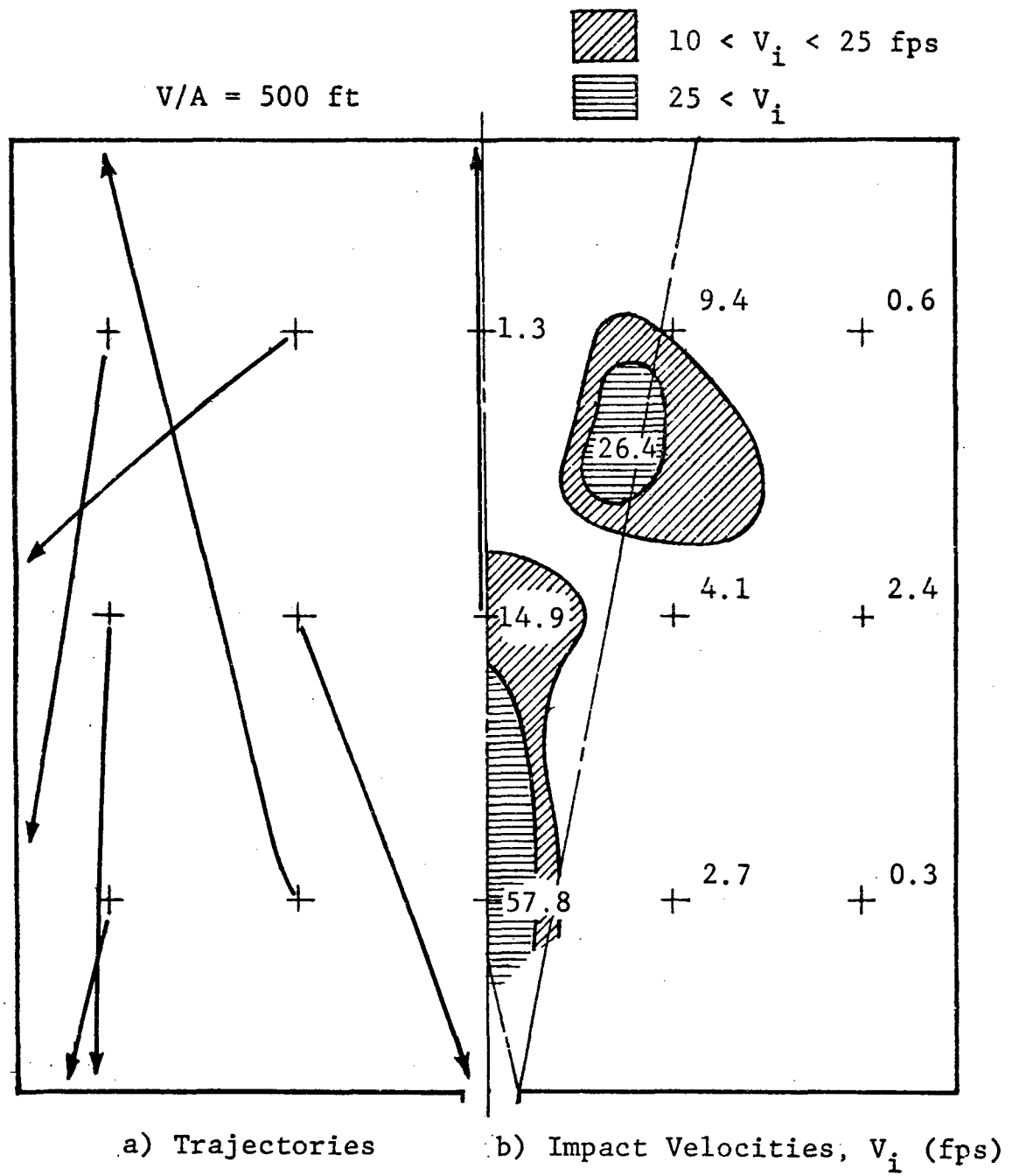
Figure 36   Transport Environment - Case E2 - 15 psi

a) Trajectories

b) Impact Boundary

Side Wall

Front Wall

Back Wall
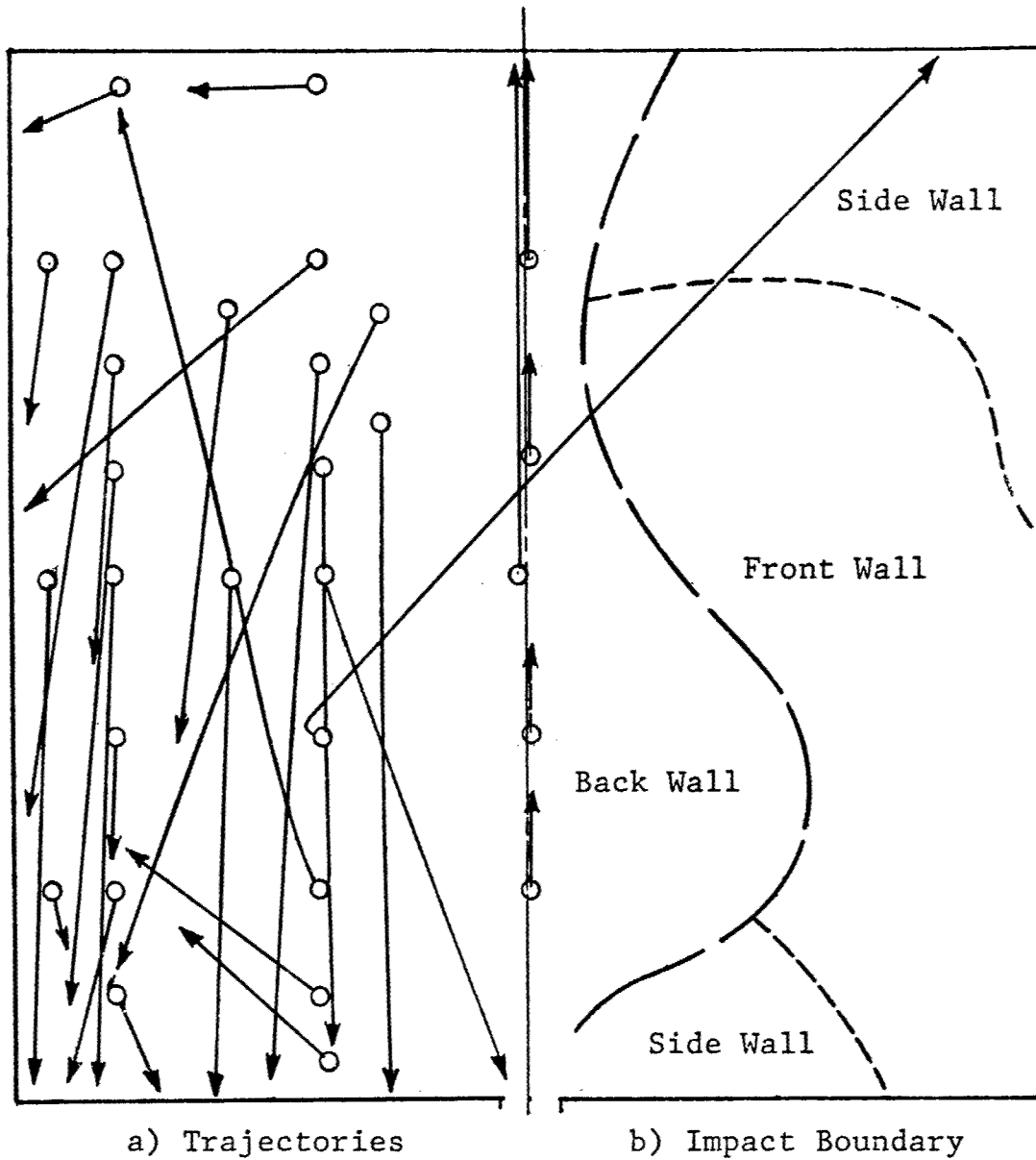
Side Wall

Figure 37   Trajectory Details - Case E2 - 15 psi

will impact. Many of the side wall impacts occur at very shallow angles hence the normal velocity component at impact is rather low eventhough the absolute velocity of the object may be fairly large. This somewhat glancing impact will not significantly impede the motion of the object and a second impact, which may be much more severe than the initial one, can be expected to occur. Most of the objects will impact the front wall suggesting that some improvement in survivability can be achieved by appropriately treating that boundary, or conversely by avoiding the placement of hazardous equipment (hazardous from the point of view of impact) along that wall.

The results for shelter case El are presented in Figure 38 for an overpressure exposure of 15 psi. This shelter is identical to that of case E2 except the inlet area and width is smaller by a factor of two. The intensity of the corresponding impacts are reduced and the size of the critical area is smaller by roughly a factor of two. The influence of the absolute size of the room is shown by the results presented in Figures 39 and 40. Figure 39 presents the results for a larger room (shelter case C2) and clearly shows that the translation-impact environment is much more severe than that for a smaller shelter. The reason for this may be the fact that the duration of the intense flow is longer and more distance and hence time is available with which to accelerate the object. A tumbling object transport model may yield less severe transport and impact conditions. Figure 38 presents results for a small shelter (shelter case D2), with a rather small inlet, and demonstrates the somewhat milder translation environment when compared to those of the related case (case E2). Both cases E2 and D2 have volume-to-area ratios of 500 ft whereas a value of 750 ft occurs for case C2.

4.4 SUMMARY, CONCULSIONS AND RECOMMENDATIONS

The transient air velocity field has been modeled which exists within a conventional basement type shelter when it is exposed to the air blast effects from the detonation of a nominal megaton-range

V/A = 1000 ft

10 < V_i < 25 fps

25 < V_i

1.0   4.0   0.2

13.0

12.3   2.0   0.2

45.5   2.1   0.2

a) Trajectories   b) Impact Velocities, V_i (fps)
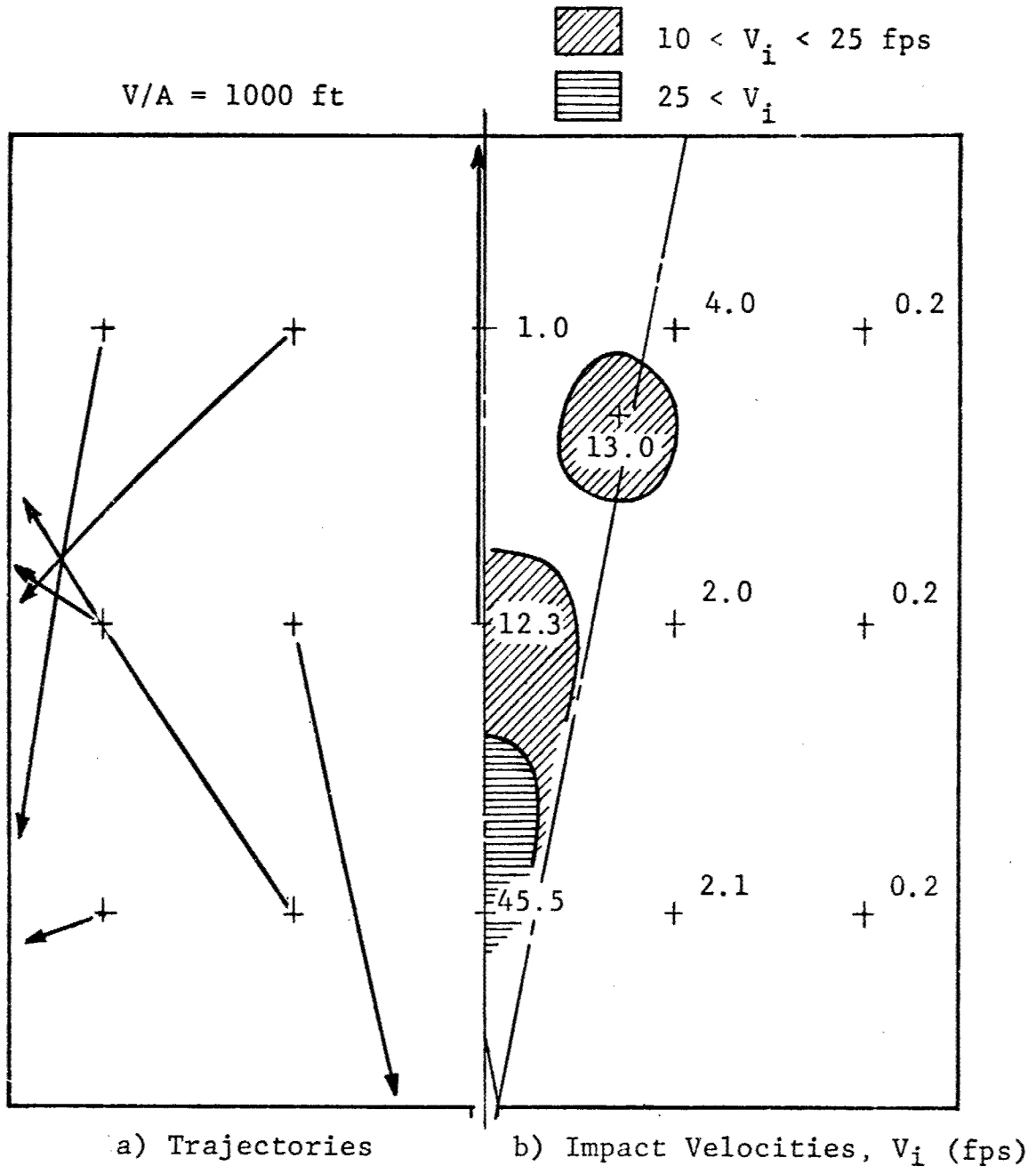
Figure 38   Transport Environment Case E1 - 15 psi

a) Trajectories

b) Impact Velocity, V_i (fps)
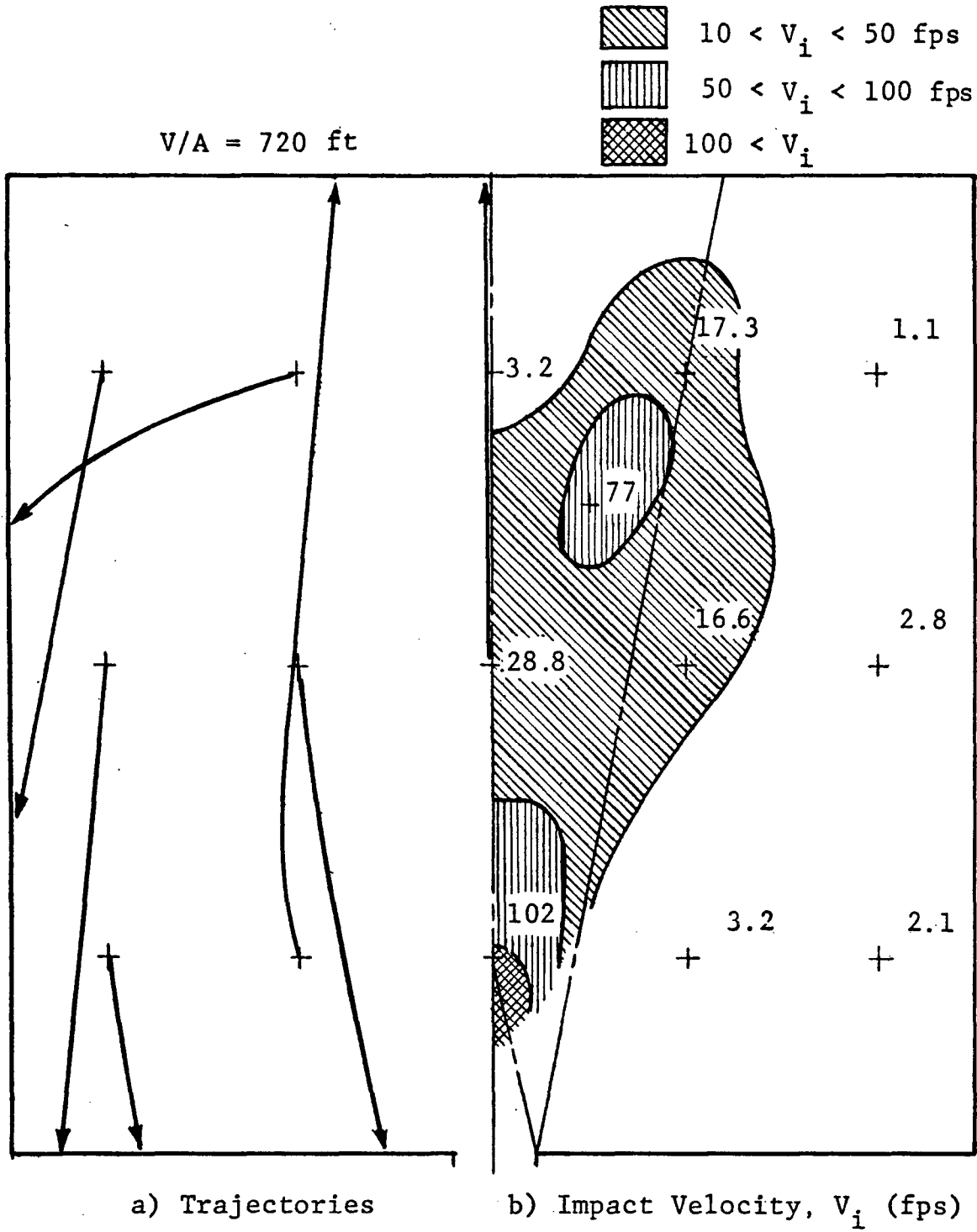
Figure 39   Transport Environment - Case C2 - 15 psi

V/A = 500 ft   ▨10 < V_i < 25 fps

a) Trajectories   b) Impact Velocity, V_i (fps)
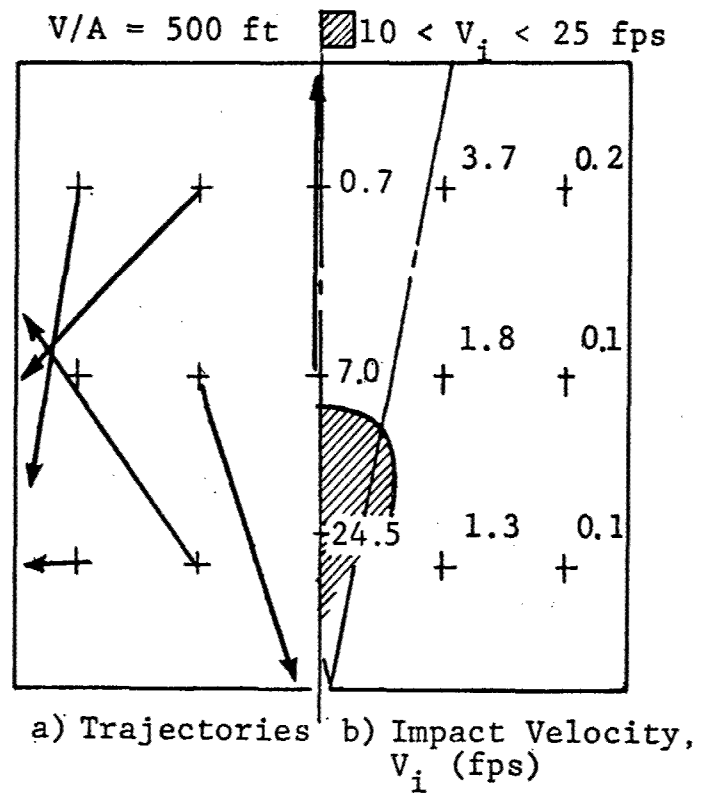
Figure 40   Transport Environment - Case D2 - 15 psi

nuclear weapon in its Mach region. This airflow model was used
in conjunction with a simple drag type transport model to examine
the translational and impact behavior of objects (i.e., personnel)
located at various positions throughout the shelter. The shel-
ter geometries treated to date were simple single-inlet shelter
configurations in which the inlet was located in the center of
one wall. A variety of shelter sizes were examined and the in-
tensity of the first wall impact was determined as a function of
the initial position of the object within the shelter. In this
manner critical regions in which unacceptable impact conditions
corresponding to head impact or total body impact injury and/or
fatality criteria have been identified for several free-air over-
pressure levels. Initial locations just inside and along the axis
of the inlet are clearly the most hazardous locations within the
shelter. However, another region in which impact conditions are
quite severe exists at the edge of the inlet flow jet near the
rear of the room. The intensity of the impact conditions and
the size (on a percentage basis) of the critical areas are larger
for the larger shelter sizes which were investigated.

The air velocity model which was developed is applicable to
a wide range of shelter configurations. These configurations are
those which can be constructed by the symmetric or alternate com-
bination of a reduced basic geometry. In this manner one or more
inlets can be placed on one or two (the opposite) walls of the
shelter in such a way that the inlets are at the center of the
wall, at one or both ends of the wall, or distributed in a uniform
manner along the wall. The inlet sizes must all be equal when
referenced to the basic geometry. A more sophisticated transport
model, such as a "tumbling man model" can readily be incorporated
into the analysis. The currently used simple drag type transport
model is adequate for the early portion of the translational phe-
nonenon. Since, for the severe impact conditions the time of free
flight is short (1 or 2 sec. maximum) the results of the
current model are applicable. The current model is also capable
of treating multiple impact conditions. This effect is important
whenever the first impact is a glancing impact, a situation which

generally underrates the severity of the potential hazard. The combined airflow, object transport and impact model will provide an adequate tool with which to assess the survivability of personnel in shelters due to airblast induced motions. This model may also be used to develop procedures and/or adopt conditions in order to eliminate or mitigate the hazardous effects which can occur.

This initial effort to establish the probability of survival within conventional basement type shelters when subjected to the blast effects from megaton-range nuclear weapons has shown that a significant hazard does exist and has identified some of the mechanisms and parameter values which significantly influence the hazard level. In some respects the models which were used initially were relatively simple and it is therefore recommended that these models, or features of these models be expanded or modified to obtain a more realistic representation of the hazard and thus improve the reliability of the survivability assessment.

The hazard produced by the collapse of the floor slab above the basement shelter area was treated without considering the influence of pressure buildup within the shelter. Such a pressure buildup could be produced by either filling through entranceways or by the blowby gasses during the failure or initial dropping phase of the slab collapse. Furthermore, it is reasonable to expect that some substantial nonstructural elements within the basement may provide some additional protection for the occupants by preventing the slab from covering the entire floor area during its total collapse.

The flow-induced translational effects models have been limited to single basement cavities as well as other flow and geometric simplifications. The models should be expanded to include the folflowing factors:

● Complex Flows:
   Flow through multiple inlets
   Flow through series cavities

130

- Interior partition failure
- Furnishings
- Partial basements.

The present models treat multiple inlets which are identical in their flow characteristics and thus any flow-through effects which will be induced by exterior pressure differentials cannot be examined. The geometric simplification of basement shelters as simple cavities is also greatly restrictive and can be readily expanded to treat a series of cavities or rooms. Such a model would permit the examination of loads on interior walls and thus allow for the inclusion of some wall failure effects. The current model does not adequately treat partial basements in that these types of basements may have inlets which possess rather local -- three-dimensional characteristics. Since these dimensional non-steady flows cannot be treated economically, the development of some rational two-dimensional equivalence factors or models will permit a survival evaluation for this class of basement shelters. Finally, we recommend that the range of weapon yields should be expanded to provide for some estimate of the influence of this important parameter.

The above suggested improvements are recommended for future activities in that they will significantly improve the degree to which the "real world" shelter environments are assessed and will provide a more realistic representation of the subject hazard. It is recognized that additional complexity or model sophistication will not necessarily improve the quality of the answer sought, however the above recommendations are intended to incorporate effects which are considered to be both significant and realistic.

CHAPTER 5

AN EXAMINATION OF THE TORNADO DEBRIS HAZARD

5.1 INTRODUCTION

Tornadoes are one of a number of violent natural phenomena which cause widespread damage, injury and death on the North American continent. This chapter examines one aspect of a destructive mechanism, namely the debris hazard, associated with tornadoes. This was done in an attempt to obtain a better understanding of the details of the mechanisms and thereby generate the opportunity to mitigate its destructive effect on the public.

The basic phenomenon of tornadoes, the wind and pressure loadings and the response of structures and equipment to the point of catastrophic failure, the aerodynamic transport of objects and debris, and the susceptibility of potential targets to the imposed debris impact environment are all complex physical problems. None-the-less each of these aspects of the overall problem are governed by the laws of physics and are to various degrees subject to statistical variations and uncertainties. For this reason the evaluation of the hazard resulting from debris produced by a tornado exposure can be approached effectively by a combination of deterministic calculations and probabalistic estimates. Furthermore, the approach can be applied at a variety of levels of precision and sophistication.

The sequence of tasks needed to evaluate the hazard produced by flying debris due to a tornado exposure are presented in Figure 41. There are three major inputs needed for this evaluation: (1) an adequate description of the basic storm environment, (2) identification and characterization of all major potential debris sources, and (3) identification of the potential target entities and their susceptibility to debris impact. The basic free-field tornado environment involves both a transient wind and pressure field. Since the debris sources and target entities will generally be located at or near grade level only the near surface storm

133

(I) Storm Description

```
┌─────────────────┐
│    Tornado      │
│   Environment   │
└─────────────────┘
```

(II) Potential Debris Sources

```
┌─────────────────┐        ┌─────────────────┐
│ "Soft" Structure│        │      Wind       │
│ Characteristics │        │   Environment   │
└─────────────────┘        └─────────────────┘

          ┌─────────┐
          │  Loads  │
          └─────────┘

     ┌─────────────┐              Debris
     │  Failure    │            Production
     │  Response   │
     └─────────────┘

     ┌─────────────┐        ┌─────────────────┐
     │   Debris    │        │     Debris      │
     │Characteristics│──────│    Transport    │
     └─────────────┘        └─────────────────┘
```

```
                              ┌─ ─ ─ ─ ─ ─ ─ ─ ─┐
                              │  Overall Site   │
                              │ Characteristics │
                              └─ ─ ─ ─ ─ ─ ─ ─ ─┘
```

(III) Potential Targets

```
┌─────────────────┐        ┌─────────────────┐
│ Critical Target │        │Debris Environment│
│ Characteristics │───────▶│   at Target     │
└─────────────────┘        └─────────────────┘

┌─────────────────┐  ┌─────────────┐  ┌─────────────┐
│     Target      │  │   Target    │  │   Hazard    │
│  Susceptibility │─▶│  Response   │─▶│ Evaluation  │
└─────────────────┘  └─────────────┘  └─────────────┘
```

Figure 41   Activity Sequence for Evaluating Debris
             Hazard Resulting from a Tornado Exposure

environment will be of direct interest. The primary driving force for the transport of the debris will be the aerodynamic forces acting upon an airborne object, thus an adequate description of the wind velocity field is needed. However, since the vertical component of the velocity is generally much smaller than the horizontal component it is the latter component which must be established with some reasonable degree of accuracy. It must be recognized that surface boundary layer and other ground interaction effects must be eventually considered. It follows then that the motion of the debris will be largely in the horizontal direction.

The transient loads acting upon neighboring structures and equipment will depend upon the combined effects of the pressure field and the interaction of the velocity field with the obstacle. The load details will most likely be dependent upon the gross response, that is, the failure of the structure as well as on the venting and filling of interior regions of the structure. The structures will respond in many instances to the imposed transient loads and fail relatively rapidly, yielding a variety of physical objects. The objects, called debris or missiles, will exist in a distribution of size, shape, weight and density, and will be released (i.e., potentially airborne) at various times, orientations, and locations with a spectrum of initial velocity conditions. Other, nonstructural sources of debris must also be considered. This aspect of the problem is referred to as the "debris production" problem (see Figure 41). Its solution will culminate in a total characterization of the debris.

The characterization of the debris together with an adequate definition of the transient wind environment will then permit an examination of the transport of the debris to be made. This can be done in general terms so as to develop an insight into the aerodynamic characteristics of classes of debris and to establish limits and other details of debris trajectories and velocities.

The application of these transport characteristics together with a description of the potential targets and debris sources can then be used to establish the debris environment at the target. The potential debris source data must be converted via the debris production analysis to the appropriate time of release and related debris characteristics form (e.g., size distribution, etc.). The debris environment at the target and target susceptibility data will permit the target response to be evaluated. In this manner the debris hazard resulting from an exposure to a tornado can be assessed.

This study is, for various reasons, restricted in scope. It is limited to: (1) a discussion of the wind environment; (2) predictions of debris transport characteristics for a simple drag behavior; (3) a brief comparative evaluation of the effect of two-dimensional lifting body influences upon debris transport characteristics; and (4) the application of the above results to a hypothetical target/debris source configuration. The latter effort demonstrates the nature and severity of the debris environment at a number of targets and begins to provide an insight into the debris hazard as this relates to injuries, fatalities, and property damage.

5.2 TORNADO WIND ENVIRONMENT

A simple description of a tornado might define it as a violently rotating column of air, pendant from a cumulonimbus cloud and nearly always observable as a "funnel cloud" or tuba. On a local scale, it is the most desctructive of all atmospheric phenomena. Its vortex, commonly several hundred feet in radius, whirls usually cyclonically with wind speeds estimated at 100 to over 300 mph. The strength of the vortex and the cyclonic flow field may increase as the tornado translates over the terrain. These speeds will generally be some small fraction of its maximum rotational velocity (perhaps 30 to 60 mph). The strength of the flow may then reach a maximum intensity and experience a decay. The tornado vortex and its significant velocity field may separate from the ground plane only to reform again at a later time.

136

The nature of tornadoes has been examined, and much literature has been written des-ribing the formation and the structure of tornadoes and their damage potential (see Ref. 50, 53, 57, 58, 59, 60, 61)

Tornadoes are rather variable in their size, structure and behavior, and are more poorly defined than most other extreme wind or storm conditions. Fujita (Ref. 51) has parameterized tornadoes by the following variables

1. maximum rotational velocity at a given height above the ground plane,

2. radius of maximum rotation velocity

3. translational velocity

4. duration of rotational velocity in excess of variable 1 above, and

5. fractional variation of gust.

The maximum wind speed would be determined by the maximum vector sum of the rotational and translational wind components multiplied by the gust factor. Typically the duration of extreme winds will be in the range of from several minutes to perhaps greater than 1 hour. Items 4 and 5 above can be incorporated into item 1 in order to establish a "worst case" situation. The cyclonic motion of the air will lower the static pressure field, such that the pressure will be the lowest at the vortex axis.

The detailed structure of the tornado cannot be readily observed precisely in nature due to the unpredictability of their occurrence in space and time, however some researchers have established sim-ulated flow fields in the laboratory to study the vortex dynamics. The work of Ting and Chang (Ref. 52) has shown that, as is ex-pected, the flow is considerably more complex than a simple plane Rankine vortex. In particular the boundary layer or surface rough-ness characteristics are important, as are the vertical or sink flow characteristics which are due to larger scale atmospheric condi-tions (i.e., pressure gradients). The current state-of-the-art in describing the velocity and pressure environment associated with a tornado is essentially restricted to the use of the Rankine

vortex model. Thus, the influence of the surface boundary layer is for the most part neglected. The sink or convergence flow feature can be readily introduced; however, this effect is generally not nearly as significant as the cyclonic flow field.

The conversion of the free field environment to specific loads acting on a structure is essentially in its infancy. Reynolds (Ref. 53) has attempted to correlate the observed damage with the characteristics of these idealized flow fields. The indication of these examinations is that the nature of the loads produced by these flow fields is substantially correct. McLaughlin (Ref. 54) has used such simple flow fields to estimate the pressure field variation as a function of distance from the center of the vortex. The application of this effort was directed toward the design of nuclear power plants. This flow field description is also applicable to the study of the transport of tornado-borne debris and missile trajectory and terminal ballistic determinations.

The simplified Rankine vortex model, which will be used initially in this effort, consists of a flow field of constant circulation outside of the tornado core, thus

$$UR = C, \quad R \leq r \tag{22}$$

where:

U = the rotational velocity component
r = the radial distance from the axis of the vortex
C = circulation ($\cong 10^5$ ft^2/sec)
R = core radius

The flow inside of the core is one of constant angular momentum, thus

$$U/r = \Omega \qquad 0 \leq r \leq R \tag{23}$$

where

Ω = the angular momentum

The intensity of the tornado can be specified by the maximum rotational velocity U^*, hence the radius of the core is given as:

$$R = \frac{C}{U^*} \tag{24}$$

This rotational field, for which the above velocity is the tangential component, moves across the terrain at a velocity, U_t. This translational or storm speed component, when added algebraically to the maximum rotational velocity yields the maximum windspeed, $U^* + U_t$. This idealized (horizontal) velocity field is illustrated in Figure 42. This vortex model can be used to establish a corresponding pressure field and both in turn can be used to estimate the nature and intensity of the transient pressure fields acting on objects such as buildings. This aspect of the problem is important in evaluating the response and failure modes of potential debris source structures, equipment, and the consequence of these velocity fields and debris on people. However, due to technical and time limits on this exploratory effort, this aspect of the problem has been set aside. Rather, a broad class of debris characteristics will be assumed to exist and then transport behavior will be examined and corresponding hazards discussed.

5.3 DEBRIS CHARACTERISTICS

When a body is immersed in an air stream it will be subjected to a variety of forces and moments which will depend upon its shape and orientation relative to the airstream as well as upon the air density and relative velocity between the object and the air stream. For objects which are grossly spherical in shape, the primary reaction will be a drag force. For moderately slender and lifting bodies, lifting forces and turning moments become more significant, however with few exceptions, drag forces will always be important. This will certainly be the case for most tornado generated debris. Thus a great deal should be learned from the examination of a simple drag type aerodynamic model. The drag force, F_d, for such a model is simply:

$$F_d = \frac{1}{2}\rho_a V_r^2 A\ C_d \tag{25}$$

where

ρ_a = air density

V_r = magnitude of the relative velocity between the air and the object
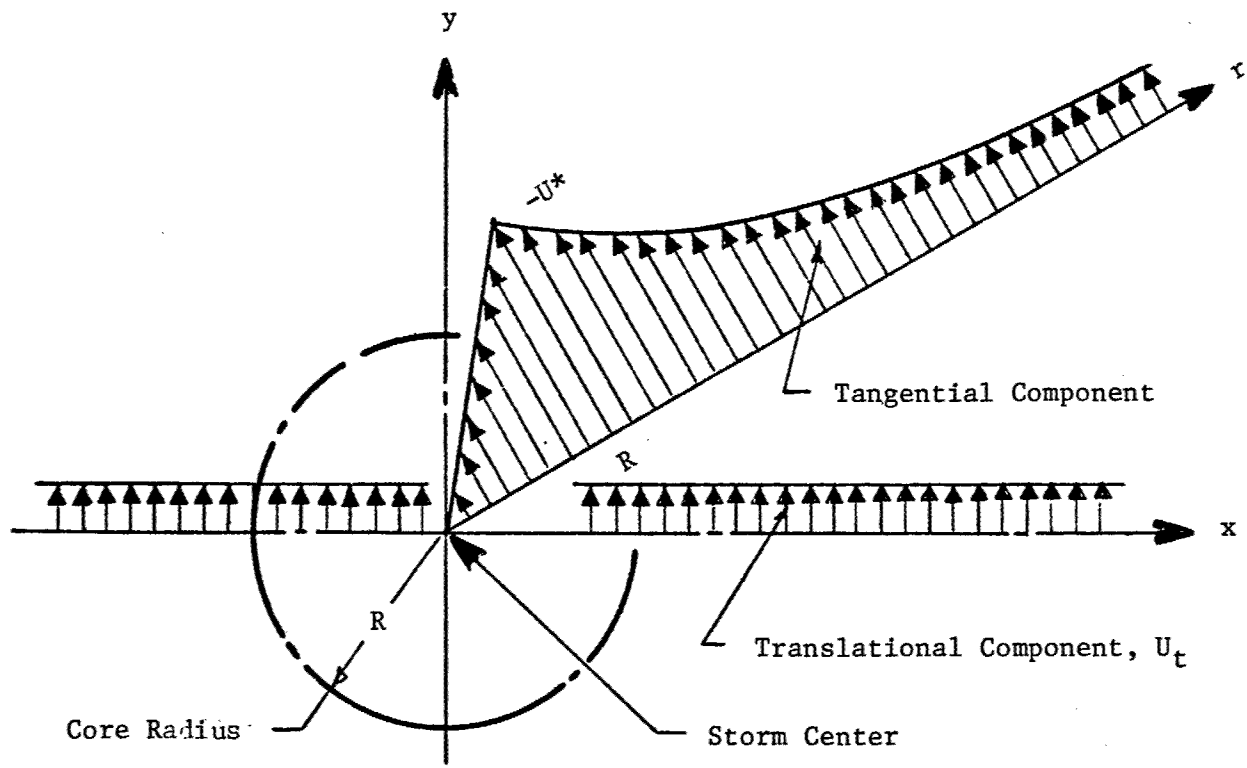
a) Velocity Field
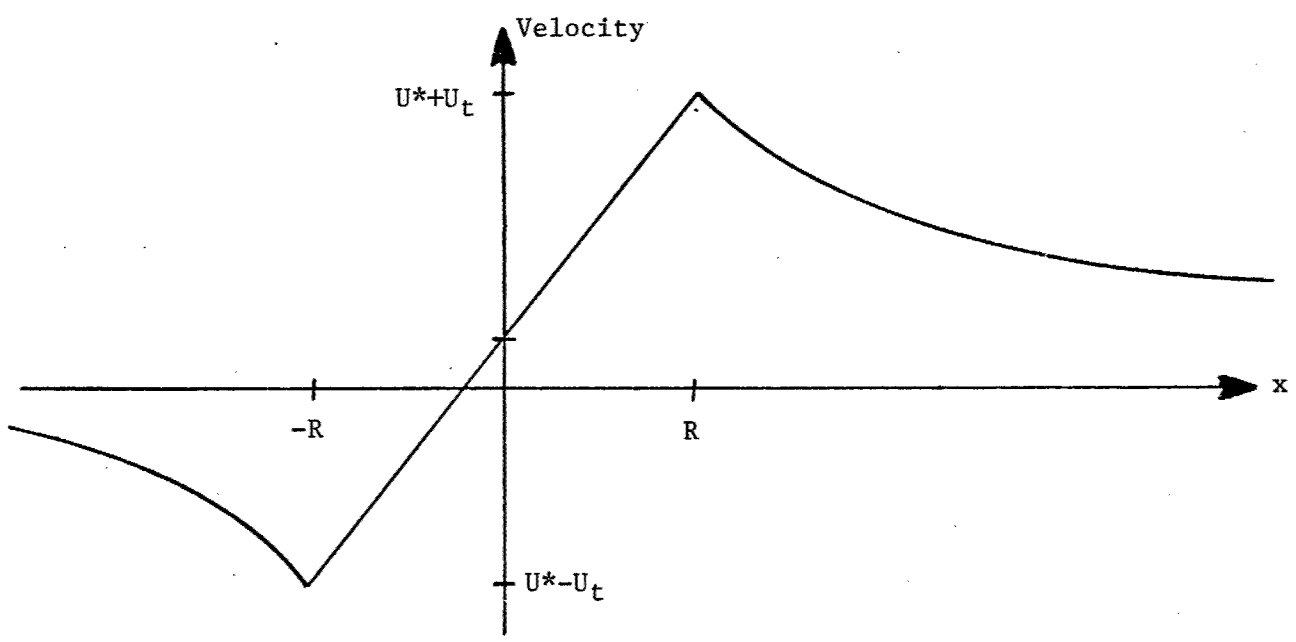
b) x-Axis Velocity Profile

Figure 42 Idealized Velocity Field

A = projected area of the object in the direction of the relative velocity vector

C_d = drag coefficient

The resulting acceleration is given by:

$$\frac{dV}{dt} = \frac{F_d}{W_d} \qquad (26)$$

where

W_d = weight of the object
V = absolute velocity of the object
t = time

and occurs in the direction of the relative velocity vector. This acceleration, together with an appropriate definition of the velocity, is

$$\frac{ds}{dt} = V$$

where s is the displacement (occurring in the direction of the relative velocity vector) and initial conditions (location and velocity) will suffice to define the trajectory and motion history of the object. Before examining the motion characteristics it will be of interest to consider the characterization of potential tornado debris in light of the above simple drag model. By combining Equations (25) and (26) and grouping the variables,

$$\frac{dV}{dt} = \frac{1}{2}\rho_\infty V_r^2 \left\{ \left(\frac{\rho_a}{\rho_\infty}\right) \cdot \frac{C_d}{(W_d/A)} \right\} \qquad (27)$$

we can define the variable ballistic weight, w (or effective ballistic weight) as

$$w = \left(\frac{W_d}{A}\right)\left(\frac{1}{C_d}\right)\left(\frac{\rho_\infty}{\rho_a}\right) \qquad (28)$$

where ρ_∞ = air density at standard conditions.

The air density ratio will always be near unity and is introduced here primarily for completeness. The drag coefficient for most two- and three-dimensional objects (see page 3-17, Ref. 55) is in the range of from 0.5 to 2, with the value 1.0 being a goal nominal or average value. Thus the value of the ballistic weight will depend most strongly upon the weight per unit projected area of the object. Equation (27) can be written as

$$\frac{dV}{dt} = \frac{1}{2}\rho_\infty V_r^2 / w \qquad (29)$$

where w characterizes the debris.

The characterization of the debris by a single variable will permit the development of the trajectory characteristics in terms of this variable and greatly simplify the prediction and interpretation of the motion of a large class of tornado debris (i.e., drag type debris). Additional analysis will ultimately be required to examine the response of lifting and rotating bodies. In a subsequent portion of this chapter it will be shown that some additional debris shape parameters can be treated as variants of the ballistic weight variable.

The ballistic weight parameter has the units of force per unit area or pressure. In this report the unit psi will be used. A 1-in. thick piece of steel thus corresponds to a ballistic weight of 0.28 psi (1-in. x 0.28 lb/in.^{3}). It will be convenient to examine an arbitrary collection of potential tornado debris objects and determine the corresponding value of the ballistic weight parameter in the direction of the principal axis of these objects. These values are listed in Table 14. The value of the drag coefficient and of the air density ratio have been taken, in this case, to be of unity magnitude. In any given instance variations in these factors will appear as an equivalent change in the actual value of the ballistic weight parameter. Since people can be (and have been) caught up in a tornado and thus be subject to being translated by its winds, ballistic weight parameters of an average man are included in Table 14 together with potential debris.

Table 14

DRAG CHARACTERISTICS OF TYPICAL DEBRIS

Description of Items	Weight (lb)	Ballistic Weight, w (psi)		
		x-axis	y-axis	z-axis
Man - medium	160.0	0.20	0.30	0.70
2x4 lumber 8 ft long	13.5	0.04	0.08	2.21
2 in. dia. rock	0.3	0.10	0.10	0.10
2 in. pipe 10 ft long (plugged ends)	36.8	0.13	0.13	0.13
1 in. dia. steel rod 4 ft long	10.6	0.22	0.22	13.40
Concrete block (4 in. x 9 in. x 18 in.)	33.7	0.23	0.52	1.03
Crate (1 ft x 2 ft x 2 ft)	150.0	0.28	0.56	0.56
2000 hp diesel-electric passenger locomotive (10 ft x 14.5 ft x 71 ft)	315,000	2.12	3.07	15.0

143

For the items examined, the value of w varies from 0.04 to 15.0 psi. Most of the values lie in the range 0.1 to 1 psi, especially if one considers the x-axis values which represent the minimum value for a nonspherical object. If one introduces a variable, S, (the ratio of the minimum projected area, A_{min}, to the maximum projected area, A_{max}) for two-dimensional objects, and then examines how the normalized projected area, h (normalized by A_{max}), varies with the orientation angle (the angle of attack), it becomes clear that the value of the normalized projected area for a rotating object will, on the average, be near unity. This fact is illustrated in Figure 43. For an infinitely thin object (i.e., an idealized flat plate)

$$h = \sin(\theta) \tag{30}$$

where θ is the angle of attack. Thus for this limiting case the average value of h is $2/\pi$ or 0.64.

It is clear that, on the average, for rotating two- and three-dimensional objects the value of the ballistic weight parameter will generally be near its minimum value. It is interesting to note (see Table 14) that the ballistic weights for very massive objects such as the diesel locomotive (2.12 for the x-axis), are not very much different from much lighter objects, such as an 8 ft length of lumber (2.21 for the z-axis). This relatively narrow range of the ballistic weight parameter suggests that much of the debris will behave in a similar manner in a tornado-wind environment.

The ballistic weight of a piece of debris will be a major factor with respect to its aerodynamic transport characteristics in a tornado environment. The weight of the piece of debris is also important, especially in its impact effect on a potential target For this reason, the distribution of both the ballistic weight, w, and the weight, W_d, must be established for a given debris source, such as a building. Even more importantly, the time at which the debris is airborne (i.e., released to the storm environment) must be established. In the case of a building, this includes the time to failure and separation of its various consitutive parts. It is
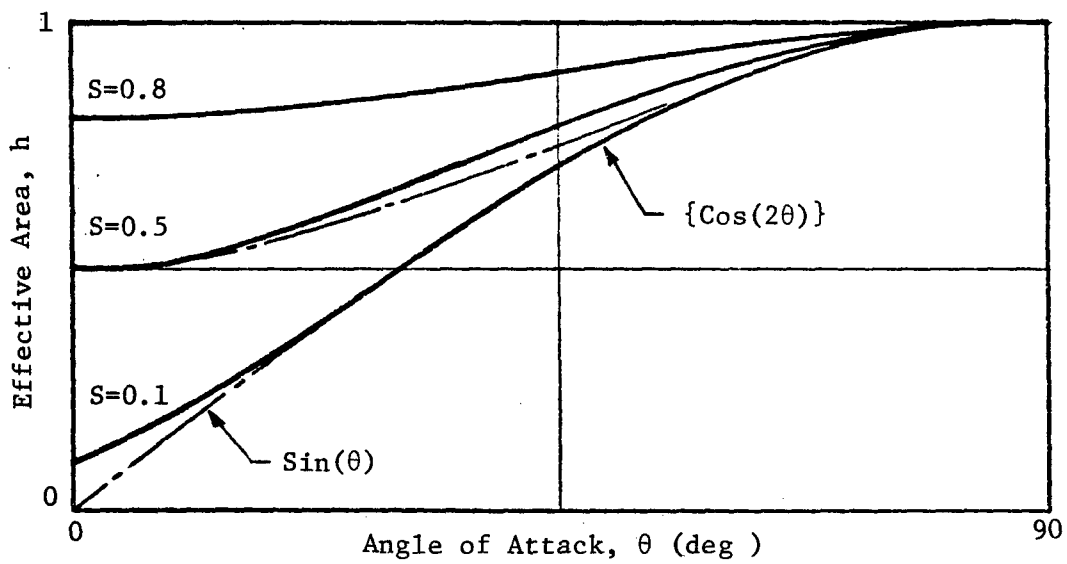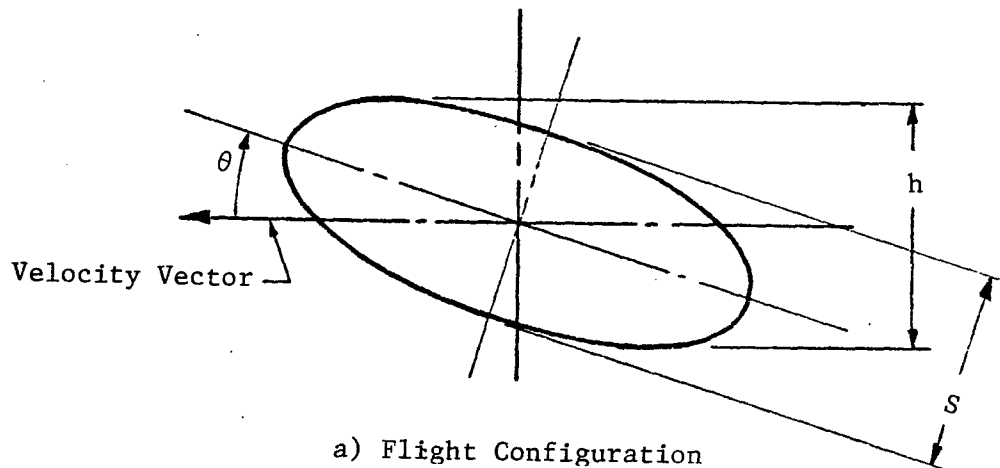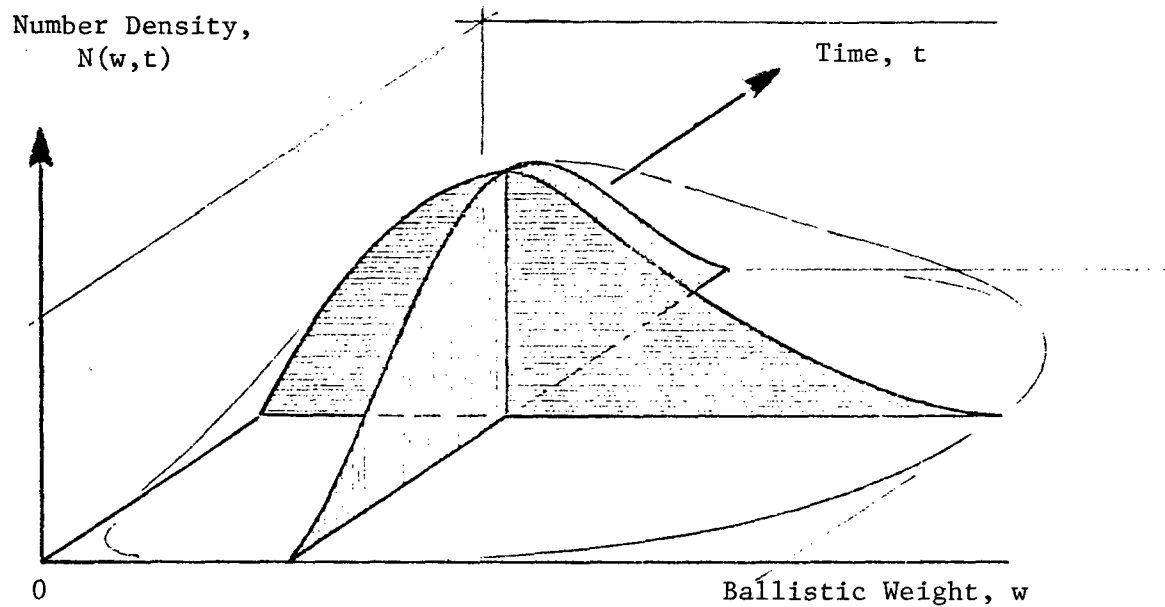
a) Flight Configuration

b) Results

Figure 43 Effective Area Variation with Orientation

presumed here that the structural response evaluation of a potential debris source will generate the number density N (w,t) of debris as a function of both ballistic weight and time, and that within each ballistic weight-time category the corresponding distribution, N_{sw}, of debris weights are estimated. These aspects of the problem will appear as statistical estimates; guided in part by engineering judgment and total mass conservation considerations. Figure 44 illustrates the general nature of these debris source characterizations. As more refinements are introduced into this overall problem, additional information expressed in distribution forms will have to be developed. The shape factor, S, could be one such debris characteristic which would have to be allocated to each of the above referenced number density estimates together with initial conditions such as time to release.

5.4 DEBRIS TRANSPORT MODEL

The motion of the debris, once airborne, will be governed by the combined effects of aerodynamic forces and gravity. For the purpose of the initial model the motion will be restricted primarily to the horizontal plane. The validity of this condition can be based upon the fact that: (1) the initial duration will be adequate so that during the time of flight the object will not reach the ground plane; or (2) an interaction with the ground plane will occur (i.e., a bounce) which will result in temporary increase in flight altitude; or (3) a lifting force will be present to maintain the motion at a near constant elevation. The ground interaction condition will result in some loss of horizontal momentum. This feature could be ultimately included into transport analysis, however for the present, if a ground interaction occurred which does not capture the piece of debris, then it is assumed that no horizontal momentum is lost. The presence of lifting forces can be expected from either aerodynamic interaction considerations or from a tilting of the nearly horizontal tornado wind field. In any event the probability of impact occurring on some target element of height, Δh, after a piece of debris has traveled a certain distance or has been airborne for a given time can be accounted for by

Number Density,
N(w,t)

Time, t

0

Ballistic Weight, w

a) Rupture History

Specific Number Density,
N_{sw}
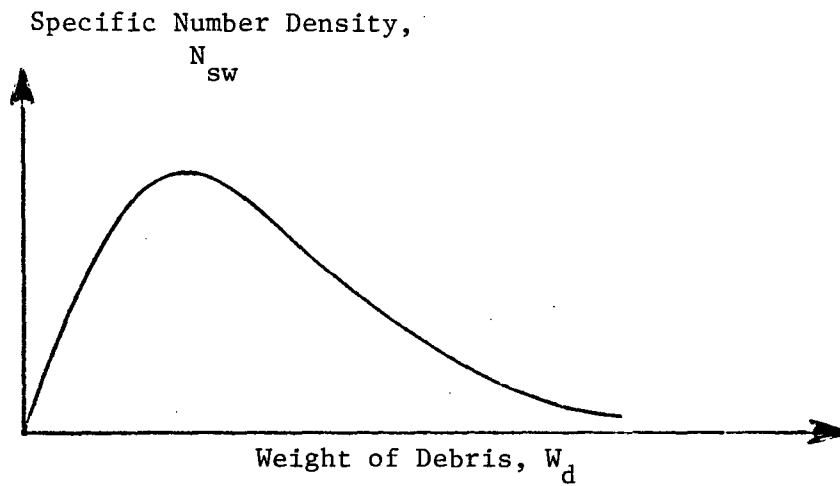
Weight of Debris, W_d

b) Debris Weight Distributions

Figure 44   Debris Characteristics of a Source

the application of some probability function. This function form is illustrated in Figure 45. Its development, for various classes of debris, should include the effects of random spreading due to tumbling, release point height, and other factors reflecting the ability of the surface perturbations (such as trees) to capture airborne debris. Not all debris which is produced by the rupture of a structure will become airborne. A large portion may drop to the ground plane due to debris/debris interactions or other such factors. The study of tornado debris surveys should shed some light on this effect.

The debris transport model which is used is composed of the combination of the horizontal wind model described in Section 5.2 and the simple aerodynamic drag model referred to in the preceeding section. The motion occurs in the horizontal plane defined by the space variables x and y where the origin is the release point and zero time is the release time. The center of the storm is thus at some position (x_o, y_o) at zero time and moves in the y direction at the speed U_t. A vector diagram for this model is illustrated in Figure 46(a). The local wind velocity is designated by the vector U, the current velocity of the object is designated by the vector V and the resultant relative velocity is designated by the vector V_r. The drag force, F_d, acts in the direction of V_r and is applied to the center of mass of the object. A computer code was written to integrate the appropriate equations and thus evaluate the trajectories and motion histories for a variety of debris characteristics and initial locations.

A single, somewhat severe storm condition was assumed; namely a peak rotational wind intensity, U*, of 360 mph (528 fps), a storm speed, U_t, of 40 mph (58 fps) and a circulation, C, of 10^5 ft-fps. Thus the radius of the core is 189.4 ft and the maximum wind speed is 400 mph (586 fps). Most of the release points examined were near the edge of the core, and since the initial debris velocity due to debris formation will be very small compared to the local wind speed at the time of release, these initial velocities were taken to be zero.
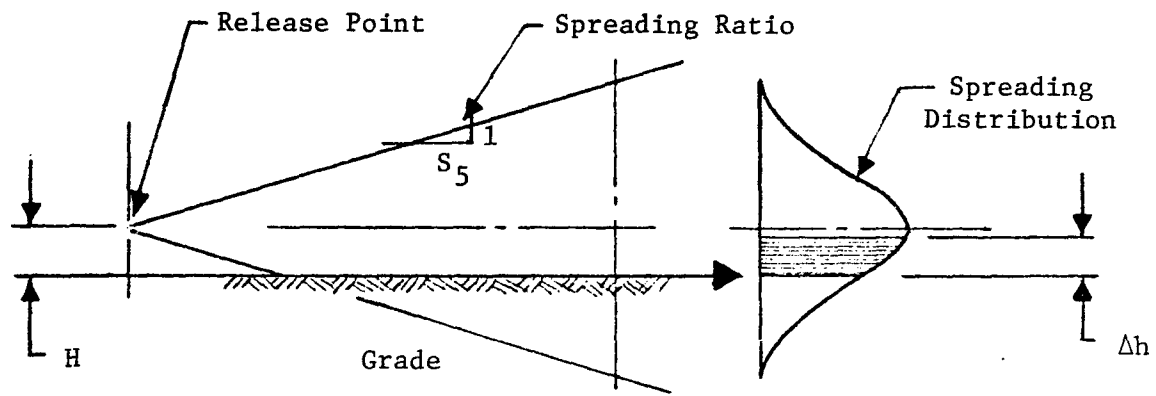
a) Vertical Spreading
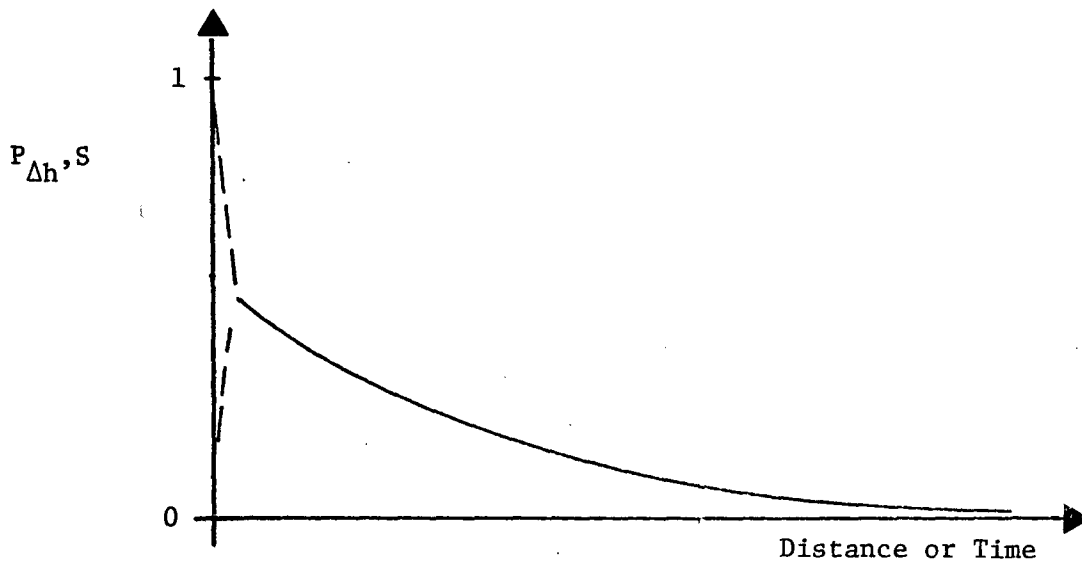
b) Probability Function

Figure 45 Probability of Impact at Elevation Increment Δh
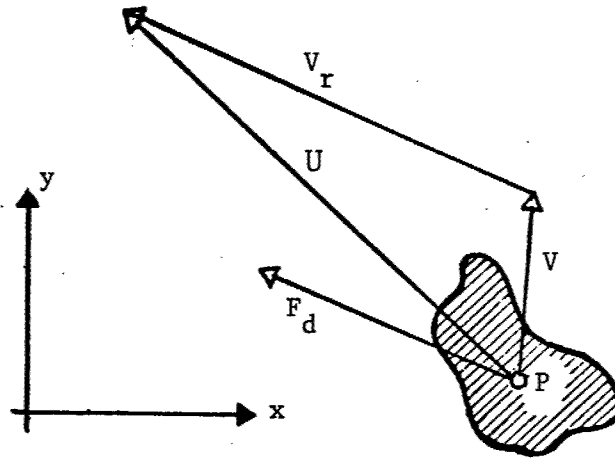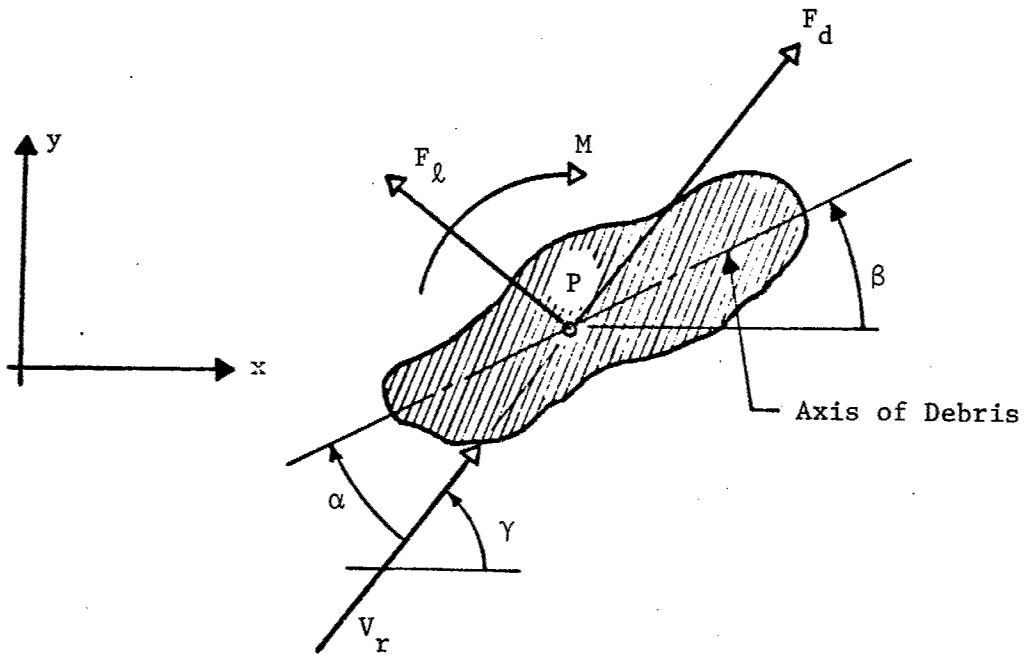
a) Simple Drag Model

b) Two-Dimensional Rotating Debris Model

Figure 46   Debris Trajectory Models

The following 11 figures describe in various forms the debris trajectories and motion histories as a function of ballistic weight and release point relative to the storm center. Most of the results correspond to release points 200 ft from the storm center (i.e., just outside the core) and cover 15° angular increments around the position circle. The position, location A, corresponds to $y_o = 0$ ft and $x_o = 200$ ft. This is nearest the point of maximum wind speed. The positions, locations B, C, and D, are the corresponding major axis positions for $y_o = -200$ ft, $x_o = 0$ ft, $y_o = +200$ ft, $x_o = 0$ ft and $y_o = 0$ ft, $x_o = 200$ ft respectively.

The influence of ballistic weight on trajectory is shown in Figure 47 for the location A. Debris with a ballistic weight of 3 psi moves generally along the +y axis and thus moves along with the storm; first lagging the storm as the object is accelerated and then outrunning the storm center. This piece of debris may be exposed to additional significant wind forces whenever and if the storm catches up to it again. Heavier debris is centrifuged outward into the first quadrant. Debris with ballistic weights in the range of from 0.1 to 1 psi (the more likely values) are thrown into the second quadrant. These objects are accelerated to peak velocities in the range of from 200 to 300 fps and maintain the value for some significant time and distance. Lines of constant velocity are plotted in Figure 47. The yet lighter particles appear to become at least partially captured by the vortex flow.

Figures 48, 49, and 50 present trajectories of objects respectively for ballistic weight values of 1.0 psi, 0.2 psi, and 0.1 psi. These trajectories correspond to the four principal locations, location A, B, C and D and five intermediate locations in each quadrant. It should be noted that in a common ground coordinate, each trajectory would initiate from different starting points. However, in these x,y plots they appear to start from a common origin (their starting point). Lines of constant velocity are shown in these figures as well as the paths along which each trajectory reaches its maximum velocity. This latter line is shown as a dotted line. Several points of general interest should be noted. First the higher values of velocity appear in the second quandrant (from starting points between locations A and B).
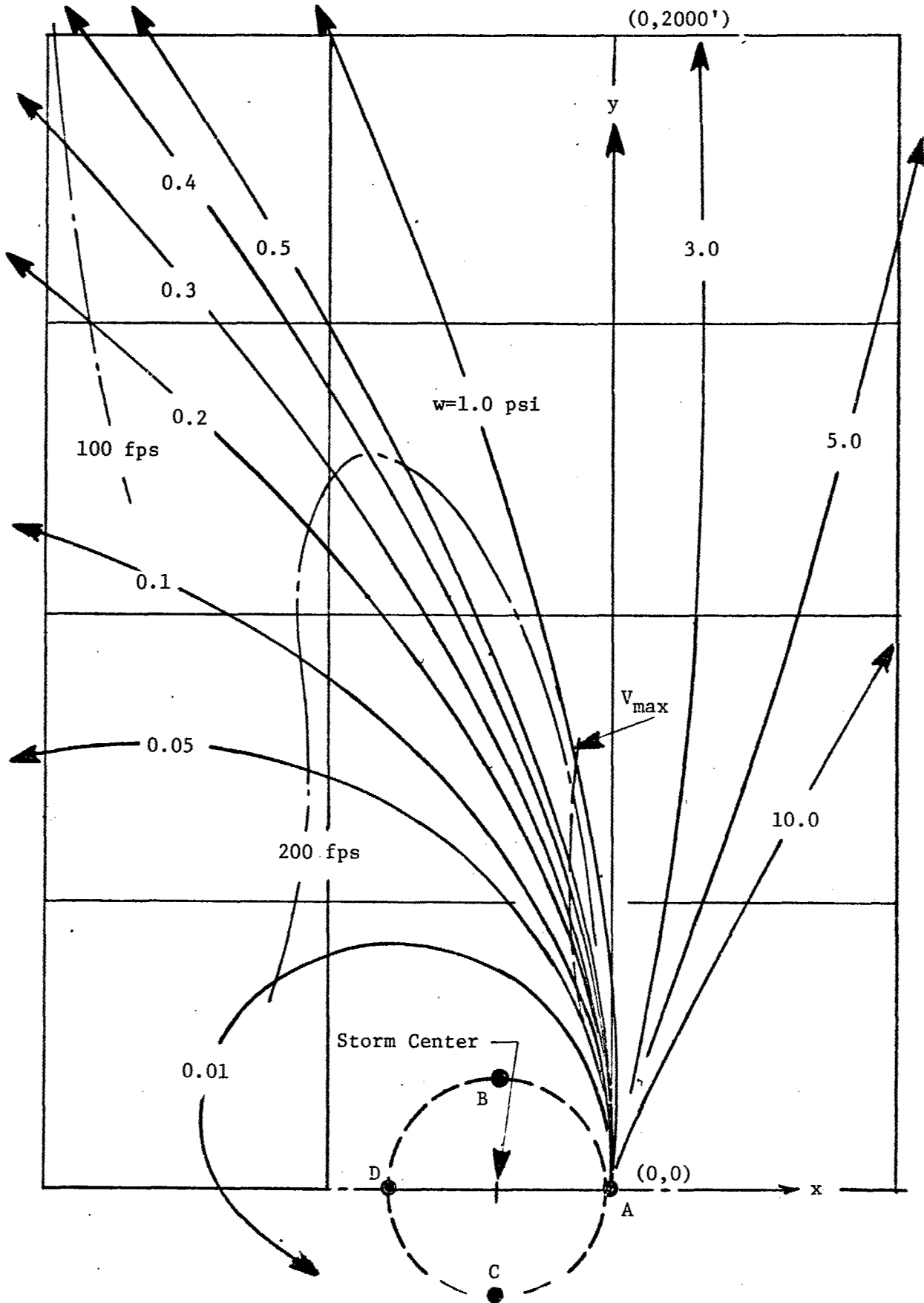
Figure 47   Influence of Ballistic Weight
on Debris Trajectories

152

(1000', 1000')

Location Nearest the Point of Maximum Wind Speed	y_0 (ft)	x_0 (ft)
A	0	200
Corresponding Major Axis Points		
B	−200	0
C	+200	0
D	0	200

Figure 48   Debris Trajectories - w = 1.0 psi
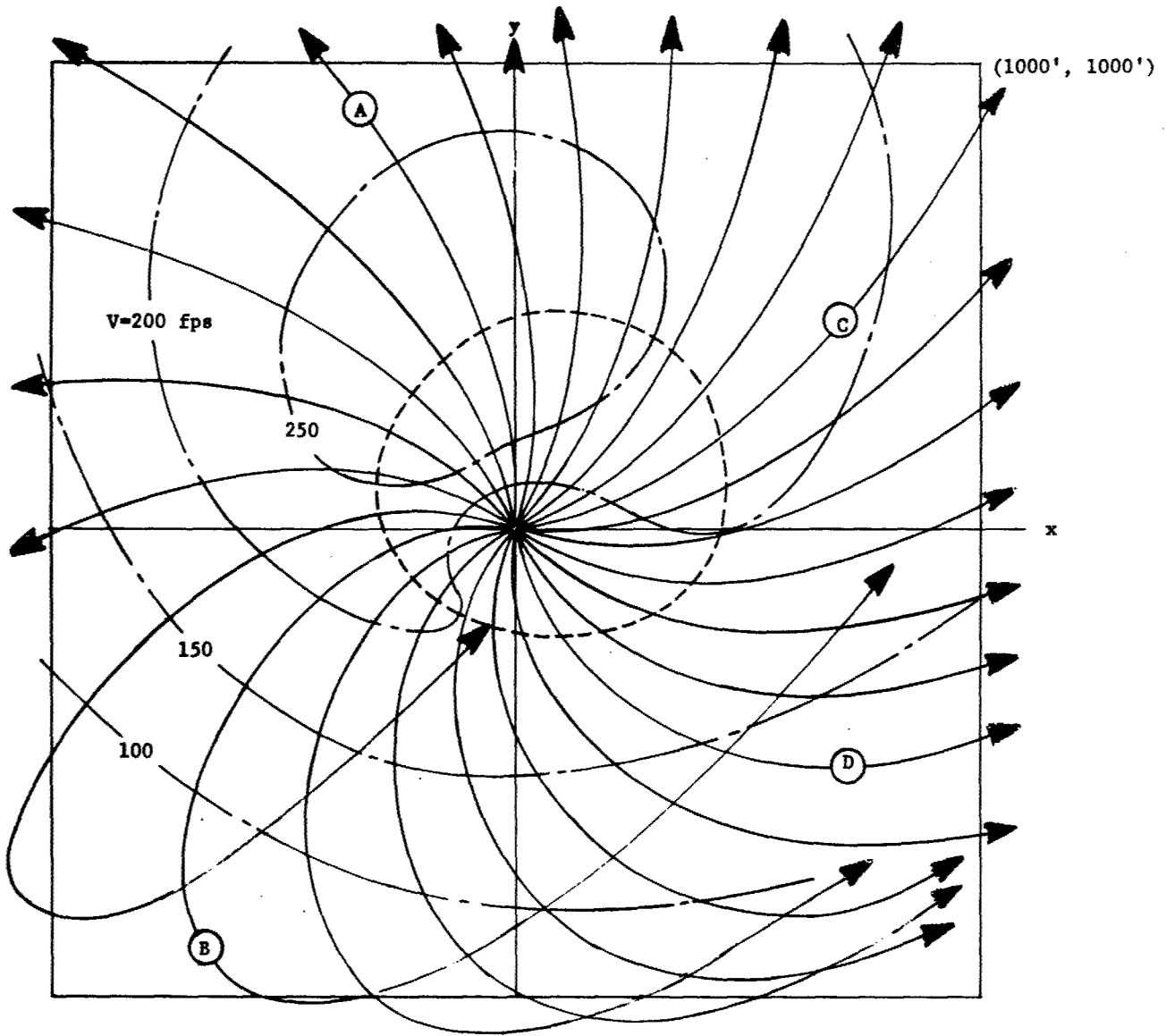
153

(1000', 1000')

V=200 fps

250

150

100

Location Nearest the Point of Maximum Wind Speed	y_0 (ft)	x_0 (ft)
A	0	200
Corresponding Major Axis Points		
B	-200	0
C	+200	0
D	0	200

Figure 49 Debris Trajectories - w = 0.2 psi
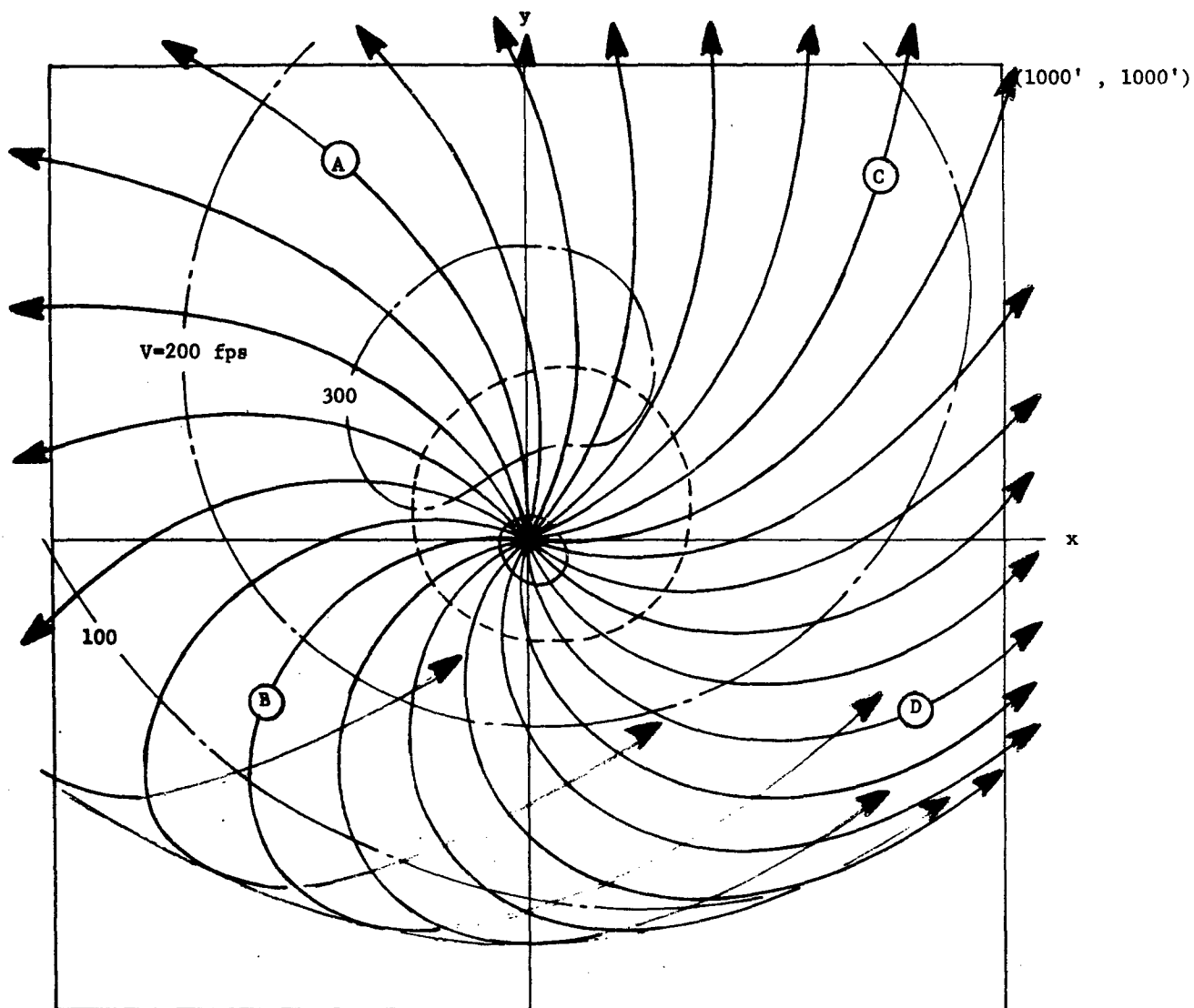
Location Nearest the Point of Maximum Wind Speed	y_0 (ft)	x_0 (ft)
A	0	200
Corresponding Major Axis Points		
B	−200	0
C	+200	0
D	0	200

Figure 50   Debris Trajectories - w = 0.1 psi

Consistent with such a behavior we note that at nominal ranges, such as at 500 ft from the release point, the density of trajectory paths per unit angle is smaller in the second quadrant indicating a greater degree of dispersion of the debris thrown in this direction. Conversely the trajectory density is larger in the direction where the velocities are lower (the fourth quadrant). Secondly, as the ballistic weight decreases, the distance that the debris travels in the upstream direction (the -y direction) becomes smaller and a pass near the release point becomes more common.

The time details of objects released from the four principal release points are presented in Figure 51 for a ballistic weight of 0.2 psi. The peak value of velocity is reached after several seconds of flight time and the velocity decays much more slowly. In the limit of long times (which will not be achieved beacuse of gravity effects) the velocity will tend to the value of the storm translational velocity (indicated as U_t). The slightly oscillatory behavior of the piece of debris released at location B is characteristic of the trajectory reversal shown in Figure 49. The influence of the magnitude of the ballistic weight upon the velocity histories is shown in Figure 52 for locations A and D. It is clear that those pieces of debris with a low ballistic weight, say 0.1 psi, will be accelerated rapidly and to larger velocities. However, it should be empahsized that they will also decelerate rapidly, thus the higher velocity conditions should be expected to be much shorter lived. The rather heavy pieces (in terms of ballistic weight) require very long times and distances before they reach their maximum value, which is, of course, somewhat smaller in magnitude.

Figure 53 presents the maximum values of velocities which debris of various ballistic weight values achieve when released from location A. It would appear that most debris will achieve peak velocities of from 30 to 60 percent of the maximum wind speed.

R = 200 ft
w = 0.2 psi
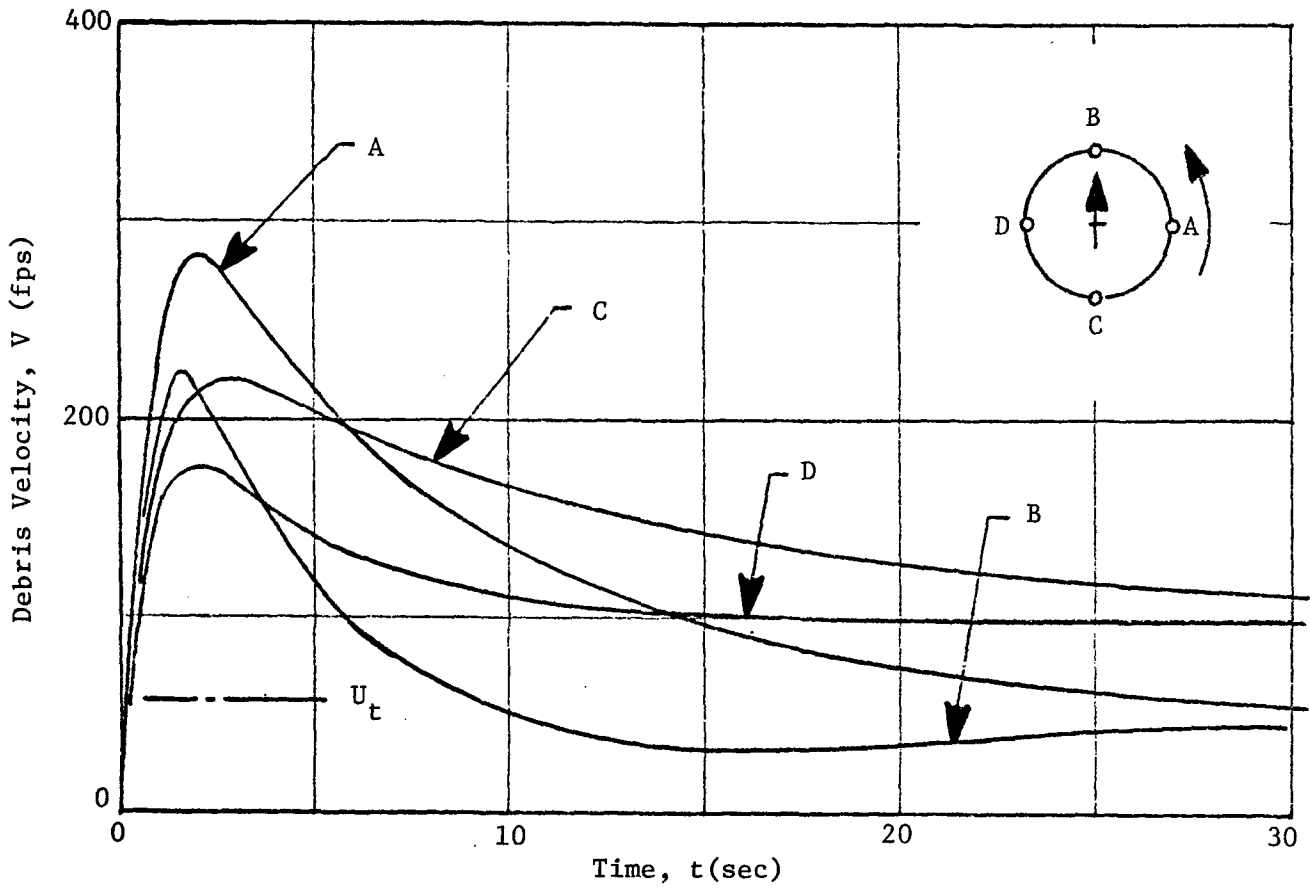
Figure 51 Velocity Histories of Debris Released in Different Quadrants
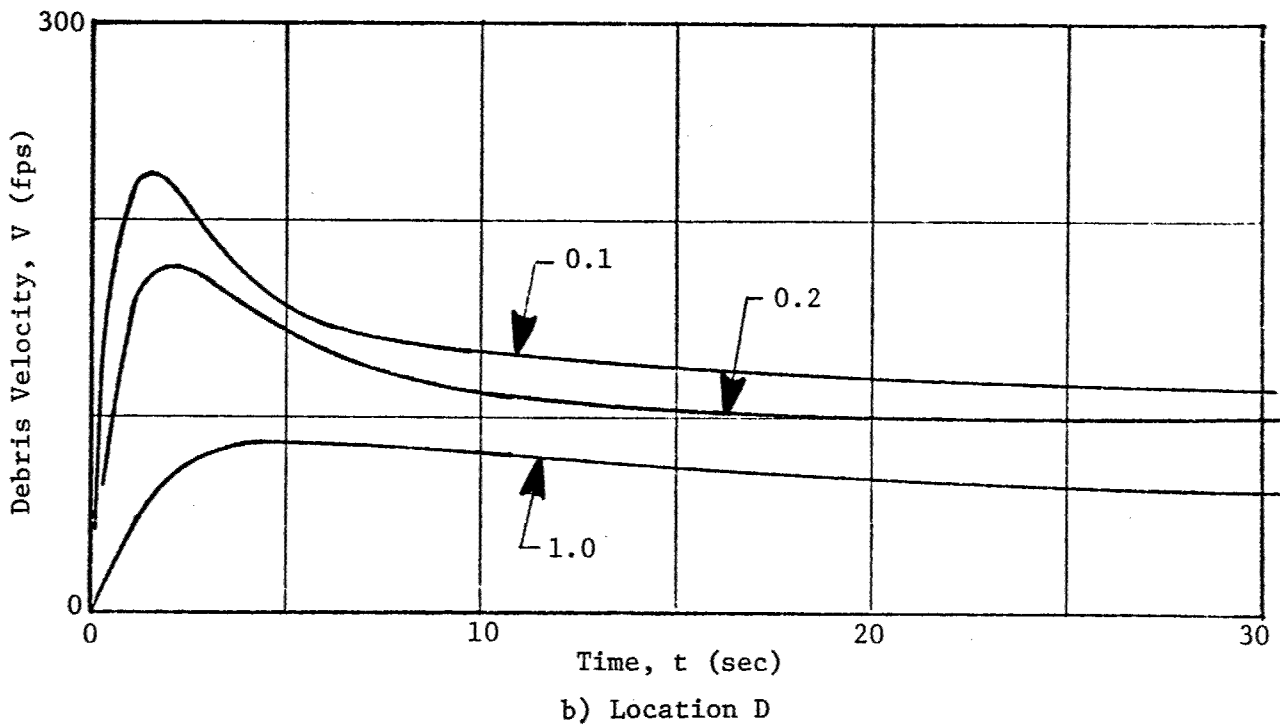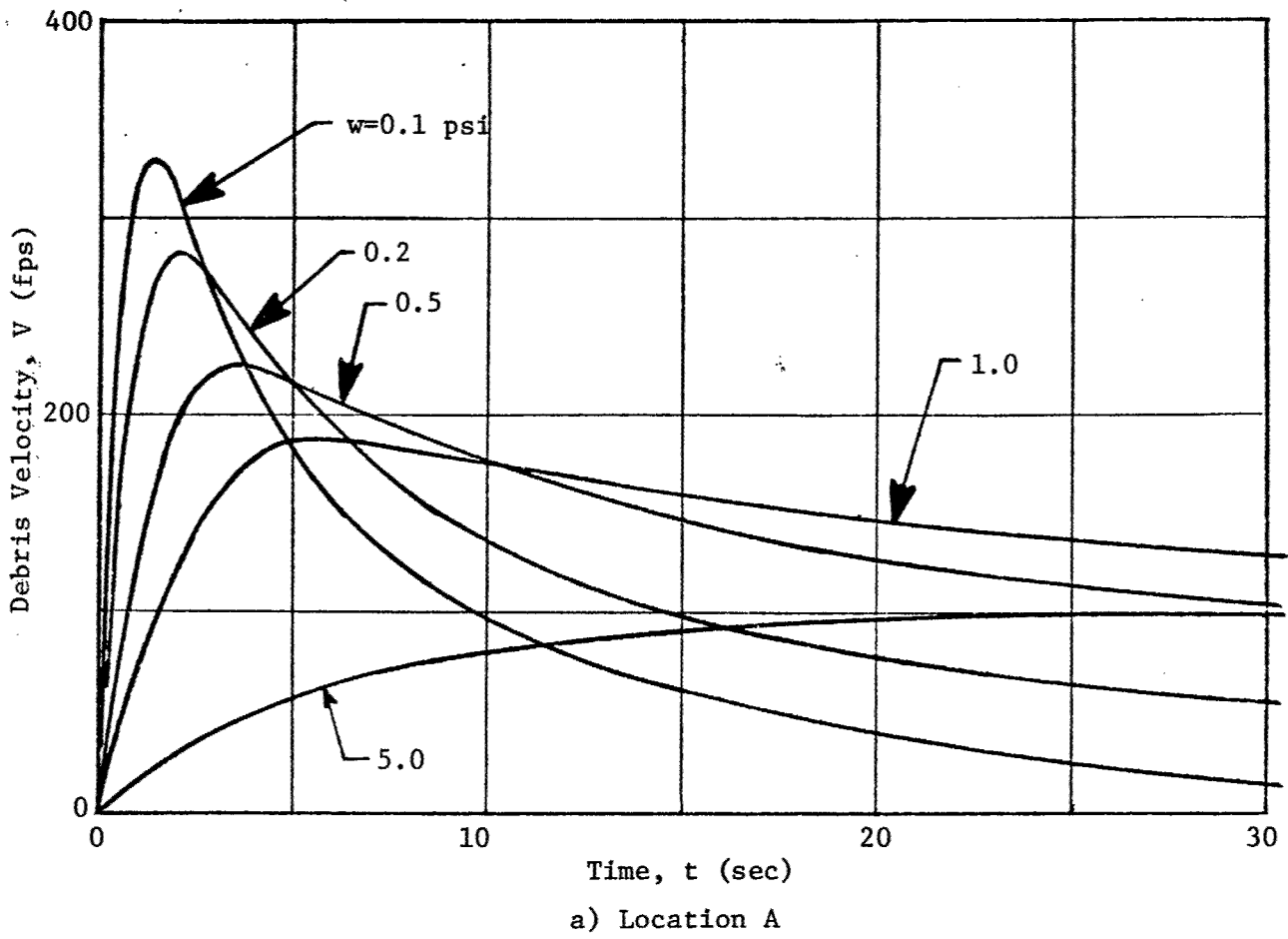
Figure 52   Influence of Ballistic Weight on Velocity Histories
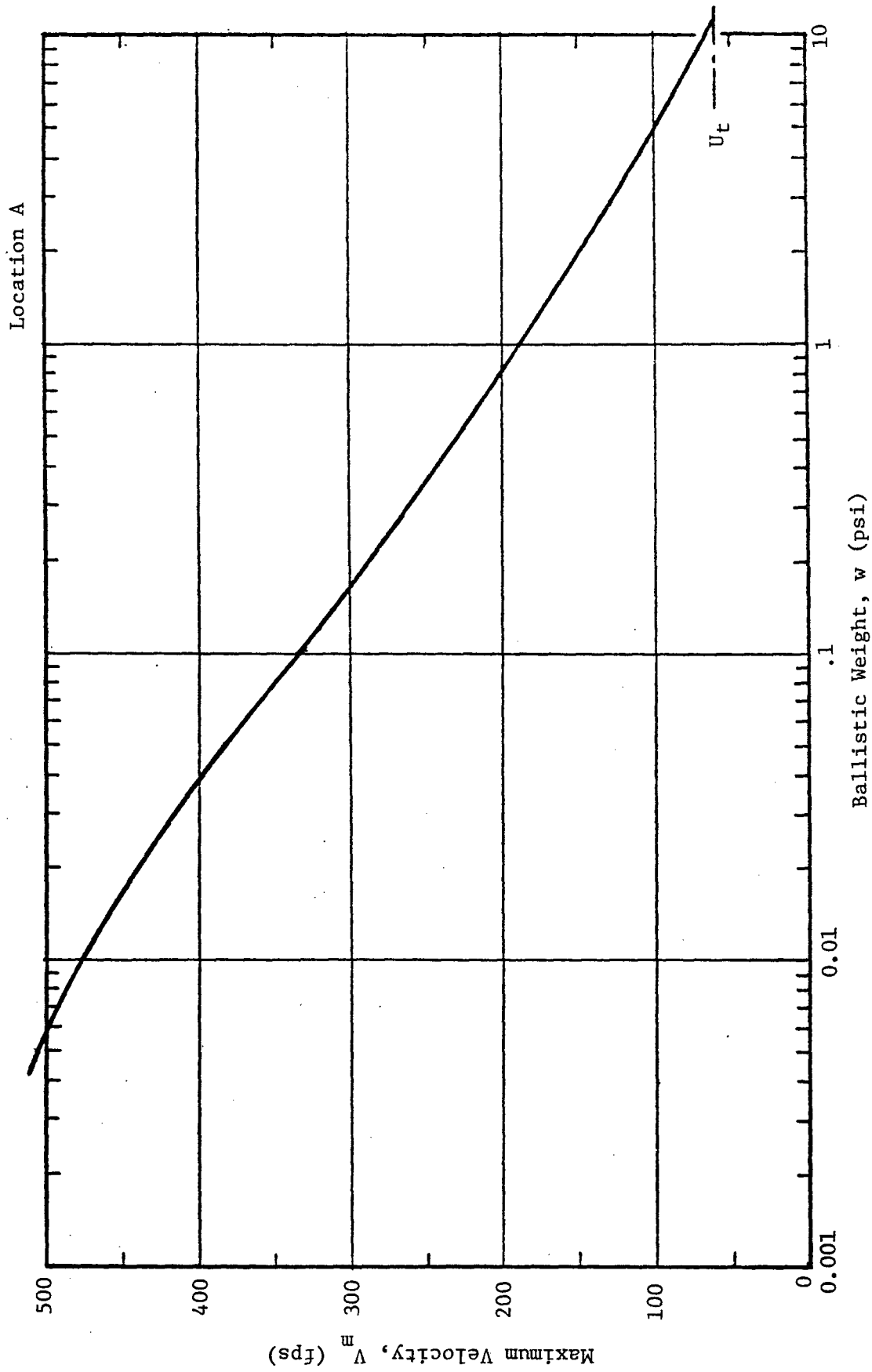
Fig. 53 Maximum Velocity Dependence on Ballistic Weight

This average velocity will be somewhat less over realistic transport distances, such as say 1000 ft. The maximum debris velocity for discrete values of the ballistic weight for all release point locations at a radius of 200 ft from the storm center are presented in Fig. 54. It is clear that substantially higher peak velocity values are achieved for release points in the BAC half of the release circle. This is especially true for the larger values of ballistic weight. Higher peak velocities are achieved for the lower ballistic weight conditions and the variation with angle is smaller.

A somewhat different perspective can be obtained by examining the trajectories relative to the storm center. These are shown in Figure 55 and can be compared to some of the same trajectories shown relative to a ground coordinate in Fig. 47. Of particular interest are the trajectories of the very low ballistic weight objects. But first note that the very heavy objects (w = 10 psi) fall behind the storm system (which is moving in the +y direction). As the value of the ballistic weight decreases the objects move ahead of the storm system after first dropping momentarily behind. The trajectories for yet smaller values of the ballistic weight (w = 0.1 psi) appear to move ahead of the storm system initially. However, all of the objects do drop momentarily behind as they are accelerated up to the magnitude of the storm translational velocity, U_t. The low ballistic weight objects are thrown ahead of the storm system and are then turned moving into the second storm quadrant. The very low ballistic weight objects (w = 0.05 to 0.005 psi) are partially trapped and circle the storm center once or more before being centrifuged outward. The time details of one of these light objects is presented in Fig. 56 Very fine soil particles such as fine sand, will be trapped in the storm system. A 2-in. diameter rock has a ballistic weight of 0.1 psi (see Table 14). The ballistic weight of such spherical items will be proportional to the size (diameter) of these objects; that is for rocks

$$w \cong 0.05 \times D \tag{31}$$

where D = diameter (in.) and w = ballistic weight (psi).
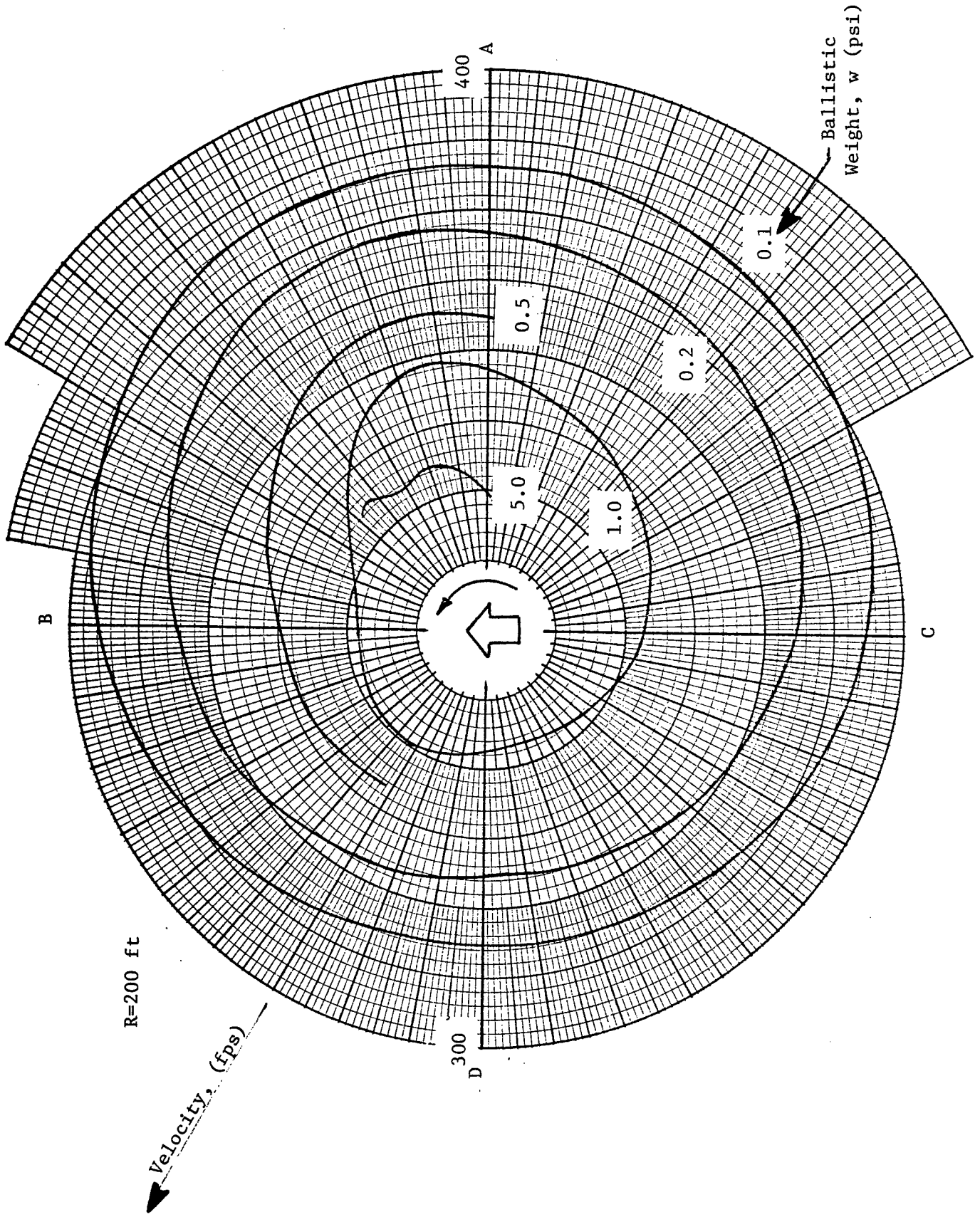
Figure 54   Maximum Debris Velocity

161
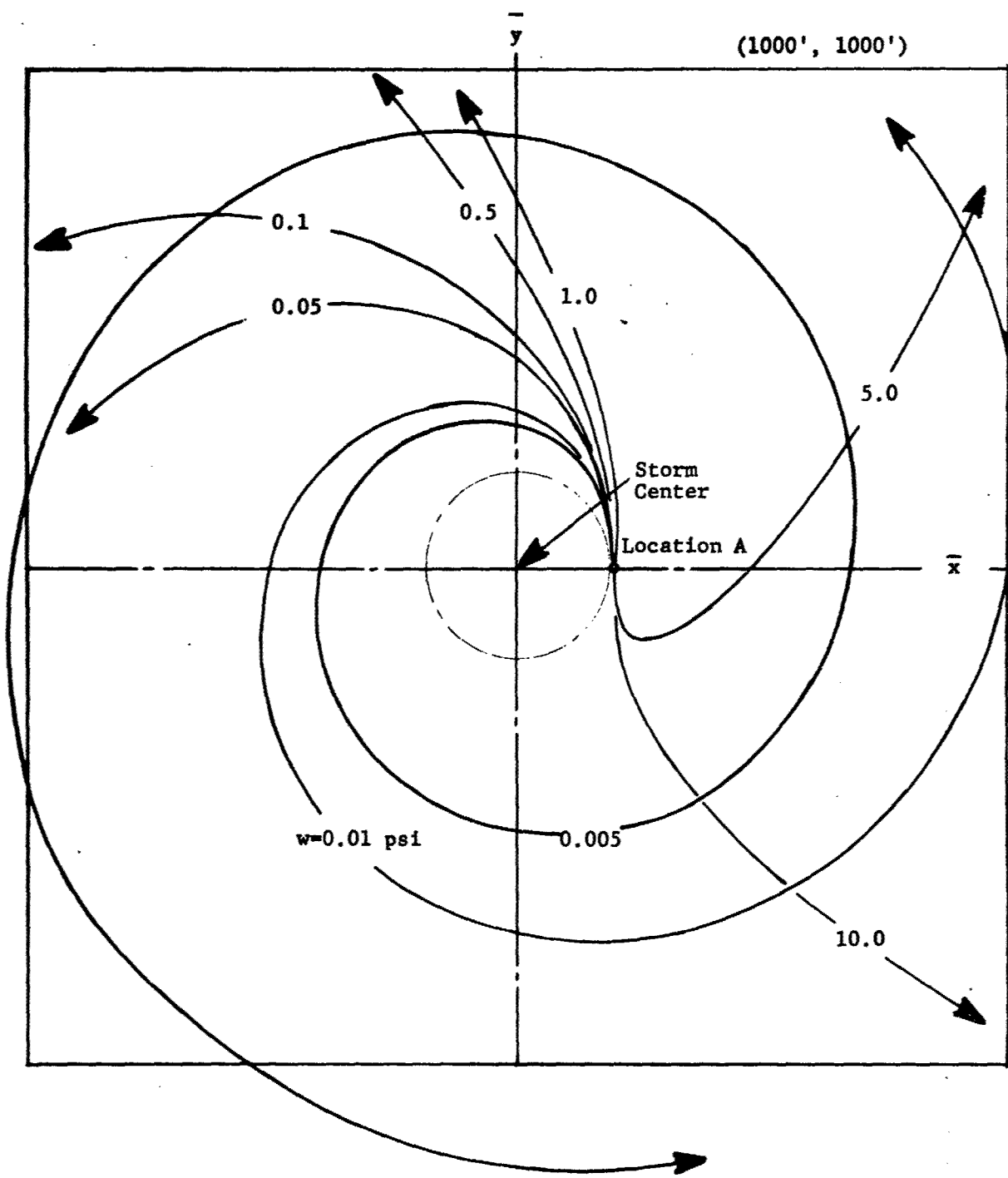
Figure 55 Debris Trajectories Relative to Storm System
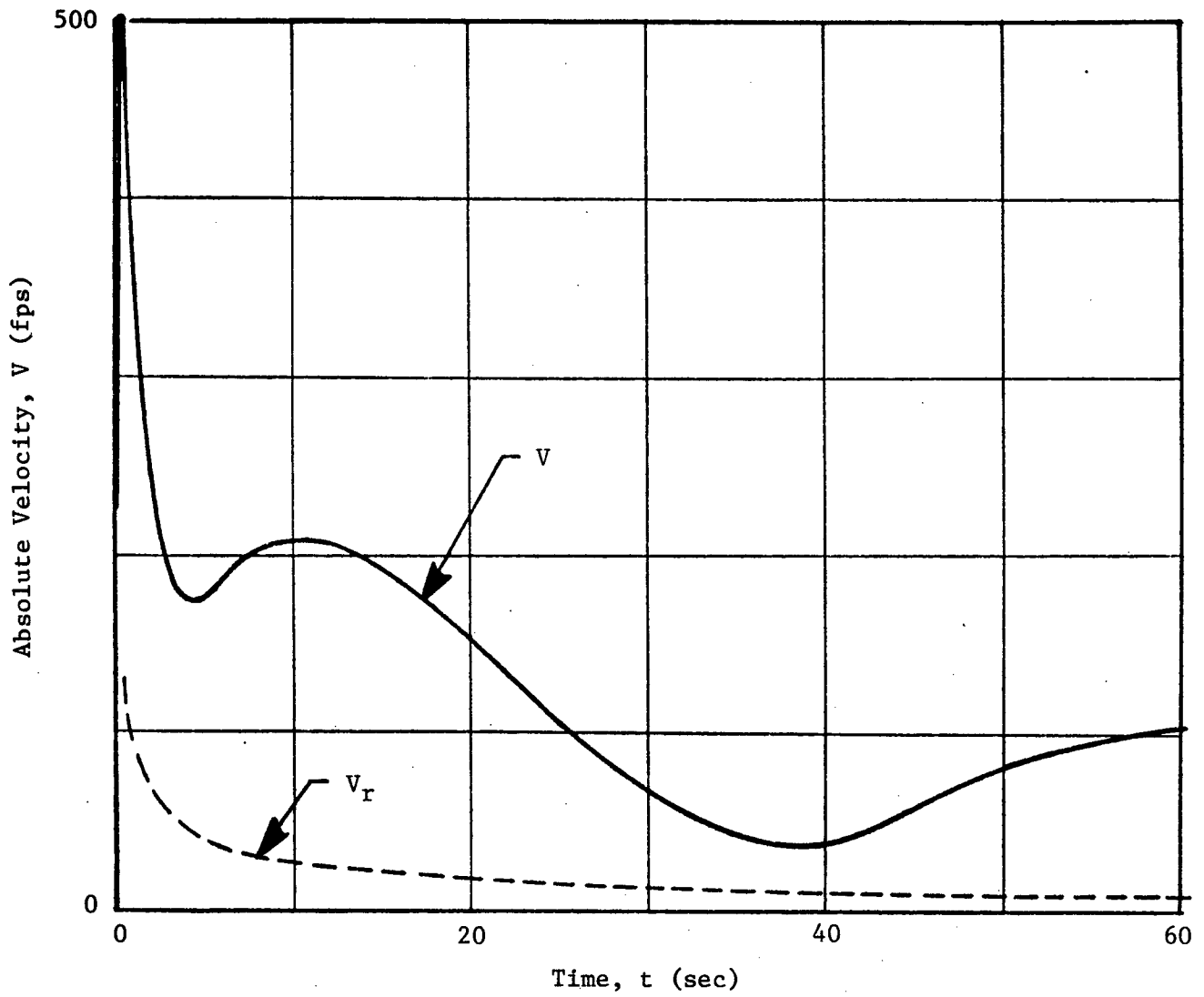
Figure 56   Velocity History of Light Particles - w = 0.005 psi

Thus pea gravel (0.1 to 0.2 in. in diameter) will have a ballistic weight in the range of 0.005 to 0.01 psi. The trajectories shown in Figure 55 were released at Location A.

Objects which become airborne within the core may have a much more complex behavior due to the larger changes in wind velocity. All of the preceding trajectory results were for debris released along locations 200 ft from the storm center and for a given set of storm parameter values. It should be noted that these results are independent of the maximum rotational velocity, U^*, provided that U^* is greater than 500 fps ($r \geq R = 200$ ft). That is because the release point and trajectory paths relative to the storm system always place the object within the constant circulation region of the storm (i.e., not within the core). Thus, the preceding results are more generally applicable to a wide range of storm conditions.

The last set of general trajectory details which will be given here deals with the maximum velocity achieved by debris as a function of release point for the ballistic weight case of 0.2 psi. Figure 54 presented these types of results for release points along a release circle of 200 ft radius (from the storm center). The complete results are presented in Figure 57 in terms of maximum velocity contours. The largest value of approximately 300 fps occurs from a point just outside the edge of the core and within the fourth quadrant. Debris released within the fourth quadrant of the core region achieve peak velocities generally in the range of from 250 to 300 fps. Debris released from the second quadrant of the core only achieve peak velocity around 200 fps. The peak velocity drops quite rapidly outside of the core. The somewhat "far field" results shown are applicable to a yet wider range of storm conditions. Release point results from positions 300 ft or more from the storm center are applicable for all maximum rotational velocity conditions greater than 333 fps (and $U_t = 40$ mph).

The usefulness of all of the preceding results and the simple drag model will be enhanced if it can be shown that the simple drag model yields an adequate representation of the dynamics of a wide class of debris.
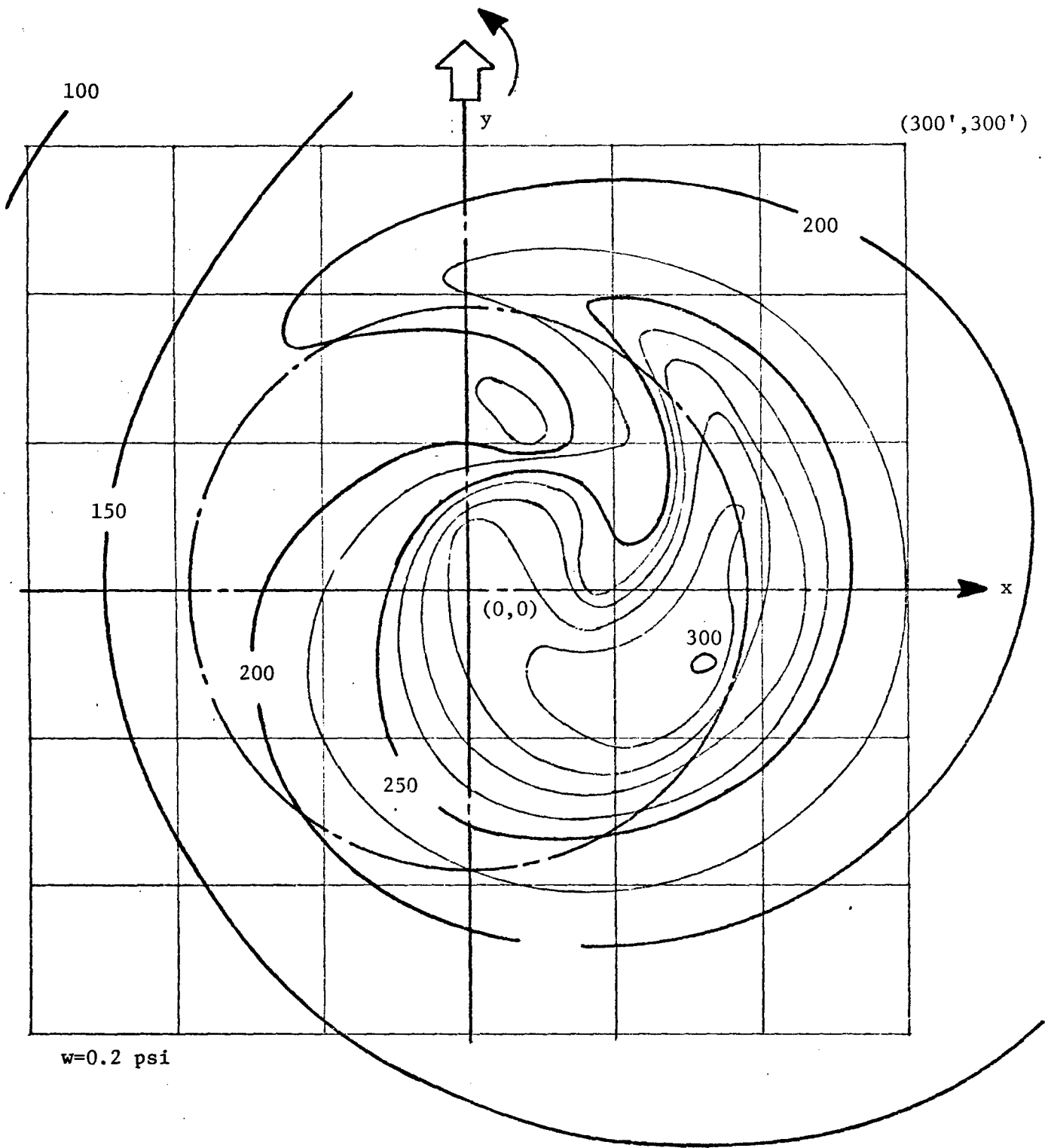
Figure 57   Influence of Release Point on Maximum Debris Velocity

Clearly the simple drag model will be adequate for debris whose shape is roughly spherical. However, most debris will be somewhat oblong in shape and an aspect ratio or the shape factor, S, can be used to characterize this broader range of debris shapes. This type of debris will be subjected to aerodynamic lifting forces and rotating moments as well as to the drag forces, and they will rotate during their flight period. A two-dimensional rotating debris model developed by IITRI (Ref. 56) was used to examine the transport of this class of debris. The generalized force diagram for this model was presented in Figure 46. Three equations of motion are required, two dealing with the two components of linear displacement and one dealing with the rotational character of the motion. The generalized driving forces are the drag force, F_d, the lifting force, F_ℓ, and the moment, M. The drag and lifting forces are proportional to the relative dynamic pressure $(\frac{1}{2}\rho V_r^2)$, an area A*, and an appropriate drag or lift coefficient. The convention used in air foil theory is followed in that the coefficients are based upon the maximum projected area, $(A^* = A_{max})$ rather than any instantaneous value. Thus the concept of an effective ballistic weight can still be used. This involves the air density ratio, the maximum projected area, the weight of the object, and a nominal drag coefficient. The lift and drag coefficients thus appear as factors which account for the shape factor, S, and the instantaneous angle of attack, α. The drag, f_d, and lift f_ℓ factors are

$$f_d = (S + (1-S) \sin^2\alpha)$$
$$f_\ell = (1-S) \sin(2\alpha)$$

(32)

The assumption of shape symmetry is implied. The equation of motion for the rotary motion of the debris is

$$\frac{d\omega}{dt} = \frac{M}{I}$$

(33)

where

ω = angular velocity

M = applied aerodynamic moment

I = moment of inertia.

166

The aerodynamic moment can be related to the lifting force by assuming a point of application. Due to the absence of any details a nominal point of application located at the quarter point was assumed, viz.,

$$M = \frac{\delta}{4} F \tag{34}$$

where δ = the length of the debris. The length of the debris can be related to the size of the debris by assuming that

$$\delta = \sqrt{A^*} \tag{35}$$

Finally the moment of inertia can be approximated as:

$$I = 0.2 \ \delta^2(S^2+1) \ W_e \tag{36}$$

Since the debris will exist in a wide variety of shapes the above form represents an average or nominal value. Its use should be reasonably good for most shapes. The orientation of the debris, γ, during free flight is given by the kinematic relation

$$\omega = \frac{d\gamma}{dt} \tag{37}$$

In addition to the previously used initial conditions for position and linear velocity, the initial orientation γ_0 and roll rate ω_0 must be specified. The initial orientation is a significant variable and one that must be examined numerically. The initial roll rate, however, is less important and it, like the initial components of linear velocity, has been assumed to be zero.

A second computer code was written with which to examine the transport of two-dimensional debris in the simplified tornado wind environment. The motion was, as before, limited to the horizontal plane. The trajectories and motion histories for a piece of debris weighing 150 lb was evaluated. The debris had a shape factor of 0.5 and a maximum projected area of 4.0 ft^2. Thus it had a minimum ballistic weight of 0.26 psi and a maximum and average ballistic weight of 0.52 and 0.35 psi respectively. It was released from location A with one of four discrete principal orientations (eight orientations due to symmetry considerations).

These resulting transport details are presented in Figure 58 and
59 and are compared to the corresponding transport details for a
simple drag model using the above cited ballistic weight values.
It is clear from these results that, for at least this case, the
two-dimensional lifting and rotating characteristics of the debris
are equivalent to a dispersion in the ballistic weight parameter
within its applicable range $(\omega_{min}$ to $\omega_{max})$. The fine details of
the transport phenomenon, such as orientation and minor velocity
oscillation are not very significant. Thus these two-dimensional
characteristics can be treated in a simple statistical manner, con-
sistent with many steps in the overall process. This result is
preliminary since it remains to be established exactly what param-
eter value domain it will be applicable to. Debris with any small
shape factors will be much more erratic in their flight behavior,
but this does not preclude the applicability or the use of the
above statistical approach to this extreme class of debris. It
also remains to be seen how sensitive any hazard evaluation is to
the value of the ballistic weight parameter. This will be done in
a limited fashion in the following section. For the moment the
simple drag model would appear to have a rather general applicability,
especially when one considers the vast variations in the debris
parameter values encountered.

5.5 SAMPLE APPLICATION

In this section the preceeding tornado wind model will be
applied to a hopefully realistic, but limited, sample problem in
order to obtain an insight into the collective behavior of a single
source as well as a spatially distributed set of debris sources.
Several targets distributed in the immediate neighborhood of the
tornado path have been used to examine the debris hazard in dif-
ferent parts of the storm system.

Figure 60 presents the layout of the physical system and the
storm path considered. The preceding storm conditions were used
and the origin of a ground plane coordinate system {x,y} is defined
with the storm center at the origin at time, t, equal to zero.
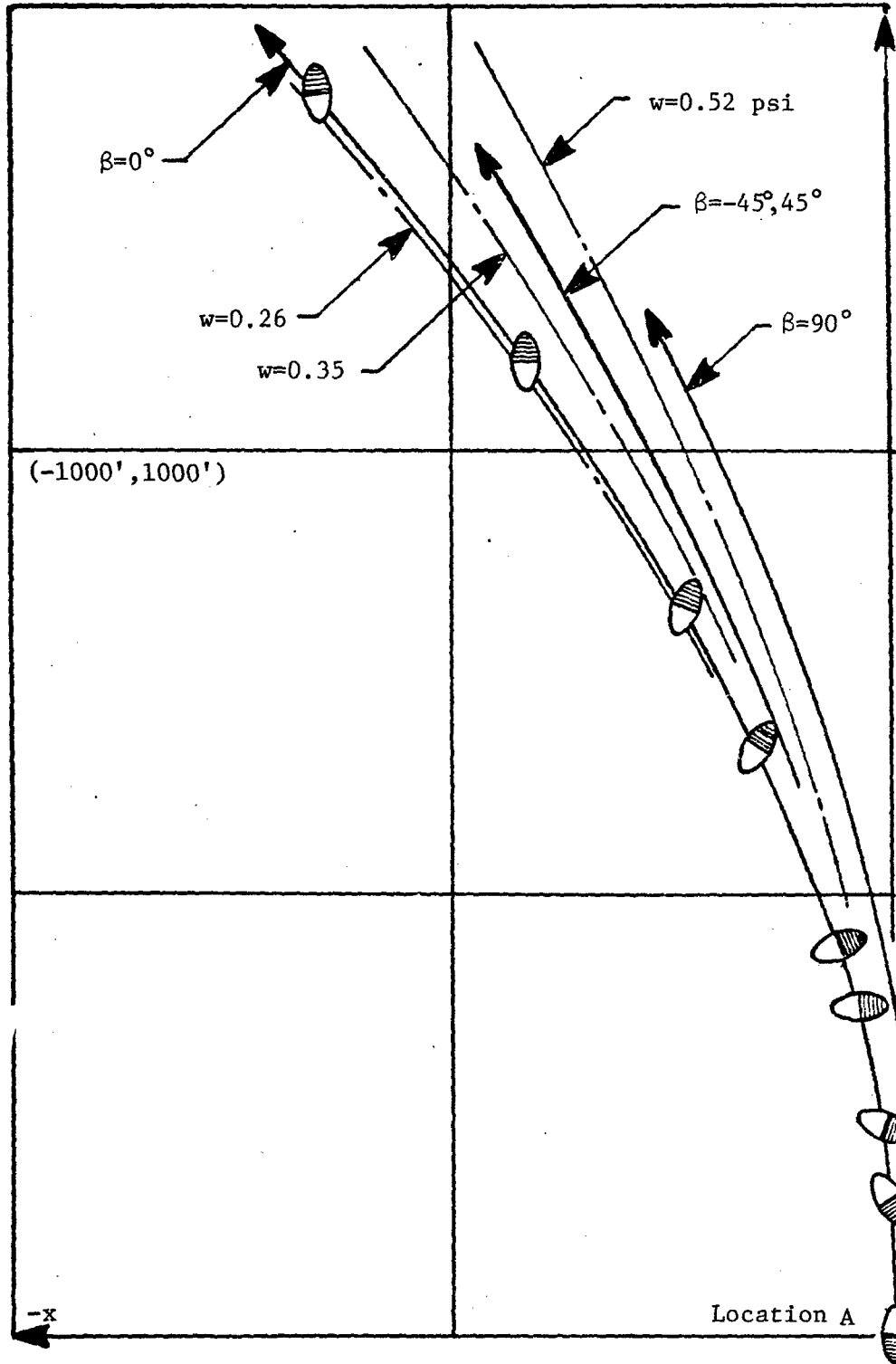
Figure 58   Trajectories of Rotating Debris - S ≈ 0.5

169
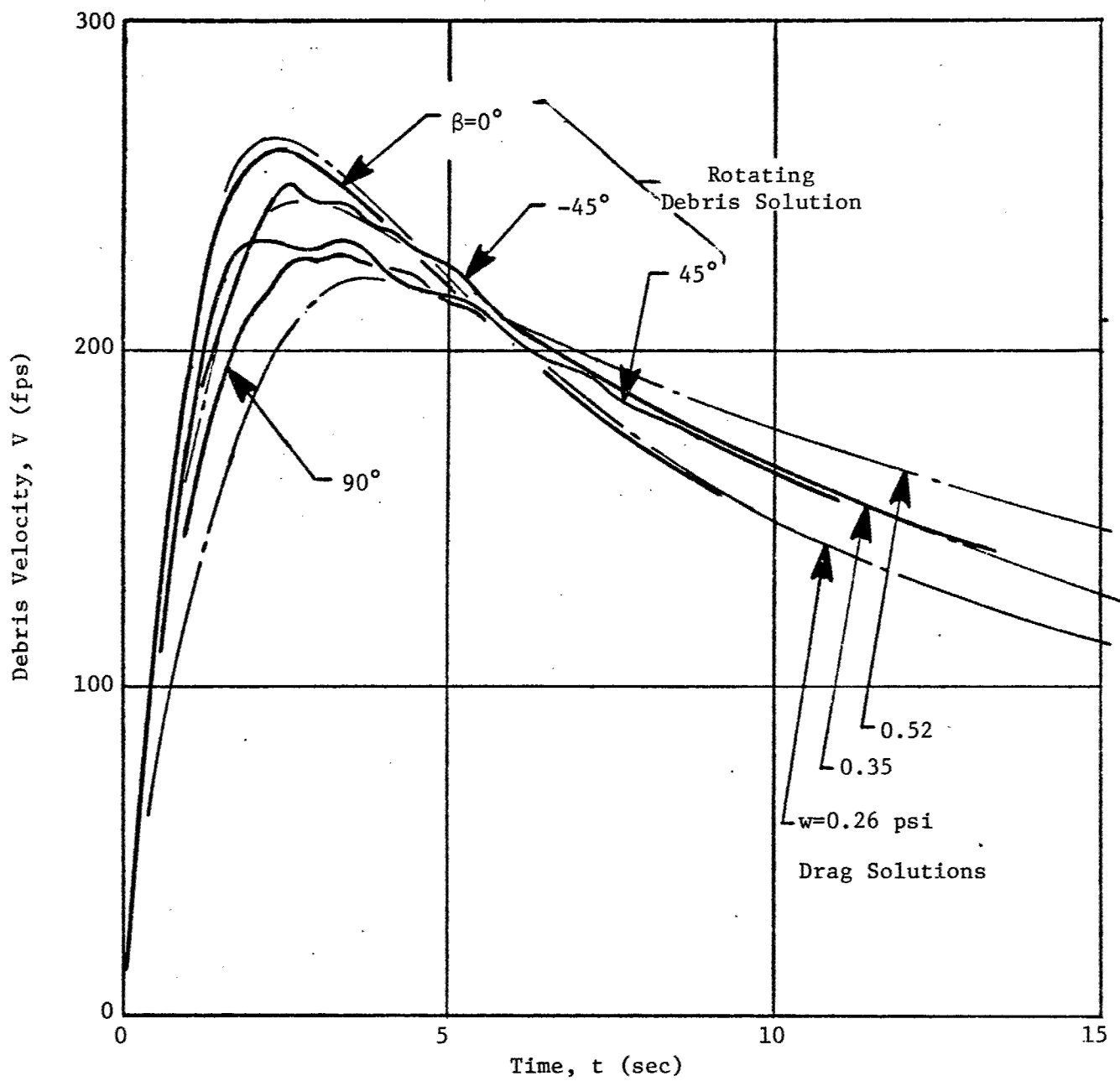
Figure 59   Velocity Histories for Rotating Debris - S = 0.5
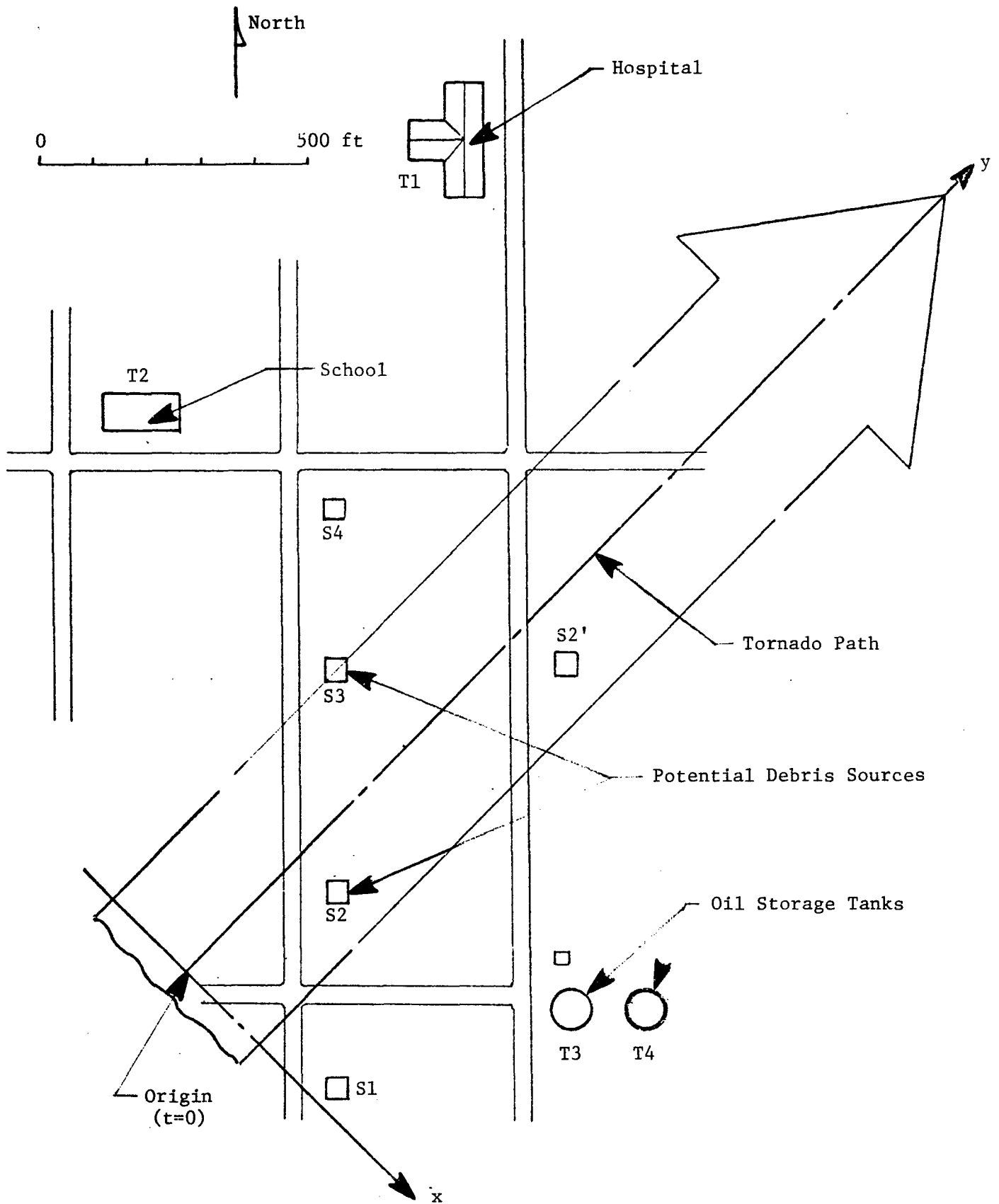
Figure 60   Layout of Targets and Potential Debris Sources

The storm moves in the northeast direction (the +y direction). An examination of storm path data clearly shows that most tornadoes move in this direction. This physical fact suggests one approach to the development of debris impact mitigation techniques. The debris impact environments may have some moderately strong directional characteristics inherent in them which can be exploited to reduce the overall hazard. A purely random system would be more difficult to protect against.

Five debris sources are indicated; however, only three are unique. These are sources S1, S2, and S3. Source S2' is identical to source S2 except for the time and corresponding distance shift. Source S4 was not used (i.e., considered to be nonfailing). The targets were assigned representative shapes, sizes and locations, and assigned names somewhat related to these factors. It is implied that the hospital is a multistory structure (say 3 to 4 stories) whereas the school might be only 1 or 1-1/2 stories high. The oil storage tanks may be 30 to 40 ft high.

In this sample application we need not deal with the number density of the debris although this parameter is a vital factor in establishing the debris impact environment. Thus, this examination will only yield the character of the environment rather than the absolute environment itself. Furthermore, the dynamic response and failure of each of the sources is omitted. Rather a failure period (t_f) is assumed which starts after an indicated period of time (a delay time, t_d) which corresponds to the location shift of the source relative to the storm center. The specific values chosen for these two time parameters for the four debris sources are indicated in Figure 61. Source S1 is the first source to rupture (at t = 0). This figure also illustrates the release points of the debris relative to the storm center. A computer code was assembled which computed the transport characteristics of debris released at discrete release points along the rupture path of a debris source. Calculations were made for the above sources for ballistic weight values ranging from 0.1 to 1.5 psi, thus covering a realistic ballistic weight interval.
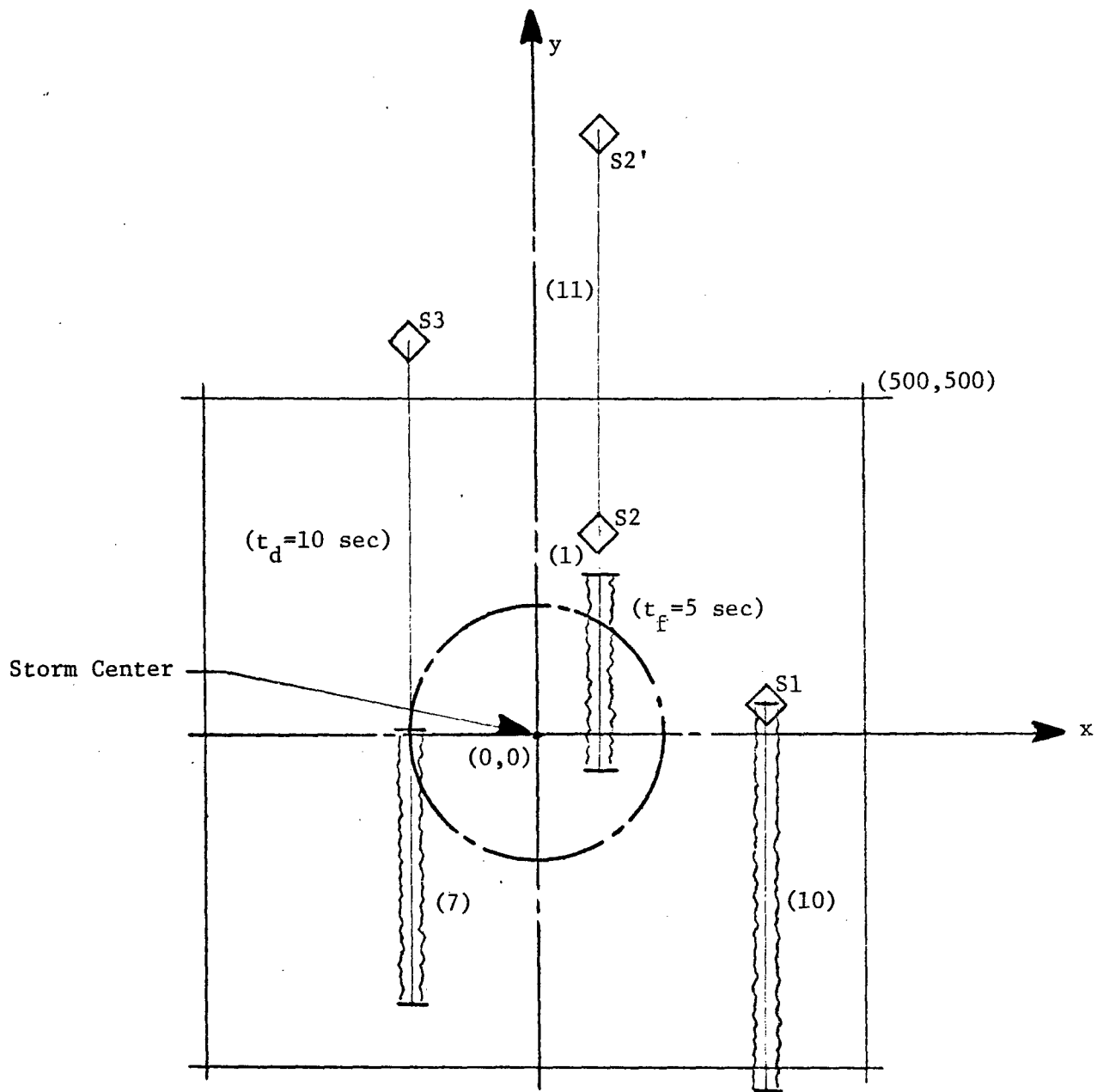
Figure 61 Location of Sources During Rupture Relative
to Storm Center

The limiting trajectories with respect to both ballistic weight and release time (t_r) are shown in Figures 62 and 63 for sources S1 and S3. The hospital (target T1) can be hit by the lighter debris (w = 0.1 psi) which is released from source S1 at the start of its rupture. The oil tanks are clearly in the path of much of the debris released from this source, however, tank T4 is substantially shielded by tank T3. The school, target T2, is not affected by this debris source. The debris coverage from source S3 behaves in a similar manner except that the tank shielding effect no longer exists.

The debris which is released by source S2 (and hence S2') is transported in a much more complex manner. The behavior of the lighter debris (a ballistic weight of 0.1 psi) is shown in Figure 64. The objects of this class of debris which are released early (1<t<3 sec) first move into the third quadrant and are then thrown back by the storm system and move into the first quadrant. Thus they can impact the oil storage tanks; or at least tank T3 since the shielding occurs. Debris released at a later time moves more strongly into the second quadrant and intersects the school location (target T2). Debris which is released late is just able to reach the location of the hospital (target T1).

The very heavy debris (ballistic weight of 1.5 psi) released from this source behaves in a very complex manner (see Figure 65). Most of it is thrown in a northwest direction toward the school and the hospital. However, much of this debris moves through the core of the storm and its motion is substantially reversed as the debris tends to move into a region of rather large relative speed difference and direction. Thus much of the debris ends up moving into the first quadrant and represents a potential hazard to the oil storage tanks. The shaded area represents a "safe" region for the conditions cited, and both the school and the hospital are immune to impacts from this class of debris.

Impact domains can be constructed from these trajectory data as a function of ballistic weight and release time from individual sources as well as from the totality of sources considered. The impact domains for targets T1 and T2 are presented in Figure 66.
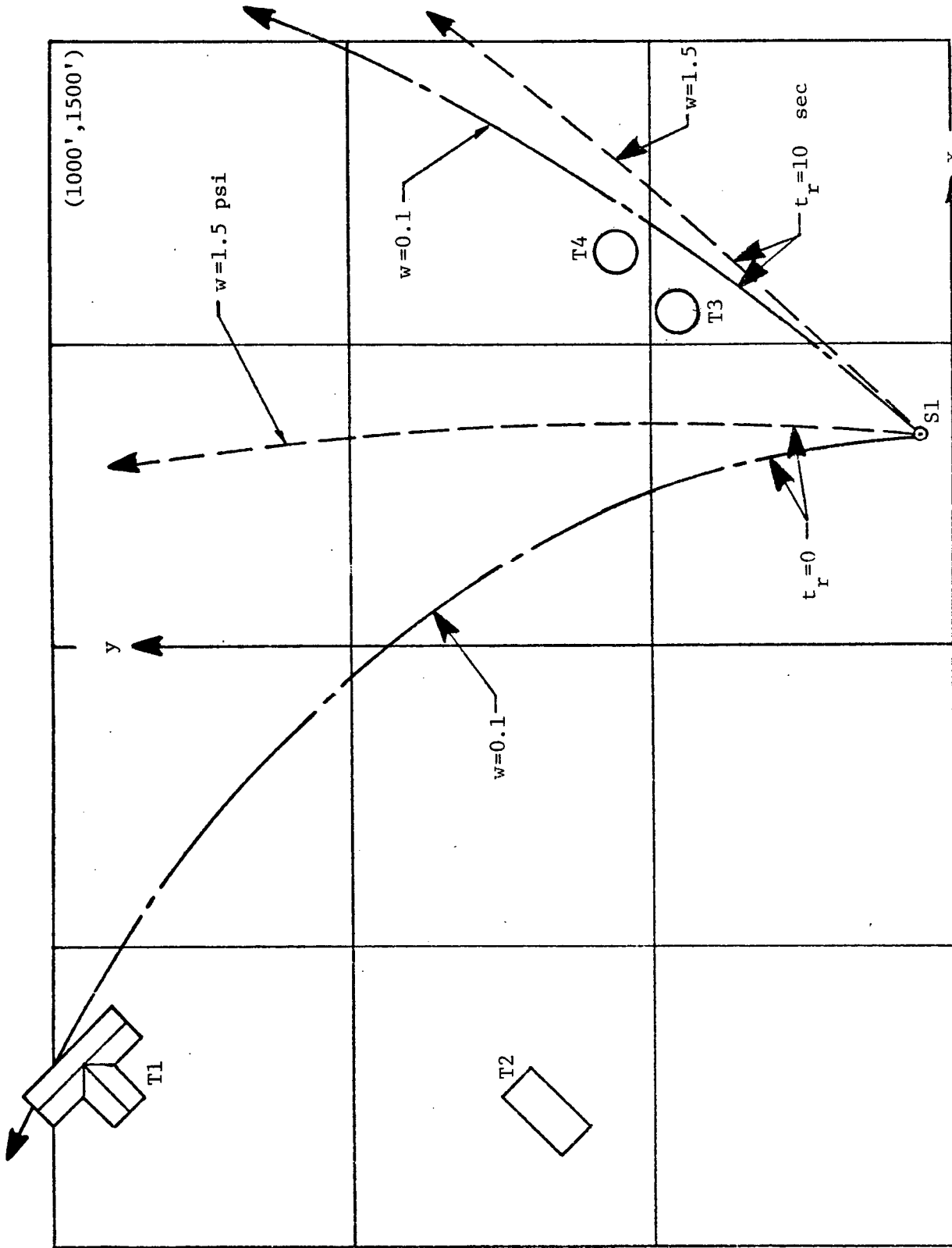
Figure 62   Debris Coverage from Source S1
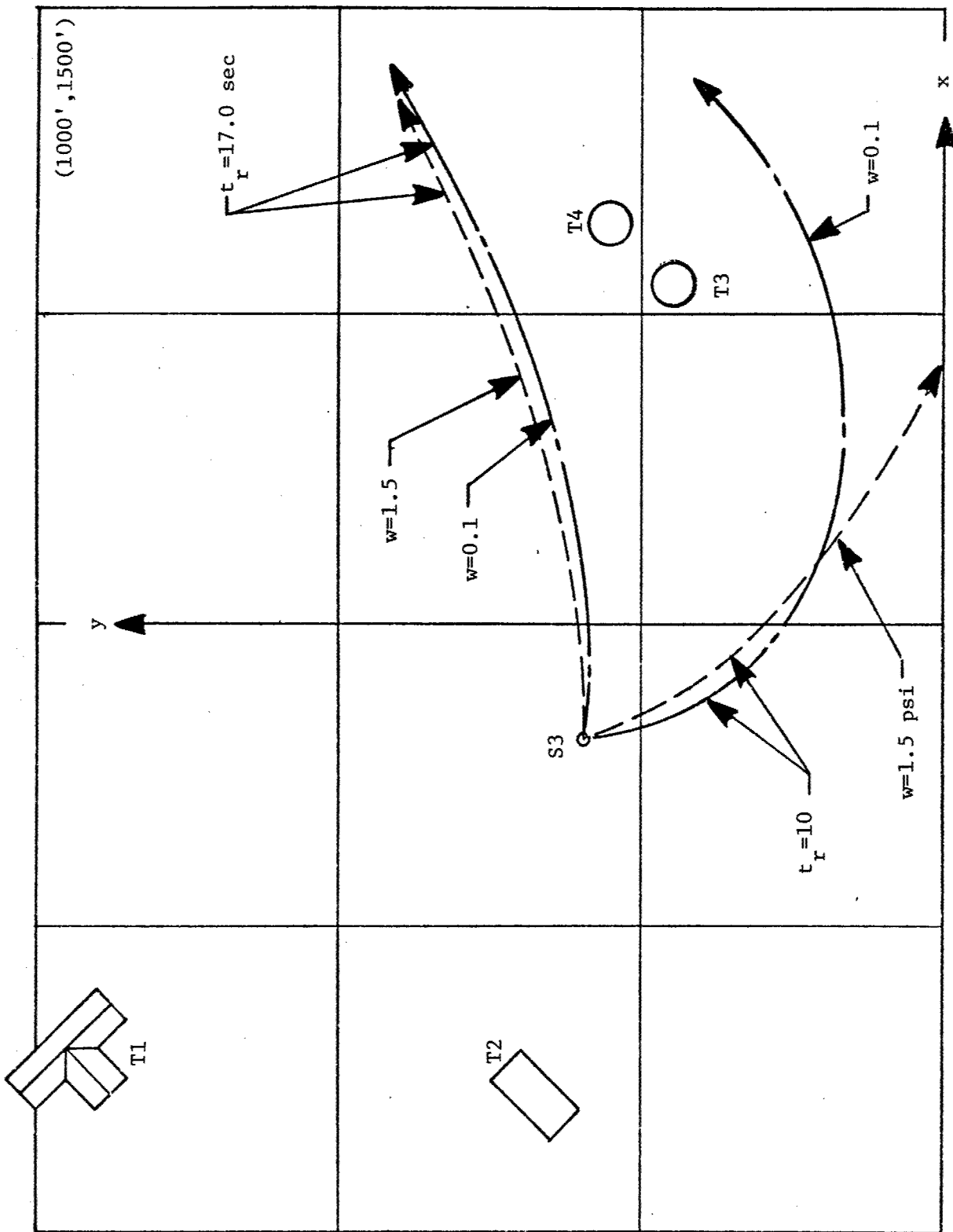
Figure 63   Debris Coverage from Source S3
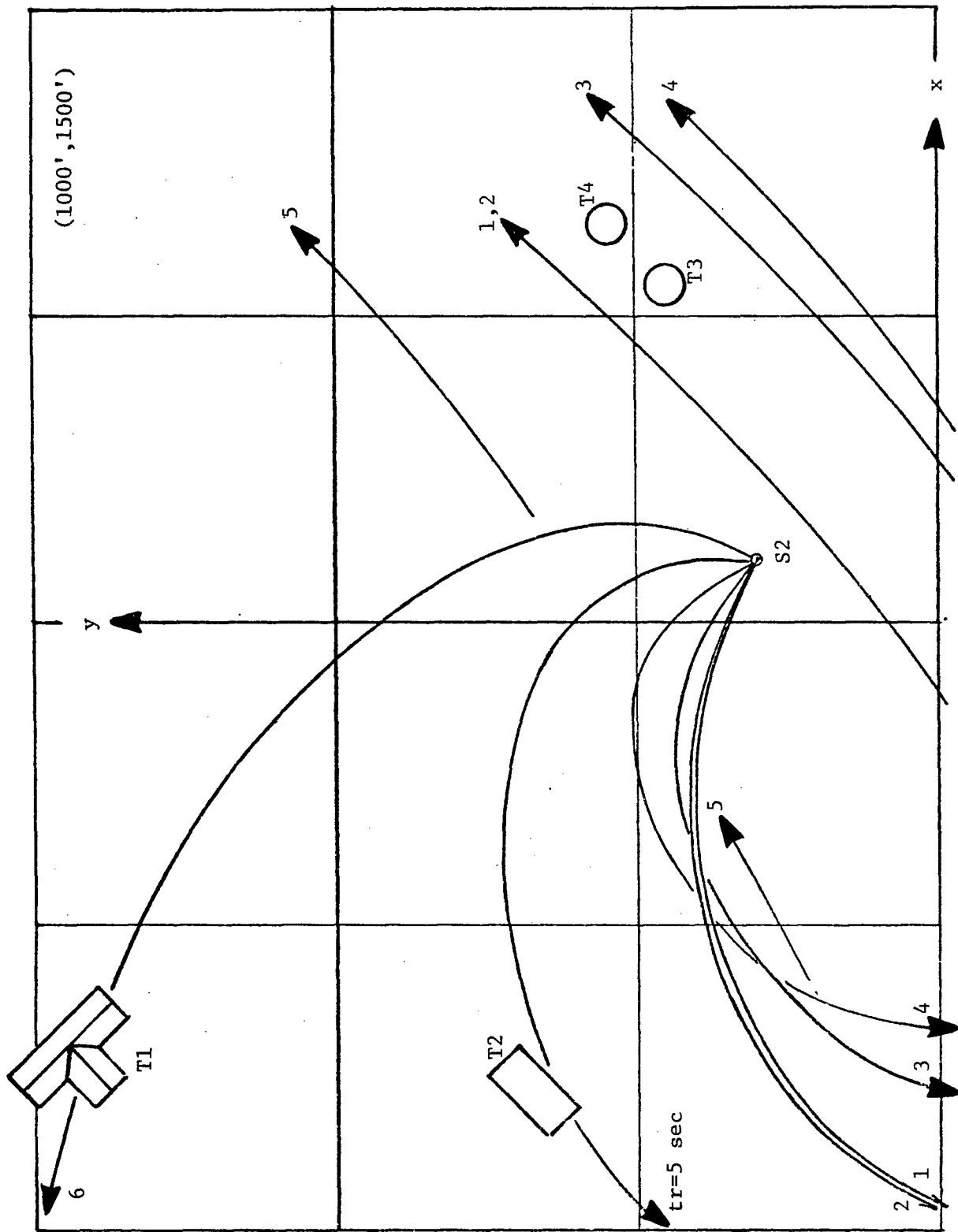
Figure 64   Debris Coverage from Source S2 - w = 0.1 psi
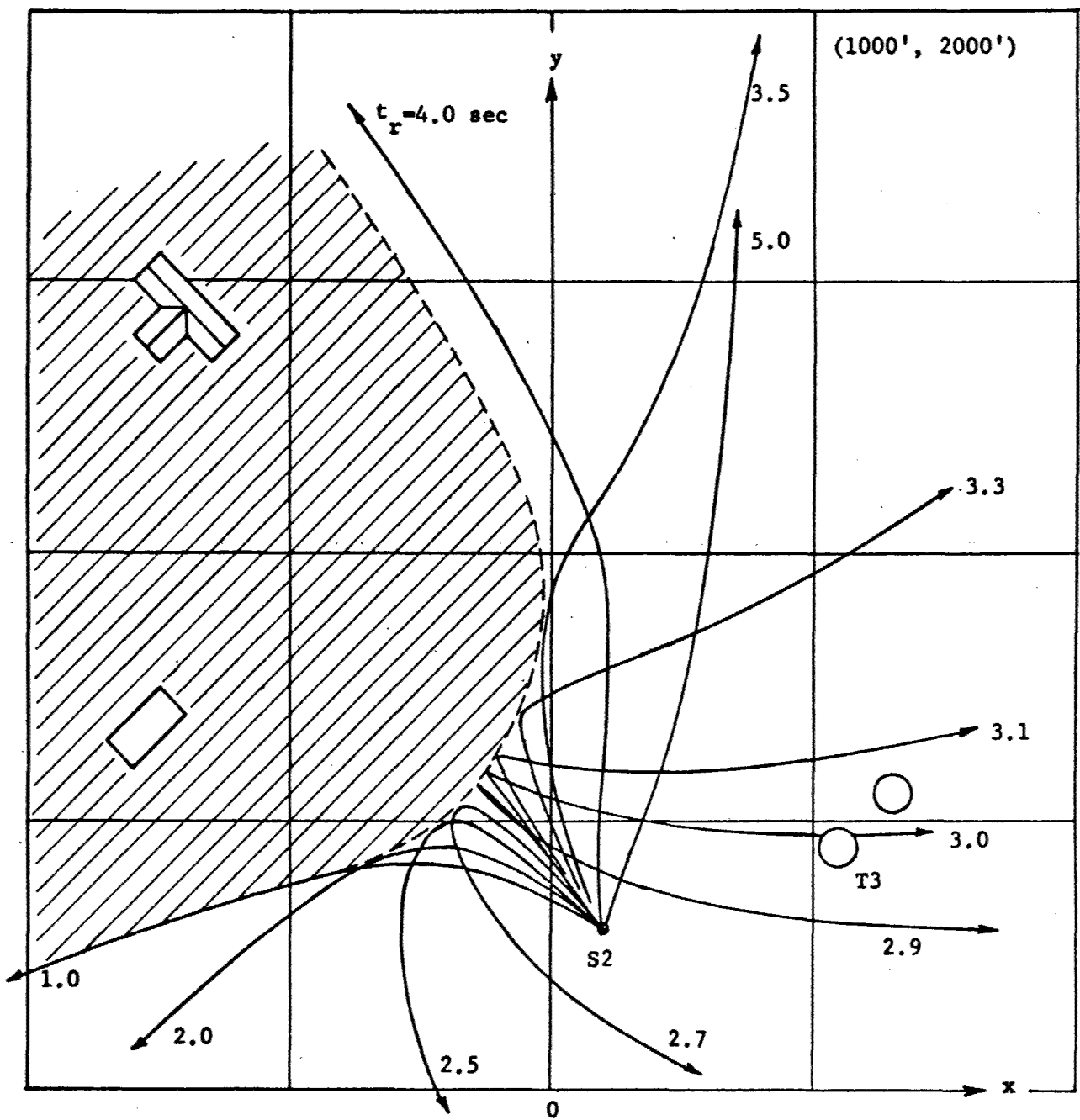
Figure 65   Debris Trajectories from Source S2 - w = 1.5 psi
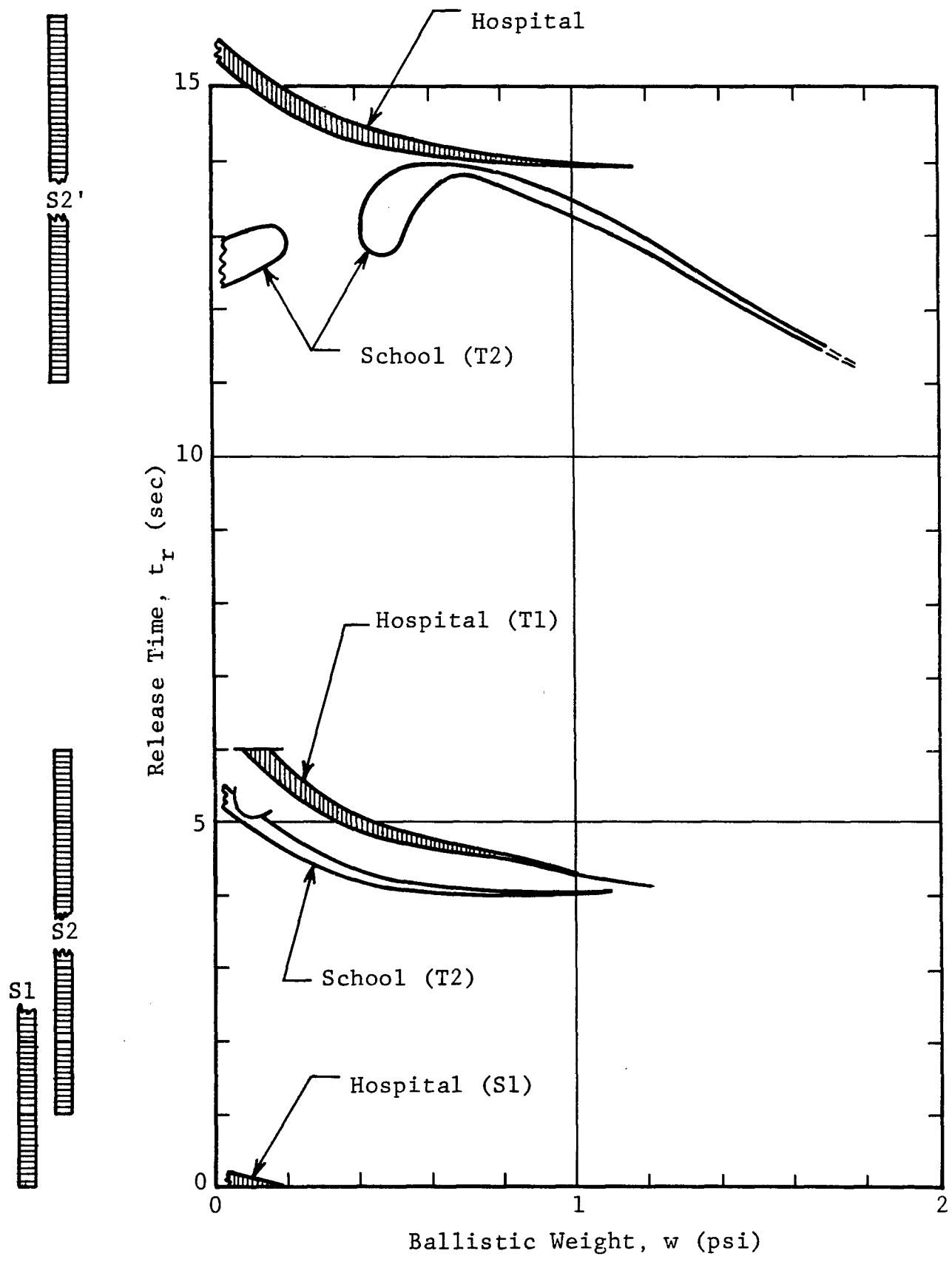
Figure 66   Impact Domains for Targets T1 and T2

179

It is possible to subdivide these targets into subtargets represent-
ing different surfaces of the target. Only specific walls of these
structures are subject to impact loads. Similar impact domains
were constructed for the oil storage tanks, targets T3 and T4.
These are presented in Figure 67.   The impact domains for these
targets are rather insensitive to the ballistic weight of the
debris and a rather broad time window exists. The impact domains
for both the school and the hospital, which are both somewhat
further from the storm center, are much more restricted both with
respect to the ballistic weight effects and to the release time
interval. It is clear from these examples that the effective dis-
persion effect the motion of two-dimensional debris will have can
be handled in a statistical manner.

The number density, and other debris characteristics such as
weight are needed before the impact environment can be completely
defined, however the preceding data will also provide both the im-
pact velocity as well as the nominal angle of incidence of impact
on specific surfaces. The impact velocity details are presented
in Figures 68 and 69 for the targets examined in this example.
As these figures show, the impact velocity varies over the range
50 to 200 fps. These values are relatively small compared to the
peak magnitude of the wind speed and suggest that, for realistic
distributions of structures, critical components or walls can
readily be made less susceptible by proper placement.

5.6 SUMMARY

An approach to the evaluation of the debris or missile hazard
produced by a tornado exposure has been outlined. This approach
is based, in part, upon a blend of deterministic calculations and
probabilistic estimates, and can be developed at several levels
of sophistication. A series of activities essential to the achieve-
ment of the above goal are identified and several are carried for-
ward in this work. A conventional tornado wind environment, together
with a simple aerodynamic drag model is used to establish debris
trajectories and motion histories for one rather severe tornado
wind field. A parameter, the effective ballistic weight, is used
to characterize the debris.
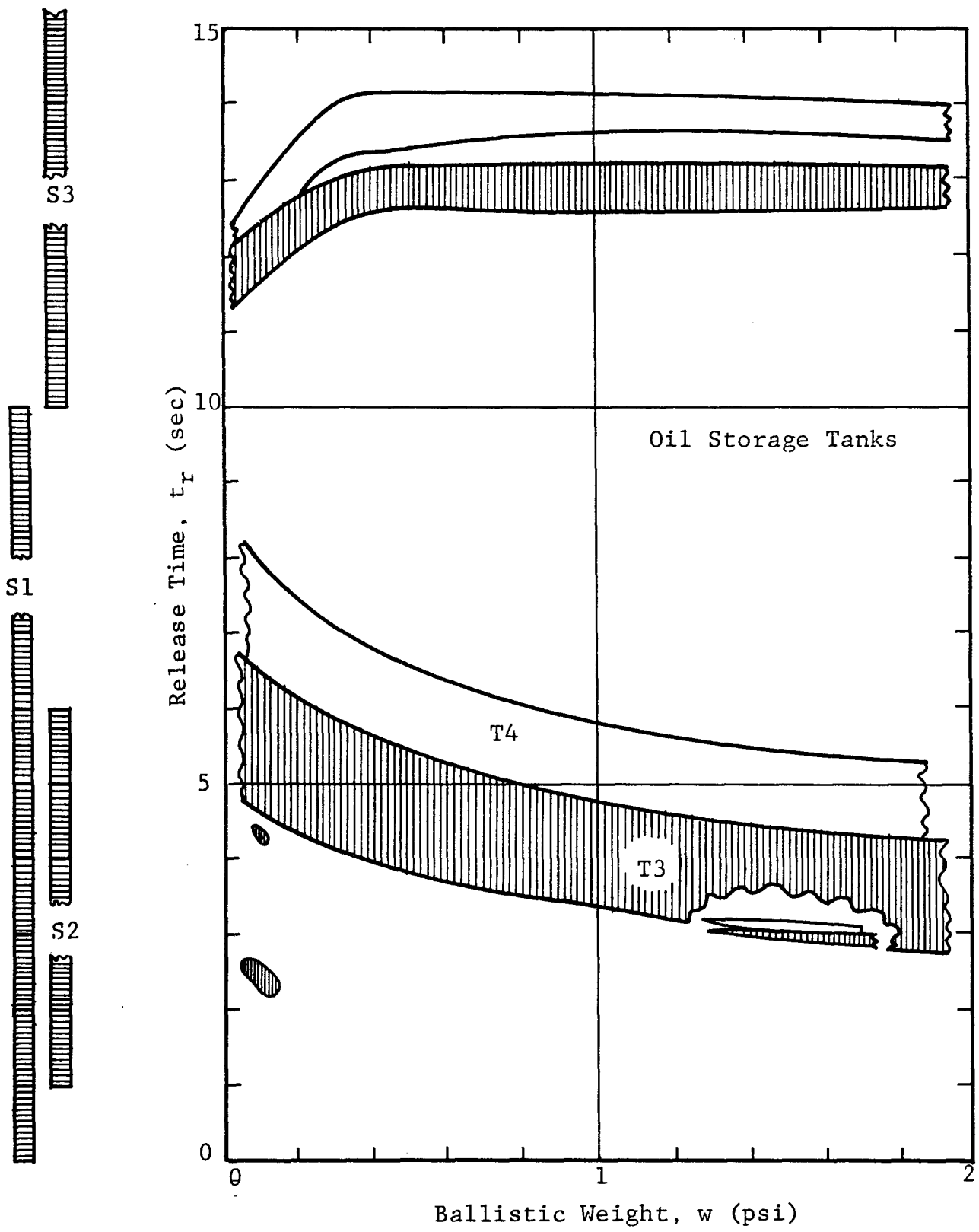
Figure 67   Impact Domains for Targets T3 and T4
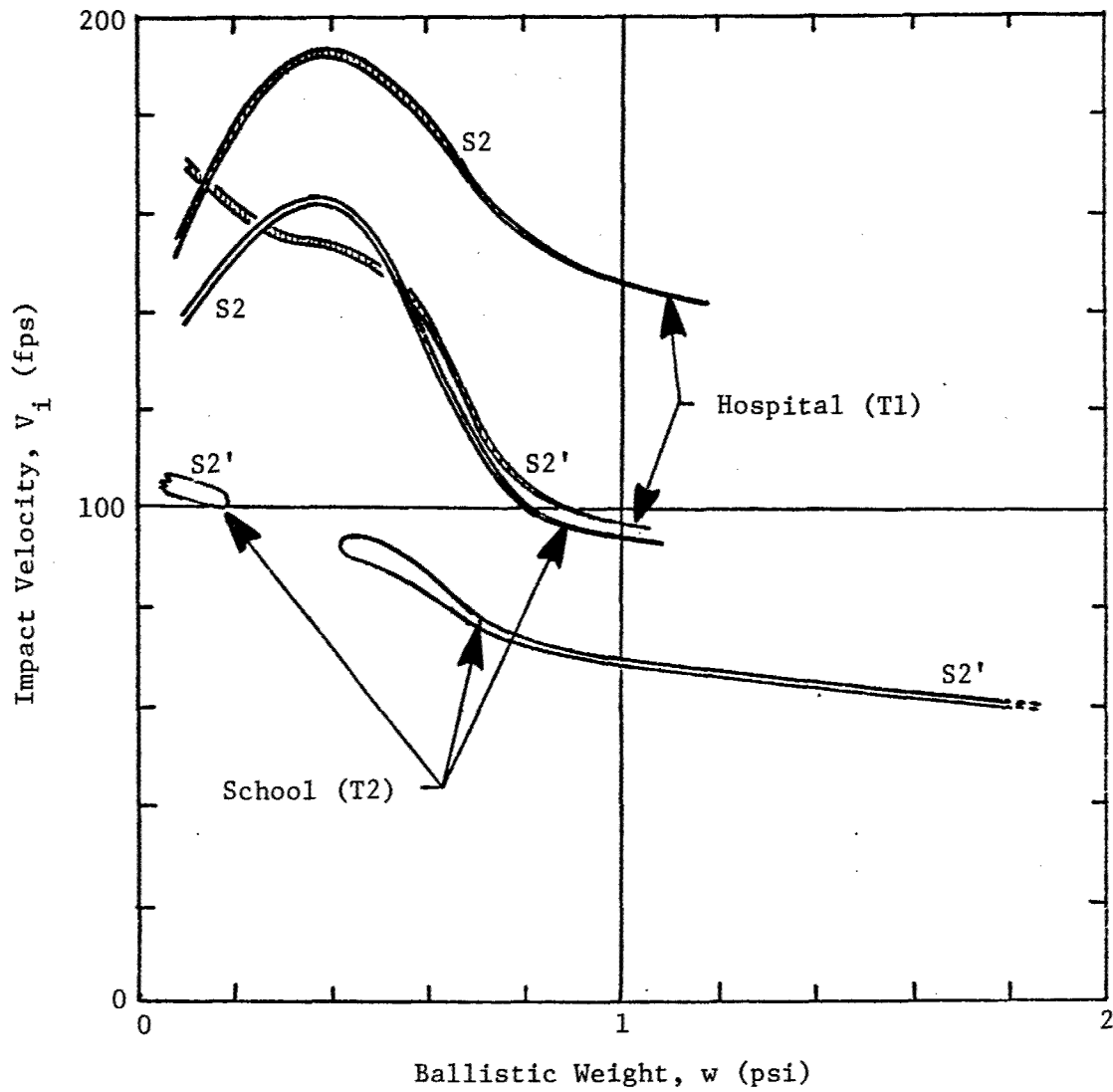
Figure 68 Impact Velocity Variations for Targets T1 and T2
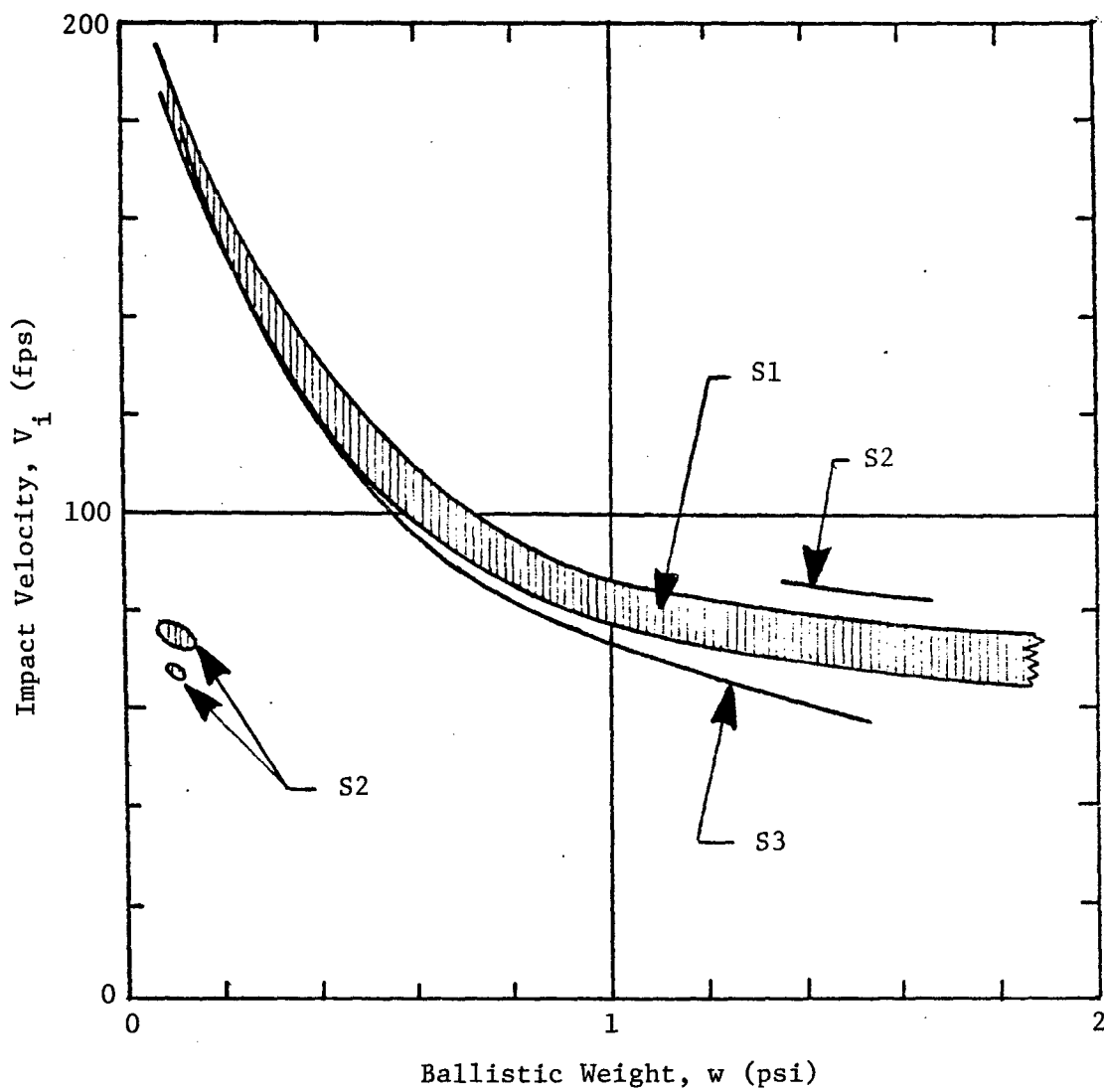
Figure 69   Impact Velocity Variations for Target T3

This parameter was evaluated for typical debris and found to be in the range 0.1 to 1.0 psi for much debris of general interest. This group of debris is accelerated by the tornado wind field to approximately 30 to 60 percent of the maximum wind speed when released in the general vicinity of the core of the tornado. The debris which is accelerated rapidly is also decelerable rather rapidly, thus its high velocity flight period tends to be short as it moves outward into the slower moving wind field.

The simple drag model is clearly applicable for debris of nearly spherical shape. However, since much debris can be expected to be more two-dimensional in shape, a two-dimensional aerodynamic model for lifting and rotating bodies was developed and a limited series of trajectories and motion histories were determined. This evaluation showed that the results obtained from the simple drag model are adequate for describing the debris transport phenomenon and that the two-dimensional features of the debris are equivalent to a dispersion (i.e., a statistical adjustment) in the ballistic weight parameter corresponding to the limiting values of this parameter for the debris evaluated. An examination of the ballistic weight parameter values for two- and three-dimensional shapes of interest show that the orientation averaged value tends to be near its minimum value.

The simple drag model and storm description were used to evaluate the integrated debris impact environment on several potential targets in a limited debris source application in which the debris production and rupture details were assumed. Thus the nature of the impact domains in terms of the ballistic weight parameter and release time were established. These results also include the magnitude of the impact velocities on the selected targets. The results of the calculation also include the impact obliquity on the various surfaces of the targets. In general, impact velocities were in the range of from 50 to 200 fps.

The analysis presented in this work was rather limited and several areas of activity require further development. The most critical, perhaps, is that dealing with debris production; namely, the definition of the loads on structures and other potential debris producing shapes and the response of these entities to the point of rapid failure, including the interaction between the response and the loads. The further evaluation of the applicability of a simple drag model to describe the transport phenomenon of more complex debris shapes and finally to gradually improve the description of the tornado wind field are considered to be important.

CHAPTER 6

CONCLUSIONS AND RECOMMENDATIONS

6.1 BACKGROUND

The current and primary concern of the United States civil defense remains "people survivability" in the narrowest and the broadest definition of this term, i.e., short- and long-term survival.

Certain population centers are at risk with respect to a nuclear weapon attack. At any given time the level of risk is variable and reaches its potentially highest level during a crisis period.

Current U.S. thinking relative to a civil defense posture includes "Crisis Relocation Planning" (CRP). CRP will result in moving a significant fraction of the (high risk) urban area population into the surrounding (low level of risk) areas.

The primary problem for CRP will be that of providing adequate "life support" (food, water, shelter, sanitation and medical services) for the displaced masses and to maintain continuity of society.

Obviously, not all of the people will or can leave the given urban areas. Most of the existing "Life Support Facilities" (LSF's) e.g. food processing plants and food storage facilities, medical supply manufacturing plants and warehouses etc. are currently located in urban areas. These urban areas are potentially at risk. People will be required to staff and operate designated LSF's at acceptable levels of productivity and performance. Before CRP can be effectively implemented, certain basic questions need to be answered among which are the following.

1. What LSF's are needed?
2. Where are they located?
3. At what fraction of normal operation are they to be operated and what are the corresponding manpower requirements for operation and maintenance?
4. What transportation (supply of goods) network is required?

5. What labor force is required?

6. Where will the labor force be located?

7. What shelters at or near to LSF's are available?

8. What level of protection is afforded by them relative to anticipated attack?

9. What level of shelter is required in host (low level of risk) areas?

10. How can the sheltering requirements (in urban and host areas) be met?

6.2 REQUIRED RESEARCH

- Field surveys should be conducted to collect the needed data for questions 1 through 10 above. Specifically, we need to identify all functional characterisitcs of LSF's and collect corresponding data so as to:

    (1) determine the adequacy of LSF's in providing the needed services, and

    (2) determine the adequacy of available personnel shelters relative to the probable attack environments (blast, fire, radiation, shelter environments).

- Should it be desirable that certain LSF's or LSF shelters be hardened, then survey information (together with appropriate analyses) can then be used in determining what hardening techniques should be used; e.g., full scale, permanent retrofitting or expedient measures. Hardening of LSF's is expected to be strongly function-dependent and therefore each LSF category would probably need to be considered on an individual basis. A task which would be concerned with identifying feasible hardening techniques for LSF's and LSF shelters should be pursued.

- Determine recovery characteristics of selected LSF's and down-time impact on the population.

- <u>People survivability</u> is the cornerstone of any viable civil defense posture. People survivability analyses should continue since, as yet, we do not have a clear picture as to what level of survivability is possible in urban or host areas with respect to probable (nuclear weapon) attack conditions. Specifically, we need to answer the following questions:

  (1) What potential for people survival (short- and long-term) exists in a given urban area subjected to a given level of risk?

  (2) What corresponding level of survivability exists in a host area?

  (3) What level of confidence can be attached to our estimates?

Up to the present time, we have considered the problem of people survivability in fairly general terms, and have succeeded in making estimates as to <u>total survivors</u>, i.e., injured and un- injured. We have recognized the importance of being able to pre- dict <u>long term</u> survivability which requires knowledge as to the number of expected <u>injured</u> personnel as part of total survivors. Overall we have accomplished the following:

- In the previous studies tools were developed to pre- dict numbers of survivors (injured and uninjured as a single group) in the immediate post-attack period. These tools have been exercised in analyzing some sixty existing buildings which were surveyed in de- tail. This was useful in broadening our understand- ing of the sheltering potential of conventional build- ings.

- As a result of the study reported herein, general in- jury criteria for predicting impact injuries have been selected. These were applied on a limited scale to people in conventional basements (see Chapter 3).

- A tool (articulated man simulation model) capable of identifying and categorizing injuries to the various parts of the body as a result of impact was developed.

189

- Casualty criteria capable of rating corresponding impact injuries on the basis of "energy density" where selected from available literature (see Chapter 2). Although still very approximate, this approach is a substantial improvement on the "rigid block" model.

To meet the goals postulated earlier, we need to perform the following tasks:

1. Develop injury and fatality criteria (short- and long-term effects) for prompt nuclear and thermal radiation.

2. Using these data and those relating impact casualties, perform systematic analysis of people survivability under probable attack situations with the object of isolating pertinent shelter and people parameters and shaking down the analysis process.

3. Determine confidence limits for results obtained.

4. Apply the analysis procedure on a systematic basis to all population centers at risk and determine what options are open to the civil defender.

The analysis process should be used on similar problems by all DOD (Department of Defense) agencies.

APPENDIX A

SLAB DESIGN PARAMETERS AND FAILURE DATA

This appendix contains all design parameters and corresponding failure data for one-way and two-way reinforced concrete slabs considered in this study and discussed in Chapter 3. One-way slab results are summarized in Table A.1. Design parameters considered with this category of slabs are given as follows:

Span length (simply supported)	- 12 ft, 16 ft, 20 ft
(two-span continuous)	- 16 ft, 20 ft, 24 ft, 28 ft
Design live load	- 50 psf, 80 psf, 125 psf, 250 psf
f'_c (ultimate compressive strength of concrete)	- 3 ksi, 4 ksi
f_y (yield strength of reinforcing steel)	- 40 ksi, 60 ksi

Table A.1 contains the corresponding slab thicknesses, required reinforcing steel and supporting analysis information such as the effective depth of slab, the ultimate bending moment and the effective moment of inertia. Also included in this table are two overpressures (P1, P2) of long duration required to fail the slab. Very generally, P1 refers to the incipient collapse of the whole slab while P2 refers to the subsequent incipient collapse of a portion of the slab. Specific collapse mechanisms considered are described in Chapter 3.

Two-way slabs considered herein belong in the flat plate - flat slab category. Design parameters used are summarized in Table A.2.

Results for two-way slabs are summarized in Table A.3. This includes slab thicknesses, reinforcement requirements, capital and drop panel sizes, etc. Nomenclature is identified in Figure A.1. Also included in this table are static and dynamic strengths of these slabs. Static strength is expressed in terms of uniform

overpressure required to yield the slab. Type of failure, i.e., shear or flexure is also indicated. Dynamic strength is expressed in terms of: (a) uniform blast pressure of long duration required to produce incipient collapse: and (b) uniform blast pressure of long duration required to produce altimate collapse, i.e., separation and dropping of the slab. Analysis procedures used herein are described in Chapter 3 together with design assumptions and design procedures.

Column Capital

Drop Panel

t

D

CAP

t_d

(a) Flat-Slab Floor

L

L

L

t
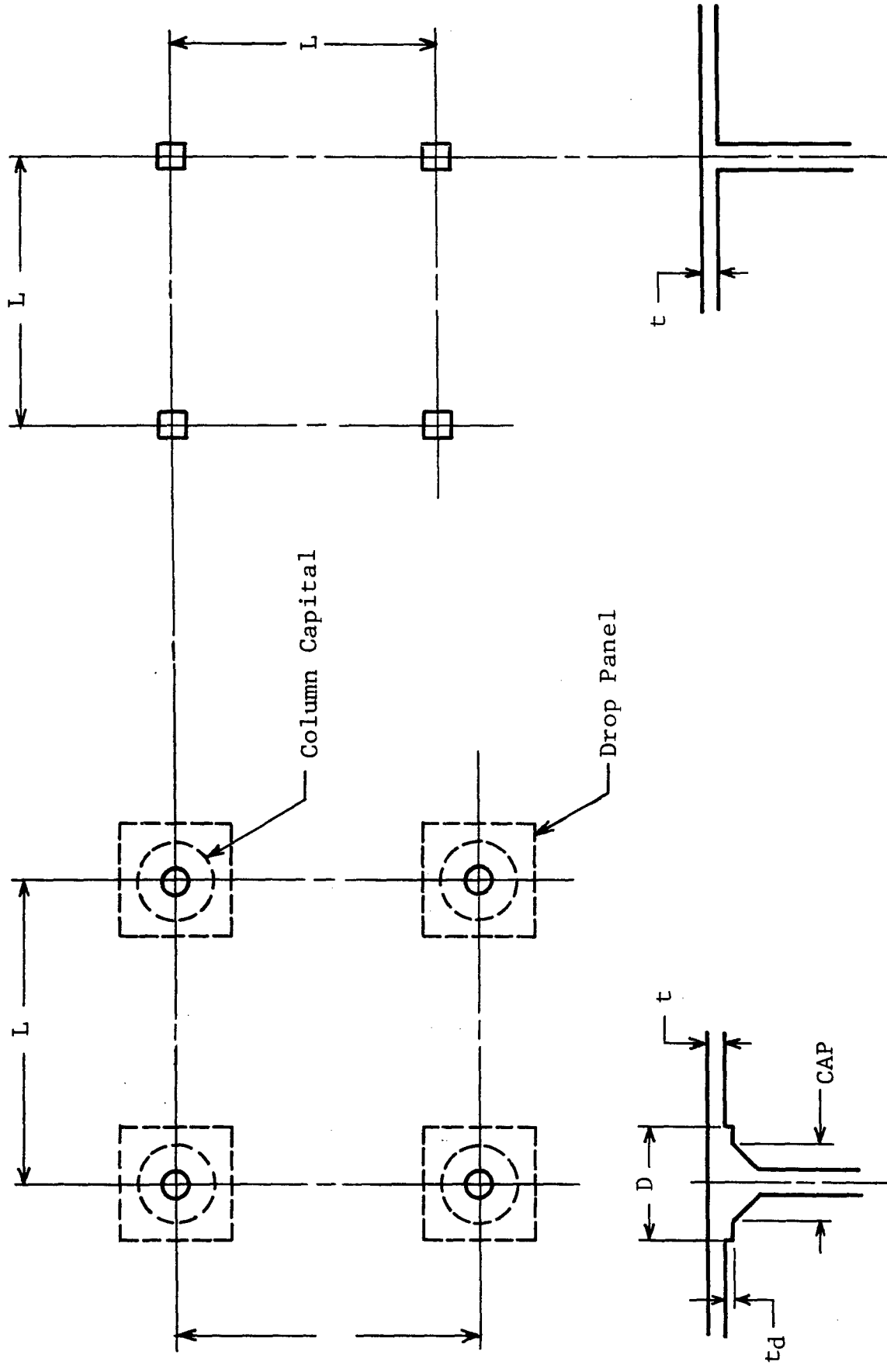
(b) Flat-Plate Floor

Figure A.1 Flat-Slab, Flat-Plate Construction and Nomenclature

193

Table A.1
ONE-WAY SLABS - DESIGN PARAMETERS AND FAILURE DATA

Concrete Compressive Strength: 3 ksi
Steel Yield Strength: 40 ksi
Slab Type: Simply Supported

Nominal Live Load (psf)	50.00	50.00	80.00	50.00	80.00	80.00
Span Length (ft)	12.00	16.00	20.00	12.00	16.00	20.00
Effective Depth (in.)	3.84	5.56	7.63	4.41	6.12	7.80
Total Slab Thickness (in.)	4.84	6.56	8.63	5.41	7.12	8.80
Ultimate Moment (ft-lb)	3052	5497	8984	4150	6905	9985
Flexural Steel Area (in.^{2}/ft)	0.28	0.34	0.47	0.33	0.39	0.44
Shear Reinforcement (in.^{2}/ft)	0.00	0.00	0.00	0.00	0.00	0.00
Effective Moment of Inertia (in.^{4})	39.40	115.00	286.40	60.30	154.80	310.10
Failure Overpressure P1 (psi)	1.18	1.06	0.96	1.70	1.42	1.14
Failure Overpressure P2 (psi)	5.94	5.90	6.05	8.16	7.50	6.78

Nominal Live Load (psf)	125.00	125.00	125.00	250.00	250.00	250.00
Span Length (ft)	12.00	16.00	20.00	12.00	16.00	20.00
Effective Depth (in.)	5.15	7.61	10.39	6.56	9.47	12.54
Total Slab Thickness (in.)	6.15	8.61	11.39	7.56	10.47	13.54
Ultimate Moment (ft-lb)	5762	11621	20586	10030	19459	33098
Flexural Steel Area (in.^{2}/ft)	0.39	0.53	0.69	0.54	0.72	0.92
Shear Reinforcement (in.^{2}/ft)	0.00	0.00	0.00	0.00	0.00	0.00
Effective Moment of Inertia (in.^{4})	96.90	304.60	763.20	204.40	601.10	1382.0
Failure Overpressure P1 (psi)	2.47	2.67	2.90	4.56	4.80	5.05
Failure Overpressure P2 (psi)	11.44	12.88	14.48	20.13	21.84	23.62

Table A.1 (Contd)

Concrete Compressive Strength: 4 ksi
Steel Yield Strength: 40 ksi
Slab Type: Simply Supported

Nominal Live Load (psf)	50.00	50.00	50.00	80.00	80.00	80.00
Span Length (ft)	12.00	16.00	20.00	12.00	16.00	20.00
Effective Depth (in.)	3.51	5.03	6.79	4.06	5.57	7.02
Total Slab Thickness (in.)	4.51	6.03	7.79	5.06	6.57	8.02
Ultimate Moment (ft-lb)	2950	5197	8245	4039	6598	9308
Flexural Steel Area (in.^{2}/ft)	0.29	0.36	0.42	0.35	0.41	0.46
Shear Reinforcement (in.^{2}/ft)	0.00	0.00	0.00	0.00	0.00	0.00
Effective Moment of Inertia (in.^{4})	31.50	88.10	208.90	48.90	121.20	234.10
Failure Overpressure P1 (psi)	1.15	1.01	0.89	1.66	1.37	1.07
Failure Overpressure P2 (psi)	5.73	5.57	5.54	7.93	7.16	6.31

Nominal Live Load (psf)	125.00	125.00	125.00	250.00	250.00	250.00
Span Length (ft)	12.00	16.00	20.00	12.00	16.00	20.00
Effective Depth (in.)	4.76	7.02	9.60	6.10	8.82	11.63
Total Slab Thickness (in.)	5.76	8.02	10.60	7.10	9.82	12.63
Ultimate Moment (ft-lb)	5638	11286	19901	9887	19094	32295
Flexural Steel Area (in.^{2}/ft)	0.41	0.56	0.72	0.57	0.75	0.97
Shear Reinforcement (in.^{2}/ft)	0.00	0.00	0.00	0.00	0.00	0.00
Effective Moment of Inertia (in.^{4})	79.40	247.80	623.20	171.30	502.50	1141
Failure Overpressure P1 (psi)	2.43	2.62	2.83	4.50	4.73	4.96
Failure Overpressure P2 (psi)	11.17	12.48	13.99	19.78	21.38	23.00

Table A.1 (Contd)

Concrete Compressive Strength: 3 ksi
Steel Yield Strength: 60 ksi
Slab Type: Simply Supported

Nominal Live Load (psf)	50.00	50.00	50.00	80.00	80.00	80.00
Span Length (ft)	12.00	16.00	20.00	12.00	16.00	20.00
Effective Depth (in.)	3.83	4.74	7.68	4.48	6.15	7.84
Total Slab Thickness (in.)	4.83	5.74	8.68	5.48	7.15	8.84
Ultimate Moment (ft-lb)	3050	4214	9025	4173	6919	10031
Flexural Steel Area (in.^{2}/ft)	0.19	0.23	0.27	0.22	0.26	0.30
Shear Reinforcement (in.^{2}/ft)	0.00	0.00	0.00	0.00	0.00	0.00
Effective Moment of Inertia (in.^{4})	35.60	104.80	269.50	56.90	143.00	290.30
Failure Overpressure P1 (psi)	1.19	1.07	0.97	1.72	1.44	1.15
Failure Overpressure P2 (psi)	5.99	5.95	6.11	8.30	7.59	6.86

Nominal Live Load (psf)	125.00	125.00	125.00	250.00	250.00	250.00
Span Length (ft)	12.00	16.00	20.00	12.00	16.00	20.00
Effective Depth (in.)	5.22	7.80	10.49	6.74	9.72	12.83
Total Slab Thickness (in.)	6.22	8.80	11.49	7.74	10.72	13.83
Ultimate Moment (ft-lb)	5781	11725	20673	10085	19601	33346
Flexural Steel Area (in.^{2}/ft)	0.26	0.35	0.46	0.35	0.47	0.61
Shear Reinforcement (in.^{2}/ft)	0.00	0.00	0.00	0.00	0.00	0.00
Effective Moment of Inertia (in.^{4})	90.10	294.60	713.30	196.10	579.40	1325.0
Failure Overpressure P1 (psi)	2.51	2.72	2.94	4.63	4.88	5.13
Failure Overpressure P2 (psi)	11.61	13.12	14.68	20.49	22.24	24.05

Table A.1 (Contd)

Concrete Compressive Strength: 4 ksi
Steel Yield Strength: 60 ksi
Slab Type: Simply Supported

Nominal Live Load (psf)	50.00	50.00	50.00	80.00	80.00	80.00
Span Length (ft)	12.00	16.00	20.00	12.00	16.00	20.00
Effective Depth (in.)	3.53	5.08	6.84	4.09	5.66	7.07
Total Slab Thickness (in.)	4.53	6.08	7.84	5.09	6.66	8.07
Ultimate Moment (ft-lb)	2954	5228	8296	4049	6646	9354
Flexural Steel Area (in.^{2}/ft)	0.19	0.24	0.28	0.23	0.27	0.30
Shear Reinforcement (in.^{2}/ft)	0.00	0.00	0.00	0.00	0.00	0.00
Effective Moment of Inertia (in.^{4})	28.50	82.20	195.50	44.60	114.20	217.60
Failure Overpressure P1 (psi)	1.16	1.03	0.90	1.69	1.40	1.08
Failure Overpressure P2 (psi)	5.80	5.66	5.62	8.04	7.29	6.40

Nominal Live Load (psf)	125.00	125.00	125.00	250.00	250.00	250.00
Span Length (ft)	12.00	16.00	20.00	12.00	16.00	20.00
Effective Depth (in.)	4.83	7.15	9.70	6.28	8.99	11.97
Total Slab Thickness (in.)	5.83	8.15	10.79	7.28	9.99	12.97
Ultimate Moment (ft-lb)	5661	11361	19983	9941	19196	32600
Flexural Steel Area (in.^{2}/ft)	0.27	0.37	0.48	0.37	0.49	0.63
Shear Reinforcement (in.^{2}/ft)	0.00	0.00	0.00	0.00	0.00	0.00
Effective Moment of Inertia (in.^{4})	73.70	233.50	577.50	163.10	472.30	1103
Failure Overpressure P1 (psi)	2.47	2.66	2.87	4.58	4.81	5.05
Failure Overpressure P2 (psi)	11.35	12.71	14.20	20.17	21.77	23.50

Concrete Compressive Strength: 3 ksi
Steel Yield Strength: 40 ksi
Slab Type: Two-Span Continuous

Nominal Live Load (psf)	50.00	50.00	50.00	50.00
Span Length (ft)	16.00	20.00	24.00	28.00
Effective Depth (in.)	4.24	5.70	7.30	9.19
Total Slab Thickness (in.)	5.24	6.70	8.30	10.19
+ Ultimate Moment (ft-lb)	3246.00	5018.00	7271.00	10687.00
- Ultimate Moment (ft-lb)	4526.00	7248.00	10878.00	16388.00
+ Flexural Steel Area (in.^{2}/ft)	0.27	0.30	0.34	0.40
- Flexural Steel Area (in.^{2}/ft)	0.38	0.45	0.52	0.62
Shear Reinforcement (in.^{2}/ft)	0.00	0.00	0.00	0.00
Effective Moment of Inertia (in.^{4})	53.80	125.60	257.40	505.10
Failure Overpressure P1 (psi)	1.07	0.97	0.89	0.88
Failure Overpressure P2 (psi)	1.82	1.71	1.62	1.66
Deflection Before Collapse (ft)	1.13	1.33	1.50	1.62

Nominal Live Load (psf)	80.00	80.00	80.00	80.00
Span Length (ft)	16.00	20.00	24.00	28.00
Effective Depth (in.)	4.84	6.16	7.60	9.30
Total Slab Thickness (in.)	5.48	7.16	8.60	10.30
+ Ultimate Moment (ft-lb)	4383.00	6251.00	8266.00	11223.00
- Ultimate Moment (ft-lb)	5980.00	8832.00	12167.00	17081.00
+ Flexural Steel Area (in.^{2}/ft)	0.32	0.35	0.37	0.41
- Flexural Steel Area (in.^{2}/ft)	0.44	0.51	0.56	0.64
Shear Reinforcement (in.^{2}/ft)	0.00	0.00	0.00	0.00
Effective Moment of Inertia (in.^{4})	80.70	160.90	293.40	526.60
Failure Overpressure P1 (psi)	1.52	1.29	1.06	0.96
Failure Overpressure P2 (psi)	2.57	2.24	1.91	1.78
Deflection Before Collapse (ft)	0.99	1.23	1.44	1.60

Table A.1 (Contd)

Concrete Compressive Strength: 3 ksi
Steel Yield Strength: 40 ksi
Slab Type: Two-Span Continuous

Nominal Live Load (psf)	125.00	125.00	125.00	125.00
Span Length (ft)	16.00	20.00	24.00	28.00
Effective Depth (in.)	6.04	8.09	10.26	12.65
Total Slab Thickness (in.)	7.04	9.09	11.26	13.65
+ Ultimate Moment (ft-lb)	7196.00	12268.00	19232.00	28513.00
- Ultimate Moment (ft-lb)	9546.00	16507.00	26207.00	39305.00
+ Flexural Steel Area (in.^{2}/ft)	0.42	0.53	0.65	0.78
- Flexural Steel Area (in.^{2}/ft)	0.56	0.72	0.90	1.10
Shear Reinforcement (in.^{2}/ft)	0.00	0.00	0.00	0.00
Effective Moment of Inertia (in.^{4})	158.70	376.30	762.90	1420.70
Failure Overpressure P1 (psi)	2.67	2.87	3.06	3.27
Failure Overpressure P2 (psi)	4.45	4.81	5.18	5.57
Deflection Before Collapse (ft)	0.80	0.93	1.04	1.14

Nominal Live Load (psf)	250.00	250.00	250.00	250.00
Span Length (ft)	16.00	20.00	24.00	28.00
Effective Depth (in.)	7.69	10.07	12.49	15.06
Total Slab Thickness (in.)	8.69	11.07	13.49	16.06
+ Ultimate Moment (ft-lb)	12671.00	20985.00	31967.00	46027.00
- Ultimate Moment (ft-lb)	16413.00	27492.00	42308.00	61501.00
+ Flexural Steel Area (in.^{2}/ft)	0.58	0.73	0.90	1.07
- Flexural Steel Area (in.^{2}/ft)	0.76	0.97	1.21	1.45
Shear Reinforcement (in.^{2}/ft)	0.00	0.00	0.00	0.00
Effective Moment of Inertia (in.^{4})	335.50	745.50	1421.20	2487.50
Failure Overpressure P1 (psi)	4.95	5.20	5.43	5.66
Failure Overpressure P2 (psi)	8.14	8.60	9.04	9.48
Deflection Before Collapse (ft)	0.62	0.73	0.84	0.94

Table A.1 (Concl)

Concrete Compressive Strength: 4 ksi
Steel Yield Strength: 40 ksi
Slab Type: Two-Span Continuous

Nominal Live Load (psf)	50.00	50.00	50.00	50.00
Span Length (ft)	16.00	20.00	24.00	28.00
Effective Depth (in.)	3.86	5.18	6.66	8.27
Total Slab Thickness (in.)	4.86	6.18	7.66	9.27
+ Ultimate Moment (ft-lb)	3126.00	4758.00	6808.00	6789.00
- Ultimate Moment (ft-lb)	4339.00	6844.00	10157.00	14992.00
+ Flexural Steel Area (in.^{2}/ft)	0.28	0.32	0.35	0.40
- Flexural Steel Area (in.^{2}/ft)	0.40	0.46	0.53	0.63
Shear Reinforcement (in.^{2}/ft)	0.00	0.00	0.00	0.00
Effective Moment of Inertia (in.^{4})	42.40	97.70	200.70	379.00
Failure Overpressure P1 (psi)	1.03	0.93	0.84	0.81
Failure Overpressure P2 (psi)	1.77	1.64	1.52	1.53
Deflection Before Collapse (ft)	1.04	1.24	1.40	1.53

Nominal Live Load (psf)	80.00	80.00	80.00	80.00
Span Length (ft)	16.00	20.00	24.00	28.00
Effective Depth (in.)	4.46	5.63	6.90	8.41
Total Slab Thickness (in.)	5.46	6.63	7.90	9.41
+ Ultimate Moment (ft-lb)	4262.00	5986.00	7761.00	10344.00
- Ultimate Moment (ft-lb)	5791.00	8421.00	11380.00	15714.00
+ Flexural Steel Area (in.^{2}/ft)	0.33	0.37	0.39	0.42
- Flexural Steel Area (in.^{2}/ft)	0.46	0.52	0.57	0.65
Shear Reinforcement (in.^{2}/ft)	0.00	0.00	0.00	0.00
Effective Moment of Inertia (in.^{4})	65.60	127.80	226.40	399.60
Failure Overpressure P1 (psi)	1.49	1.25	1.00	0.88
Failure Overpressure P2 (psi)	2.51	2.16	1.81	1.65
Deflection Before Collapse (ft)	0.91	1.13	1.34	1.50

Table A.1 (Contd)

Concrete Compressive Strength: 3 ksi
Steel Yield Strength: 60 ksi
Slab Type: Two-Span Continuous

Nominal Live Load (psf)	50.00	50.00	50.00	50.00
Span Length (ft)	16.00	20.00	24.00	28.00
Effective Depth (in.)	4.25	5.81	7.49	9.24
Total Slab Thickness (in.)	5.25	6.81	8.49	10.24
+ Ultimate Moment (ft-lb)	3250.00	5073.00	7406.00	10732.00
- Ultimate Moment (ft-lb)	4530.00	7335.00	11088.00	16458.00
+ Flexural Steel Area (in.^{2}/ft)	0.18	0.20	0.23	0.27
- Flexural Steel Area (in.^{2}/ft)	0.25	0.30	0.35	0.41
Shear Reinforcement (in.^{2}/ft)	0.00	0.00	0.00	0.00
Effective Moment of Inertia (in.^{4})	48.80	120.70	253.10	472.50
Failure Overpressure P1 (psi)	1.08	0.99	0.91	0.90
Failure Overpressure P2 (psi)	1.80	1.70	1.61	1.64
Deflection Before Collapse (ft)	1.88	2.16	2.41	2.63

Nominal Live Load (psf)	80.00	80.00	80.00	80.00
Span Length (ft)	16.00	20.00	24.00	28.00
Effective Depth (in.)	4.89	6.27	7.69	9.49
Total Slab Thickness (in.)	5.89	7.27	8.69	10.49
+ Ultimate Moment (ft-lb)	4399.00	6306.00	8328.00	11400.00
- Ultimate Moment (ft-lb)	6004.00	8918.00	12263.00	17356.00
+ Flexural Steel Area (in.^{2}/ft)	0.21	0.23	0.25	0.28
- Flexural Steel Area (in.^{2}/ft)	0.29	0.33	0.37	0.43
Shear Reinforcement (in.^{2}/ft)	0.00	0.00	0.00	0.00
Effective Moment of Inertia (in.^{4})	74.60	153.20	276.70	512.00
Failure Overpressure P1 (psi)	1.55	1.32	1.08	0.98
Failure Overpressure P2 (psi)	2.56	2.22	1.89	1.78
Deflection Before Collapse (ft)	1.65	2.00	2.34	2.57

Concrete Compressive Strength: 3 ksi
Steel Yield Strength: 60 ksi
Slab Type: Two-Span Continuous

Nominal Live Load (psf)	125.00	125.00	125.00	125.00
Span Length (ft)	16.00	20.00	24.00	28.00
Effective Depth (in.)	6.19	8.31	10.46	12.97
Total Slab Thickness (in.)	7.19	9.31	11.46	13.97
+ Ultimate Moment (ft-lb)	7244.00	12383.00	19378.00	28827.00
- Ultimate Moment (ft-lb)	9619.00	16686.00	26434.00	39793.00
+ Flexural Steel Area (in.^{2}/ft)	0.27	0.35	0.43	0.51
- Flexural Steel Area (in.^{2}/ft)	0.37	0.47	0.60	0.72
Shear Reinforcement (in.^{2}/ft)	0.00	0.00	0.00	0.00
Effective Moment of Inertia (in.^{4})	151.80	363.90	724.70	1371.90
Failure Overpressure P1 (psi)	2.72	2.93	3.12	3.34
Failure Overpressure P2 (psi)	4.46	4.85	5.21	5.63
Deflection Before Collapse (ft)	1.32	1.52	1.72	1.87

Nominal Live Load (psf)	250.00	250.00	250.00	250.00
Span Length (ft)	16.00	20.00	24.00	28.00
Effective Depth (in.)	7.97	10.42	12.94	15.61
Total Slab Thickness (in.)	8.97	11.42	13.94	16.61
+ Ultimate Moment (ft-lb)	12759.00	21164.00	32287.00	46566.00
- Ultimate Moment (ft-lb)	16550.00	27770.00	42806.00	62340.00
+ Flexural Steel Area (in.^{2}/ft)	0.37	0.47	0.58	0.69
- Flexural Steel Area (in.^{2}/ft)	0.49	0.63	0.78	0.94
Shear Reinforcement (in.^{2}/ft)	0.00	0.00	0.00	0.00
Effective Moment of Inertia (in.^{4})	327.70	728.00	1391.90	2443.80
Failure Overpressure P1 (psi)	5.05	5.31	5.55	5.79
Failure Overpressure P2 (psi)	8.22	8.70	9.16	9.62
Deflection Before Collapse (ft)	1.02	1.21	1.38	1.54

Table A.1 (Contd)

Concrete Compressive Strength: 4 ksi
Steel Yield Strength: 60 ksi
Slab Type: Two-Span Continuous

Nominal Live Load (psf)	50.00	50.00	50.00	50.00
Span Length (ft)	16.00	20.00	24.00	28.00
Effective Depth (in.)	3.90	5.22	6.70	8.50
Total Slab Thickness (in.)	4.90	6.22	7.70	9.50
+ Ultimate Moment (ft-lb)	3139.00	4781.00	6839.00	10004.00
- Ultimate Moment (ft-lb)	4358.00	6880.00	10206.00	15327.00
+ Flexural Steel Area (in.^{2}/ft)	0.19	0.21	0.23	0.27
- Flexural Steel Area (in.^{2}/ft)	0.26	0.31	0.35	0.42
Shear Reinforcement (in.^{2}/ft)	0.00	0.00	0.00	0.00
Effective Moment of Inertia (in.^{4})	38.90	90.30	185.90	373.20
Failure Overpressure P1 (psi)	1.05	0.95	0.85	0.84
Failure Overpressure P2 (psi)	1.75	1.62	1.51	1.54
Deflection Before Collapse (ft)	1.74	2.04	2.30	2.46

Nominal Live Load (psf)	80.00	80.00	80.00	80.00
Span Length (ft)	16.00	20.00	24.00	28.00
Effective Depth (in.)	4.50	5.68	7.05	8.57
Total Slab Thickness (in.)	5.50	6.68	8.05	9.57
+ Ultimate Moment (ft-lb)	4276.00	6014.00	7865.00	10500.00
- Ultimate Moment (ft-lb)	5812.00	8464.00	11542.00	15957.00
+ Flexural Steel Area (in.^{2}/ft)	0.22	0.24	0.26	0.28
- Flexural Steel Area (in.^{2}/ft)	0.30	0.35	0.38	0.43
Shear Reinforcement (in.^{2}/ft)	0.00	0.00	0.00	0.00
Effective Moment of Inertia (in.^{4})	60.00	117.60	217.60	384.80
Failure Overpressure P1 (psi)	1.51	1.27	1.03	0.91
Failure Overpressure P2 (psi)	2.51	2.15	1.81	1.65
Deflection Before Collapse (ft)	1.52	1.88	2.19	2.43

Concrete Compressive Strength: 4 ksi
Steel Yield Strength: 60 ksi
Slab Type: Two-Span Continuous

Nominal Live Load (psf)	125.00	125.00	125.00	125.00
Span Length (ft)	16.00	20.00	24.00	28.00
Effective Depth (in.)	5.72	7.64	9.70	11.98
Total Slab Thickness (in.)	6.72	8.64	10.70	12.98
+ Ultimate Moment (ft-lb)	7095.00	12048.00	18829.00	27856.00
- Ultimate Moment (ft-lb)	9388.00	16165.00	25581.00	38284.00
+ Flexural Steel Area (in.^{2}/ft)	0.29	0.36	0.45	0.53
- Flexural Steel Area (in.^{2}/ft)	0.38	0.49	0.62	0.74
Shear Reinforcement (in.^{2}/ft)	0.00	0.00	0.00	0.00
Effective Moment of Inertia (in.^{4})	123.60	291.20	592.00	1107.70
Failure Overpressure P1 (psi)	2.68	2.87	3.05	3.25
Failure Overpressure P2 (psi)	4.40	4.75	5.10	5.48
Deflection Before Collapse (ft)	1.21	1.41	1.58	1.74

Nominal Live Load (psf)	250.00	250.00	250.00	250.00
Span Length (ft)	16.00	20.00	24.00	28.00
Effective Depth (in.)	7.41	9.75	12.09	14.56
Total Slab Thickness (in.)	8.41	10.75	13.09	15.56
+ Ultimate Moment (ft-lb)	12581.00	20831.00	31676.00	45537.00
- Ultimate Moment (ft-lb)	15273.00	27252.00	41856.00	60739.00
+ Flexural Steel Area (in.^{2}/ft)	0.39	0.49	0.61	0.72
- Flexural Steel Area (in.^{2}/ft)	0.51	0.65	0.81	0.98
Shear Reinforcement (in.^{2}/ft)	0.00	0.00	0.00	0.00
Effective Moment of Inertia (in.^{4})	271.30	612.00	1163.70	2032.30
Failure Overpressure P1 (psi)	4.99	5.24	5.47	5.70
Failure Overpressure P2 (psi)	8.14	8.60	9.02	9.45
Deflection Before Collapse (ft)	0.94	1.11	1.27	1.42

Table A.1 (Contd)

Concrete Compressive Strength: 4 ksi
Steel Yield Strength: 40 ksi
Slab Type: Two-Span Continuous

Nominal Live Load (psf)	125.00	125.00	125.00	125.00
Span Length (ft)	16.00	20.00	24.00	28.00
Effective Depth (in.)	5.63	7.51	9.49	11.74
Total Slab Thickness (in.)	6.63	8.51	10.49	12.74
+ Ultimate Moment (ft-lb)	7066.00	11977.00	18676.00	27630.00
- Ultimate Moment (ft-lb)	9343.00	16055.00	25342.00	37931.00
+ Flexural Steel Area (in.^{2}/ft)	0.44	0.55	0.68	0.81
- Flexural Steel Area (in.^{2}/ft)	0.58	0.75	0.94	1.13
Shear Reinforcement (in.^{2}/ft)	0.00	0.00	0.00	0.00
Effective Moment of Inertia (in.^{4})	133.30	311.60	625.20	1174.60
Failure Overpressure P1 (psi)	2.63	2.81	2.99	3.19
Failure Overpressure P2 (psi)	4.38	4.72	5.06	5.43
Deflection Before Collapse (ft)	0.72	0.85	0.95	1.05

Nominal Live Load (psf)	250.00	250.00	250.00	250.00
Span Length (ft)	16.00	20.00	24.00	28.00
Effective Depth (in.)	7.22	9.42	11.74	14.13
Total Slab Thickness (in.)	8.22	10.42	12.74	15.13
+ Ultimate Moment (ft-lb)	12519.00	20660.00	31424.00	45114.00
- Ultimate Moment (ft-lb)	16176.00	26987.00	41463.00	60080.00
+ Flexural Steel Area (in.^{2}/ft)	0.60	0.76	0.93	1.11
- Flexural Steel Area (in.^{2}/ft)	0.79	1.01	1.24	1.50
Shear Reinforcement (in.^{2}/ft)	0.00	0.00	0.00	0.00
Effective Moment of Inertia (in.^{4})	286.80	631.90	1216.20	2118.40
Failure Overpressure P1 (psi)	4.89	5.13	5.35	5.57
Failure Overpressure P2 (psi)	8.05	8.48	8.91	9.32
Deflection Before Collapse (ft)	0.56	0.66	0.76	0.85

Table A.2

MATRIX OF TWO-WAY SLAB DESIGN PARAMETERS

Live Load \ Span	16 ft	20 ft	24 ft	28 ft
50 psf	FP WSD	FP WSD	FP WSD	CAPS USD
80 psf	FS WSD	FS WSD	FS WSD	CAPS USD
125 psf	FS WSD	FS WSD	FS WSD	--
125 psf	FS USD	FS USD	FS USD	--
125 psf	CAPS USD	CAPS USD	CAPS USD	CAPS USD
250 psf	CAPS USD	CAPS USD	CAPS USD	CAPS USD

Notation: FP   - Flat plate
           FS   - Flat slab with drop panel and no capital
           CAPS - Flat slab with drop panel and capital
           WSD - Working stress design
           USD - Ultimate strength design

Table A.3
TWO-WAY SLAB DESIGN PARAMETERS AND FAILURE DATA

Design Live Load, Nominal: 50 psf
Length: 16 ft
Type: Flat Plate
Working Stress Design

f'_c, ksi	3		4	
f_y, ksi	40	60	40	60
Slab Weight, psf	75.00	75.00	68.75	68.75
Total Dead Load, psf	85.00	85.00	78.75	78.75
Live Load, psf	40.00	40.00	40.00	40.00
M_o, k-in.	552.30	552.30	531.00	531.00
t, in.	6.00	6.00	5.50	5.50
t_d, in.	-	-	-	-
D, ft	-	-	-	-
Capital, ft	-	-	-	-
Square Column, in.	12.00	12.00	11.00	11.00
Round Column, in.	-	-	-	-
Approximate Bar Size	4's	4's	4's	4's
+ Column Strip } d, in.	5.00	5.00	4.50	4.50
A_s, in.^{2}	1.54	1.16	1.65	1.24
- Column Strip } d, in.	4.50	4.50	4.00	4.00
A_s, in.^{2}	3.59	2.69	3.88	2.91
+ Middle Strip } d, in.	4.50	4.50	4.00	4.00
A_s, in.^{2}	1.25	1.04	1.35	1.02
- Middle Strip } d, in.	5.00	5.00	4.50	4.50
A_s, in.^{2}	1.25	1.04	1.35	1.02
Static Failure Overpressure:				
Shear, psi	-	1.22	-	1.19
Flexural, psi	1.06	-	1.04	-
Dynamic Failure Overpressure:				
Shear, psi	0.81	0.72	0.68	0.67
Flexural, psi	-	-	-	-
Time, sec	0.03	0.04	0.04	0.04
Ultimate Collapse Overpressure, psi	2.40	2.10	2.40	2.10

Table A.3 (Contd)

Design Live Load, Nominal: 50 psf
Length: 20 ft
Type: Flat Plate
Working Stress Design

f'_c, ksi	3		4	
f_y, ksi	40	60	40	60
Slab Weight, psf	93.75	93.75	87.50	87.50
Total Dead Load, psf	103.75	103.75	97.50	97.50
Live Load, psf	34.00	34.00	34.00	34.00
M_o, k-in.	1200.20	1200.20	1156.80	1156.80
t, in.	7.50	7.50	7.00	7.00
t_d, in.	-	-	-	-
D, ft	-	-	-	-
Capital, ft	-	-	-	-
Square Column, in.	14.00	14.00	13.00	13.00
Round Column, in.	-	-	-	-
Approximate Bar Size	4's	4's	4's	4's
+ Column Strip d, in.	6.50	6.50	6.00	6.00
A_s, in.^{2}	2.58	1.94	2.70	2.02
- Column Strip d, in.	6.00	6.00	5.50	5.50
A_s, in.^{2}	5.84	4.38	6.15	4.61
+ Middle Strip d, in.	6.00	6.00	5.50	5.50
A_s, in.^{2}	2.04	1.62	2.14	1.61
- Middle Strip d, in.	6.50	6.50	6.00	6.00
A_s, in.^{2}	2.04	1.62	2.14	1.61
Static Failure Overpressure:				
Shear, psi	1.03	1.03	1.06	1.06
Flexural, psi	-	-	-	-
Dynamic Failure Overpressure:				
Shear, psi	0.61	0.60	0.60	0.57
Flexural, psi	-	-	-	-
Time, sec	0.05	0.05	0.05	0.06
Ultimate Collapse Overpressure, psi	1.90	1.80	2.00	2.00

Table A.3 (Contd)

Design Live Load, Nominal: 50 psf
Length: 24 ft
Type: Flat Plate
Working Stress Design

f'_c, ksi	3		4	
f_y, ksi	40	60	40	60
Slab Weight, psf	112.50	112.50	106.25	106.25
Total Dead Load, psf	122.50	122.50	116.25	116.25
Live Load, psf	27.00	27.00	27.00	27.00
M_o, k-in.	2229.20	2229.20	2170.50	2170.50
t, in.	9.00	9.00	8.50	8.50
t_d, in.	-	-	-	-
D, ft	-	-	-	-
Capital, ft	-	-	-	-
Square Column, in.	18.00	18.00	16.00	16.00
Round Column, in.	-	-	-	-
Approximate Bar Size	5's	5's	5's	5's
+ Column Strip d, in.	7.94	7.94	7.44	7.44
A_s, in.^{2}	3.93	2.95	4.08	3.06
- Column Strip d, in.	7.31	7.31	6.81	6.81
A_s, in.^{2}	8.90	6.68	9.31	6.98
+ Middle Strip d, in.	7.31	7.31	6.81	6.81
A_s, in.^{2}	3.10	2.33	3.24	2.43
- Middle Strip d, in.	7.94	7.94	7.44	7.44
A_s, in.^{2}	3.10	2.33	3.24	2.43
Static Failure Overpressure:				
Shear, psi	0.99	0.99	1.00	1.00
Flexural, psi	-	-	-	-
Dynamic Failure Overpressure:				
Shear, psi	0.62	0.60	0.61	0.59
Flexural, psi	-	-	-	-
Time, sec	0.05	0.06	0.05	0.06
Ultimate Collapse Overpressure, psi	2.30	2.10	2.10	2.10

Table A.3 (Contd)

Design Live Load, Nominal: 80 psf
Length: 16 ft
Type: Flat Slab
Working Stress Design

f'_c, ksi	3		4	
f_y, ksi	40	60	40	60
Slab Weight, psf	66.75	66.75	66.75	66.75
Total Dead Load, psf	76.75	76.75	76.75	76.75
Live Load, psf	63.60	63.60	63.60	63.60
M_o, k-in.	627.60	627.60	627.60	627.60
t, in.	5.00	5.00	5.00	5.00
t_d, in.	2.25	2.25	2.25	2.25
D, ft	5.26	6.25	6.25	6.25
Capital, ft	-	-	-	-
Square Column, in.	11.00	11.00	11.00	11.00
Round Column, in.	-	-	-	-
Approximate Bar Size	3's	3's	3's	3's
+ Column Strip } d, in.	4.06	4.06	4.06	4.06
A_s, in.^{2}	1.97	1.48	1.97	1.48
− Column Strip } d, in.	5.94	5.94	5.94	5.94
A_s, in^2	3.36	2.52	3.36	2.52
+ Middle Strip } d, in.	3.69	3.69	3.69	3.69
A_s, in.	1.62	1.22	1.62	1.22
− Middle Strip } d, in.	4.06	4.06	4.06	4.06
A_s, in.	1.62	1.22	1.62	1.22
Static Failure Overpressure:				
Shear, psi	-	1.58	-	-
Flexural, psi	1.36	-	1.38	1.61
Dynamic Failure Overpressure:				
Shear, psi	-	-	-	-
Flexural, psi	1.48	1.71	1.50	1.74
Time, sec	0.41	0.54	0.39	0.50
Ultimate Collapse Overpressure, psi	1.80	1.80	1.80	1.80

Design Live Load, Nominal: 80 psf
Length: 20 ft
Type: Flat Slab
Working Stress Design

f'_c, ksi	3		4	
f_y, ksi	40	60	40	60
Slab Weight, psf	81.45	81.45	81.45	81.45
Total Dead Load, psf	91.45	91.45	91.45	91.45
Live Load, psf	54.40	54.40	54.40	54.40
M_o, k-in.	1307.70	1307.70	1307.70	1307.70
t, in.	6.00	6.00	6.00	6.00
t_d, in.	3.00	3.00	3.00	3.00
D, ft	8.25	8.25	8.25	8.25
Capital, ft	-	-	-	-
Square Column, in.	11.00	11.00	11.00	11.00
Round Column, in.	-	-	-	-
Approximate Bar Size	4's	4's	4's	4's
+ Column d, in.	5.00	5.00	5.00	5.00
Strip A_s, in.^{2}	3.33	2.49	3.33	2.49
- Column d, in.	7.50	7.50	7.50	7.50
Strip A_s, in.^{2}	5.54	4.16	5.54	4.16
+ Middle d, in.	4.50	4.50	4.50	4.50
Strip A_s, in.^{2}	2.77	2.08	2.77	2.08
- Middle d, in.	5.00	5.00	5.00	5.00
Strip A_s, in.^{2}	2.77	2.08	2.77	2.08
Static Failure Overpressure:				
Shear, psi	1.19	1.19	-	1.47
Flexural, psi	-	-	1.39	-
Dynamic Failure Overpressure:				
Shear, psi	1.04	0.87	-	1.59
Flexural, psi	-	-	1.52	-
Time, sec	0.05	0.06	0.46	0.04
Ultimate Collapse Overpressure, psi	1.50	1.30	1.50	1.30

Table A.3 (Contd)

Design Live Load, Nominal: 80 psf
Length: 24 ft
Type: Flat Slab
Working Stress Design

f'_c, ksi	3		4	
f_y, ksi	40	60	40	60
Slab Weight, psf	100.50	100.50	100.50	100.50
Total Dead Load, psf	110.50	110.50	110.50	110.50
Live Load, psf	43.20	43.20	43.20	43.20
M_o, k-in.	2404.00	2404.00	2404.00	2404.00
t, in.	7.50	7.50	7.50	7.50
t_d, in.	3.50	3.50	3.50	3.50
D, ft	9.25	9.25	9.25	9.25
Capital, ft	-	-	-	-
Square Column, in.	12.00	12.00	12.00	12.00
Round Column, in.	-	-	-	-
Approximate Bar Size	5's	5's	5's	5's
+ Column Strip } d, in.	6.44	6.44	6.44	6.44
A_s, in.^{2}	4.75	3.56	4.75	3.56
- Column Strip } d, in.	9.31	9.31	9.31	9.31
A_s, in.^{2}	8.20	6.15	8.20	6.15
+ Middle Strip } d, in.	5.81	5.81	5.81	5.81
A_s, in.^{2}	3.94	2.96	3.94	2.96
- Middle Strip } d, in.	6.44	6.44	6.44	6.44
A_s, in.^{2}	3.94	2.96	3.94	2.96
Static Failure Overpressure:				
Shear, psi	1.02	1.02	1.29	1.29
Flexural, psi	-	-	-	-
Dynamic Failure Overpressure:				
Shear, psi	0.74	0.70	-	0.89
Flexural, psi	-	-	1.51	-
Time, sec	0.07	0.08	0.57	0.07
Ultimate Collapse Overpressure, psi	1.10	1.10	1.10	1.10

Table A.3 (Contd)

Design Live Load, Nominal: 125 psf
Length: 16 ft
Type: Flat Slab
Working Stress Design

f'_c, ksi	3		4	
f_y, ksi	40	60	40	60
Slab Weight, psf	73.50	73.50	73.50	73.50
Total Dead Load, psf	83.50	83.50	83.50	83.50
Live Load, psf	125.00	125.00	125.00	125.00
M_o, k-in.	921.20	921.20	921.20	921.20
t, in.	5.50	5.50	5.50	5.50
t_d, in.	2.50	2.50	2.50	2.50
D, ft	6.25	6.25	6.25	6.25
Capital, ft	-	-	-	-
Square Column, in.	12.00	12.00	12.00	12.00
Round Column, in.	-	-	-	-
Approximate Bar Size	3's	3's	3's	3's
+ Column Strip d, in.	4.56	4.56	4.56	4.56
A_s, in.^{2}	2.57	1.93	2.57	0.93
- Column Strip d, in.	6.69	6.69	6.69	6.69
A_s, in.^{2}	4.38	3.28	4.38	3.28
+ Middle Strip d, in.	4.19	4.19	4.19	4.19
A_s, in.^{2}	2.10	1.58	2.10	1.58
- Middle Strip d, in.	4.56	4.56	4.56	4.56
A_s, in.^{2}	2.10	1.58	2.10	1.58
Static Failure Overpressure:				
Shear, psi	1.99	1.99	-	2.38
Flexural, psi	-	-	2.22	-
Dynamic Failure Overpressure:				
Shear, psi	2.12	1.35	-	-
Flexural, psi	-	-	2.39	2.74
Time, sec	0.03	0.04	0.31	0.40
Ultimate Collapse Overpressure, psi	2.80	2.60	2.80	2.60

Table A.3 (Contd)

Design Live Load, Nominal: 125 psf
Length: 20 ft
Type: Flat Slab
Working Stress Design

f'_c, ksi	3		4	
f_y, ksi	40	60	40	60
Slab Weight, psf	88.20	88.20	88.20	88.20
Total Dead Load, psf	98.20	98.20	98.20	98.20
Live Load, psf	125.00	125.00	125.00	125.00
M_o, k-in.	1944.80	1944.80	1944.80	1944.80
t, in.	6.50	6.50	6.50	6.50
t_d, in.	3.75	3.75	3.75	3.75
D, ft	8.25	8.25	8.25	8.25
Capital, ft	-	-	-	-
Square Column, in.	14.00	14.00	14.00	14.00
Round Column, in.	-	-	-	-
Approximate Bar Size	4's	4's	4's	4's
+ Column Strip } d, in.	5.50	5.50	5.50	5.50
A_s, in.^{2}	4.49	3.37	4.49	3.37
- Column Strip } d, in.	8.75	8.75	8.25	8.25
A_s, in.^{2}	7.06	5.30	7.49	5.62
+ Middle Strip } d, in.	5.00	5.00	5.00	5.00
A_s, in.^{2}	3.71	2.78	3.71	2.78
- Middle Strip } d, in.	5.50	5.50	5.50	5.50
A_s, in.^{2}	3.71	2.78	3.71	2.78
Static Failure Overpressure:				
Shear, psi	1.86	1.86	2.07	2.07
Flexural, psi	-	-	-	-
Dynamic Failure Overpressure:				
Shear, psi	1.24	1.42	2.26	1.44
Flexural, psi	-	-	-	-
Time, sec	0.07	0.05	0.34	0.06
Ultimate Collapse Overpressure, psi	2.60	2.50	2.80	2.70

Table A.3 (Contd)

Design Live Load, Nominal: 125 psf
Length: 24 ft
Type: Flat Slab
Working Stress Design

f'_c, ksi	3		4	
f_y, ksi	40	60	40	60
Slab Weight, psf	114.80	114.80	107.55	107.55
Total Dead Load, psf	124.80	124.80	117.55	117.55
Live Load, psf	125.00	125.00	125.00	125.00
M_o, k-in.	3724.90	3724.90	3645.90	3645.90
t, in.	8.50	8.50	8.00	8.00
t_d, in.	4.25	4.25	3.75	3.75
D, ft	9.25	9.25	9.25	9.25
Capital, ft	-	-	-	-
Square Column, in.	18.00	18.00	17.00	17.00
Round Column, in.	-	-	-	-
Approximate Bar Size	6's	6's	6's	6's
+ Column Strip d, in.	7.37	7.37	6.87	6.87
+ Column Strip A_s, in.^{2}	6.42	4.81	6.74	5.05
- Column Strip d, in.	10.87	10.87	9.87	9.87
- Column Strip A_s, in.^{2}	10.88	8.16	11.72	8.80
+ Middle Strip d, in.	6.62	6.62	6.12	6.12
+ Middle Strip A_s, in.^{2}	5.36	4.02	5.68	4.27
- Middle Strip d, in.	7.37	7.37	6.87	6.87
- Middle Strip A_s, in.^{2}	5.36	4.02	5.68	4.27
Static Failure Overpressure:				
Shear, psi	1.96	1.96	1.99	1.99
Flexural, psi	-	-	-	-
Dynamic Failure Overpressure:				
Shear, psi	1.33	1.54	1.32	1.53
Flexural, psi	-	-	-	-
Time, sec	0.06	0.06	0.06	0.06
Ultimate Collapse Overpressure, psi	3.00	2.90	3.00	3.00

Table A.3 (Contd)

Design Live Load, Nominal: 125 psf
Length: 16 ft
Type: Flat Slab
Ultimate Strength Design

f'_c, ksi	3		4	
f_y, ksi	40	60	40	60
Slab Weight, psf	77.40	77.40	77.40	77.40
Total Dead Load, psf	87.40	87.40	87.40	87.40
Live Load, psf	125.00	125.00	125.00	125.00
M_o, k-in.	1748.10	1748.10	1769.30	1769.30
t, in.	6.00	6.00	6.00	6.00
t_d, in.	1.75	1.75	1.75	1.75
D, ft	5.33	5.33	5.33	5.33
Capital, ft	-	-	-	-
Square Column, in.	12.00	12.00	11.00	11.00
Round Column, in.	-	-	-	-
Approximate Bar Size	4's	4's	4's	4's
+ Column d, in.	5.00	5.00	5.00	5.00
Strip A_s, in.^{2}	2.04	1.36	2.04	1.36
- Column d, in.	6.25	6.25	6.25	6.25
Strip A_s, in.^{2}	4.40	2.93	4.30	2.87
+ Middle d, in.	4.50	4.50	4.50	4.50
Strip A_s, in.^{2}	1.69	1.13	1.69	1.13
- Middle d, in.	5.00	5.00	5.00	5.00
Strip A_s, in.^{2}	1.69	1.13	1.69	1.13
Static Failure Overpressure:				
Shear, psi	1.87	1.87	-	-
Flexural, psi	-	-	1.87	1.88
Dynamic Failure Overpressure:				
Shear, psi	1.84	1.84	-	-
Flexural, psi	-	-	2.03	2.03
Time, sec	0.03	0.03	0.37	0.42
Ultimate Collapse Overpressure, psi	3.00	2.40	2.40	2.10

Table A.3 (Contd)

Design Live Load, Nominal: 125 psf
Length: 20 ft
Type: Flat Slab
Ultimate Strength Design

f'_c, ksi	3		4	
f_y, ksi	40	60	40	60
Slab Weight, psf	96.60	96.60	96.60	96.60
Total Dead Load, psf	106.60	106.60	106.60	106.60
Live Load, psf	125.00	125.00	125.00	125.00
M_o, k-in.	3619.90	3619.90	3726.10	3726.10
t, in.	7.50	7.50	7.50	7.50
t_d, in.	2.00	2.00	2.00	2.00
D, ft	6.67	6.67	6.67	6.67
Capital, ft	-	-	-	-
Square Column, in.	17.00	17.00	14.00	14.00
Round Column, in.	-	-	-	-
Approximate Bar Size	4's	4's	4's	4's
+ Column } d, in.	6.50	6.50	6.50	6.50
Strip) A_s, in.^{2}	3.24	2.16	3.30	2.20
- Column } d, in.	8.00	8.00	8.00	8.00
Strip) A_s, in.^{2}	7.12	4.75	7.09	4.73
+ Middle } d, in.	6.00	6.00	6.00	6.00
Strip) A_s, in.^{2}	2.62	1.80	2.67	1.78
- Middle } d, in.	6.50	6.50	6.50	6.50
Strip) A_s, in.^{2}	2.62	1.80	2.67	1.78
Static Failure Overpressure:				
Shear, psi	-	1.94	-	-
Flexural, psi	1.92	-	1.93	1.93
Dynamic Failure Overpressure:				
Shear, psi	-	-	-	-
Flexural, psi	2.08	2.11	2.10	2.10
Time, sec	0.52	0.54	0.48	0.51
Ultimate Collapse Overpressure, psi	3.30	2.70	2.50	2.20

Table A.3 (Contd)

Design Live Load, Nominal: 125 psf
Length: 24 ft
Type: Flat Slab
Ultimate Strength Design

f'_c, ksi	3		4	
f_y, ksi	40	60	40	60
Slab Weight, psf	115.95	115.95	115.95	115.95
Total Dead Load, psf	125.95	125.95	125.95	125.95
Live Load, psf	125.00	125.00	125.00	125.00
M_o, k-in.	6533.10	6533.10	6858.00	6858.00
t, in.	9.00	9.00	9.00	9.00
t_d, in.	2.50	2.50	2.50	2.50
D, ft	8.00	8.00	8.00	8.00
Capital, ft	-	-	-	-
Square Column, in.	24.00	24.00	18.00	18.00
Round Column, in.	-	-	-	-
Approximate Bar Size	6's	6's	6's	6's
+ Column } d, in.	7.87	7.87	7.87	7.87
Strip } A_s, in.^{2}	4.83	3.22	5.02	3.35
- Column } d, in.	9.62	9.62	9.62	9.62
Strip } A_s, in.^{2}	10.74	7.16	10.91	7.28
+ Middle } d, in.	7.12	7.12	7.12	7.12
Strip } A_s, in.^{2}	3.99	2.66	4.15	2.77
- Middle } d, in.	7.87	7.87	7.87	7.87
Strip } A_s, in.^{2}	3.99	2.66	4.15	2.77
Static Failure Overpressure:				
Shear, psi	-	-	1.99	1.99
Flexural, psi	1.95	1.95	-	-
Dynamic Failure Overpressure:				
Shear, psi	-	-	-	-
Flexural, psi	2.13	2.13	2.18	2.18
Time, sec	0.57	0.64	0.53	0.61
Ultimate Collapse Overpressure, psi	4.20	3.30	3.00	2.60

Table A.3 (Contd)

Design Live Load, Nominal: 125 psf
Length: 16 ft
Type: Capitals
Ultimate Strength Design

f'_c, ksi	3		4	
f_y, ksi	40	60	40	60
Slab Weight, psf	77.40	77.40	77.40	77.40
Total Dead Load, psf	87.40	87.40	87.40	87.40
Live Load, psf	125.00	125.00	125.00	125.00
M_o, k-in.	1507.50	1507.50	1404.60	1404.60
t, in.	6.00	6.00	6.00	6.00
t_d, in.	1.75	1.75	1.75	1.75
D, ft	5.33	5.33	5.33	5.33
Capital, ft	2.00	2.00	2.50	2.50
Square Column, in.	-	-	-	-
Round Column, in.	14.00	14.00	14.00	14.00
Approximate Bar Size	4's	4's	4's	4's
+ Column Strip d, in.	5.00	5.00	5.00	5.00
A_s, in.^{2}	1.75	1.17	1.62	1.08
- Column Strip d, in.	6.25	6.25	6.25	6.25
A_s, in.^{2}	3.72	2.48	3.43	2.29
+ Middle Strip d, in.	4.50	4.50	4.50	4.50
A_s, in.^{2}	1.45	0.97	1.35	0.90
- Middle Strip d, in.	5.00	5.00	5.00	5.00
A_s, in.^{2}	1.45	0.97	1.35	0.90
Static Failure Overpressure:				
Shear, psi	-	-	-	-
Flexural, psi	1.69	1.69	1.60	1.60
Dynamic Failure Overpressure:				
Shear, psi	-	-	-	-
Flexural, psi	1.83	1.83	1.74	1.74
Time, sec	0.42	0.42	0.40	0.40
Ultimate Collapse Overpressure, psi	4.50	3.80	5.30	4.40

Design Live Load, Nominal: 125 psf
Length: 20 ft
Type: Capitals
Ultimate Strength Design

f'_c, ksi	3		4	
f_y, ksi	40	60	40	60
Slab Weight, psf	96.60	96.60	96.60	96.60
Total Dead Load, psf	106.60	106.60	106.60	106.60
Live Load, psf	125.00	125.00	125.00	125.00
M_o, k-in.	3379.70	3379.70	2993.00	2993.00
t, in.	7.50	7.50	7.50	7.50
t_d, in.	2.00	2.00	2.00	2.00
D, ft	6.67	6.67	6.67	6.67
Capital, ft	2.00	2.00	3.00	3.00
Square Column, in.	-	-	-	-
Round Column, in.	15.00	15.00	15.00	15.00
Approximate Bar Size	4's	4's	4's	4's
+ Column } d, in.	6.50	6.50	6.50	6.50
Strip } A_s, in.^{2}	3.01	2.01	2.66	1.77
- Column } d, in.	8.00	8.00	8.00	8.00
Strip } A_s, in.^{2}	6.58	4.39	5.74	3.83
+ Middle } d, in.	6.00	6.00	6.00	6.00
Strip } A_s, in.^{2}	2.42	1.68	2.15	1.48
- Middle } d, in.	6.50	6.50	6.50	6.50
Strip } A_s, in.^{2}	2.42	1.68	2.15	1.48
Static Failure Overpressure:				
Shear, psi	-	-	-	-
Flexural, psi	1.81	1.84	1.65	1.67
Dynamic Failure Overpressure:				
Shear, psi	-	-	-	-
Flexural, psi	1.96	2.00	1.79	1.82
Time, sec	0.53	0.53	0.50	0.50
Ultimate Collapse Overpressure, psi	3.90	3.20	5.40	4.50

Design Live Load, Nominal: 125 psf
Length: 24 ft
Type: Capitals
Ultimate Strength Design

f'_c, ksi	3		4	
f_y, ksi	40	60	40	60
Slab Weight, psf	115.95	115.95	115.95	115.95
Total Dead Load, psf	125.95	125.95	125.95	125.95
Live Load, psf	125.00	125.00	125.00	125.00
M_o, k-in.	5914.00	5914.00	5619.60	5619.60
t, in.	9.00	9.00	9.00	9.00
t_d, in.	2.50	2.50	2.50	2.50
D, ft	8.00	8.00	8.00	8.00
Capital, ft	3.00	3.00	3.50	3.50
Square Column, in.	-	-	-	-
Round Column, in.	17.00	17.00	17.00	17.00
Approximate Bar Size	6's	6's	6's	6's
+ Column ⎫ d, in.	7.87	7.87	7.87	7.87
Strip ⎭ A_s, in.^{2}	4.35	2.90	4.13	2.75
- Column ⎫ d, in.	9.62	9.62	9.62	9.62
Strip ⎭ A_s, in.^{2}	9.58	6.39	9.04	6.03
+ Middle ⎫ d, in.	7.12	7.12	7.12	7.12
Strip ⎭ A_s, in.^{2}	3.59	2.40	3.41	2.27
- Middle ⎫ d, in.	7.87	7.87	7.87	7.87
Strip ⎭ A_s, in.^{2}	3.59	2.40	3.41	2.27
Static Failure Overpressure:				
Shear, psi	-	-	-	-
Flexural, psi	1.79	1.80	1.72	1.72
Dynamic Failure Overpressure:				
Shear, psi	-	-	-	-
Flexural, psi	1.96	1.96	1.88	1.88
Time, sec	0.61	0.61	0.60	0.60
Ultimate Collapse Overpressure, psi	5.00	4.10	5.60	4.70

Design Live Load, Nominal: 250 psf
Length: 16 ft
Type: Capitals
Ultimate Strength Design

f'_c, ksi	3		4	
f_y, ksi	40	60	40	60
Slab Weight, psf	77.40	77.40	77.40	77.40
Total Dead Load, psf	87.40	87.40	87.40	87.40
Live Load, psf	250.00	250.00	250.00	250.00
M_o, k-in.	2186.80	2186.80	2186.80	2186.80
t, in.	6.00	6.00	6.00	6.00
t_d, in.	1.75	1.75	1.75	1.75
D, ft	5.33	5.33	5.33	5.33
Capital, ft	3.00	3.00	3.00	3.00
Square Column, in.	-	-	-	-
Round Column, in.	16.00	16.00	15.00	15.00
Approximate Bar Size	4's	4's	4's	4's
+ Column Strip d, in.	5.00	5.00	5.00	5.00
A_s, in.^{2}	2.58	1.72	2.54	1.69
- Column Strip d, in.	6.25	6.25	6.25	6.25
A_s, in.^{2}	5.72	3.82	5.45	3.63
+ Middle Strip d, in.	4.50	4.50	4.50	4.50
A_s, in.^{2}	2.14	1.43	2.11	1.41
- Middle Strip d, in.	5.00	5.00	5.00	5.00
A_s, in.^{2}	2.14	1.43	2.11	1.41
Static Failure Overpressure:				
Shear, psi	-	-	-	-
Flexural, psi	3.03	3.03	2.97	2.97
Dynamic Failure Overpressure:				
Shear, psi	-	-	-	-
Flexural, psi	3.25	3.26	3.20	3.20
Time, sec	0.28	0.39	0.26	0.36
Ultimate Collapse Overpressure, psi	11.30	9.60	10.70	9.20

Table A.3 (Contd)

Design Live Load, Nominal: 250 psf
Length: 20 ft
Type: Capitals
Ultimate Strength Design

f'_c, ksi	3		4	
f_y, ksi	40	60	40	60
Slab Weight, psf	103.20	103.20	96.60	96.60
Total Dead Load, psf	113.20	113.30	106.60	106.60
Live Load, psf	250.00	250.00	250.00	250.00
M_o, k-in.	4642.70	4642.70	4568.60	4568.60
t, in.	8.00	8.00	7.50	7.50
t_d, in.	2.25	2.25	2.00	2.00
D, ft	6.67	6.67	6.67	6.67
Capital, ft	3.50	3.50	3.50	3.50
Square Column, in.	-	-	-	-
Round Column, in.	19.00	19.00	17.00	17.00
Approximate Bar Size	5's	5's	5's	5's
+ Column Strip d, in.	6.94	6.94	6.44	6.44
A_s, in.^{2}	3.91	2.61	4.12	2.75
- Column Strip d, in.	8.56	8.56	7.81	7.81
A_s, in.^{2}	8.69	5.79	9.19	6.13
+ Middle Strip d, in.	6.31	6.31	5.81	5.81
A_s, in.^{2}	3.21	2.14	3.41	2.28
- Middle Strip d, in.	6.94	6.94	6.44	6.44
A_s, in.^{2}	3.21	2.14	3.41	2.28
Static Failure Overpressure:				
Shear, psi	-	-	-	-
Flexural, psi	3.07	3.07	3.04	3.04
Dynamic Failure Overpressure:				
Shear, psi	-	-	-	-
Flexural, psi	3.31	3.31	3.27	3.28
Time, sec	0.38	0.45	0.33	0.45
Ultimate Collapse Overpressure, psi	10.10	8.40	10.70	9.00

Table A.3 (Contd)

Design Live Load, Nominal: 250 psf
Length: 24 ft
Type: Capitals
Ultimate Strength Design

f'_c, ksi	3		4	
f_y, ksi	40	60	40	60
Slab Weight, psf	115.95	115.95	103.20	115.95
Total Dead Load, psf	125.95	125.95	113.20	125.95
Live Load, psf	250.00	250.00	250.00	250.00
M_o, k-in.	8114.90	8114.90	7872.00	8114.90
t, in.	9.00	9.00	8.00	9.00
t_d, in.	2.50	2.50	2.25	2.50
D, ft	8.00	8.00	8.00	8.00
Capital, ft	4.50	4.50	4.50	4.50
Square Column, in.	-	-	-	-
Round Column, in.	21.00	21.00	19.00	19.00
Approximate Bar Size	6's	6's	6's	6's
+ Column } d, in.	7.87	7.87	6.87	7.87
Strip } A_s, in.^{2}	6.07	4.05	6.72	3.99
- Column } d, in.	9.62	9.62	8.37	9.62
Strip } A_s, in.^{2}	13.91	9.28	15.37	8.80
+ Middle } d, in.	7.12	7.12	6.12	7.12
Strip } A_s, in.^{2}	5.01	3.34	5.64	3.29
- Middle } d, in.	7.87	7.87	6.87	7.87
Strip } A_s, in.^{2}	5.01	3.34	5.64	3.29
Static Failure Overpressure:				
Shear, psi	-	-	-	-
Flexural, psi	3.13	3.13	3.09	3.06
Dynamic Failure Overpressure:				
Shear, psi	-	-	-	-
Flexural, psi	3.38	3.38	3.33	3.31
Time, sec	0.41	0.57	0.34	0.53
Ultimate Collapse Overpressure, psi	12.00	10.10	13.50	9.50

Table A.3 (Concl)

Design Live Load, Nominal: 250 psf
Length: 28 ft
Type: Capitals
Ultimate Strength Design

Design Live Load, psf	50	80	125	250
f_c', ksi	4	4	4	4
f_y, ksi	60	60	60	60
Slab Weight, psf	135.00	135.00	135.00	135.00
Total Dead Load, psf	145.00	145.00	145.00	145.00
Live Load, psf	20.00	32.00	250.00	250.00
M_o, k-in.	5604.80	6798.90	10039.60	13646.20
t, in.	10.50	10.50	10.50	10.50
t_d, in.	2.75	2.75	2.75	2.75
D, ft	9.33	9.33	9.33	9.33
Capital, ft	2.00	2.50	3.50	5.00
Square Column, in.	-	-	-	-
Round Column, in.	12.00	12.00	17.00	21.00
Approximate Bar Size	5's	5's	6's	6's
+ Column Strip } d, in.	9.44	9.44	9.37	9.37
A_s, in.^{2}	2.24	2.73	4.10	5.63
- Column Strip } d, in.	11.56	11.56	11.37	11.37
A_s, in.^{2}	4.69	5.75	8.91	12.57
+ Middle Strip } d, in.	8.81	8.81	8.62	8.62
A_s, in.^{2}	1.80	2.19	3.33	4.57
- Middle Strip } d, in.	9.44	9.44	8.62	9.37
A_s, in.^{2}	1.80	2.19	3.33	4.57
Static Failure Overpressure:				
Shear, psi	-	-	-	-
Flexural, psi	0.47	0.82	1.78	3.11
Dynamic Failure Overpressure:				
Shear, psi	-	-	-	-
Flexural, psi	0.56	0.93	1.95	3.37
Time, sec	0.70	0.68	0.66	0.62
Ultimate Collapse Overpressure, psi	0.60	1.30	4.10	9.30

225

REFERENCES

1. Perrone, N., "Biomechanical Problems Related to Vehicle Impact," Chapter 22 of Biomechanics, Its Foundations and Objectives, edited by Y. C. Fung, N. Perrone and M. Anliker, Prentice-Hall, Inc. 1972.

2. Metropolitan Life Insurance Co., "Motorcycle Accident Deaths Rising Rapidly," Statistical Bulletin, Vol. 48, April 1967.

3. Metropolitan Life Insurance Co., "Fatal and Nonfatal Accidental Falls," Statistical Bulletin, Vol. 49, October 1968.

4. Webster's New Collegiate Dictionary, G. & C. Merriam Co., Publishers, Springfield, Massachusetts.

5. Gurdjian, E. S., Webster, J. E., and Lissner, H. R., "The Mechanism of Skull Fracture," Radiology, Vol. 54, No. 313, 1950.

6. Gurdjian, E. S., "Experiences in Head Injury and Skeletal Research," Proceedings Symposium on Impact Acceleration Stress, Publ. 977, pp 145-157, November 27-29, 1961.

7. Gurdjian, E. A., Lissner, H. R. and Patrick, L. M., "Protection of the Head and Neck in Sports," Journal of the American Medical Association, Vol. 182, No. 5, November 3, 1962.

8. Snyder, R. G., "State-of-the-Art -- Human Impact Tolerance," Reprinted from 1970 International Automotive Safety Conference Compendium, P-30 by Society of Automotive Engineers, Inc., 2 Pennsylvania Plaza, New York, N. Y. 10001, May 1970.

9. Hodgson, V. R. and Thomas, L. M., "Effect of Long-Duration Impact on Head," Proceedings of Sixteenth Stapp Car Crash Conference, Detroit, Michigan, pp 292-295, November 8-10, 1972.

10. Gadd, C. W., "Use of a Weighted-Impulse Criterion for Estimating Injury Hazard," Tenth Stapp Car Crash Conference, pp 164-174, November 8-9, 1966.

11. White, C. S., Bowen, I. G. and Richmond, D. R., "Biological Tolerance to Airblast and Related Biomedical Criteria," Civil Effects Test Operations, U.S. Atomic Energy Commission, 1965.

12. Zukerman, S. and Black, A. N., The Effect of Impact on the Head and Back on Monkeys, Report R. C. 124, Ministry of Home Security, Oxford, England, August 12, 1940.

REFERENCES (Contd)

13. Gurdjian, E. S.; Webster, J. E. and Lissner, H. L., "Studies
     on Skull Fracture with Particular Reference to Engineering
     Factors," American Journal of Surgery, Vol. 78, pp 276-742,
     1949.

14. White, C. S., et al, The Biodynamics of Airblast, for Defense
     Nuclear Agency, Washington, D.C. 20305, Contract DASA
     01-70-C-0075, Lovelace Foundation, DNA 2738T, July 1, 1971.

15. Longinow, A. and Ojdrovich, G., Survivability in a Direct
     Effects Environment (Analysis of 25 NFSS Buildings), for
     Defense Civil Preparedness Agency, Contract DAHC20-72-C-
     0318, IIT Research Institute, January 1973.

16. Longinow, A., et al, People Survivability in A Direct Effects
     Environment and Related Topics, for Defense Civil Prepared-
     ness Agency, Contract DAHC20-68-C-0126, DCPA Work Unit 1614D,
     IIT Research Institute, May 1973.

17. Longinow, A., Survivability in a Direct Effects Environment
     (Analysis of 50 NFSS Buildings), for Defense Civil Prepared-
     ness Agency, Contract DASC20-73-C-0227, IIT Research Institute,
     July 1974.

18. DeHaven, H., "Mechanical Analysis of Survival in Falls from
     Heights of Fifty to One Hundred and Fifty Feet," War Medicine,
     1(2), pp 586-596, January 1942.

19. Snyder, R. G., "Human Survivability of Extreme Impacts in
     Free-Fall," 63-15, Federal Aviation Agency, Oklahoma City,
     Oklahoma, August 1963.

20. Stech, E. L. and Payne, P. R., "Dynamic Models of the Human
     Body," AMRL-TR-66-157, Aerospace Medical Research Laboratory,
     Wright-Patterson Air Force Base, Ohio.

21. Lewis, W. S.; Lee, A. B., Jr. and Grantham, S. A., "Jumpers'
     Syndrome -- The Trauma of High, Free-Fall as Seen at Harlem
     Hospital," J. Trauma, 5, pp 812-818, 1965.

22. Richmond, D. R., et al, "Tertiary Blast Effects -- Effects
     of Impact on Mice, Rats, Guinea Pigs and Rabbits," Aerospace
     Medicine, Vol. 32, pp 789-805, September 1961.

23. Roth, H. P., "Impact and Dynamic Response of the Body,"
     Symposium on Frontiers of Man-Controlled Flight, edited by
     H. Haber, The Institute of Transportation and Traffic Engineer-
     ing, University of California, Los Angeles, pp 48-54, April 3,
     1975.

REFERENCES (Contd)

24. States, J. D., "The Abbreviated and the Comprehensive Research Injury Scales," Proceedings of the Thirteenth Stapp Car Crash Conference, Society of Automotive Engineers, Inc., New York, pp 282-294, 1969.

25. States, J. D. et al, "Field Application and Research Development of the Abbreviated Injury Scale," Fifteenth Stapp Car Crash Conference, Coronado, California, November 17-19, 1971.

26. Glasstone, S. (editor), The Effects of Nuclear Weapons, U.S. Government Printing Office (Revised Edition) (Section 4.81, p 182) 1962.

27. Hoerner, S. F., Fluid Dyanmic Drag, published by the author, (Chapter III, Section 5) 1965.

28. Wiedermann, A. and Nielsen, H., Debris and Fire Environment from Soft Oil Storage Tanks Under Nuclear Attack Conditions, IIT Research Institute, for U.S. Army Engineer Division, Huntsville Corps of Engineers, Contract DACA 87-70-C-0001, 1971.

29. Damon, A.; Stoudt, H. W. and McFarland, R. A., The Human Body in Equipment Design, Harvard University Press, 1964.

30. Dempster, W. T., Space Requirements of the Seated Operator, WACD Tech. Report 55-159, Aero Medical Laboratory, Wright Air Development Center, 1955.

31. Bartz, J. A. and Butler, F. E., A Three-Dimensional Computer Simulation of a Motor Vehicle Crash Victim, Phase 2 - Validation of the Model, DOT-HS 800795, Calspan Report VU-2978-V-2, Department of Transportation, National Highway Traffic Safety Administration, Washington, D.C. 20590, 1972.

32. Krouskop, T. A.; Newell, P. H. and Swarts, A. E., Vehicle Exteriors and Pedestrian Injury Prevention, Vol. III - The Texas A&M University Injury Severity Index, DOT-HS-065-1-217, Texas A&M Research Foundation Report DOT HS-801 543 for U.S. Department of Transportation, National Highway Traffic Safety Administration, Washington, D.C. 20590, May 1975.

33. Hognestad, E., "Yield-Line Theory for the Ultimate Flexural Strength of Reinforced Concrete Slabs," ACI Journal (ACI Proceedings Vol. 29) p 637, March 1953.

34. Keenan, W. A., Strength and Behavior of Restrained Reinforced Concrete Slabs Under Static and Dynamic Loading, Technical Report R621, U.S. Naval Civil Engineering Laboratory, Port Hueneme, California, April 1969.

REFERENCES (Contd)

35. Brown, W. M. and Black, M. S., Dynamic Strength Study of Small, Fixed-Edge, Longitudinally Restrained, Two-Way Reinforced Concrete Slabs, Technical Report N-73-8, U.S. Army Engineer Waterways Experiment Station, CE, Vicksburg, Mississippi, December 1973.

36. Huff, W. J., Collapse Strength of a Two-Way Reinforced Concete Slab Contained Within a Steel Frame Structure, Technical Report N-75-2, U.S. Army Engineer Waterways Experiment Station, CE, Vicksburg, Mississippi, June 1975.

37. Denton, D. R., A Dynamic Ultimate Strength Study of Simply Supported Two-Way Reinforced Concrete Slabs, Technical Report 1-789, U.S. Army Engineer Waterways Experiment Station, CE, Vicksburg, Mississippi, July 1967.

38. Newmark, N. M. and Haltiwanger, J. D., Air Force Design Manual; Principles and Practices for Design of Hardened Structures, Technical Documentary Report AFSWC-TDR-62-138, Air Force Special Weapons Center, Kirtland Air Force Base, New Mexico, December 1962.

39. ACI Standard 318-63 - Building Code Requirements for Reinforced Concrete, (ACI 318-63), American Concrete Institute, P.O. Box 4754, Redford Station Detroit, Michigan 48219.

40. Excerpts from the American Standard Building Code Requirements for "Minimum Design Loads in Buildings and Other Structures," A58.1-1955, Section 3.5, Manual of Steel Construction, American Institute of Steel Construction, Inc. 101 Park Avenue, New York, N.Y. 10017, Sixth Edition, pp 5-163.

41. CRSI Design Handbook, Working Stress Design, Revised 1963 ACI Code, Concrete Reinforcing Steel Institute, 228 North LaSalle Street, Chicago, Illinois 60601.

42. CRSI Handbook, Ultimate Strength Design, 1963 ACI Code, Concrete Reinforcing Steel Institute, 228 North LaSalle Street, Chicago, Illinois 60601.

43. Criswell, M. E., Strength and Behavior of Reinforced Concrete Slab-Column Connections Subjected to Static and Dynamic Loading, Technical Report N-70-1, U.S. Army Engineer Waterways Experiment Station, Vicksburg, Mississippi, December 1970.

44. Biggs, J. M., Introduction to Structural Dynamics, McGraw-Hill Book Company, 1964.

45. Criswell, M. E., Design and Testing of a Blast-Resistant Reinforced Concrete Slab System, Technical Report N-72-10, U.S. Army Engineer Waterways Experiment Station, Vicksburg, Mississippi, November 1972.

46. Longinow, A., et al, Civil Defense Shelter Options: Deliberate Shelters, IIT Research Institute, Final Report IITRI J6144, Vol. II, December 1971.

47. Kot, C., et al, Air Blast Attenuation, IIT Research Institute, Final Report IITRI J6014(2), July 1969 (SECRET)

48. Coulter, G. A., Flow in Model Rooms Caused by Air Shock Waves, BRL Report BRLMR2044, July 1970.

49. Coulter, G. A., Blast Loading of Objects in Basement Shelter Models, Ballistics Research Lab. Report BRLMR2348, January 1974.

50. "Tornado," U.S. Department of Commerce, National Oceanic and Atmospheric Administration, 1970.

51. Fujita, T. T., "Tornado Parameters," Proceedings, Tornado Conference, University of Wisconsin, April 1970.

52. Ting, S. J. and Chang, C. C., "Exploratory Model Study of Tornado-Like Vortex Dynamics," Journal of Atmospheric Sciences, 27, No. 1, January 1970.

53. Reynolds, G. W., "A Practical Look at Tornado Forces," Proceedings, Tornado Conference, University of Wisconsin, April 1970.

54. McLaughlin, J. M., "Design of Nuclear Power Plants for Tornadoes," Proceedings of the Tornado Conference, University of Wisconsin, April 1970.

55. Hoerner, S. F., Fluid Dynamic Drag, 1965.

56. Nielson, H. and Wiedermann, A. H., Debris and Fire Environment from Soft Oil Storage Tanks Under Nuclear Attack Conditions, (S-3), IIT Research Institute, ca June 1970.

57. Minor, R. R. and Sanger, A. J., "Observations of the Response of Metal Building Systems to the Lubbock Tornado," Texas Tech University Storm Research Report 02, Texas Tech University, Lubbock, Texas, February 1971.

58. McDonald, J. R.; Mehta, K. C. and Cartwright, E., "Economic Feasibility of Tornado Resistant Design," presented at ASCE National Water Resources Meeting, Atlanta, Georgia, January 24-28, 1972.

REFERENCES (Concl)

59. Minor, J. E.; Lambert, B. K. and Wittman, J., "Impact of the Lubbock Storm on Regional Systems," Texas Tech University Storm Research Report 05 (TTU SRR05), prepared for the Defense Civil Preparedness Agency, Washington, D.C., June 1972.

60. Mehta, K. C.; McDonald, J. R. and Minor, J. E., "Response of Structural Systems to the Lubbock Storm," TTU SRR 03, Texas Tech University, Lubbock, Texas, October 1971.

61. McDonald, J. R., "Structural Response of a Twenty-Story Building to the Lubbock Tornado," TTU SRR 01, Texas Tech University, Lubbock, Texas, October 1970.

DISTRIBUTION LIST

	Copies
Defense Civil Preparedness Agency Research and Engineering Washington, D.C. 20301 Attention: Administrative Officer	50
Assistant Secretary of the Army (R&D) Washington, D.C. 20310 Attention: Assistant for Research	1
Chief of Naval Research Washington, D.C. 20306	1
Commander, Naval Supply Systems Command (0421G) Department of the Navy Washington, D.C. 20376	1
Commander Naval Facilities Engineering Command Research and Development (Code 0322C) Department of the Navy Washingotn, D.C. 20390	1
Defense Documentation Center Cameron Station Alexandria, Virginia 22314	12
Emergency Technology Division Civil Defense Research Project Oak Ridge National Laboratory P.O. Box X Oak Ridge, Tennessee 37830 Attention: Librarian	1
Director Lovelace Foundation 5200 Gibson Boulevard, S.E. Albuquerque, New Mexico 87108	1
Mr. Edward L. Hill Research Triangle Institute Post Office Box 12194	1
Mr. H. L. Murphy Stanford Research Institute 333 Ravenswood Avenue Menlo Park, California 94025	1
Chief of Engineers Attention: ENGME-RD Department of the Army Washington, D.C. 20314	1

Copies

Commanding Officer
U.S. Naval Civil Engineering Laboratory
Attention: Document Library
Port Hueneme, California 93041   1

AFWL/Civil Engineering Division
Attention: Technical Library
Kirtland Air Force Base
Albuquerque, New Mexico 87117   1

Director, U. S. Army Engineer
  Waterways Experiment Station
Attention: Nuclear Weapons Effects Branch
Post Office Box 631
Vicksburg, Mississippi 39180   1

Dikewood Industries, Inc.
1009 Bradbury Drive, S.E.
University Research Park
Albuquerque, New Mexico 87106   1

Mr. William H, Van Horn
URS Research Company
155 Bovet Road
San Mateo, California 94402   1

Dr. Rudolf J. Engelmann
Energy Research and Development
  Administration (DBER)
Washington, D.C. 20545   1

Mr. Carl K. Wiehle
Stanford Research Institute
333 Ravenswood Avenue
Menlo Park, California 94025   1

Director
Ballistic Research Laboratory
Attention: Document Library
Aberdeen Proving Ground, Maryland 21005   1

Civil Engineering Center/AF/PRECET
Attention: Technical Library
Wright-Patterson Air Force Base
Dayton, Ohio 45433   1

Director, Army Materials and
  Mechanics Research Center
Attention: Technical Library
Watertown, Massachusetts 02172   1

DISTRIBUTION LIST (Contd)

Copies

Commanding Officer
U.S. Army Combat Developments Command
Institute of Nuclear Studies
Fort Bliss, Texas 79916   1

Director, U.S. Army Engineer
  Waterways Experiment Station
Attention: Document Library
Post Office Box 631
Vicksburg, Mississippi 29180   1

Mr. Donald A. Bettge
Research and Engineering Directorate
Defense Civil Preparedness Agency
Washington, D.C. 20301   1

Dr. Lewis V. Spencer
Radiation Theory Section 4.3
National Bureau of Standards
Washington, D.C. 20234   1

Mr. Anatole Longinow
IIT Research Institute
10 West 35th Street
Chicago, Illinois 60616   1

Mr. Samuel Kramer, Chief
Office of Federal Building Technology
Center for Building Technology
National Bureau of Standards
Washington, D.C. 20234   1

Dr. Clarence R. Mehl
Department 5230
Sandia Corporation
Box 5800, Sandia Base
Albuquerque, New Mexico 87115   1

Director, Defense Nuclear Agency
Attention: Mr. Jack R. Kelso
Washington, D.C. 20305   1

Mr. Bert Greenglass
Director, Office of Administration
Program Planning and Control
Department of Housing & Urban Development
Washington, D.C. 20410   1

DISTRIBUTION LIST (Concl)

DEBRIS MOTION AND INJURY RELATIONSHIPS IN ALL HAZARD   (Unclassified)
Environments

Final Report   236 pages

Contract DCPA01-74-C-0251   IIT Research Institute
DCPA Work Unit 1614E   July 1976

This report contains the results of a study concerned with producing
casualty (injury and fatality) relationships for people located in con-
ventional buildings when subjected to man-made and natural disaster haz-
ard environments. Emphasis is on the direct effects produced by nuclear
weapons. Limited consideration is given to debris effects produced by
a tornado.

The key portion of this effort was concerned with selecting impact cas-
ualty criteria and developing a simulation model for people subjected
to blast winds and debris. Portions of available literature dealing
with impact casualties are reviewed and discussed. Impact casualty cri-
teria applicable for evaluating casualties in a nuclear weapon blast
environment are selected. A two-dimensional, articulated man simulation
model developed herein is described.

People survivability estimates for people located in conventional base-
ments of multistory buildings subjected to blast effects of megaton

range nuclear weapons are presented. Results are presented for full basements with one-way and two-way (flat plate, flat slab) reinforced concrete overhead floor systems and large V/A (basement volume to entranceway area) ratios, i.e., large basements with proportionally small entranceways in which blast penetration is not a significant hazard. A separate task is devoted to basements having small V/A ratios. The transient air velocity field which may exist in such basements is modeled. This model is used in conjunction with a simple drag-type transport model to examine the impact hazard to personnel.

A limited effort is devoted to evaluating debris hazards posed by a tornado. A conventional tornado wind environment together with a simple aerodyamic model is used to establish hazards posed by debris for one severe tornado wind field.

IITRI IIT Research Institute
10 West 35 Street, Chicago, Illinois 60616
312/225-9630

September 9, 1974

Defense Civil Preparedness Agency
The Pentagon
Washington, D.C.   20301

Attention: Mr. D. A. Bettge

Subject: First Quarterly Report on IITRI Project J6334,
          Contract DCPA01-74-C-0251, Work Unit 1614E,
          Entitled "Debris Motion and Injury Relation-
          ships in All Hazard Environments"

Gentlemen:

1. <u>Selection of Casualty Criteria</u>

       Over the first reporting period the emphasis of this study
was on the review of available literature dealing with casualties
and casualty criteria with respect to impact. Approximately 50
references were obtained and have been reviewed. Most of these
deal with impacts produced as a result of automobile accidents.
Based on our evaluation of these references it is concluded that
currently available casualty criteria are very limited.

       This subject was discussed with Dr. L. Ovenshire of NHTSA
(National Highway Traffic Safety Administration) who coordinates
studies dealing with casualty prediction in connection with auto-
mobile accidents. Dr. Ovenshire has several studies underway
whose ultimate objective is to provide the capability for pre-
dicting impact casualties. One of these studies, dealing with
head impact, is being conducted at NCEL (Naval Civil Engineering
Laboratory). The other, dealing with thorax impact, is being
conducted at the Franklin Institute. These are large scale
analytic modeling studies. They are currently in progress and
readily usable information is not expected to be available in the
near future.

       Dr. Ovenshire reviewed the status of his projects and was
helpful in recommending references and workers in this field whose
suggestions might prove useful. Based on his recommendations we
we plan to review a number of papers presented at the 15th Stapp
Car Crash Conference and contact Dr. J. D. States at the University
of Rochester, Mr. L. M. Patrick at Wayne State University and Dr.
R. G. Snyder at the University of Michigan. Based on available
references these people appear to be very active in this field.
Dr. States is the author of the abbreviated injury scale which was
adapted by the AMA (American Medical Association).

The problem of adopting available casualty criteria for predicting injuries and fatalities in a blast environment is a difficult task. However, at this point we feel that at least crude, though defensible criteria can be formulated on a problem oriented basis.

2. Fiscal Report

Project Appropriation $58,062
Billable Fee   - 3,287

Billable Cost $54,775

Project start - April 15, 1974

(1) Expenditures for the second calendar quarter
  ending June 30, 1974 $2,833.21

(2) Anticipated expenditures for the third
  calendar quarter ending September 30, 1974 15,200.79

(3) Anticipated expenditures for the fourth
  calendar quarter ending December 31, 1974 15,052.00

(4) Anticipated expenditures for the first
  calendar quarter ending March 31, 1975 15,689.00

(5) Anticipated expenditures for the second
  calendar quarter ending June 30, 1975   4,000.00

(6) Anticipated expenditures for the third
  calendar quarter ending September 30, 1975 2,000.00

                $54,775.00

Respectfully submitted,
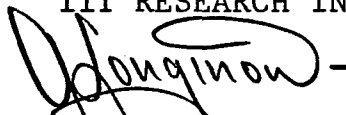
IIT RESEARCH INSTITUTE

A. Longinow
Manager
Structural Analysis Section

APPROVED:

I. B. Fieldhouse
Assistant Director of Research
Engineering Mechanics Division

October 31, 1974   J6334

Defense Civil Preparedness Agency
The Pentagon
Washington, D.C. 20301

Attention: Mr. D. A. Bettge

Subject: Second Quarterly Report on IITRI Project J6334, Con-
            tract DCPA01-74-C-0251, Work Unit 1614E, entitled
            "Debris Motion and Injury Relationships in All Hazard
            Environments"

Gentlemen:

1. Selection of Casualty Criteria

The objective of this task is to explore the feasibility of
developing impact casualty criteria (based on available information)
capable of separating shelter survivors in two categories, i.e., in-
jured and uninjured. This task was initiated in the previous re-
porting period and is continuing.

To date approximately 80 references dealing with impact casual-
ties (and specifically with human tolerance limitations to impact)
have been collected. The majority of these have been reviewed.
References collected do not cover a single method for measuring
human tolerance, instead several methods are used. These include

- Human volunteers

- Clinical reports of accidents

- Cadavers

- Experimental animals

- Anthropomorphic dummies

- Accidental free-falls

- Mathematical models

A significant portion of information collected deals with some as-
pect of automobile safety.

We feel that relevant information has been collected. How-
ever, before specific criteria are selected for evaluation, it is
important to first define and quantify casualty mechanisms prevalent
in shelters. The following, general classes of information are
relevant to the problem.

Debris

Size distribution

Ranges of debris transport

Impact velocities

Dynamic pressure in the interior of shelters

Pressure-time histories

Peak pressures

Durations

People

Transport distances

Orientations

Impact velocities

Portions of body impacted

At the present time we are in the process of identifying casualty
mechanisms and levels of their intensity for basement shelters.
Building parameters considered include the strength of overhead slab
as a function of geometry and floor area. In the initial task only
one-way, simply supported, reinforced concrete slabs are being con-
sidered. We will quantify failure overpressures, times to failure,
debris sizes, impact velocities and portions of floor area affected.
This information will then be related to casualty, i.e., injury
and/or fatality in terms of acceptable criteria.

2. Fiscal Report

Project Appropriation $58,062
Billable Fee   -   3,287

Billable Cost $54,775

Project start - April 15, 1974

(1) Expenditures for the second calendar quarter
    ending June 30, 1974 $2,833.21

(2) Expenditures for the third calendar quarter
    ending September 30, 1974   11,430.21

(3) Anticipated expenditures for the fourth
    calendar quarter ending December 31, 1974   15,052.00

(4) Anticipated expenditures for the first
     calendar quarter ending March 31, 1975   15,689.00

(5) Anticipated expenditures for the second
     calendar quarter ending June 30, 1975   7,770.58

(6) Anticipated expenditures for the third
     calendar quarter ending September 30, 1975   2,000.00

                                   Total $54,775.00

Respectfully submitted,
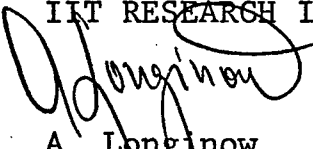
IIT RESEARCH INSTITUTE

AL:ms

A. Longinow
Manager
Structural Analysis Section

APPROVED:
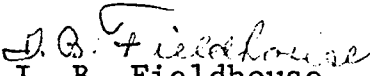
I. B. Fieldhouse
Assistant Director of Research
Engineering Mechanics Division

January 13, 1975   J6334

Defense Civil Preparedness Agency
The Pentagon
Washington, D.C.   20301

Attention: Mr. D. A. Bettge

Subject: Third Quarterly Report on IITRI Project J6334,
            Contract DCPA01-740C-0251, Work Unit 1614E,
            entitled "Debris Motion and Injury Relation-
            ships in All Hazard Environments"

Gentlemen:

    During the course of this reporting period a task was ini-
tiated to estimate the extent of survivability afforded by base-
ments of conventional buildings when subjected to the direct
effects of nuclear weapons. The object is to estimate percent
survivors and to separate them into two groups, i.e., injured
and uninjured. To date a representative group of basements
having one-way reinforced concrete slabs was analyzed. The pro-
cedure and some results are discussed in the following section.
The analysis procedure developed is to be expanded to include
different floor systems over basements and upper story spaces.

1. People Survivability in Basement Spaces

    The objective of this task is to estimate the extent of
sheltering provided by conventionally designed basements of
existing buildings when subjected to the direct effects of megaton-
range nuclear weapons. In this task the "extent of sheltering"
is measured in terms of number or percent survivors. Survivors
include two categories of people, i.e., injured and uninjured.
The percent (or number) of each is estimated.

    The reason for considering basements first is that by virtue
of their location relative to the ground surface basements gen-
erally provide more protection than upper stories. Also, since
fewer casualty mechanisms are generally involved, the problem
of estimating the number of survivors and then separating them
in two categories, i.e., injured and uninjured, is generally
simpler than in the case of people located in the upper stories.

    This task considers basements of the type generally found in
office buildings, schools and apartment buildings. The first
portion of the task considers basements whose overhead floor

systems are at grade. This restriction eliminates exposed basement walls, direct external entranceways into the basement area and windows. The basic geometry considered is shown in Fig. 1.

Readily available designs of basements with different floor systems, representative ranges of design loads, span lengths and support conditions do not exist. It was therefore necessary to design several sets of floor systems allowing for a sufficiently broad variation of pertinent design parameters. For the simply-supported one-way slabs discussed in this report, the following design parameters were varied over the ranges indicated.

Design live load	– 40, 60, 80, 100, 120, 140, 160, 180, 200, 220, 240 psf
Span length	14, 16, 18, 20, 22, 24, 26, 28, 30, 32, 34, 36, 38, 40 ft
f'_c (ultimate compressive strength of concrete)	2500, 3000, 3500, 4000, 4500, 5000, 5500, 6000 psi
f_y (yield strength of reinforcing steel)	40000, 50000, 60000, 75000 psi

As indicated in Fig. 1, a clear ceiling height of 8 ft was kept constant. A total of 4928 slabs were designed using the design criteria stipulated in ACI 318-71.

Estimates of people survivability are made on the assumption that the only possible collapse mechanisms are those shown in Fig. 2 and that each is equally likely. Experience and theory indicate that a uniform, simply-supported slab subjected to a uniformly applied dynamic load of sufficiently high magnitude will develop a plastic hinge at midspan and will thus become a mechanism. Since the design stipulates a uniform slab and symmetric loading, then a symmetric collapse is a logical conclusion. However, since these conditions are not expected to be uniform in every case, an unsymmetric collapse mode, i.e., rotation about point A or point B is also likely. Since the likelihood of these collapse modes is not known, it is reasonable to assume that each of the three is equally likely. The assumptions described have some experimental basis. For example in Ref. approximately one-half of the symmetrically designed, supported and loaded slabs experienced unsymmetric collapse.

After the slab has experienced its collapse deflection at overpressure p_1 or higher (see point 1, Fig. 2a and b), the unsymmetric and symmetric collapse mechanisms can be described as follows.

2. Rotation of total span about support point A or B resulting in unstable position 2.

3. Further rotation and falling to a stable position 3.

4. Failure and collapse of half-span due to overpres-
   sure p_2 (or higher) resulting in collapse mode 4.

The symmetric collapse (see Fig. 2b), is followed by a stable
position "2". At sufficiently high overpressures (p_2 or higher)
this is followed by failure and collapse of the half-spans result-
ing in collapse mode 3.

A computerized procedure was formulated which computes geo-
metric parameters h_2, h_3, h_4, S_2, S_3 as a function of span length,
clear ceiling height and the collapse assumptions.

Survivors are estimated on the basis of collapse overpressures
p_1 and p_2, corresponding to collapsed states of slabs resulting in
h_2, h_3, h_4, S_2 and S_3 and respective impact velocities in areas
occupied by people. It is assumed that basement occupants are dis-
tributed in one of the preparatory postures illustrated in Fig. 3,
and do not change the given posture during the course of slab
failure.

People located in areas unaffected by portions of collapsed
slab are classified as uninjured survivors. Injury or fatality
is assumed to be produced when shelter occupant interacts with the
collapsing slab. Injury or fatality depends on the magnitude of
impact velocity and the portion of the body affected.

Results of analyses performed on several slabs in which span
lengths and material properties were varied are illustrated in
Fig. 4 through Fig. 12. Designations for the various graphs shown
are given below.

<center>Legend (Fig. 4 through Fig. 12)</center>

——————————— Percent surviving initial slab collapse or percent
             surviving initial and secondary slab collapse, as-
             suming availability of rescue equipment irrelevant

— — — — —   Percent surviving initial slab collapse injured,
             or percent surviving initial and secondary slab
             collapse injured, assuming rescue equipment available.

——— — ———   Percent surviving initial and secondary slab collapse
             assuming rescue equipment unavailable

——— · ———   Percent surviving initial and secondary slab collapse,
             assuming equipment available

The graphs shown in Figs. 4 through 12 were all based on an assumed equally lumped 50 percent population along each wall and the unsymmetric collapse mode shown in Fig. 2. The four positions illustrated in the top half of Fig. 3A were assumed to be equally likely for the 50 percent of the population located in the basement corner opposite the slab pivot point, with the two prone positions in the bottom half of the page being equally likely for the 50 percent of the population located in the corner adjacent to the pivot point.

Furthermore, the question of availability of rescue equipment had to be raised with regards to survivability estimates following the secondary slab collapse, i.e., the possibility of people being alive but unable to extricate themselves from the fallen debris without outside help and equipment was recognized.

Following these assumptions, pertinent distances and clearances were geometrically approximated and translated into survivability estimates. Based upon the analyses of nine separate cases (Figs. 4 through 12) the following statements can be made:

1. Failure overpressure for both initial and secondary slab collapse increases significantly with both span length and design live load.

2. Span length is the governing factor in the survivability estimates themselves.

Fiscal Report

Project Appripriation	$58,062	
Billable Fee	- 3,287	
Billable Cost	$54,775	

Project start - April 15, 1974

(1) Expenditures for the second calendar
    quarter ending June 30, 1974 $ 2,833.21

(2) Expenditures for the third calendar
    quarter ending September 30, 1974   11,430.11

(3) Expenditures for the fourth calendar
    quarter ending December 31, 1974   11,657.52

(4) Anticipated expenditures for the first
    calendar quarter ending March 31, 1975   15,689.00

(5) Anticipated expenditures for the second
calendar quarter ending June 30, 1975 $10,770.58

(6) Anticipated expenditures for the third
calendar quarter ending September 30, 1975   2,394.48

Total $54.775.00

Respectfully submitted,

IIT RESEARCH INSTITUTE

A. Longinow
Manager, Structural Analysis

AL:ms

APPROVED:

K. E. McKee
Director of Research
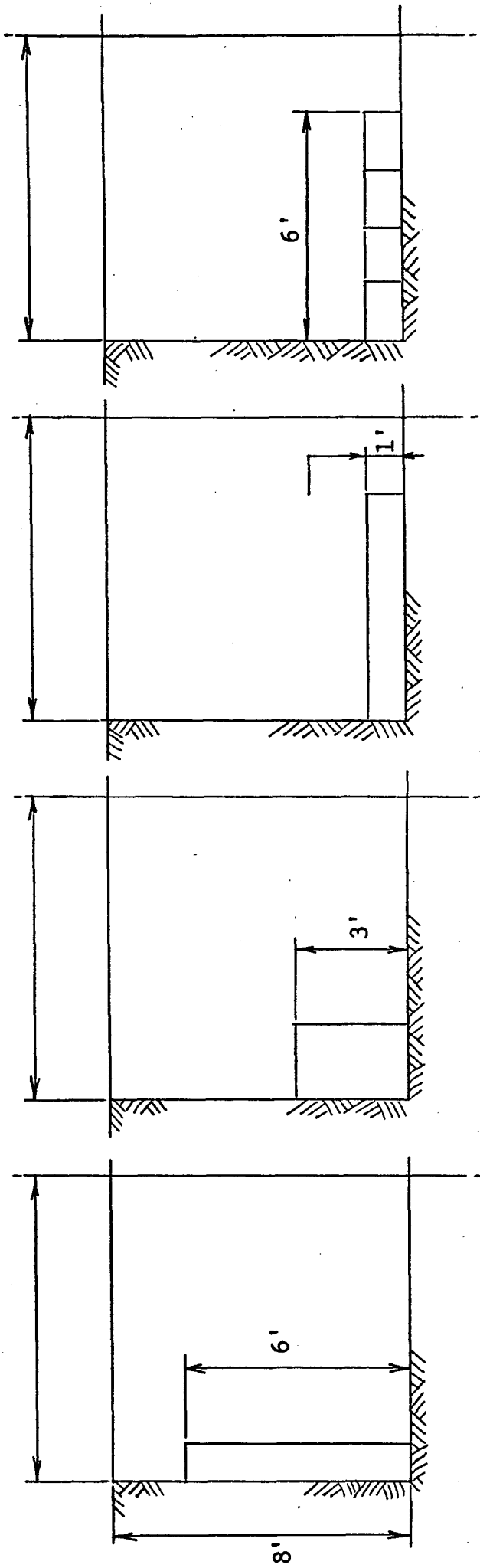Engineering Mechanics Division
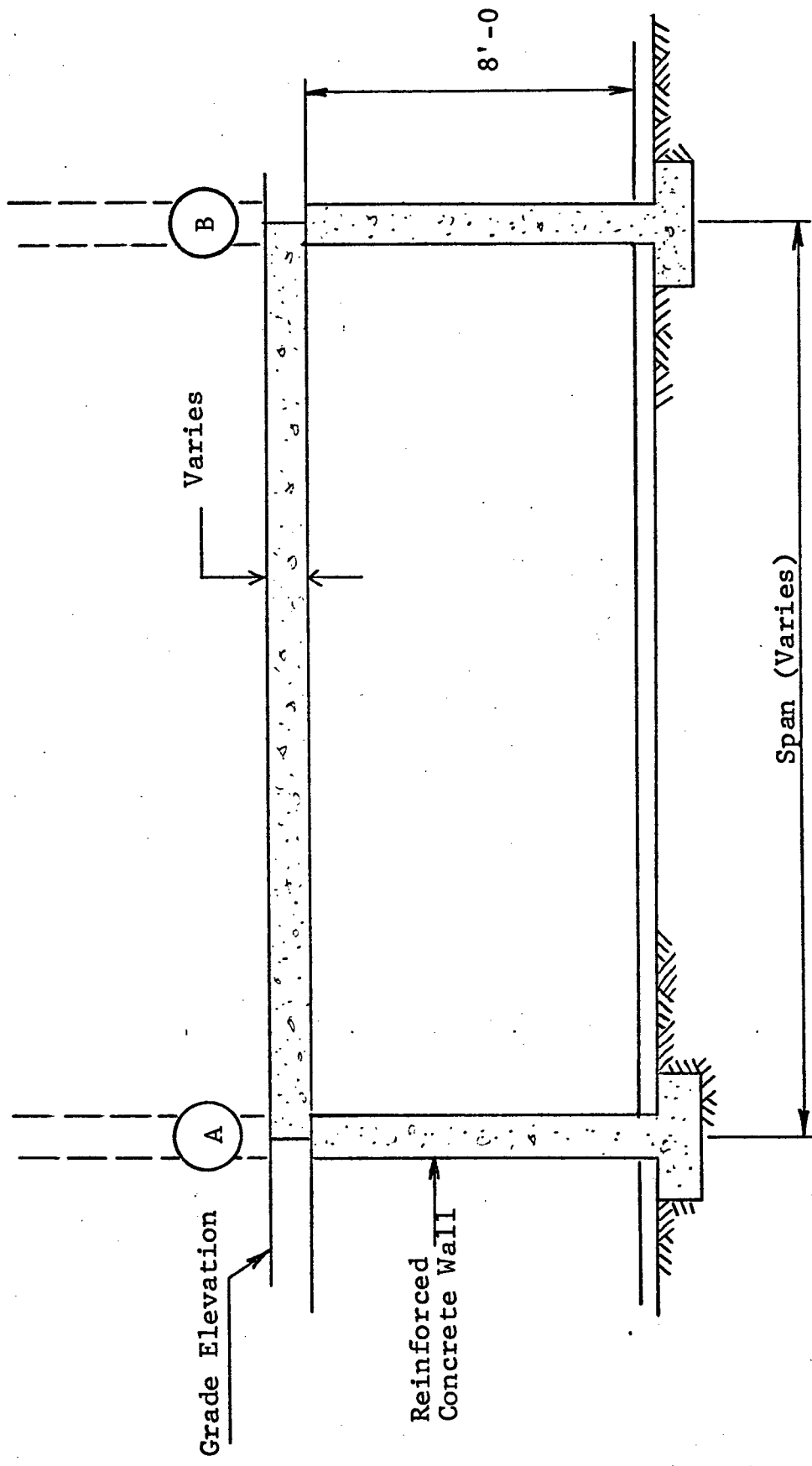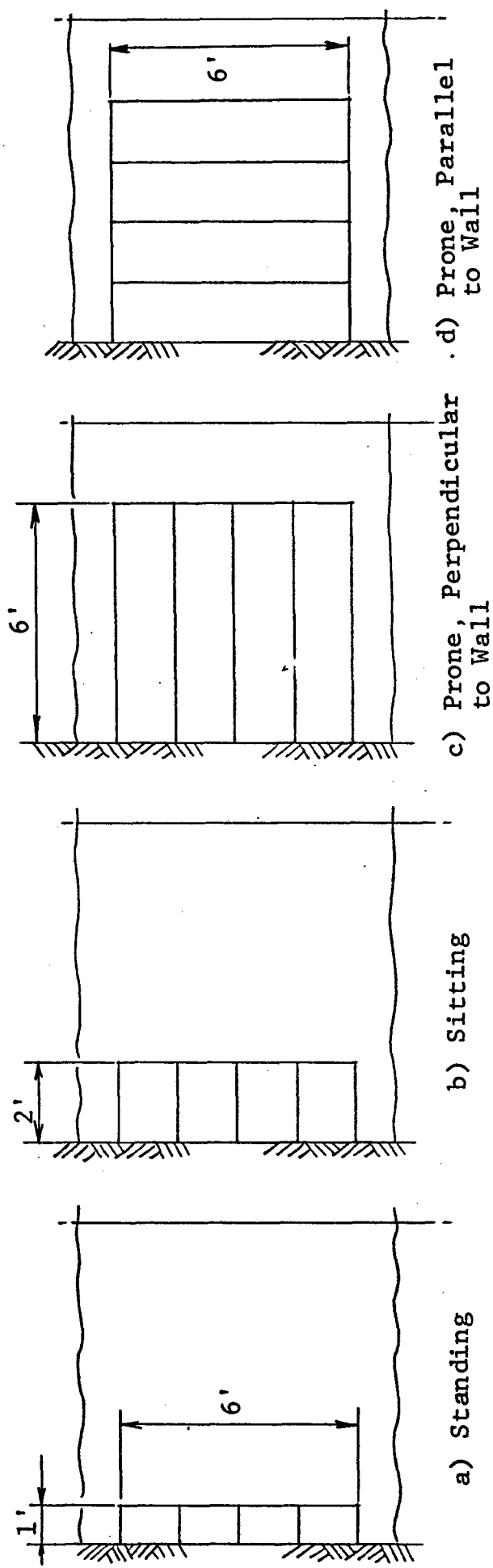
Fig. 1 Basic Basement Geometry
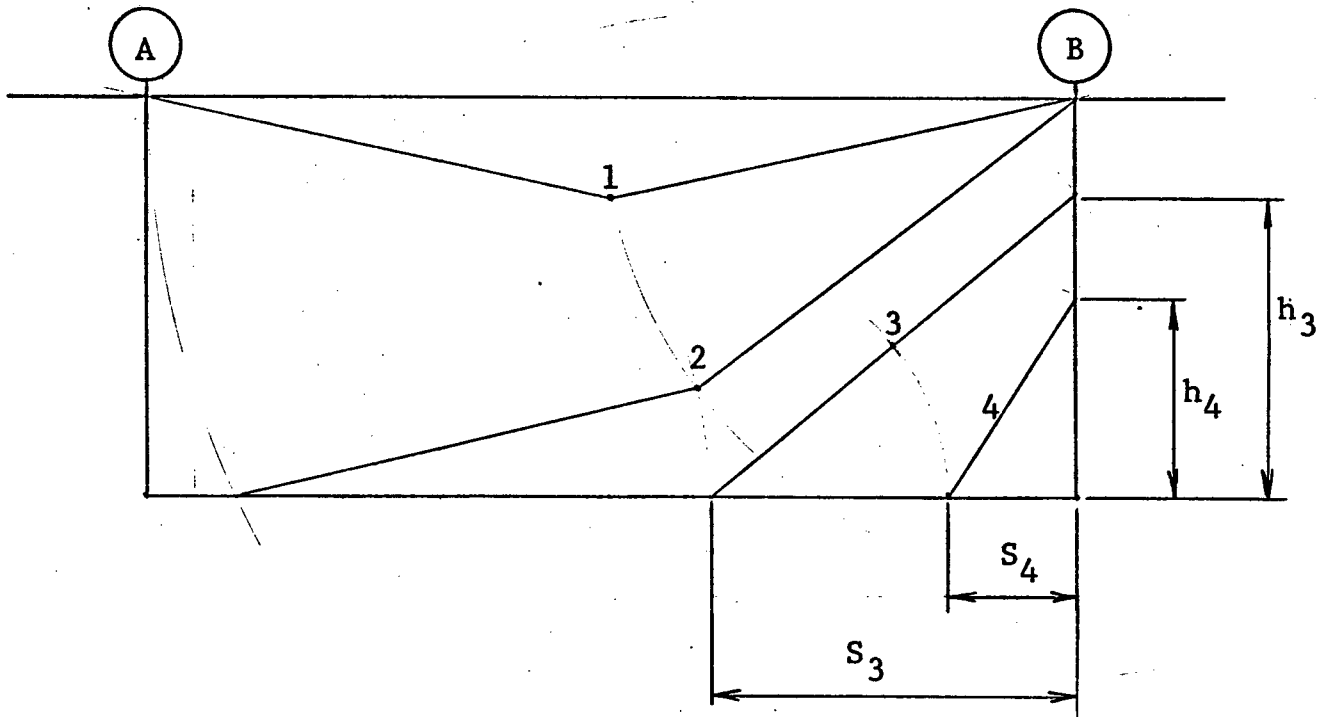
a) Unsymmetric Collapse Mode
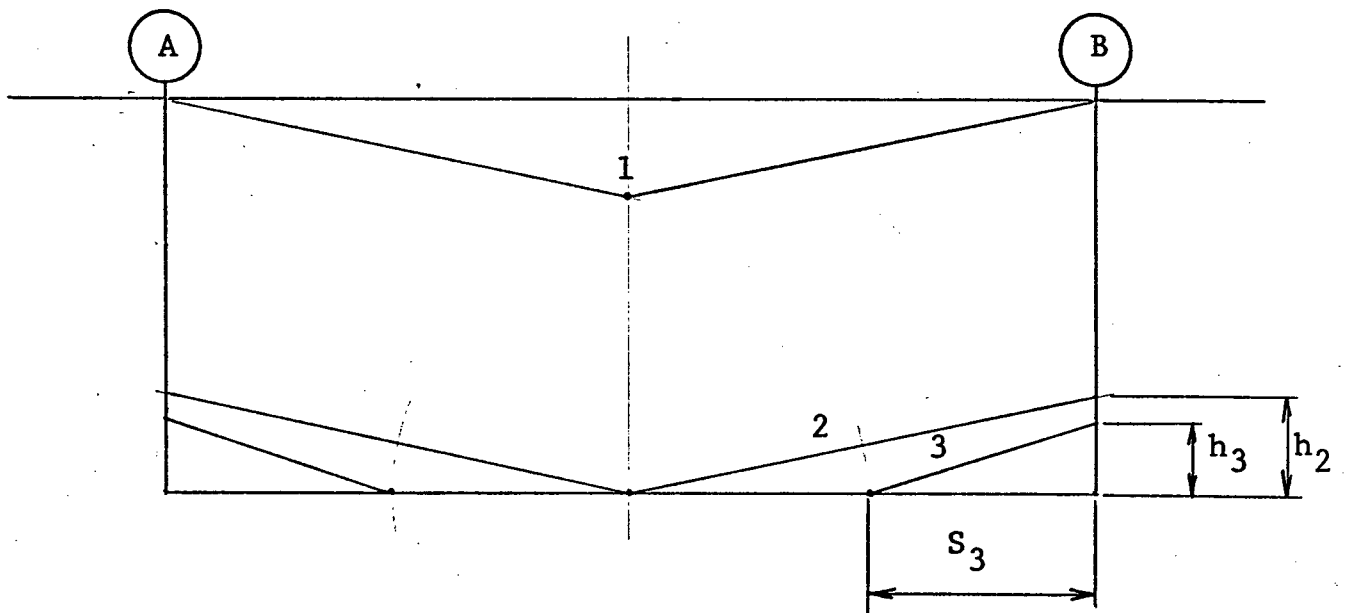
b) Symmetric Collapse Mode

Fig. 2 Slab Collapse Modes

a) Standing   b) Sitting   c) Prone, Perpendicular to Wall   d) Prone, Parallel to Wall

Fig. 3   Distributions of Personnel in Basements
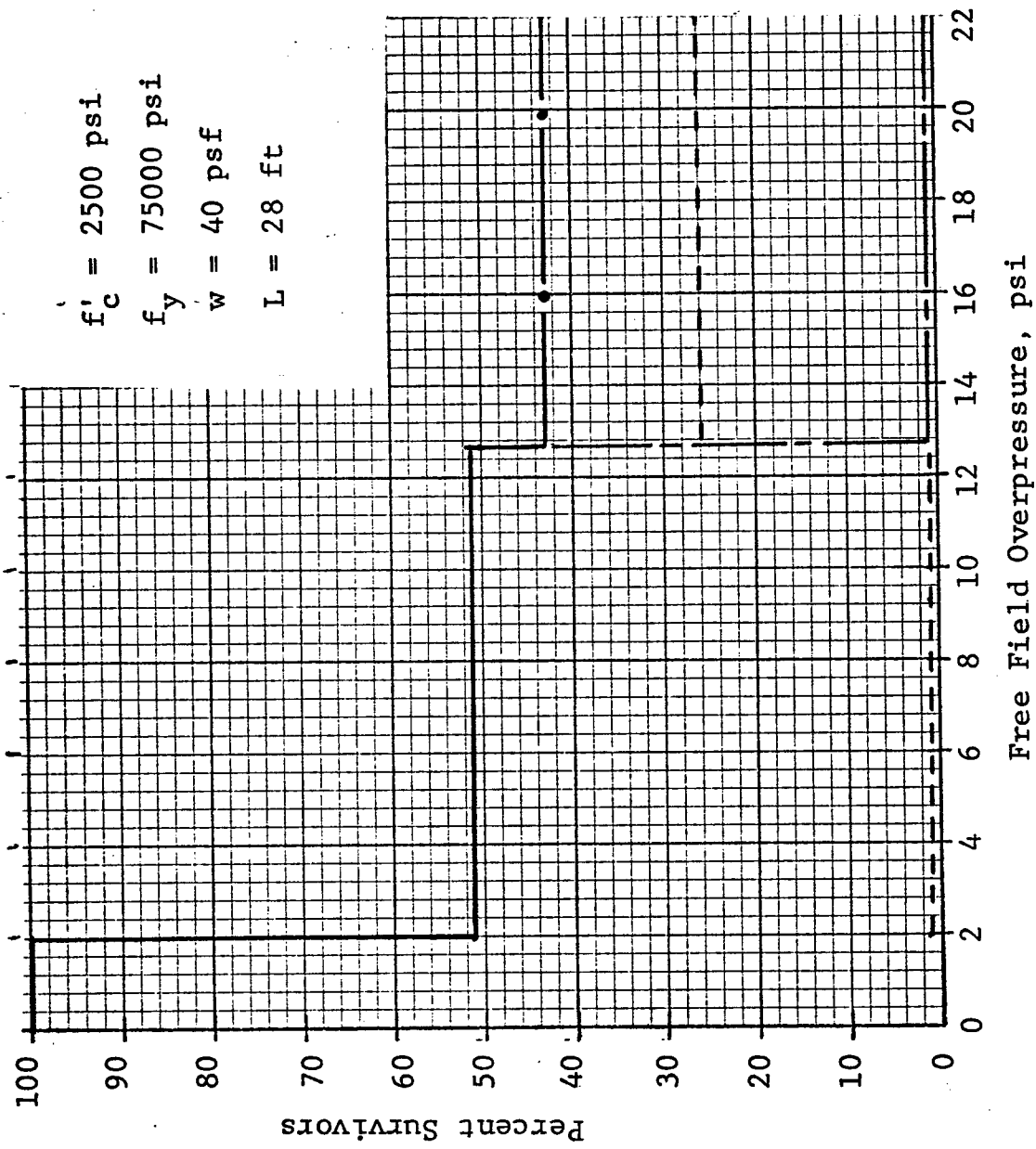
Fig. 3A Distribution of Personnel in Basements
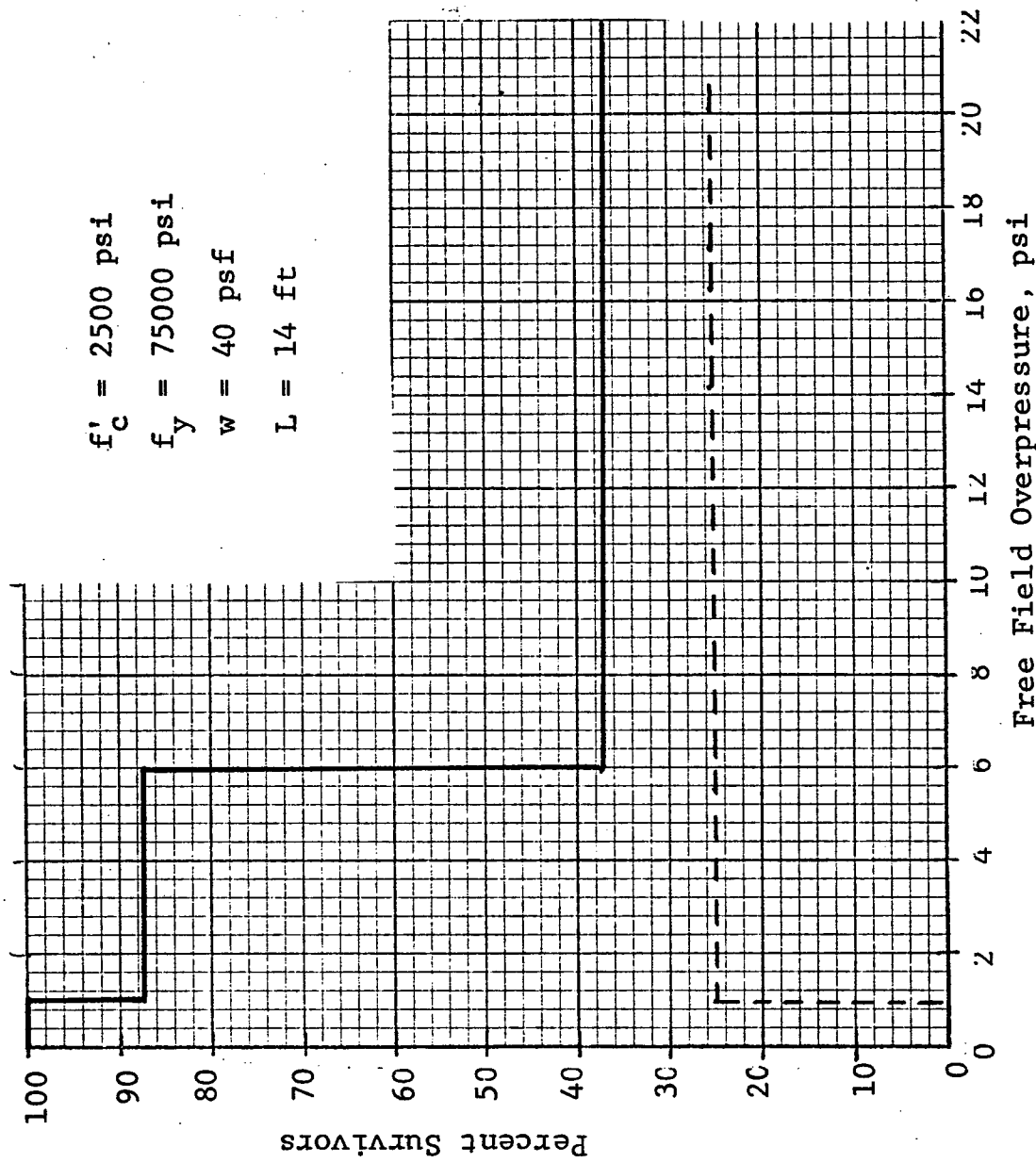
Fig. 4 People Survivability Estimate (Full Basement, One-Way
Simply Supported Slab)

f'_c = 2500 psi

f_y = 75000 psi

w = 40 psf

L = 40 ft

Percent Survivors

Free Field Overpressure, psi
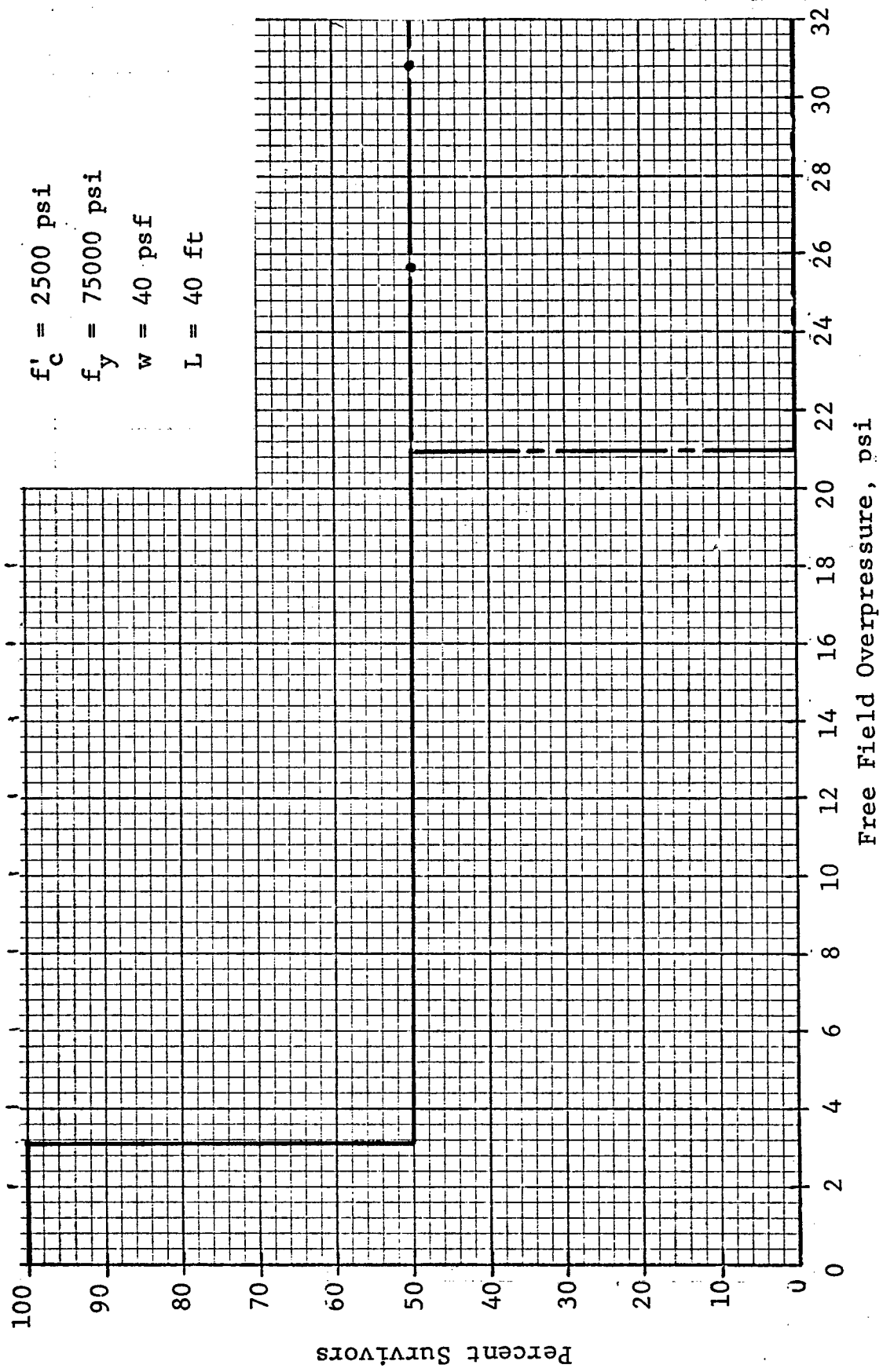
Fig. 5 People Survivability Estimate (Full Basement, One-Way Simply Supported Slab)

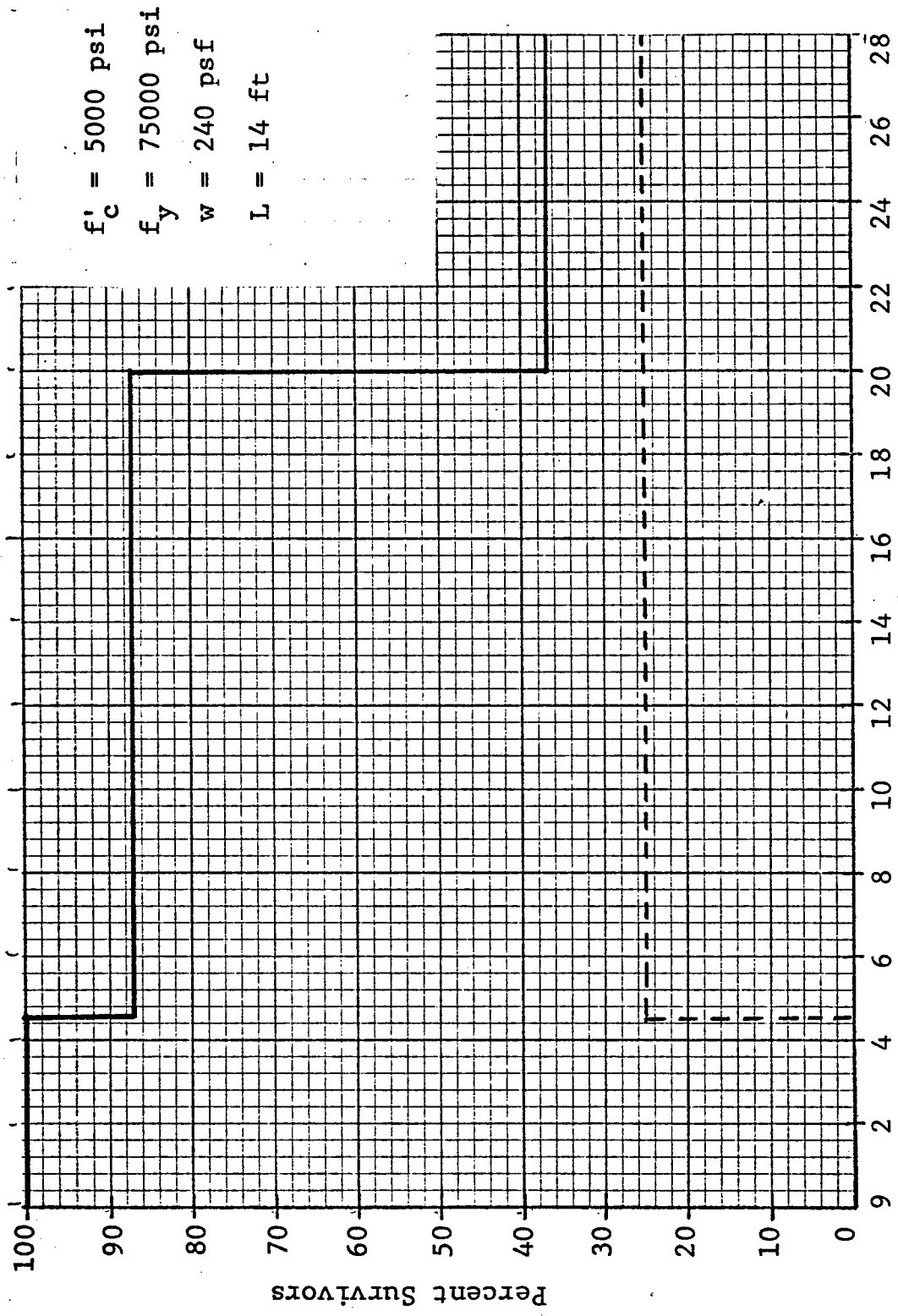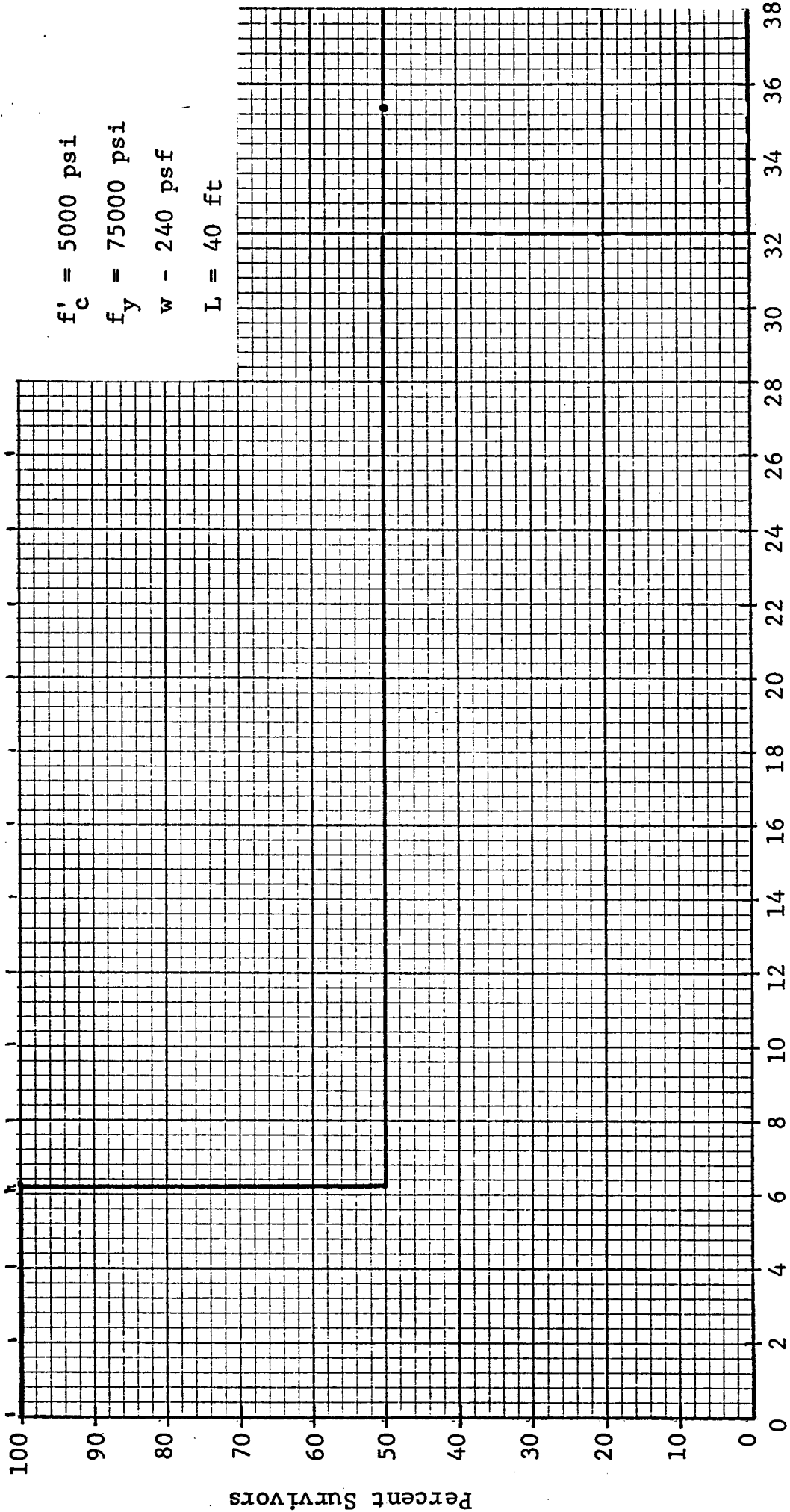Fig. 6   People Survivability Estimate (Full Basement, One-Way Simply Supported Slab)
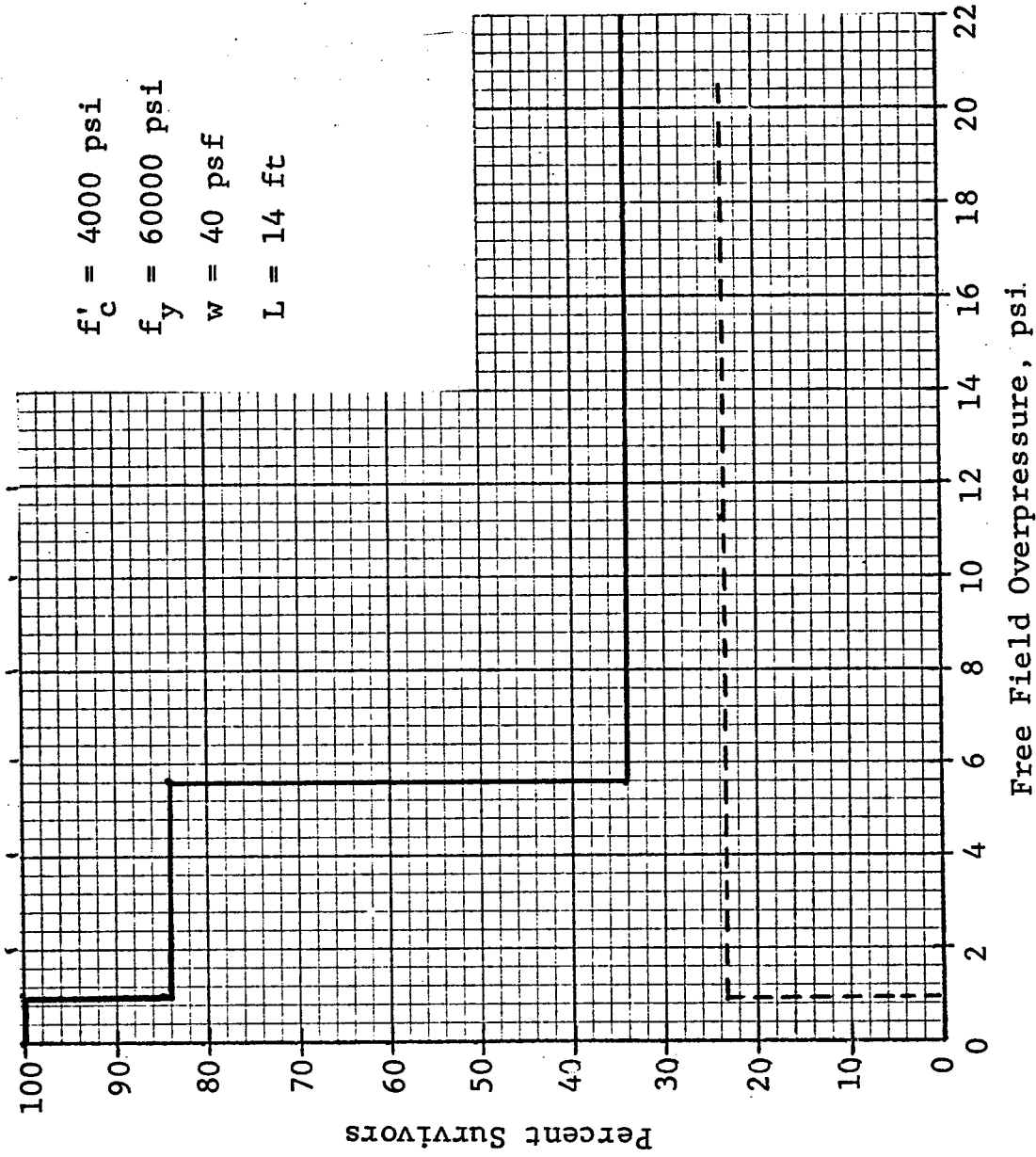
Fig. 7 People Survivability Estimate (Full Basement, One-Way Simply Supported Slab)

$f'_c = 5000$ psi

$f_y = 75000$ psi

$w = 240$ psf

$L = 14$ ft

Fig. 8 People Survivability Estimate (Full Basement, One-Way Simply Supported Slab)

Fig. 9 People Survivability Estimate (Full Basement, One-Way Simply Supported Slab)
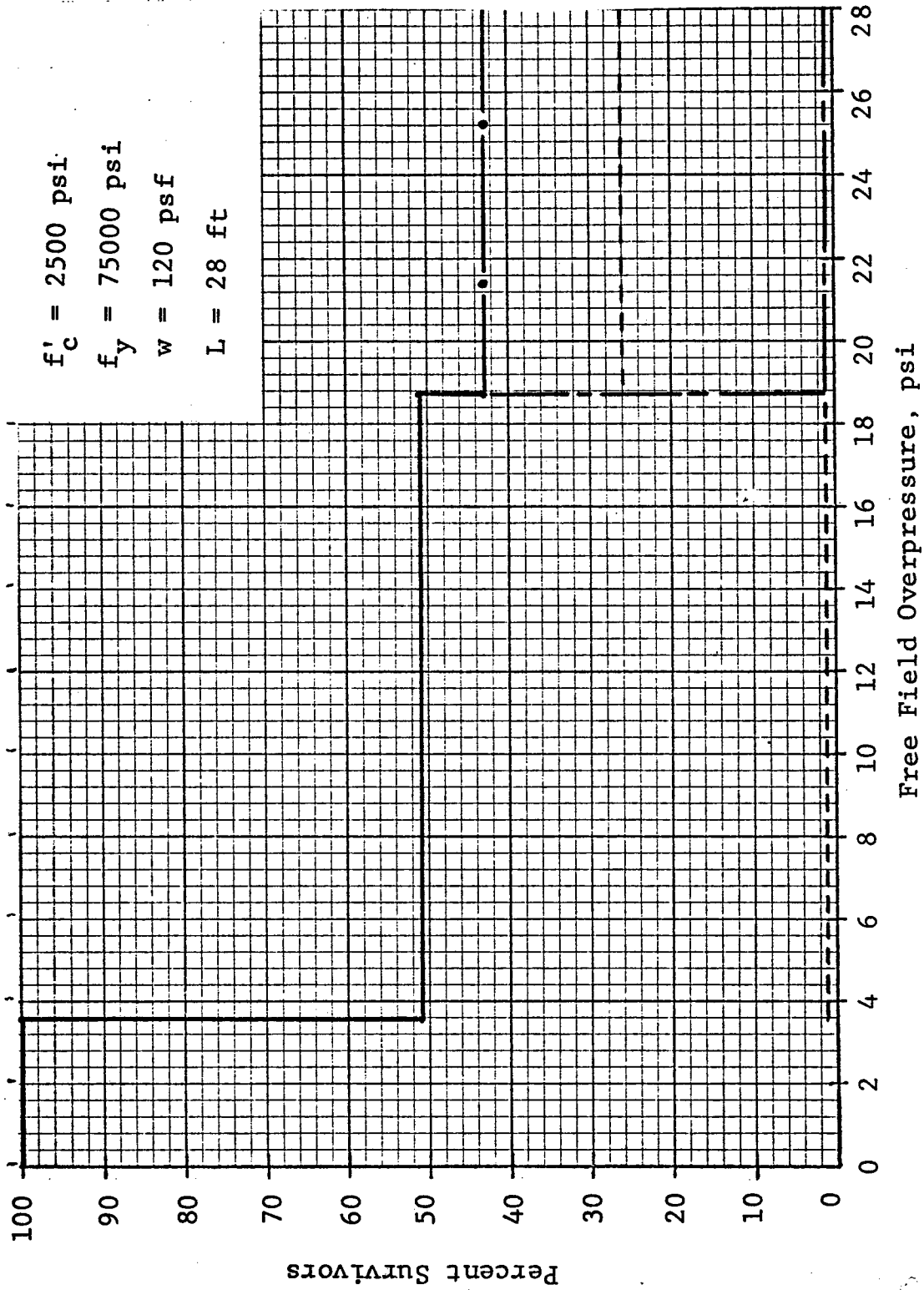
Fig. 10 People Survivability Estimate (Full Basement, One-Way Simply Supported Slab)
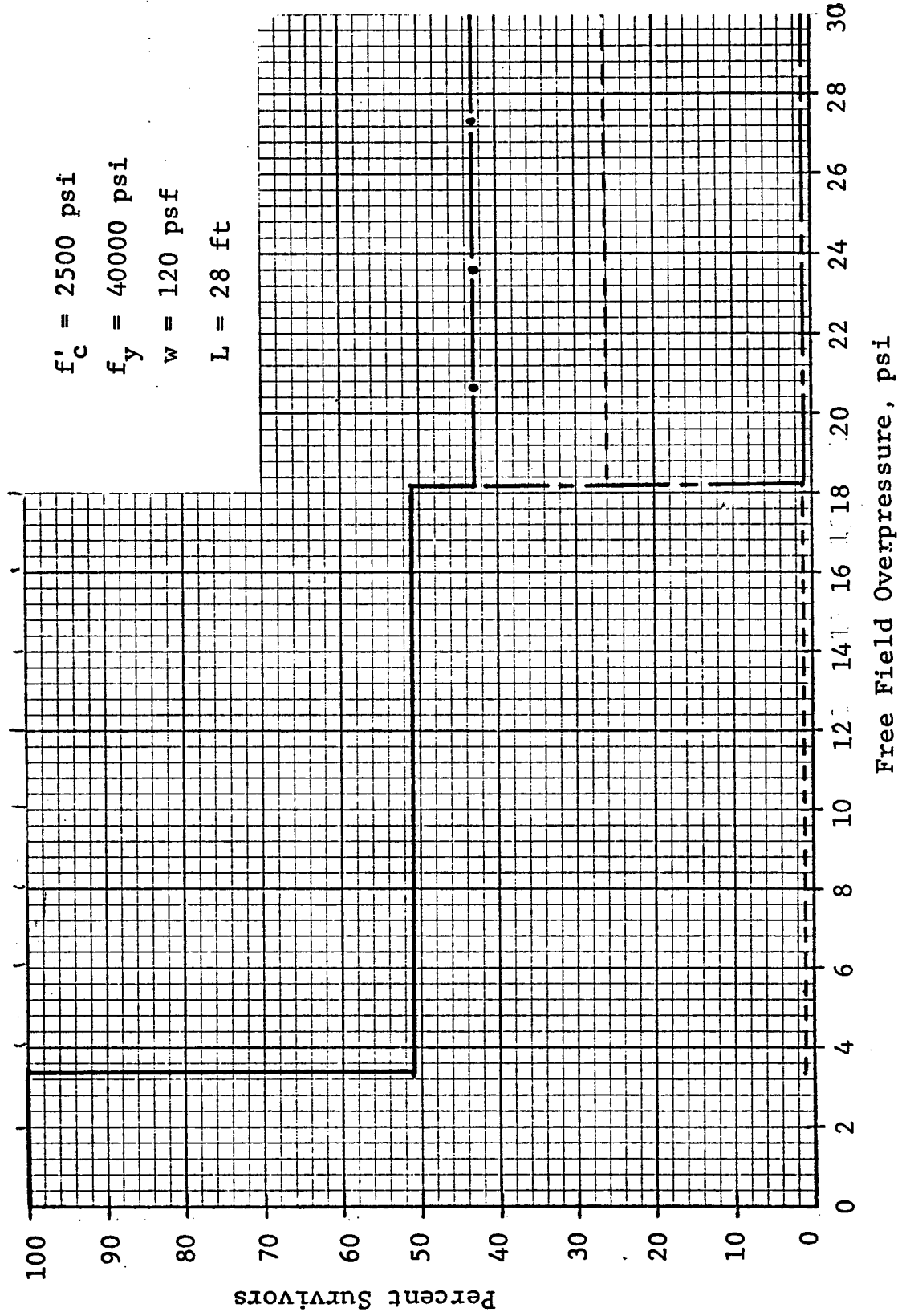
Fig. 11   People Survivability Estimate (Full Basement, One-Way Simply Supported Slab)
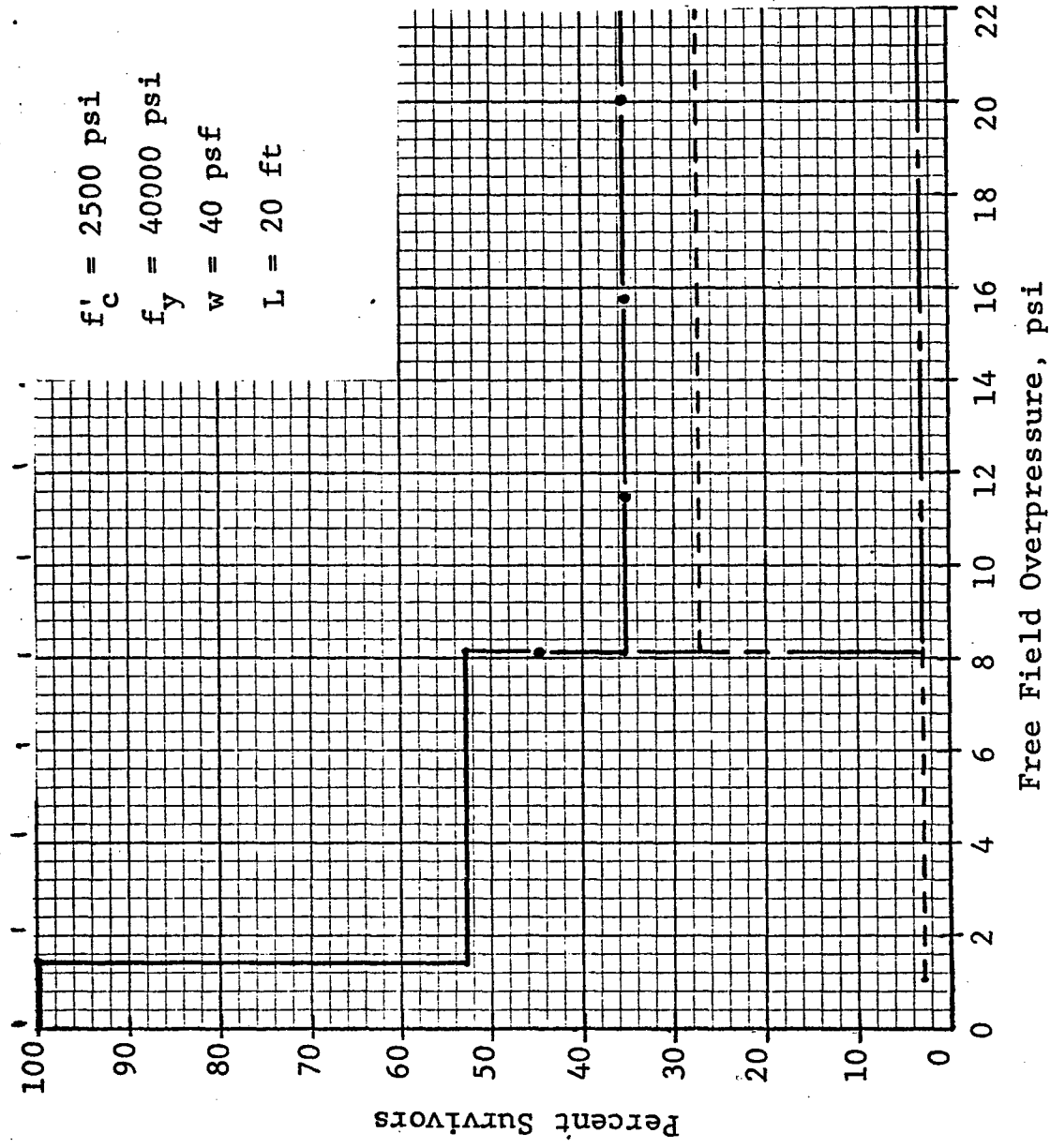
Fig. 12 People Survivability Estimate (Full Basement, One-Way
Simply Supported Slab

Free Field Overpressure, psi

Percent Survivors

f'_c = 2500 psi
f_y = 40000 psi
w = 40 psf
L = 20 ft

IIT Research Institute
10 West 35 Street, Chicago, Illinois 60616
312/225-9630

June 17, 1975   J6334

Defense Civil Preparedness Agency
The Pentagon
Washington, D.C.   20301

Attention: Mr. D. A. Bettge

Subject: Fourth Quarterly Report on IITRI Project J6334,
             Contract DCPA01-74-C-0251, Work Unit 1614E,
             "Debris Motion and Injury Relationships in All
             Hazard Environments"

Gentlemen:

     During the course of this reporting period the subject study
was conducted along the lines discussed in the following paragraphs.

1. People Survivability in Basement Spaces

     This task was initiated in the previous reporting period. Its
objective is to estimate the extent of sheltering provided by con-
ventional basements of existing buildings against the direct effects
of megaton-range nuclear weapons. The *extent of sheltering provided*
is measured in terms of number or percent survivors. Survivors in-
clude *injured* and *uninjured* personnel.

     Since readily available designs of basements with a representa-
tive range of design parameters do not exist, it was necessary to
design a representative sample of basement overhead floor systems.
The sample chosen includes one-way and two-way reinforced concrete
floor systems without beams or girders. The design parameters for
this sample are listed in Table 1.

     One way slab designs performed previously and discussed in the
last progress report were revised to reflect ACI 318-63 building
code requirements since this code more realistically reflects the
current inventory of basement spaces than does the ACI 318-71 code.
Also, a coarser gradation of parameter values was finally used than
was indicated in the last progress report. Differences in corre-
sponding slab thicknesses were too small to justify using a finer
gradation of values than that indicated in Table 1. One-way slabs
were designed using the USD (Ultimate Strength Design) approach.

     In keeping with the construction practice it was not practical
to match *all* parameters (one to one) listed in Table 1 for *two-way
slab* designs. Parameters which were matched are shown in Table 2.
The reasons are as follows.

Table 1
BASEMENT OVERHEAD SLAB PARAMETERS

1. Type of Slab — *One-way*; simply supported and continuous

   Two-way; flat plate; flat slab with drop panel and no capital, flat slab with drop panel and capital

2. Design Method — Working stress design
   Ultimate strength design

3. Design Live Load (nominal) — 50, 80, 125, 250 psf

4. Span — 16, 20, 24, 28 ft

5. Ultimate Compressive Strength of Concrete — 3, 4 ksi

6. Yield Strength of Reinforcing Steel — 40, 60 ksi

Table 2
MATRIX OF TWO-WAY SLAB DESIGN PARAMETERS

Span / Live Load	16 ft	20 ft	24 ft	28 ft
50 psf	FP WSD	FP WSD	FP WSD	CAPS USD
80 psf	FS WSD	FS WSD	FS WSD	CAPS USD
125 psf	FS WSD	FS WSD	FS WSD	--
125 psf	FS USD	FS USD	FS USD	--
125 psf	CAPS USD	CAPS USD	CAPS USD	CAPS USD
250 psf	CAPS USD	CAPS USD	CAPS USD	CAPS USD

Notation:
FP — Flat plate
FS — Flat slab with drop panel and no capital
CAPS — Flat slab with drop panel and capital
WSD — Working stress design
USD — Ultimate strength design

2

It is very unlikely that a two-way (square) slab (without beams) with a 16 ft span and 50 psf live load would be designed with drop panels and capitals. For this span and load magnitude a flat plate is more practical. Also, since we are dealing with ACI 318-63, working stress design (WSD) would produce a more economical slab than would the ultimate strength design (USD). The reason for this is that ACI 318-63 imposed a penalty on the use of USD for short spans and light loads of two-way slabs. The result was an increased slab thickness over that produced by using WSD. The effect of this penalty vanishes as the span or the load magnitude increases. At this end of the scale, the USD produces a more practical design. Thus, for a live load of 250 psf the likelihood is that two-way slabs without beams would be designed using the USD and would have drop panels and capitals. The middle ground is approximately at the 125 psf live load (see Table 2). At this load magnitude the use of WSD and USD is equally likely. Also, it is possible to have flat slabs with or without capitals. For these reasons, three sets of designs were produced for the 125 psf live load as shown in Table 2. Material (steel and concrete) properties used with these designs were as given in Table 1. The set of slab designs as indicated in Table 2 is considered to be representative of the current inventory for this category of slabs.

Under the assumption that each slab design represents a basement overhead slab system, each slab was analyzed to determine its response when subjected to the blast effects of megaton range nuclear weapons, i.e., blast pulse of long duration. This analysis determined overpressure levels necessary to produce yielding and catastrophic collapse. This information was then used to estimate percent survivors in two categories, i.e., injured and uninjured personnel. Survivors were estimated using several initial body positions for sheltered personnel, i.e.,

prone - uniformly distributed

prone - along peripheral walls

sitting - along peripheral walls

Some representative results for one-way and two-way floor systems are shown in Figures 1 and 2. In each case people are assumed to be uniformly distributed at approximately 10 sq ft per person. A much more detailed comparison of basement types and initial body positions will be included in the draft final report which is currently being prepared.

2. Prediction of Flow Fields in Basement Areas

The translational response of people and objects in a basement shelter during a nuclear attack requires a complete description of the complex flow fields which occur in this region during these transient events for the full range of weapon yield, overpressure level, and shelter sizes and geometries of interest. Current methodologies will permit such a description to be determined for two-dimensional shelter configurations by using a two-dimensional
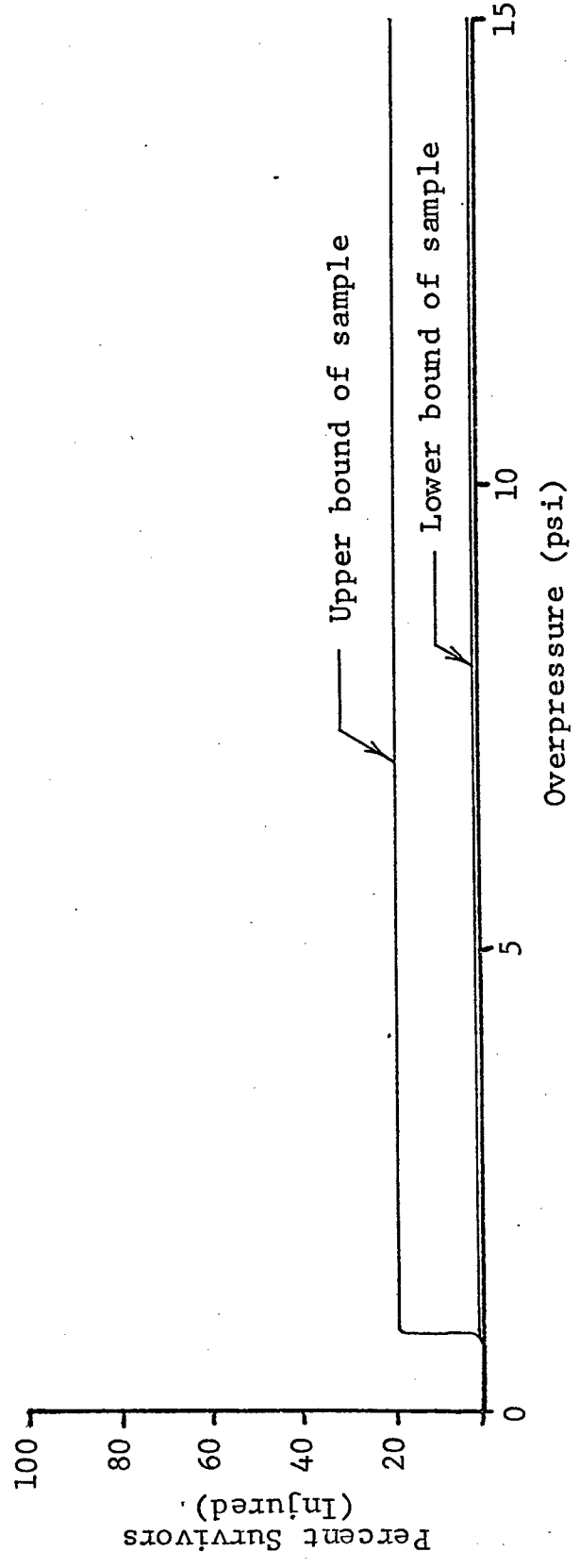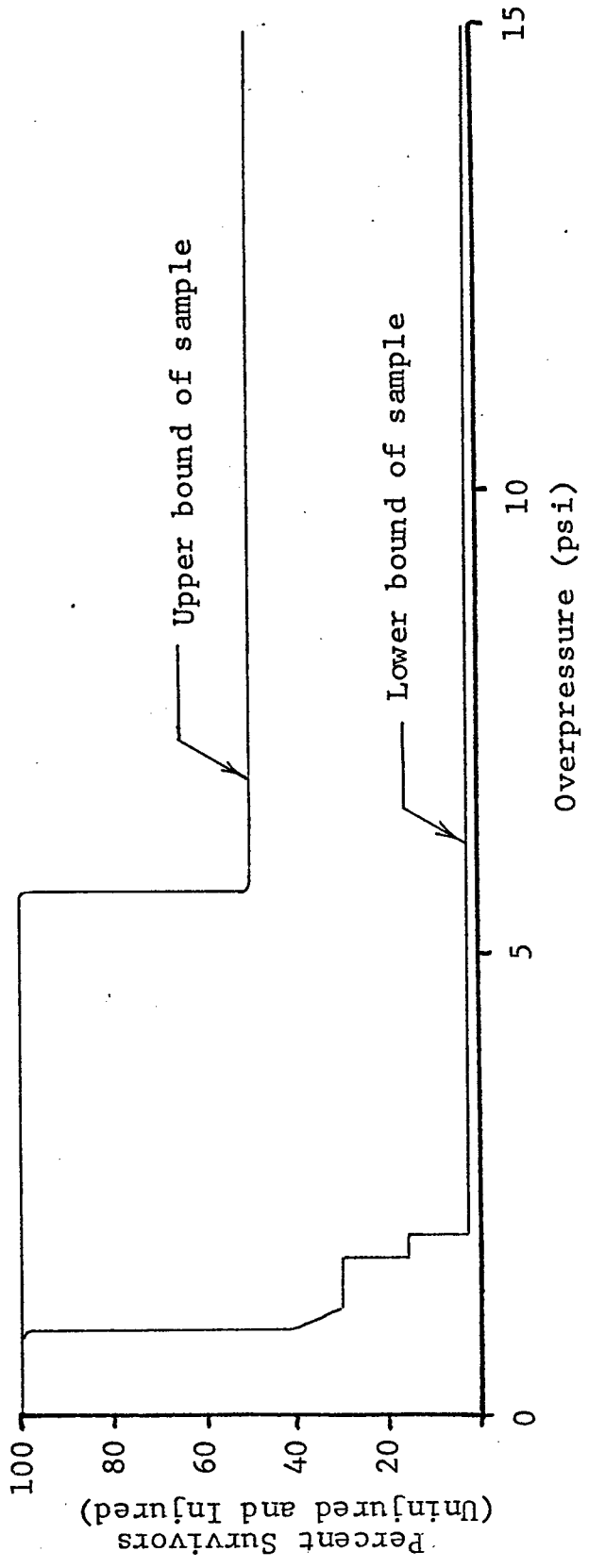
3

Figure 1 Upper and Lower Bound Estimates of Survivability and Injury for Two-Span Continuous Slabs
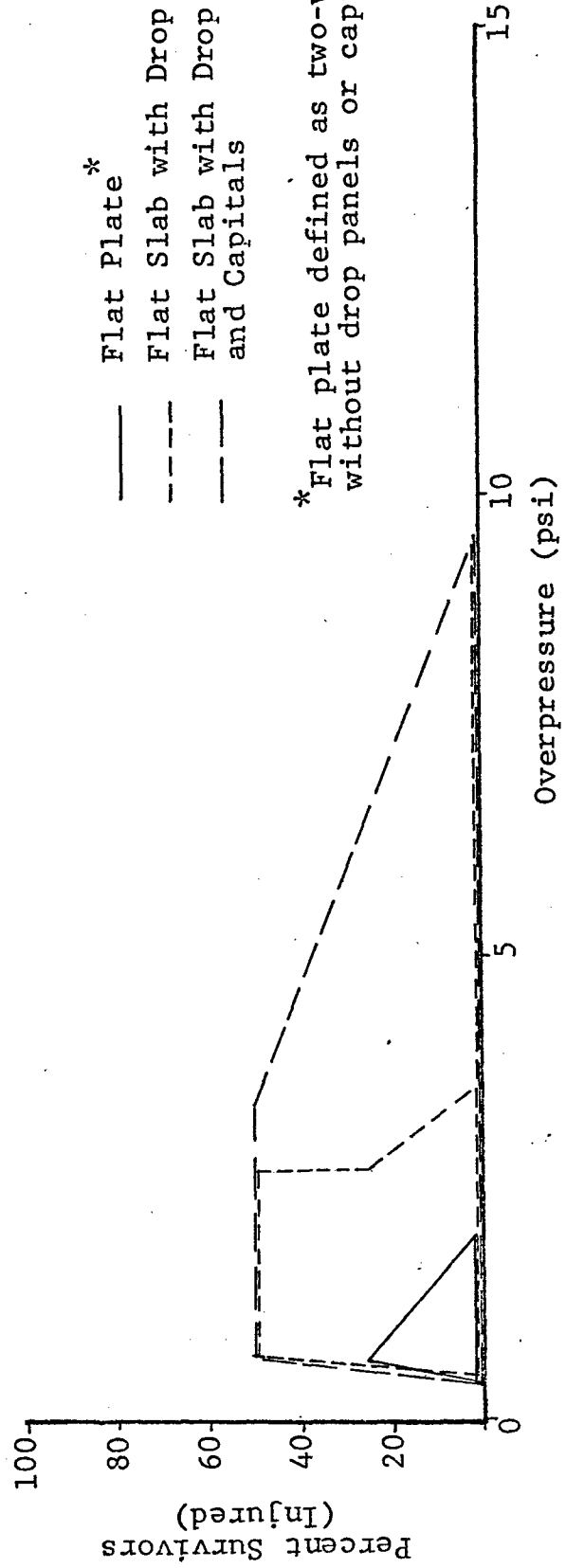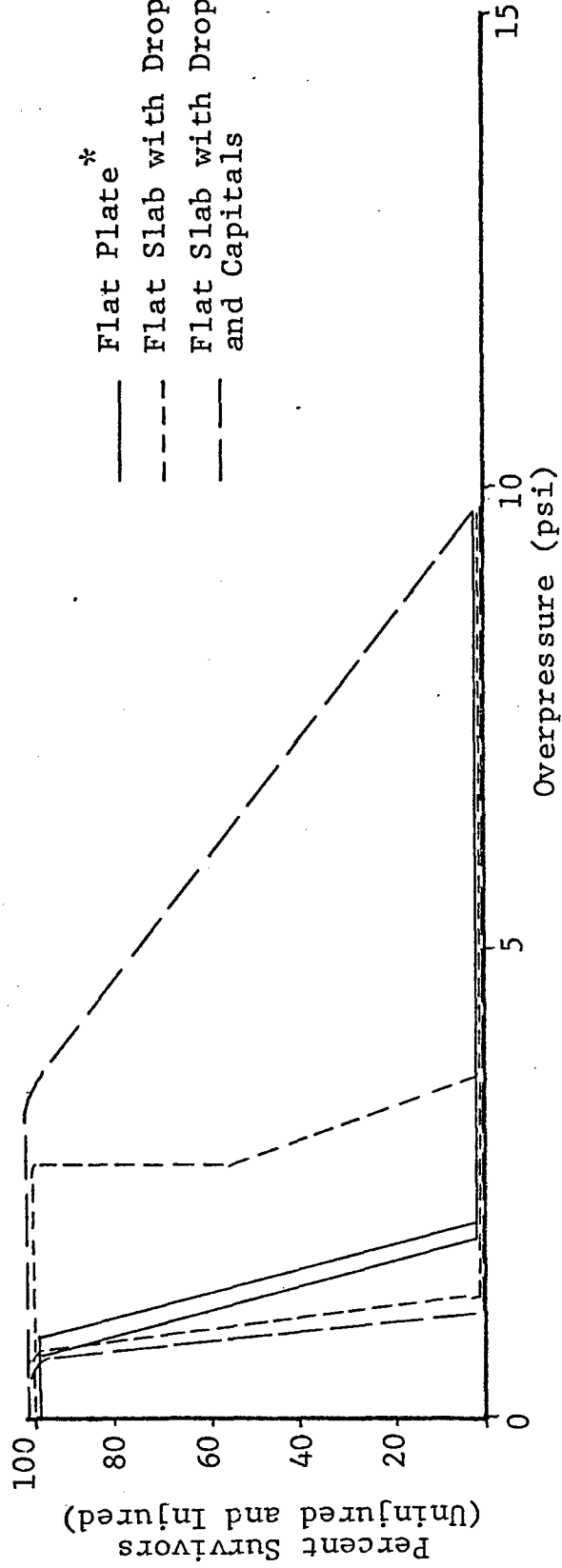
4

Figure 2   Upper and Lower Bound Estimates of Survivability and Injury for Two-Way Slabs

Eulerian nonsteady hydrodynamic computer code such as the BRL RIPPLE Program. The use of such a large computer code for this application would be expensive and time consuming. A more expeditious method is therefore required.

Simple quasi-steady cavity filling analysis will provide both an internal shelter pressure and inlet mass flow history. The latter can then be used as input data to define the flow in the neighborhood of a free jet. This is the limit of the current simplified methods. This type of model is inadequate because the shelter sizes of interest are frequently smaller than the free jet and thus the (no flow) boundaries of the shelter are not taken into consideration with respect to their influence in modifying the velocity field. In addition, secondary swirl flows which will be present are not treated. Furthermore this model does not consider the initial shock wave transient and its associated velocity field. To overcome these deficiencies an internal shelter flow model was constructed in the current study. The model treats three velocity fiels, i.e., 1) the initial transient, 2) the jet in a confined region, and 3) the swirl flows. Several solutions for internal flows in simple rectangular regions obtained by the RIPPLE Program were used as the basis for the development of this model. Inlet mass flow details, obtained from quasi-steady cavity filling solutions, were used as input data for this simplified model. At the present time the model is restricted to two-dimensional rectangular (basement) shelter configurations with a simple centrally located or edge located inlet.

This model has been exercised for a range of possible basement geometries shown in Table 3 and Figure 3, and for a range of free field overpressures between 6 and 15 psi.

At the writing of this report all the work on this study is essentially complete and is being written up for submission for your review. A draft final report is expected to be submitted within four to six weeks of this date.

3. Fiscal Report

Project Appropriation	$58,062
Billable Fee	- 3,287
Billable Cost	$54,775

Project Start - April 15, 1974

(1) Expenditures for the second calendar quarter ending June 30, 1974 $ 2,833.21

(2) Expenditures for the third calendar quarter ending September 30, 1974   11,430.11

6

Table 3

BASEMENT PARAMETERS

Case	Volume	$H \times \overline{W} \times H_c$	A	V/A	H	W	B
A	4×10^5 ft	200 x 200 x 10	400 ft^2	1000 ft	200	100	20.00
B1	10^5	100 x 100 x 10	25	4000	100	50	1.25
B2			100	1000	100	50	5.00
C1	3.6×10	60 x 60 x 10	10	3600	60	30	0.50
C2			50	720	60	30	2.50
D1	2048	16 x 16 x 8	2.05	1000	16	8	0.13
D2			4.10	500	16	8	0.26
E1	6270	28 x 28 x 8	6.27	1000	28	14	0.39
E2			12.54	500	28	14	0.78

Note: $\overline{W}$ = 2W

H_c = Clear ceiling height
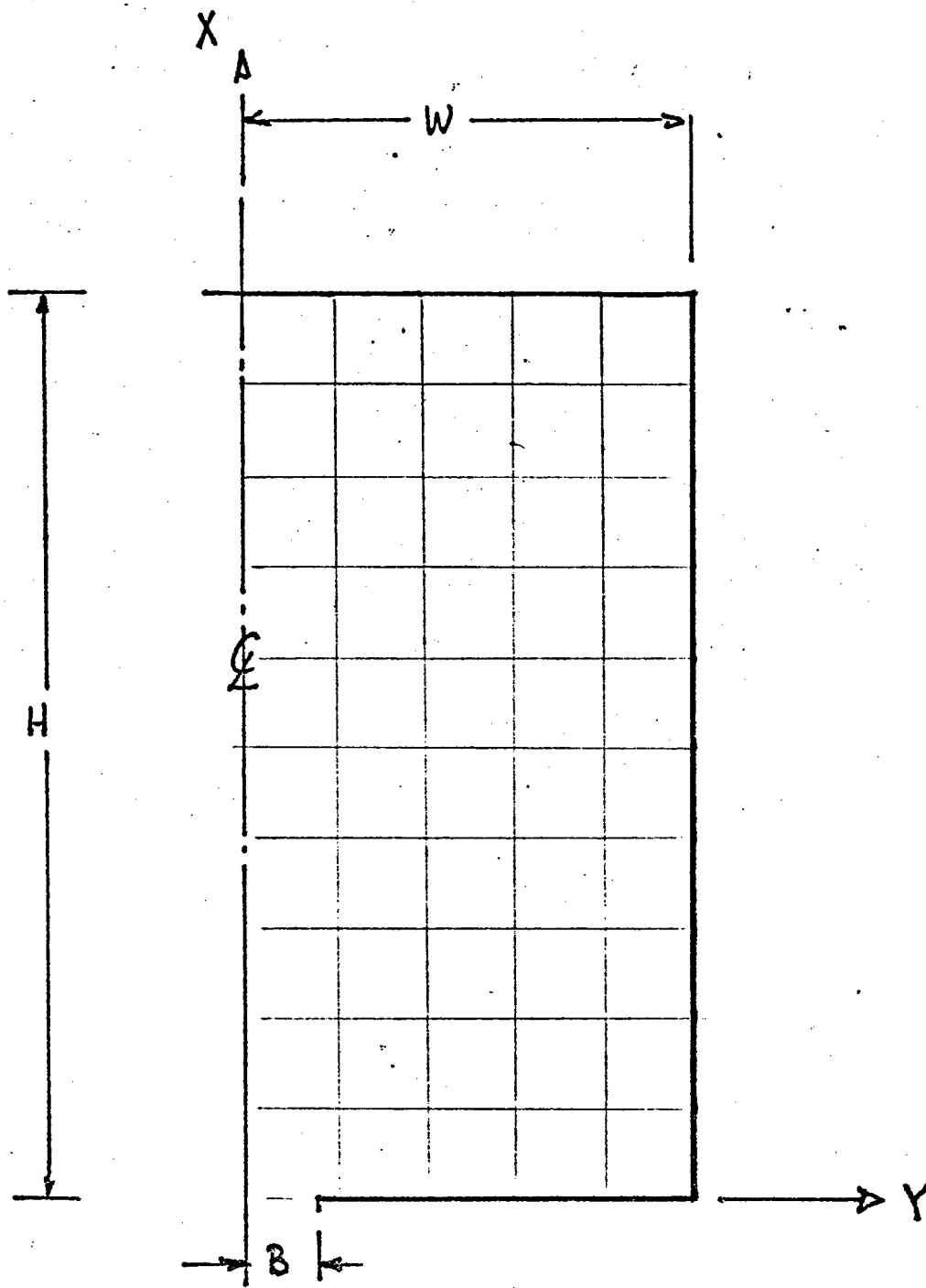
Figure 3 Basement Plan (Definition of Terms Used
in Flow Field Prediction)

(3) Expenditures for the fourth calendar
quarter ending December 31, 1974 $11,657.52

(4) Expenditures for the first calendar
quarter ending March 31, 1975   8,034.99

(5) Anticipated expenditures for the
second calendar quarter ending
June 30, 1975   18,000.00

(6) Anticipated expenditures for the
third calendar quarter ending
September 30, 1975   2,819.17

Total $54,775.00

Respectfully submitted,

IIT RESEARCH INSTITUTE

A. Longinow
Manager
Structural Analysis

AL:ms

APPROVED:

K. E. McKee
Director of Research
Engineering Mechanics Division

9